USING SUBSTRATE ANALOGUES TO PROBE THE MECHANISMS OF TWO BIOSYNTHETIC ENZYMES

A thesis presented in partial fulfillment of the requirements for the degree of

**Doctor of Philosophy**
In
Chemistry

At Massey University, Turitea, Palmerston North
New Zealand

Amy Lorraine Pietersma
2007

ABSTRACT

3-Deoxy-D-*arabino*-heptulosonate 7-phosphate (DAH7P) synthase and 3-deoxy-D-*manno*-octulosonate 8-phosphate synthase (KDO8P) synthase are two enzymes that catalyse very similar reactions. DAH7P synthase is the first enzyme of the shikimate pathway and catalyses the condensation reaction between the four-carbon sugar erythrose 4-phosphate (E4P) **1** and the three-carbon sugar phosphoenolpyruvate (PEP) **2** to give the seven-carbon sugar DAH7P **3**. KDO8P synthase catalyses a similar condensation reaction between the five-carbon sugar arabinose 5-phosphate (A5P) **8** and PEP **2** to give the eight-carbon sugar KDO8P **9**. Early mechanistic studies have shown the reaction mechanisms of these two enzymes to be very similar and structural and phylogenic analysis has suggested that the two enzymes share a common ancestor.
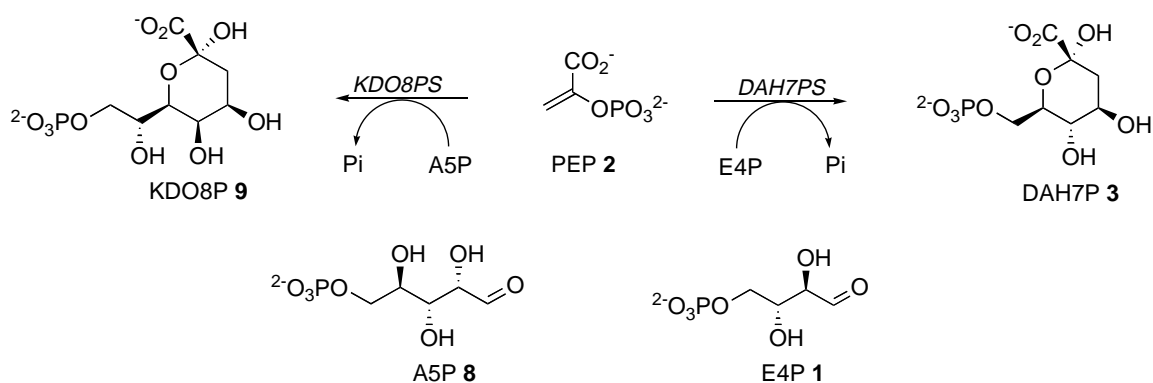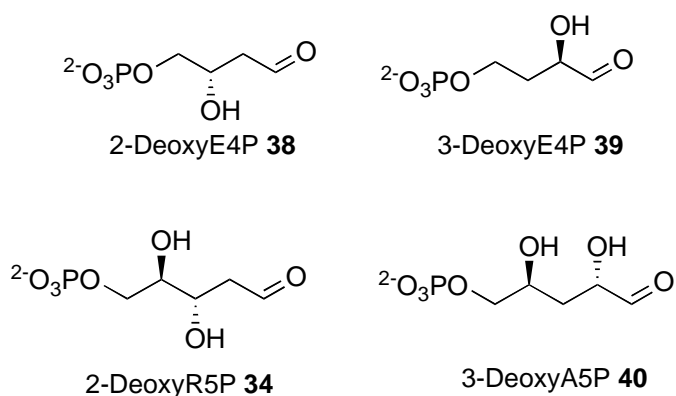

However, there are differences between the two enzymes that have not been explained by the current literature. Whereas all DAH7P synthases require a divalent metal ion for activity, there exists both metallo and non-metallo KDO8P synthases. As well as this, there is the difference in substrate specificity. The natural substrate of KDO8P synthase, A5P, is one carbon longer and has the opposite C2 stereochemistry to E4P, the natural substrate of DAH7P synthase.

This study investigates the role of the C2 and C3 hydroxyl groups of E4P and A5P in the enzyme catalysed reactions. The E4P analogues 2-deoxyE4P **38** and 3-deoxyE4P **39** have been synthesised from β-hydroxy-γ-butyrolactone and malic acid respectively. The two analogues were tested as substrates for DAH7P synthase from a variety of organisms, including *N. meningitidis*, the purification and characterisation of which was

carried out during the course of these studies. It was found that both analogues were substrates for DAH7P synthase. 2-DeoxyE4P was found to be the best alternative substrate for DAH7P synthase to date.

The analogous study was carried out on KDO8P synthase from *N. meningitidis* with 2-deoxyR5P **34** and 3-deoxyA5P **40**.   It was found that removal of the C2 and C3 hydroxyl groups of A5P was much more catastrophic for the KDO8P synthase catalysed reaction. Commercially available 2-deoxyR5P was found to be a very poor substrate, whereas 3-deoxyA5P, which was prepared according to a literature procedure was not a substrate.

The difference in substrate specificities of DAH7P synthase and KDO8P synthase is consistent with the hypothesis that despite their similarities, these two related enzymes have different mechanisms.   The key step for DAH7P synthase appears to be coordination of the E4P carbonyl to the divalent metal. The metal appears to play a less important role in the KDO8P synthase reaction and the key step is the correct orientation of A5P in the active site.

2-DeoxyE4P **38**

3-DeoxyE4P **39**

2-DeoxyR5P **34**

3-DeoxyA5P **40**

ACKNOWLEDGEMENTS

TABLE OF CONTENTS

CHAPTER ONE: INTRODUCTION

CHAPTER TWO: PURIFICATION AND CHARACTERISATION OF A TYPE Iα DAH7P SYNTHASE FROM *NEISSERIA MENINGITIDIS*

CHAPTER THREE: EVALUATION OF 2-DEOXYE4P AND A5P ANALOGUES WITH DAH7P AND KDO8P SYNTHASES

CHAPTER FOUR: SYNTHESIS AND EVALUATION OF 3-DEOXYE4P AND 3-DEOXYA5P WITH DAH7P AND KDO8P SYNTHASES

CHAPTER FIVE: MECHANISTIC INSIGHT INTO DAH7P AND KDO8P SYNTHASES

CHAPTER SIX: EXPERIMENTAL METHODS

ABBREVIATIONS

A5P   arabinose 5-phosphate

AEC   anion exchange chromatography

ATP   adenosine triphosphate

BSA   bovine serum albumin

BTCA   benzyltrichloroacetimidate

BTP   1,3-(tris(hydroxymethyl)-methylamino)propane

CSA   camphor sulfonic acid

Conc.   concentrated

Da   dalton

DAH7P   3-deoxy-D-*arabino*-heptulosonate-7-phosphate

DAST   diethylaminosulfurtrifluoride

DIBAL   diisobutylaluminium hydride

DMF   N, N-dimethylformamide

E4P   erythrose-4-phosphate

EDTA   ethylenediaminetetraacetic acid

EPSP   5-enolpyruvyl shikimate 3-phosphate

EtOAc   ethyl acetate

EtOH   ethanol

FPLC   fast protein liquid chromatography

G3P   glyceraldehyde 3-phosphate

G6P   glucose 6-phosphate

Hex   hexane

HIC   hydrophobic interaction chromatography

IPTG   isopropyl-1-thio-β-D-galactopyranoside

K_{cat} turnover number

KDO   3-deoxy-D-*manno*-octulosonic acid

KDO8P   3-deoxy-D-*manno*-octulosonate 8-phosphate

K_i inhibition constant

K_M Michaelis constant

L5P   lyxose 5-phosphate

LAH   lithium aluminum hydride

LB   luria broth

MWCO molecular weight cut-off

NAD^+ nicotinamide adenine dinucleotide

NADH nicotinamide adenine dinucleotide reduced form

OD   optical density

PAGE   polyacrylamide gel electrophoresis

PEP   phosphoenolpyruvate

2-PGA 2-phosphoglyceric acids

Phe   phenylalanine

P_i inorganic phosphate

pI   isoelectric point

ppm   parts per million

R5P   ribose 5-phosphate

R_F retention factor

Rpm   revolutions per minute

Sat.   saturated

SDS   sodium dodecyl sulfate

SEC   size exclusion chromatography

T4P   threose 4-phosphate

TBDMS *tert*-butyldimethylsilyl

TBDPS *tert*-butyldiphenylsilyl

THF   tetrahydrofuran

TLC   thin layer chromatography

Trp   tryptophan

Tyr   tyrosine

UV   ultra-violet

DAH7P synthase   3-deoxy-D-*arabino*-heptulosonate-7-phosphate

EPSP synthase   5-enolpyruvyl shikimate 3-phosphate synthase

G6P dehydrogenase   glucose 6-phosphate dehydrogenase

KDO8P synthase   3-deoxy-D-*manno*-octulosonate 8-phosphate synthase

A. aeolicus   *Aquifex aeolicus*

A. pyrophilus   *Aquifex pyrophilus*

B. subtilis   *Bacillus subtilis*

C. psittaci   *Chlamydia psittaci*

E. coli   *Escherichia coli*

H. pylori   *Helicobacter pylori*

M. tuberculosis   *Mycobacterium tuberculosis*

N. crassa   *Neurospora crassa*

N. gonorrhoeae   *Neisseria gonorrhoeae*

P. furiosus   *Pyrococcus furiosus*

S. typhimurium   *Salmonella typhimurium*

S. cerevisiae   *Saccharomyces cerevisiae*

T. maritima   *Thermotoga maritima*

N. meningitidis   *Neisseria meningitidis*

INDEX OF FIGURES

INDEX OF TABLES

PUBLICATIONS

Parts of this thesis have been published in the following publications:

Ahn, M.; Pietersma, A. L.; Schofield, L. R.; Parker, E. J., Mechanistic divergence of two closely related aldol-like enzyme-catalysed reactions. *Organic & Biomolecular Chemistry* **2005,** 3, (22), 4046-4049.

Williamson, R. M.; Pietersma, A. L.; Jameson, G. B.; Parker, E. J., Stereospecific deuteration of 2-deoxyerythrose 4-phosphate using 3-deoxy-D-*arabino*-heptulosonate 7-phosphate synthase. *Bioorganic & Medicinal Chemistry Letters* **2005,** 15, (9), 2339-2342.

CHAPTER ONE: INTRODUCTION

1.1   The Shikimate Pathway

The shikimate pathway (Figure 1.1) is an enzyme pathway consisting of seven enzyme-catalysed reactions, ultimately responsible for the formation of chorismate **4**. Chorismate is a precursor to aromatic compounds, including the essential aromatic amino acids phenylalanine **5**, tyrosine **6,** and tryptophan **7**.[1]
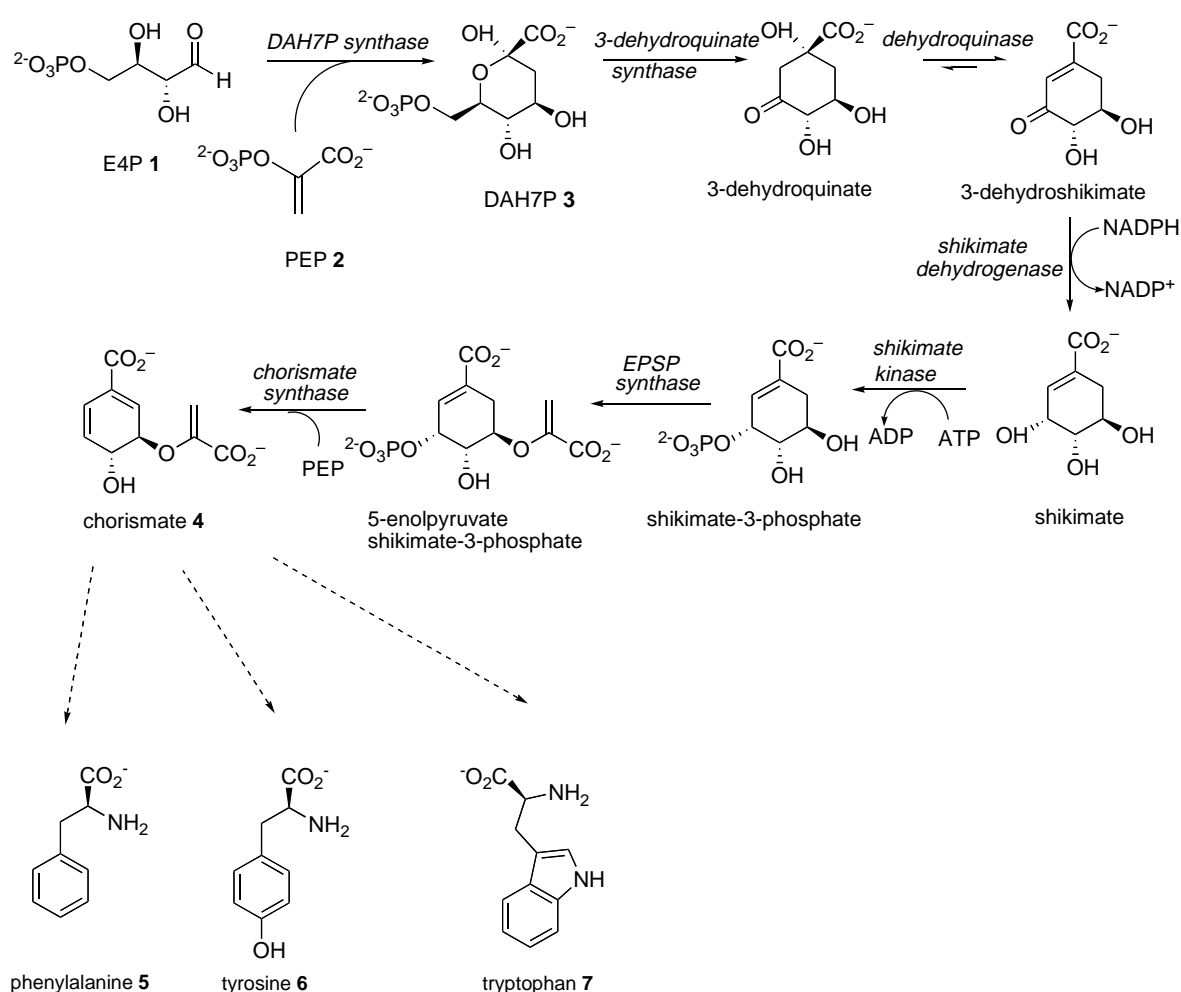
Figure 1.1: The seven enzyme-catalysed reactions of the shikimate pathway

The shikimate pathway exists in plants, bacteria and fungi, but not in mammals, making the aromatic amino acids an essential part of our diets. The absence of this pathway in mammals also makes the enzymes of the shikimate pathway attractive targets for novel

antibiotics, herbicides and fungicides. This potential is demonstrated in the success of Roundup® an effective herbicide containing the active ingredient glyphosate (*N*-(phosphomethyl)glycine), which inhibits the sixth enzyme of the shikimate pathway, 5-enolpyruvylshikimate-3-phosphate (EPSP) synthase.[2]

1.2   3-Deoxy-D-*arabino*-heptulosonate 7-phosphate (DAH7P) synthase

The first step of the shikimate pathway is catalysed by 3-deoxy-D-*arabino*-heptulosonate 7-phosphate (DAH7P) synthase (Figure 1.2). The reaction is an aldol-like condensation reaction between erythrose 4-phosphate (E4P) **1,** and phosphoenol pyruvate (PEP) **2** to form the seven-carbon sugar DAH7P **3**, along with inorganic phosphate. This reaction is a major control point of the shikimate pathway. In *Escherichia coli*, there are three isozymes of DAH7P synthase, each being specifically feedback regulated by one of the three aromatic amino acids, phenylalanine, tyrosine and tryptophan. The work presented in this report relates to DAH7P synthase, as well as to a related enzyme, 3-deoxy-D-*manno*-octulosonate 8-phosphate (KDO8P) synthase.
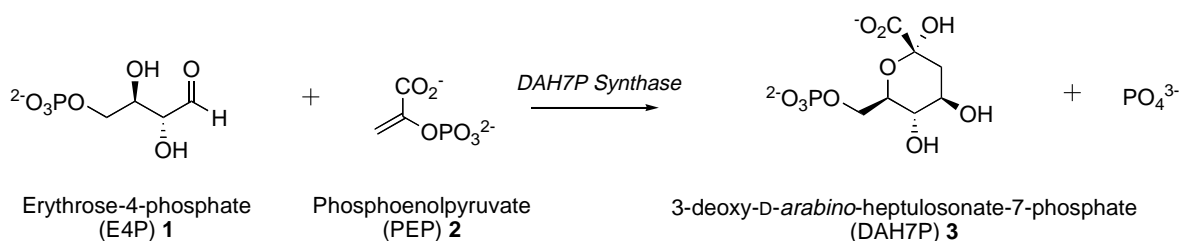
Figure 1.2: The reaction catalysed by DAH7P synthase

1.3   3-Deoxy-D-*manno*-octulosonate 8-phosphate (KDO8P) synthase

3-Deoxy-D-*manno*-octulosonate 8-phosphate (KDO8P) synthase catalyses a similar aldol-like reaction to DAH7P synthase between the five-carbon sugar arabinose 5-phosphate (A5P) **8** and the three-carbon sugar PEP **2**, to produce KDO8P **9** and

inorganic phosphate (Figure 1.3). A5P differs from E4P in that its chain length is one carbon longer, and its stereochemistry at C2 is the opposite to that of E4P. The KDO8P synthase catalysed reaction is the first committed step in the formation of KDO, which is an essential sugar of lipopolysaccharide, a component of cell walls in Gram-negative bacteria.[3] As formation of the lipopolysaccharide is necessary for growth and virulence of Gram-negative bacteria,[4] KDO8P synthase has been identified as a possible target for antibiotics.[5] Due to the similarities in their mechanisms and structures, as described later, DAH7P synthase and KDO8P synthase have often been studied together.
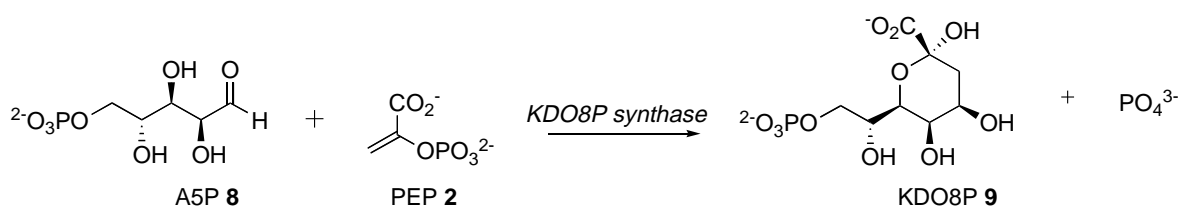
Figure 1.3: The reaction catalysed by KDO8P synthase

1.4 Classification

It has recently been proposed that DAH7P synthase and KDO8P synthase belong to the same enzyme family and are related by evolution.[6] There are two classes of DAH7P synthase, based on amino acid sequence and molecular mass. Walker and coworkers[7] defined the type I DAH7P synthases as having an *E. coli*-like sequence and as smaller proteins (M_r around 39000), whereas type II DAH7P synthases have plant-like sequences and are larger, with M_r around 54000. Gosset *et al*[8] use the terminology AroA$_I$ and AroA$_{II}$ for type I and II DAH7P synthases respectively. The type I DAH7P synthases were later identified as having two sub-classes, denoted Iα and Iβ.[9] The type Iα proteins consist entirely of DAH7P synthases and include the characterised enzymes from *Escherichia coli*[10-15] and *Saccharomyces cerevisiae*,[16-18] whereas the type Iβ proteins can be further split into the Iβ_D and Iβ_K subfamilies. Iβ_D type proteins are all DAH7P synthases and characterised enzymes include *Pyrococcus furiosus*[19,20] and *Thermotoga maritima*,[21,22] whereas the Iβ_K subfamily consists only of KDO8P synthases. The KDO8P synthases can be further split into metallo (*Aquifex aeolicus*[23,24] and *Helicobacter pylori*[25]) and non-metallo (*E. coli*[26]) enzymes. Although the Iβ_D

enzymes are functionally related to the Iα proteins, they show greater structure similarity to the Iβ_K enzymes, as described in Section 1.7.2.[9] It has been suggested that the type I proteins be renamed the 3-deoxy-ald-2-ulosonate-phosphate synthase family, due to the two different substrate specificities of its members.[6]

Type II DAH7P synthases were originally identified in plants and are now known to encompass a diverse set of microbial proteins of which the plant proteins form a subcluster.[1,8] Some organisms, such as *Stigmatella aurantiaca*[27] have genes encoding both type I and II DAH7P synthases, in some of these, the type II enzymes are apparently required for the biosynthesis of secondary metabolites,[27,28] but other organisms, such as *Mycobacterium tuberculosis*, have only type II DAH7P synthases. This lead to the conclusion that type II DAH7P synthases, in these organisms, must play a role in primary biosynthesis.[8]

A phylogenetic tree based on sequence similarity, showing the relationship between the type I enzymes, has been constructed by Jensen *et al*.[6] Although the lack of obvious sequence similarity, particularly between DAH7P synthase and KDO8P synthase had initially suggested convergent evolution of the enzymes, many other factors, such as the very similar monomer structure, conserved active site residues (Section 1.7), and similar proposed mechanisms (Section 1.5) all are consistent with divergent evolution.[29] Gosset *et al*[8] have proposed that the ancestral form of DAH7P synthase must be a Iβ-like protein, as this subfamily contains organisms that are the most widely distributed in nature. It has been proposed by Jensen *et al* that the ancestor of the type I enzymes had a broad substrate specificity, the ability to coordinate metal, and was not subject to allosteric inhibition.[6] Potential criteria characterising the individual subfamilies have been proposed. Birck and Woodard initially suggested that the requirement for a metal may distinguish between the type Iα and Iβ DAH7P synthases, although it was later shown that Iβ DAH7P synthases did require a metal ion for activity.[19,21]. A later study by Wu *et al* suggested that allosteric regulation may be the evolutionary link between the two classes. Subramaniam *et al* suggested that substrate specificity could explain the difference between the two subfamilies and that the ancient proteins had broad substrate specificities, which narrowed over time.[9] Ancient proteins generally have broad substrate specificity with evolution resulting in the narrowing of substrate

specificity.[30]   *P. furiosus*, a Iβ$_D$ DAH7P synthase, as described later, fulfils all these predictions, with a broad substrate specificity and no allosteric regulation and therefore is potentially the contemporary protein most closely related to the ancestral protein.[20]

Until recently, the limited structural information on the type II DAH7P synthases has meant that it is unclear how they relate to the type I enzymes. However, the structure of *M. tuberculosis* DAH7P synthase has been solved recently, and this has shown that the basic structure and key active site residues are conserved, suggesting that these proteins do belong to the same enzyme family as the other DAH7P synthases and KDO8P synthase.[31]

1.5   Mechanism

Although it is clear that both DAH7P and KDO8P are formed *via* an aldol-like reaction between the monosaccharide and PEP, there has been much interest in the detail of these enzyme-catalysed reactions. This information could then be used in the design of mechanism-based inhibitors for these enzymes. Most of the early reaction mechanism studies were carried out on DAH7P synthase. These have shown that the reaction is carried out stereospecifically, with the *si* face of PEP attacking the *re* face of E4P (Figure 1.4),[32] and that the reaction, rather than following a ping-pong mechanism, as originally thought,[33] follows an ordered sequential kinetic mechanism, with PEP binding before E4P, and the sugar phosphate product being released prior to inorganic phosphate.[34] It has also been shown that the loss of phosphate from PEP is achieved by the cleavage of the C-O bond, rather than O-P bond.[34] Hence, the anomeric oxygen in DAH7P must originate from bulk solvent. This type of bond cleavage is unusual and only seen in a few PEP-utilising enzymes, such as EPSP synthase, the sixth enzyme of the shikimate pathway (which is inhibited by the successful herbicide glyphosate)[2] and UDP-*N*-acetyl-glucosamine enolpyruvyltransferase (MurA), which is targeted by the antibiotic fosfomycin.[35]
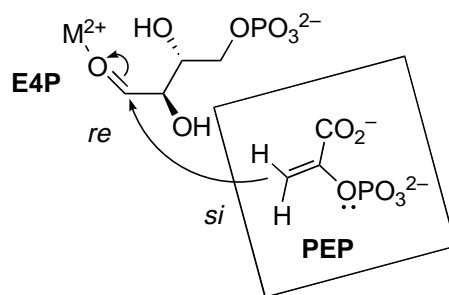
Figure 1.4: The steric course of the DAH7P synthase reaction between E4P and PEP

Similar studies on KDO8P synthase have found these aspects of the mechanism to be identical. The kinetic mechanism of the reaction is also ordered sequential, with PEP binding first and inorganic phosphate released last.[36,37] It involves cleavage of the C-O bond of PEP,[38] and the use of stereospecifically labeled 3-deutero and 3-fluoro PEP analogues has established that the overall stereochemical course of the reaction involves the *si* face of PEP attacking the *re* face of A5P.[39] Unlike E4P, A5P has a cyclic, furanose form; however, substrate analogue studies with 4-deoxyA5P, which cannot cyclise, have indicated that the enzyme acts upon the acyclic form of A5P.[36] Due to these similarities in the reactions catalysed by these two enzymes and their almost identical active sites, it has been assumed that the two enzyme-catalysed reactions share a common mechanism and mechanistic findings have therefore, tended to be extrapolated from one enzyme system to another.

The finer details of the mechanisms of these two enzymes have been the subject of ongoing controversy. DeLeo *et al*[34] proposed a mechanism for DAH7P synthase that was consistent with the information then available (fig 1.5 path A). It was proposed that in the initial step, C2 of PEP **2** was attacked by a water molecule, forming a tetrahedral carbanion at C3 of PEP, which then acts as a nucleophile on the aldehyde of E4P **1**. Loss of inorganic phosphate then gives the seven-carbon sugar DAH7P **3** in its acyclic form. Asojo *et al*[40] suggested a variation (Figure 1.5, path B) in which nucleophilic attack of the aldehyde of E4P **1** by C3 of PEP **2** results in the formation of an oxocarbenium ion intermediate or transition state **11,** which is then susceptible to attack by water to form the acyclic bisphosphate intermediate **12**. Both of these proposed mechanisms initially form the acyclic form of DAH7P **3**, which can then cyclise into the more stable hemiacetal form.[41]
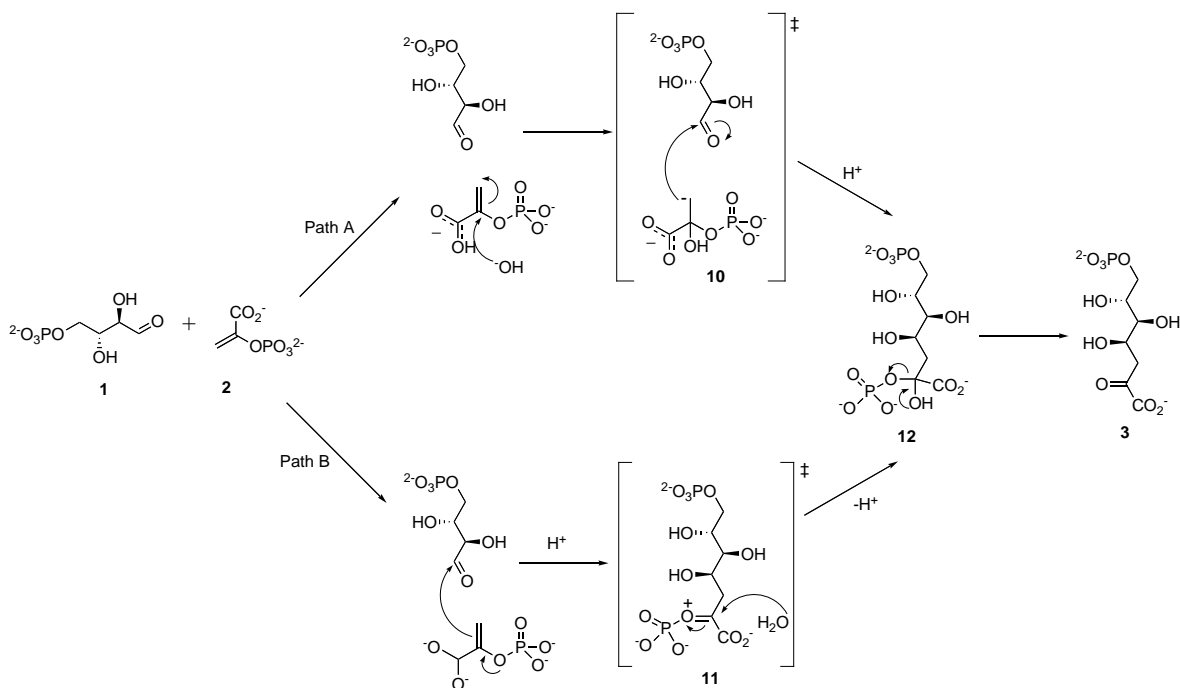
Figure 1.5; Two proposed mechanisms for DAH7P synthase catalysis

Hedstrom and Abeles[38] later proposed that the same mechanism operated for KDO8P synthase as shown in path A in Figure 1.5 above, where the first step is attack by a water molecule on C2 of PEP. It has been suggested that this water molecule may be activated by abstraction of a proton, making it more likely to attack C2 of PEP.[42] The mechanism proposed by Asojo *et al*, involving the oxocarbenium ion **11** (path B, Figure 1.5), was inclusive of both DAH7P synthases and KDO8P synthases.

Sheffer-Dee-Noor *et al*[43] initially proposed an alternative mechanism for KDO8P synthases, which involved a cyclic intermediate **13**. They proposed that the nucleophile that attacks the forming oxocarbenium ion **11** is not water, but the C3-hydroxyl of A5P, resulting in the direct formation of the cyclic form of KDO8P **9** after loss of inorganic phosphate. As aspects of the mechanisms of DAH7P and KDO8P synthases have been shown to be so similar, it has been inferred that the cyclic mechanism may also operate for DAH7P synthase.
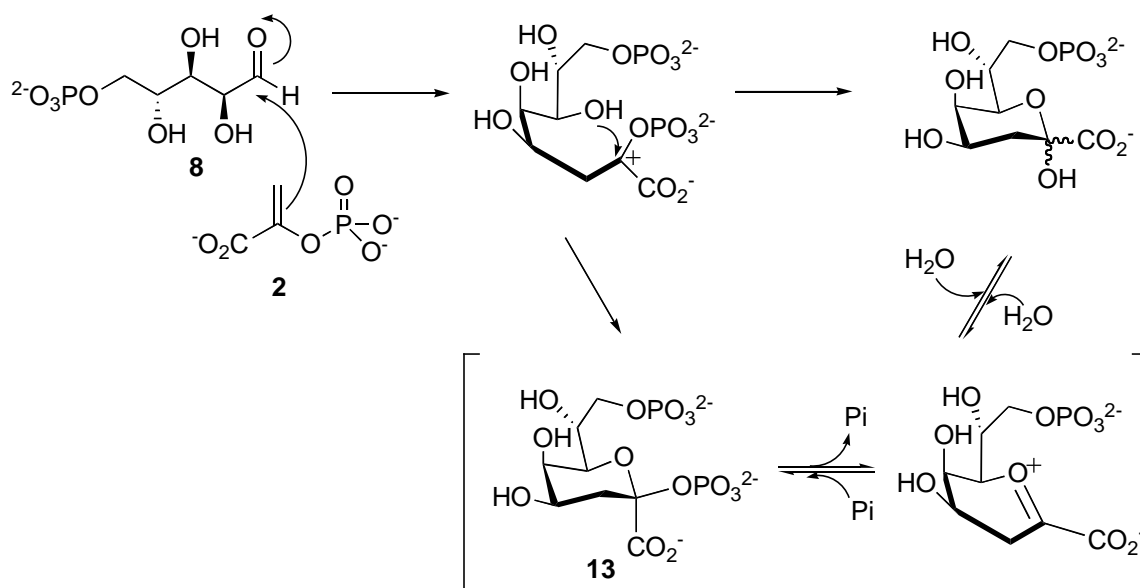
Figure 1.6: Proposed cyclic mechanism for the formation of KDO8P

This mechanism involving a cyclic intermediate **13** was originally supported by the observation that the phosphonate analogue **14** of the proposed cyclic intermediate **13** was found to be a potent inhibitor of KDO8P synthase, with a K_i of 5μM. Also, it was shown that 3-deoxyA5P was not a substrate for KDO8P synthase from *E. coli*, implying that the C3-hydroxyl of A5P **8** had a vital role in the reaction.[44] However, later studies[45,46] supported an acyclic mechanism, as the proposed cyclic intermediate **13** itself was found to not be a substrate or inhibitor for *E. coli* KDO8P synthase, and rapid chemical quench flow experiments showed no evidence of the cyclic intermediate **13** being formed.[47] Structural studies detailed in Section 1.7 are also inconsistent with the formation of a cyclic intermediate, as the C3-OH of E4P **1** or A5P **8** in either enzyme is not close enough to the C2 of PEP **2** to form a bond.[48]
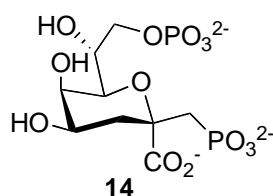
Figure 1.7: Phosphonate analogue **14** of proposed cyclic intermediate **13**

1.6 Metal activation

1.6.1 DAH7P synthase

Another unclear feature in the condensation reaction catalysed by DAH7P synthase and KDO8P synthase is the role of the divalent metal ion. All DAH7P synthases characterised to date require a divalent metal for activity, with the presence of the metal ion chelator EDTA shown to cause a complete loss of activity, that is reversible by the addition of metal ions.[49] Although some early reports characterising the tyrosine-sensitive and phenylalanine-sensitive isozymes of *E. coli* DAH7P synthase and *Bacillus subtilis* DAH7PS[11,50,51] stated that DAH7P synthase activity was not hindered by the addition of EDTA and therefore they were not metalloenzymes, it was later shown that some DAH7P synthases bind metal ions very tightly and hence needed a stronger metal chelator such as dipicolinic acid to form the apoenzyme.[52] Sequence alignments have shown that all identified DAH7P synthases possess the metal-binding residues Cys, His, Glu and Asp.[21] Mutations of Cys61 in *E. coli* DAH7P synthase have shown the residue to be essential for metal-binding.[10,53]

A variety of divalent metal ions are able to reactivate enzyme that has been treated with a metal chelator. The extent to which the metal ions can do this *in vitro* differs in the different organisms that the enzyme comes from, and also differs in the different isozymes of the same organism. For example, the tyrosine-regulated isozyme of *S. cerevisiae* is most activated by Co(II), whereas the phenylalanine isozyme is most activated by Mn(II).[17] The most extensively characterised DAH7P synthase, the phenylalanine-regulated *E. coli* DAH7P synthase is most activated by Mn(II).[14] DAH7P synthases from *E. coli* (Tyr),[54] *S. cerevisiae* (phe),[17] *S. cerevisiae* (tyr),[18] *P. furiosus,*[19] and *T. maritima*[21] have also been characterised and are activated by a wide variety of divalent metal ions.

Studies have also been carried out to determine the *in vivo* metal ion required for *E. coli* DAH7P synthase (phe). Staub and Dénes[49] found that the purified enzyme contained Co(II); however, Simpson and Davidson[55] later found that the purified enzyme neither had any significant quantity of Co(II) and nor was it stimulated by Co(II). McCandliss and Herrman[56] also found no evidence for *E. coli* DAH7P synthase (phe) being a Co(II)

metalloenzyme, after using atomic absorption spectroscopy to determine that their enzyme preparation contained one mole of Fe(II) per mole of enzyme and no Co(II). Stephens and Bauerle[14] later suggested that the most likely *in vivo* metal for all the *E. coli* DAH7P synthase isozymes is either Fe(II) or Zn(II), based on their high presence in purified enzyme preparations, their high binding affinity *in vitro*, and their relatively high bioavailability.

For *E. coli* (Tyr) DAH7P synthase, evidence suggests that the *in vivo* metal is copper.[54] Purified preparations of the enzyme showed high levels of bound copper(II) and copper(II) was the most activating metal out of the divalent metal ions tested. Other evidence points towards Fe(II), as the native enzyme was most activated by Fe(II) and also contained high levels of Fe(II).[13]

It is clear from these studies that *E. coli* DAH7P synthase (phe) is activated by a wide variety of divalent metals. The *in vivo* metal ion is likely to depend on various factors, such as bioavailability and growth conditions.

It has been shown that in the absence of the substrate PEP, redox-active metal ions catalyse the inactivation of *E. coli* DAH7P synthase (phe).[57] The inactivation is due to the metal-catalysed oxidation of two active site cysteine residues, Cys61 and Cys328, which is not seen when the enzyme is treated with EDTA. The presence of high metal concentrations allows a conformational change in the active site, enabling a disulfide bond to form between these two residues. The binding of PEP in the active site presumably hinders this conformational change. Recent studies on the type II DAH7P synthases from *M. tuberculosis* and *H. pylori* have also reported the need for a reducing agent in order to maintain full enzyme activity, and structural studies on *M. tuberculosis* DAH7P synthase have identified the formation of a disulfide bond between the metal-binding Cys87 and another Cys residue.[58] The stabilisation of DAH7P synthase by PEP is well documented[11,12,59] whereas the other substrate, E4P is known to inactivate *E. coli* DAH7P synthase (phe) by the formation of an imine linkage between a lysine residue and the aldehyde of E4P.[60]

1.6.2 KDO8P synthase

In contrast to the DAH7P synthases, both metallo and non-metallo KDO8P synthases have been characterised. Known non-metallo KDO8P synthases, the activity of which is unaffected by the presence of divalent metal ions or EDTA include those from *E. coli*,[26] *Salmonella typhimurium*,[61] *Neisseria gonorrhoeae*,[62] and *Neisseria meningitidis*, the last of which has recently been extensively characterised within our laboratory.[63] Initially it was assumed that all KDO8P synthases were non-metallo; however, it was later shown that KDO8P synthase from *A. aeolicus* was inhibited by the presence of EDTA and that activity could be restored with a variety of divalent metal ions.[24] This led to the proposal that a separate class of KDO8P synthases existed, based on active site sequence, which were metalloenzyymes.[6,29] Analysis of the metal requirement of *H. pylori* KDO8P synthase confirmed the prediction that a divalent metal ion was essential for activity and mass-spectral analysis showed one equivalent of Zn(II) bound per monomer.[25] The KDO8P synthases *Aquifex pyrophilus*[64] and *Chlamydia psittaci*[29] have also been shown to be metalloenzymes.

Sequence alignments of metallo KDO8P synthases and DAH7P synthases with non-metallo KDO8P synthases have shown a conserved metal-binding cysteine, found in all metalloenzymes, is replaced by a conserved asparagine in their non-metallo counterparts. Mutation of the metal-binding cysteine to an asparagine has been shown to convert a metalloenzyme into a non-metalloenzyme for *A. aeolicus*[65] and *A. pyrophilus*[66] KDO8P synthases. There is some disagreement as to whether the opposite mutation can be carried out. Although in one case it has been found that the reciprocal mutation of Asn26 to cysteine in the non-metallo *E. coli* KDO8P synthase does not result in a metal-binding enzyme,[65] other studies have found that it does.[66,67]

The difference in the metal requirement of DAH7P synthase and KDO8P synthase has prompted discussion over the role of the divalent metal ion that is necessary for activity of only some KDO8P synthases but all DAH7P synthases. Theories for the role of the metal in the enzyme-catalysed reaction include a catalytic role, where the metal is required to interact with a water molecule, lowering its pKa and allowing it to dissociate a proton in order to act as a nucleophile on C2 of PEP (mechanism path A, Figure 1.5).[42] Or that the metal ion acts as a Lewis acid, activating the carbonyl of E4P (or

A5P) for attack (mechanism path B, Figure 1.5).[68] It has also been proposed that the metal has a structural role, and is required to maintain the active site in the correct conformation for binding of the substrates.[10] In the non-metallo KDO8P synthases, this structural role may instead be fulfilled by the conserved Asn reside (Asn26 in *E. coli* KDO8P synthase), which is replaced by a Cys in the metallo counterparts. Structural studies described in the next section provide some insight as to the most likely role for the metal ion.

1.7 Structural analysis

While functional studies have managed to deduce many aspects of the mechanism of DAH7P synthase and KDO8P synthase, there are still many issues yet to be resolved. Recently, structural analysis with various substrates, substrate analogues and inhibitors bound has allowed for more detailed study of the mechanisms of these two enzymes.

1.7.1 Type Iα

Structures of the type Iα DAH7P synthases from *E. coli* (phe)[10,48,69] and *S. cerevisiae* (tyr)[68] have been solved. Both enzymes crystallised as tetramers of four identical subunits. Two of the subunits form a very tightly interacting dimer. The two tight dimers are held together in the *E. coli* enzyme by a saltbridge, hydrogen bonds and hydrophobic interactions, while in the case of *S. cerevisiae*, the interdimer interactions are hydrophobic only. The *S. cerevisiae* tetramer also has a much greater tetrahedral twist at the dimer-dimer interface than the *E. coli* tetramer.

The main residues involved in the interdimer interactions of *E. coli* DAH7P synthase (phe) and *S. cerevisiae* DAH7P synthase (tyr) are substituted in the tryptophan- and tyrosine-sensitive isozymes of *E. coli.* This explains why they are dimers in solution, rather than tetramers like the *E. coli* (phe) isozyme.[11,13] Mutational studies in which one of these residues, Glu24 is replaced by a Gln have resulted in an active dimer of the phenylalanine isozyme in solution,[48] although it still crystallises as a tetramer.
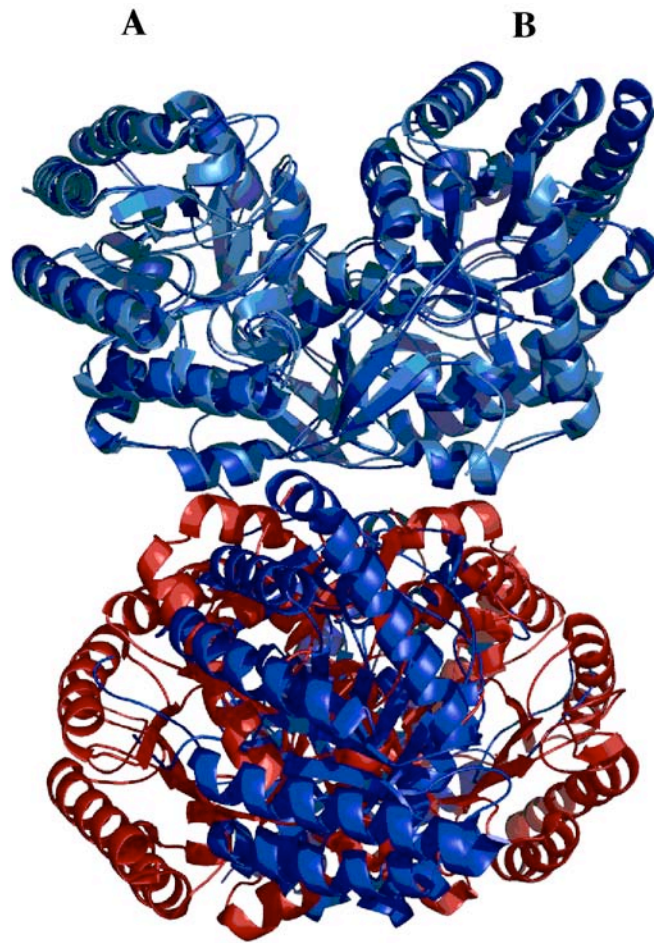
Figure 1.8: Comparison of the quaternary structures of *E. coli* DAH7P synthase (phe) (PDB code 1KFL) and *S. cerevisiae* DAH7P synthase (tyr) (PDB code 1HFB). The shared dimer (A and B) is in blue and the tetrameric association (the second dimer) of the type Iα enzymes is shown in red for *E. coli* (phe) and blue for *S. cerevisiae* (tyr).

Each monomer folds as a $(\beta/\alpha)_8$ barrel, enhanced by two additional elements. There is an N-terminal extension of 53 residues, as well as a two-stranded anti-parallel β-sheet, β6a/β6b inserted between α5 and β6 strands of the barrel (Figure 1.9). These two additional structural elements have been shown to be essential for feedback regulation.[16,70] The active site is located at the C-terminal end of the $(\beta/\alpha)_8$ barrel and is formed by the residues of a single subunit.
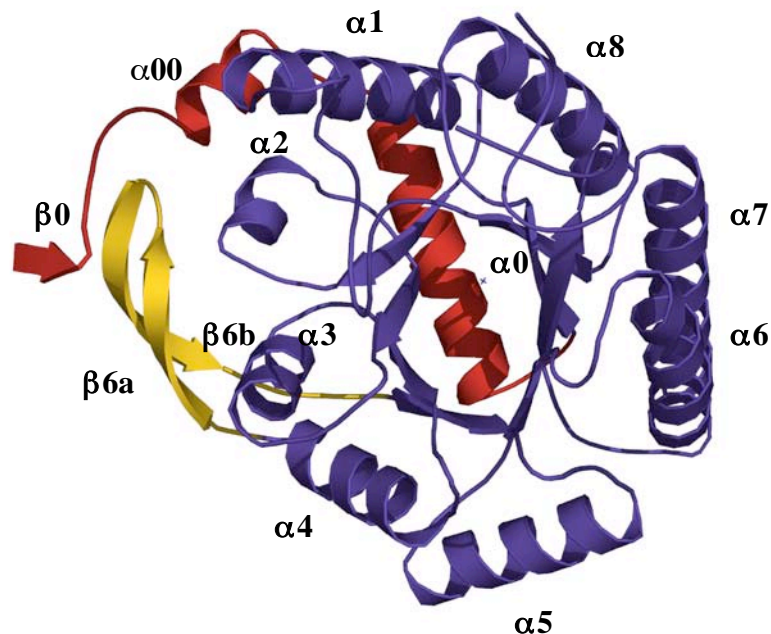
Figure 1.9: *E. coli* DAH7P synthase (phe) (PDB code 1KFL) monomer structure with α-helices of the basic (β/α)$_8$ barrel labeled. Additional structural elements are coloured red for the N-terminal extension and yellow for the inserted β-sheet.

The metal in the *E. coli* structure displays an approximately octahedral geometry with the residues Cys61, His268, Glu302 and Asp326 as ligands, as well as a water molecule that also binds to Lys97 and to PEP. Lys97 has been shown to be an essential residue for activity. The location of the metal and coordinated residues in the *S. cerevisiae* structure is identical to that of *E. coli*, but it displays a trigonal bipyramidal geometry rather than octahedral.

PEP is found at the bottom of the active site cleft with C3 pointing towards the opening of the cleft, surrounded by a positively charged binding pocket. It is held in place by multiple salt bridges and hydrogen bonds. One of the carboxylate oxygens forms a salt bridge with Lys97 (or Lys112 in the *S. cerevisiae* structure). PEP appears to deviate from planar geometry, with a 30° twist around the C1-C2 bond.
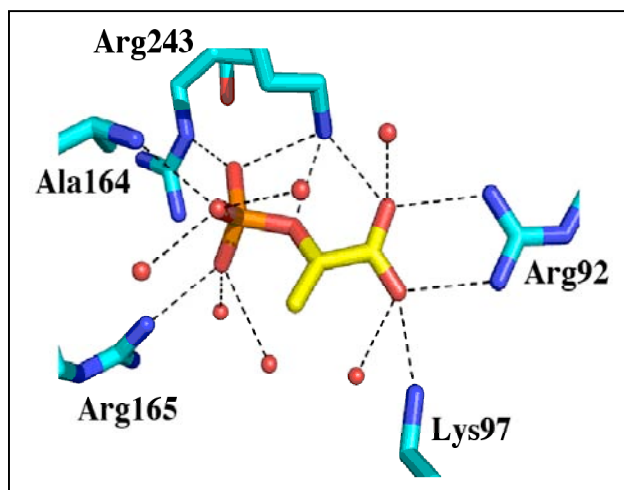
Figure 1.10: PEP binding site of *E. coli* DAH7P synthase (phe)-E24Q (PDB code 1N8F). Dashed lines indicate interactions between PEP and surrounding water molecules and protein residues.

Although E4P is not present in any of the structures, there is a sulfate ion located above PEP in the active site of the *E. coli* structure.[69] This is thought to take the place of the E4P phosphate group, and the *S. cerevisiae* structure supports this hypothesis, as a glycerol 3-phosphate molecule is found bound with its phosphate group in the same location. Mutation of the *S. cerevisiae* Arg114 residue (Arg92 in *E. coli* (phe)), which is involved in binding of the phosphate results in an inactive enzyme, as does mutation of Arg180 (Arg165 in *E. coli* (phe)), which binds the PEP phosphate.[68] Modeling of E4P in this site in its extended conformation confirms that C1 of E4P can approach within 3Å of the C3 of PEP and that the *si* face of PEP faces the *re* face of E4P, in accordance with the established stereochemistry. It also places the carbonyl of E4P in a position where it can coordinate to the metal ion, activating it for attack and supporting the mechanism in path B of Figure 1.5

1.7.2 Type Iβ_D

Recently structures of type Iβ_D DAH7P synthases from *T. maritima*[22] and *P. furiosus*[20] have been solved. The active site of these structures closely resembles that of the characterised Iα proteins, although the quaternary structure is more similar to the related Iβ_K enzymes. Both enzymes crystallise as tetramers, despite *P. furiosus* being observed as a dimer in solution.[19] A lack of intersubunit interactions for the solution-state dimer of the *P. furiosus* enzyme is thought to lead to additional flexibility in the active site and hence explain the broad substrate specificity of this enzyme, as described in Section 1.11.1. Each subunit is made up of a $(\beta/\alpha)_8$ barrel with a 2-stranded β-

hairpin near the N-terminus, which covers the end of the barrel. *T. maritima* also exhibits this β-hairpin, as well as an N-terminal ferredoxin-like domain, which has been implicated in feedback regulation by the aromatic amino acids phenylalanine **5** and tyrosine **6**.[21] *P. furiosus*, which shows no feedback inhibition by any of the aromatic amino acids, does not exhibit this additional decoration.
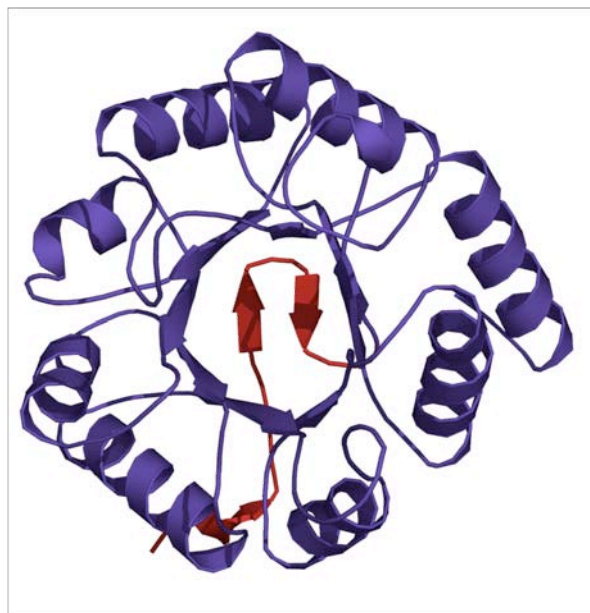
Figure 1.11: Monomer structure of *P. furiosus* DAH7P synthase (PDB code 1ZCO), showing the N-terminal -hairpin in red.

Due to *T. maritima* being a hyperthermophile and hence exhibiting little activity at room-temperature, the active site, which is located in the same place as in the Iα structures, contains both substrates PEP **2** and E4P **1**, as well as Co(II), without there being any evidence of a reaction taking place. All residues that have been shown to interact with PEP in the Iα structures are conserved in the Iβ structures except that a water molecule that was bound to the PEP carboxylate group in the Iα enzymes has been replaced by a Gln residue in the Iβ enzymes. PEP is found bound with a twist around the C1-C2 bond, consistent with the Iα structures. The binding of PEP within the active site also closely resembles that of KDO8P synthases structurally characterised.

The E4P bound in the structure is found in an orientation not correctly set up for reaction. However, rotation about the bonds allows it to be modeled into the active site in a catalytically competent orientation which agrees with that proposed for the

S. cerevisiae model.[68] The metal-binding site in the Iα, Iβ$_D$, and metallo Iβ$_K$ enzymes is identical.

1.7.3 Type Iβ$_K$ (non metallo)

The structure of the non-metallo type Iβ$_K$ protein from *E. coli* has been solved.[40,71,72] Like the type Iα proteins, it is a tetramer of (α/β)$_8$ barrels, and has a β-hairpin sealing off the active site cavity as observed in the Iβ$_D$ structures. As in *P. furiosus* DAH7P synthase, there are no additional elements, which supports the hypothesis that the additional elements observed in some DAH7P synthases are involved in feedback regulation. KDO8P synthase exhibits no such end-product inhibition.

The active sites are similar, with most of the DAH7P synthase residues conserved, except for the metal-binding Cys being replaced by an Asn. There are also some differences in the binding of PEP, which are described in Section 1.7.4. The position of bound PEP in the structure of *E. coli* KDO8P synthase solved by Asojo *et al*[40] is different to that observed by Radaev[72] and Wagner.[71] Asojo *et al* claim that the difference in the PEP binding found in their structure explains the lack of need for a divalent metal ion for catalysis in *E. coli* DAH7P synthase. Although the latter two structures do not contain PEP, they do contain sulfate ions in the proposed binding sites of the PEP and A5P phosphate groups and on this basis, the two substrates have been modeled into the active site. These two structures concur with the later published KDO8PS structures from *A. aeolicus*[42] and the DAH7P synthase structures from *E. coli*,[10,69] whereas the Asojo structure does not.

The relative positions of PEP **2** and A5P **8** when modeled into the active site are not consistent with a cyclic mechanism (Figure 1.6) as the C3-hydroxyl of A5P is not close enough to C2 of PEP to form a bond without significant conformational changes within the active site.

1.7.4 Type Iβ$_K$ (metallo)

Several structures of *A. aeolicus* KDO8P synthase with various combinations of substrates and metal ion have been solved at high resolution (1.9Å).[42] The structure is very similar to that of the non-metallo enzyme from *E. coli*. It is a tetramer with (α/β)$_8$

topology, but unlike the *E. coli* KDO8P synthase structure and $I\beta_D$ structures, it has no β-hairpin sealing off the end of the barrel. The active site is located in the same position. The metal is bound with octahedral coordination and interacts with the equivalent metal-binding residues as in the metallo DAH7P synthases, with Cys11 and His185 as axial ligands, and Glu222, Asp233 and a water molecule (which interacts with Lys46, equivalent to Lys97 in *E. coli* DAH7P synthase) occupying the equatorial positions.

PEP binding is similar to that seen in *E. coli* KDO8P synthase, which in turn shows some differences to the binding interactions observed in the DAH7P synthases. An Arg, which binds the PEP phosphate in DAH7P synthase is replaced by a Phe in *E. coli* KDO8P synthase and the interactions of the PEP carboxylate with an Arg in DAH7P synthases are replaced by a salt bridge with a Lys. Additionally, a water molecule in DAH7P synthases is replaced by a Ser in the type $I\beta_K$ enzymes. This different environment around PEP is thought to explain the lack of necessity for a metal to be present for catalysis. Due to the different interactions, PEP has a higher nucleophilic character, and hence there is less need for activation of the carbonyl for the condensation reaction to proceed.
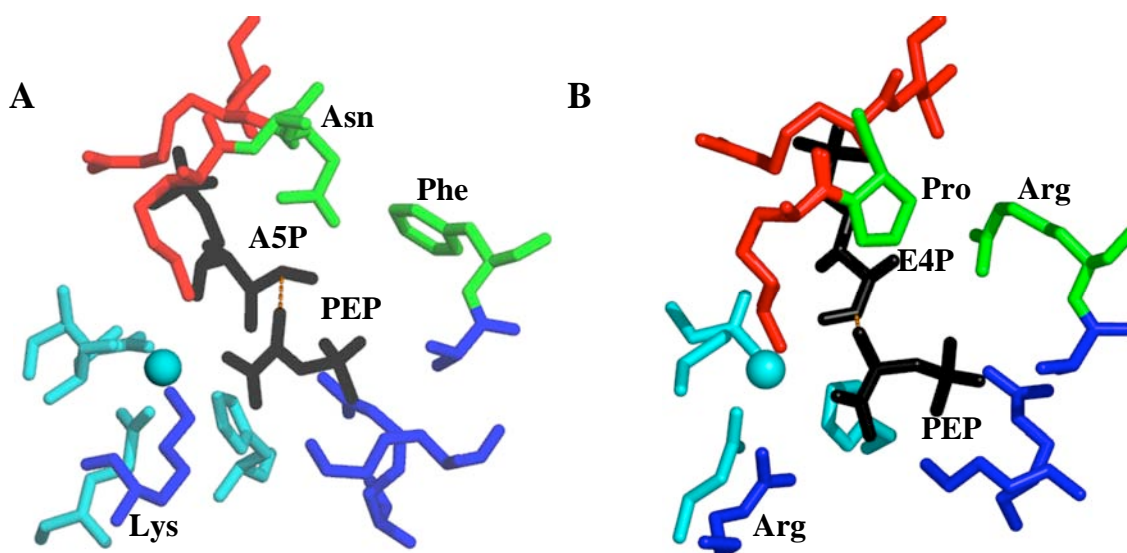
Figure 1.12: Comparison of the active sites of (A) *Aquifex aeolicus* KDO8P synthase (PDB code 1FWW) and (B). *P. furiosus* DAH7P synthase (PDB code 1ZCO). E4P has been modelled into this structure based on the observed binding of glycerol 3-phosphate to *S. cerevisiae* DAH7P synthase[68] and the proposed binding of E4P to *T. maritima* DAH7PS.[22] Metal and metal ligands are in cyan and PEP ligands are shown in blue. Substrates, PEP and A5P (or E4P), are shown in black.

As *A. aeolicus* usually operates at elevated temperatures and has no detectable activity at 4˚C, X-ray crystal structures containing both PEP and A5P were able to be determined. The position of binding of A5P agrees with the modeling of A5P in the *E. coli* KDO8P synthase structure.[71] Two conformations of A5P are observed, which may represent different binding modes during different stages of the reaction. In both conformations, there is no evidence that the carbonyl oxygen of A5P coordinates the metal as predicted for E4P in DAH7P synthase.[68]

When PEP and A5P are both present, the L7 loop, which was disordered in the *E. coli* KDO8P synthase structure[72] becomes ordered, isolating the active site from the external environment. Residues in this loop bind to the phosphate of A5P. When only one or the other substrate is bound, L7 remains disordered and the active site remains open until both substrates are bound. As PEP binds down at the bottom of the active site cavity and A5P at the top, this result is consistent with earlier kinetic results indicating an ordered sequential mechanism.[37]

A structure was also solved containing PEP **2**, along with E4P **1** in the A5P **8** binding site. E4P has previously been found to not be a substrate for *E. coli* KDO8P synthase, but to be a competitive inhibitor.[5] It is found with its phosphate group bound in the same place as the A5P phosphate. This explains the lack of reaction between PEP and E4P, as E4P being one carbon shorter than A5P is probably not close enough for bond formation to occur.

1.7.5 Type II

A type II DAH7P synthase structure from *M. tuberculosis* has been solved.[31] Despite the type II DAH7P synthases having low sequence identity (less than 10%) with the type I enzymes, the crystal structures are very similar.

The quartenary structure is a homotetramer consisting of two tight dimers. Like the Iα and Iβ enzymes, the monomer consists of a $(\beta/\alpha)_8$ barrel. Rather than the ferredoxin-like domain of the Iβ *T. maritima* enzyme, or the N-terminal extension seen in the Iα structures, the additional elements on the barrel of *M. tuberculosis* are unique. There is

a major extension at the N-terminus consisting of a β-strand and two α-helices. There is also a pair of α-helices inserted into the α2-β3 connecting loop. It has been suggested that these two additional elements each have an inhibitor binding site and are responsible for the synergistic inhibition observed with this enzyme with tryptophan and phenylalanine.[58]

The active site is in the same position as observed for the type I enzymes, and contains Mn(II), PEP **2**, and a sulfate ion, in the same position as previously established to be the E4P phosphate binding site, near the opening of the cleft, 10Å from PEP. The metal is bound at the bottom of the active site cavity in approximately trigonal bipyramidal coordination, with Cys, His, Glu and Asp as ligands. PEP has a 30-40˚ twist about the C1-C2 bond as previously observed in the type I enzymes. Most of the PEP and E4P binding ligands are found in the same positions as observed in the type I enzymes. Overall, the active site is very similar to that of the type I enzymes. The superimposition of the *M. tuberculosis* structure over that of *E. coli* DAH7P synthase aligns all of the active site residues, which is consistent with a common reaction mechanism, despite the low sequence similarity.

1.8   Structural analysis and the implications for the catalytic mechanism

As discussed in Section 1.5, a water molecule is required to add to PEP during the catalytic reaction, either before the condensation reaction between PEP and the monosaccharide, or after. The structures of DAH7P synthase and KDO8P synthase have identified two water molecules frequently present within the active site, which could fulfill this role.

One is located on the *si* side of PEP **2**, and also binds to the metal and Lys97 (*E. coli* numbering). It has been proposed that the coordination of this water to the metal ion could lower its pK_a enough for hydroxide ion formation, allowing for path A in the mechanism in Figure 1.5 above to take place.[42] Structures of *A. aeolicus* with ribose 5-phosphate (R5P) bound in place of A5P, show that this water molecule is not present.[73]

As R5P has been reported to not be a substrate for *E. coli* KDO8P synthase,[74] it is claimed that this suggests this water molecule is essential for reaction, and hence is more likely to be the water molecule that adds to PEP. However, this would result in the unfavourable *syn* addition of water and the monosaccharide to the double bond of PEP. As well as this, modeling of E4P into the active site of *S. cerevisiae* DAH7P synthase suggests that this water may be displaced by the carbonyl moiety.[68] This would allow E4P to coordinate to the metal, activating it for attack, and hence supporting the path B mechanism in Figure 1.5. Finally, this water molecule shows a high level of mobility, which is not consistent with a strong enough interaction with the metal to allow a reduction of the water's pKa to the extent where it becomes deprotonated.

Another water molecule which could potentially add to PEP is found on the *re* side of PEP, 3.0-3.1Å away from C2 of PEP, a distance less than the sums of the Van der waals radii. This would allow for more favourable *anti* addition. Although there are no residues identified that could be responsible for the deprotonation of this water to allow the path A mechanism to take place, it has been postulated by Duewel *et al*[42] that there could be a chain of hydrogen-bonds involved in transferring a proton from the water molecule on the *re* side to His83 *via* Asp81. Asp81 is conserved in all KDO8P synthases and replaced by a Glu in DAH7P synthases. Although Glu or Asp would not usually be anticipated to accept a proton readily at neutral pH, the authors claim that the microenvironment created in the active site by the closing off by L7, may alter expected pK_a values. The hydroxide ion formed could then attack C2 of PEP as in mechanism A, resulting in favourable *anti* addition.

König *et al* claim that the path B mechanism is more feasible.[68] They suggest that that the conserved active site Lys (Lys112 in *S. cerevisiae* DAH7P synthase) is ideally placed to first of all donate a proton to the forming hydroxyl group at C1 of E4P or A5P and then accept a proton leftover from the water that adds to the oxocarbenium ion. The Iβ$_D$ structures also support the path B mechanism above, as modeling studies with E4P in the *T. maritima* structure suggest electrophilic activation of E4P by the metal ion and a Lys residue.[22]

1.9   Regulation

Feedback regulation is the major mechanism for control of the shikimate pathway.[75]   *E. coli* DAH7P synthase has three isozymes, each sensitive to feedback regulation by one of the three aromatic amino acid products of the pathway, phenylalanine **5**, tyrosine **6** and tryptophan **7**.   DAH7P synthase (phe) and DAH7P synthase (tyr) account for approximately 80% and 20% respectively of the total DAH7P synthase activity on *E. coli*, with DAH7P synthase (trp) contributing less than 1%.[76]   Similarly, *S. typhimurium* and *Neurospora crassa* also possess three isozymes, whereas in *S. cerevisiae*, there are two isozymes, regulated by phenylalanine **5** and tyrosine **6**.[16]   Kinetic studies on *E. coli* DAH7P synthase (phe) have shown that phenylalanine **5** inhibits the enzyme non-competitively with respect to both E4P and PEP.[49]

Crystal structures have provided some insight into the mechanism by which this feedback regulation works.   All DAH7P synthases structurally characterised to date, except for *P. furiosus*, which is unregulated, have some kind of decoration on the basic $(\alpha/\beta)_8$ barrel.   The Iα proteins from *E. coli* and *S. cerevisiae* have an N-terminal extension and a β-sheet inserted between the $\alpha5$ and $\beta6$ strands of the barrel.   The Iβ_D *T. maritima* has an N-terminal ferredoxin-like domain.   The type II *M. tuberculosis* has a major extension at the N-terminus, and a pair of α-helices inserted into the $\alpha2$-$\beta3$ connecting loop.   These decorations contain the binding sites for the allosteric inhibitors.   Studies on the tyrosine-sensitive isozyme of *S. cerevisiae* have shown that deletion of the N-terminal extension results in an unregulated enzyme.[16]   All KDO8P synthases and the Iβ_D *P. furiosus* DAH7P synthase have only the basic barrel structure. Like *P. furiosus* DAH7P synthase, KDO8P synthases are unregulated.[26]

A structure of *E. coli* DAH7P synthase (phe) with the phenylalanine inhibitor bound has been solved.[70]   The structure shows phenylalanine bound in a cavity on the outer side of the barrel, near the N-terminus, in each monomer.   Phenylalanine is bound 18Å from PEP and 23Å from the metal ion.   The hydrophobic pocket around the aromatic ring of phenylalanine includes the residues Pro150, Gln151, Met147 and Ser180, which have previously been shown to be involved in phenylalanine binding.[10]

The binding of phenylalanine appears to initiate a transmission pathway in which an inhibitory signal is transmitted from the β6a/β6b segment, which binds phenylalanine, to the β2-α2 segment which contains both PEP and E4P binding residues. This transmission results in significant conformational changes in the enzyme, including those residues which usually bind PEP **2** and E4P **1**. There is no sulfate ion present in the E4P phosphate binding site, despite crystallization conditions being identical (except for added phenylalanine) to those that previously resulted in a sulfate ion in this site. As well as this, the bound PEP has a different conformation to that previously observed.

1.10 Inhibition

The design of mechanism-based inhibitors has been hindered by the uncertainty regarding the correct mechanism of DAH7P and KDO8P synthases. Early studies in which analogues of the proposed KDO8P cyclic intermediate **13** were synthesised and tested as inhibitors of *E. coli* KDO8P synthase suggested that the cyclic mechanism was not valid.[77] Reduction of KDO8P **9** to give a C2 epimeric mixture **15** has been found to have a K_i of 0.5mM with *E. coli* KDO8P synthase,[78] which also supports an acyclic mechanism.
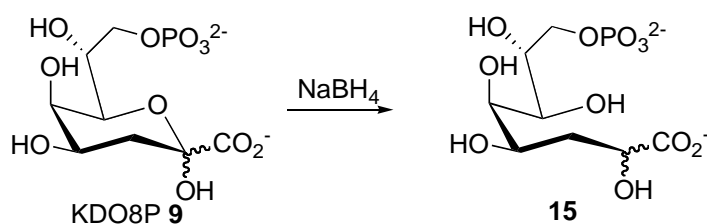
Figure 1.13: Borohydride reduction of KDO8P, giving a C2 epimeric mixture **15**

An amino-phosphonate analogue **17** of the proposed intermediate oxocarbenium ion **16** has been synthesised (Figure 1.14) incorporating features of both PEP and A5P, which bears a phosphonate instead of a phosphate group and an amine at the position corresponding to C2 of PEP. It was found to be an effective, slow-binding inhibitor of *E. coli* KDO8P synthase, with a K_i of 0.42μM[78,79] and 7.0μM for *A. aeolicus*.[73] It was also found that the free amine, present at lower pHs, binds more tightly to the enzyme

than the charged ammonium form, which supports a concerted mechanism (mechanism path A, Figure 1.5), with no formation of an oxocarbenium ion intermediate.

Structures with inhibitor **17** bound in the active site of *E. coli* and *A. aeolicus* KDO8PS synthases have been solved.[40,73] The inhibitor fits well in an area covering the combined binding sites of A5P and PEP, with the phosphate and phosphonate moieties occupying the positions of the phosphates of A5P and PEP. There are no large changes to the active site to accommodate the inhibitor.

Further work has been carried out to deduce the important features of this inhibitor.[80] The corresponding compound without the carboxylate group **18** was found to have the same K_i as the original inhibitor, indicating that the carboxylate group is not important for inhibition. Crystal structures show that it binds in the same position as the original inhibitor. However, the phosphonate group does seem to be important. The inhibitor prepared without this group **19** does not appear to bind to *A. aeolicus* or inhibit KDO8P synthase from *H. pylori* or *E. coli*. This can be explained by the fact that release of the product by the active site is initiated by the cleavage of phosphate, hence this group is important for binding.
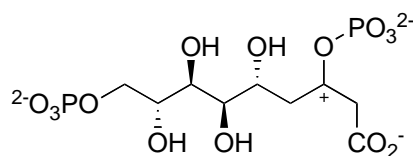
Proposed oxocarbenium intermediate for KDO8P formation **16**
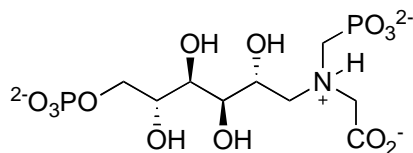
Amino phosphonate inhibitor **17**
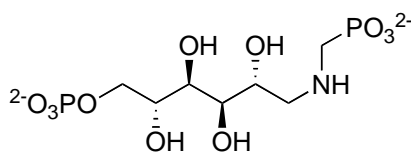
18
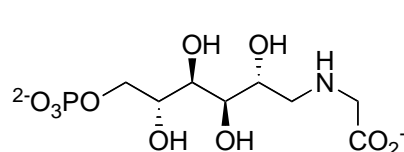
19

Figure 1.14: Inhibitors for KDO8P synthase

Two other variations of mechanism-based inhibitors have been synthesised, one which lacks the phosphate from the A5P end and retains the PEP C2-C3 double bond (**20**), and another that also has an extra hydroxyl group on C2 of the PEP end (**21**).[80] Both of these were found to inhibit *H. pylori* KDO8P synthase at µM concentrations. Structural studies also suggest that the C3 and C4 hydroxyl groups may not be essential for binding, as the electron density of the C3-hydroxyl group is not well defined, and the C4-hydroxyl group does not seem to be involved in any hydrogen bonds.
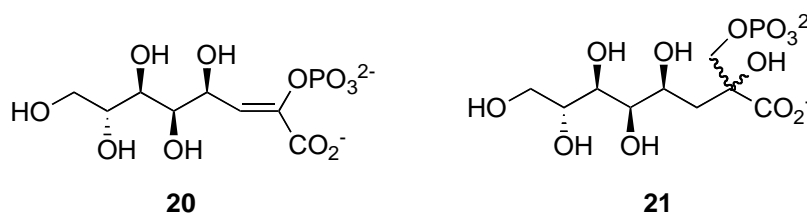
Figure 1.15 Modified KDO8P synthase inhibitors

Unfortunately, the amino-phosphonate inhibitor **17**, although effective in inhibiting KDO8P synthase *in vitro* failed to inhibit bacterial growth,[81] possibly due to hydrolysis of its C6 phosphate monoester. This resulted in the design of a new isosteric phosphonate analogue inhibitor **22**. This analogue was found to be a competitive inhibitor of KDO8P synthase, although 15-fold weaker than the original inhibitor. However, again, no inhibition of *E. coli* cells was observed, which is thought to be caused by low permeability through the bacterial cell membrane.
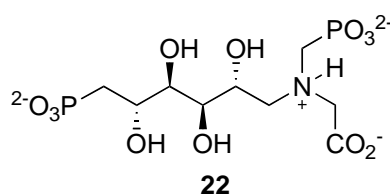
Figure 1.16: Isosteric phosphonate inhibitor for KDO8P synthase

An equivalent inhibitor for DAH7P synthase, one carbon atom shorter (**23**), has recently been synthesised and evaluated as an inhibitor of DAH7P synthase. This has been shown to be a slow-binding inhibitor of *E. coli* DAH7P synthase.[82]

23
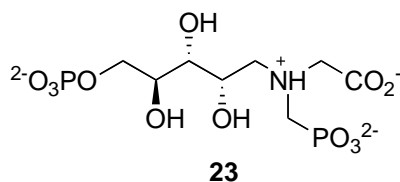
Figure 1.17: Amino phosphonate inhibitor for DAH7P synthase

1.11 Substrate specificity

1.11.1 DAH7P synthase

Substrate analogue studies with PEP have found that DAH7P synthase is reasonably intolerant of changes to PEP. Analogues of PEP with a substituent at C3 that have been tested as substrates include (*Z*)-3-chloroPEP **24,** (*Z*)-3-bromoPEP **25**, (*Z*)-and (*E*)-3-fluoroPEP **26**, and (*Z*)-3-methylPEP **27**.[83] It was found that both the (*Z*)- and (*E*)-diastereomers of 3-fluoroPEP were substrates for *E. coli* DAH7P synthase (Phe). Fluorinated DAH7P products were isolated with both stereochemistries at C3 of DAH7P, indicating that both fluorinated PEP analogues resulted in DAH7P-like products. None of the other analogues with C3 substituents were found to be substrates for DAH7P, and they were only found to be weak inhibitors. It appears from these results that the size of the substituent on C3 of PEP is a factor, as fluorine is the only substituent that is comparable in size with the corresponding hydrogen in PEP.

As well as 3-substituted PEP analogues, the methylene phosphonate **28**, difluoromethylenephoshonate **29**, and the phosphoamidate analogues **30** of PEP have been tested as substrates for *E. coli* (phe) DAH7P synthase.[83] None of these analogues were found to be substrates.

3-ChloroPEP **24**   3-BromoPEP **25**   3-FluoroPEP **26**   3-methylPEP **27**

28   **29**   **30**
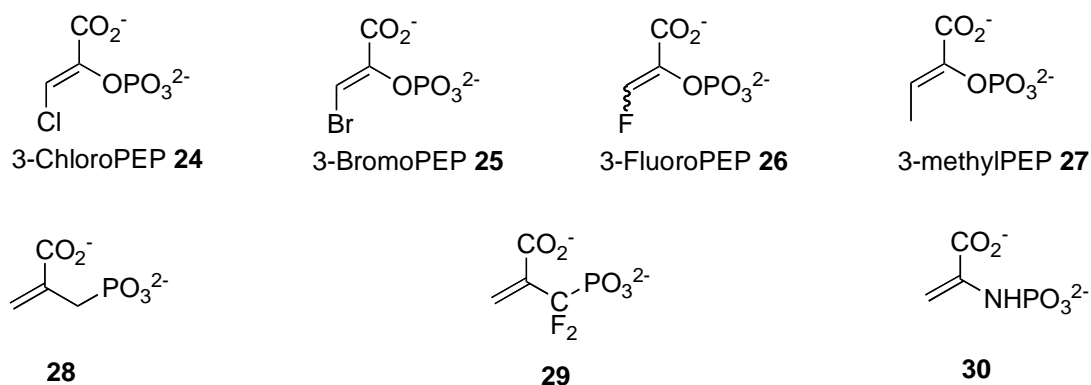
Figure 1.18: PEP analogues tested as substrates for *E. coli* (phe) DAH7P synthase

The majority of the substrate specificity studies of DAH7P synthase have focused on the phosphorylated monosaccharide. Both the phosphonate **31** and the homophosphonate **32** analogues of E4P **1** in which the oxygen of the C-O-P bond is either absent or replaced with a CH_2 group have been synthesised and tested as substrates for *E. coli* DAH7P synthase (tyr).[84] It was found that both analogues were substrates, with the homophosphonate **32** a significantly better substrate. This observation likely reflects the fact that the homophosphonate, with the CH_2 group in place of the oxygen atom allows the space between the carbonyl and phosphate groups to be very similar to E4P itself.

31   **32**
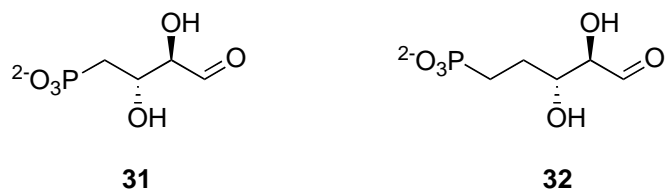
Figure 1.19: Phosphonate **31** and homophosphophonate **32** E4P analogues

Extensive substrate specificity studies carried out by Sheflyan *et al*[15] have demonstrated that the five-carbon sugars A5P **8** (with the opposite C2 stereochemistry to E4P **1**), ribose-5-phosphate **33** (R5P) (with the same C2 configuration as E4P **1**) and 2-deoxyR5P **34** (with no C2-hydroxyl) are all weak substrates for *E. coli* DAH7P synthase (phe). All three monosaccharides were shown by ^{1}H NMR to form KDO8P-like condensation products with PEP, with the *re* face of the monosaccharide being attacked by PEP. The three-carbon sugar D,L-glyceraldehyde 3-phosphate (G3P) **35** and the six-carbon sugar D-glucose-6-phosphate (G6P) **36** were not substrates. Howe *et al*[74] found that in the presence of G3P and DAH7P synthase, PEP was converted to

pyruvate. This is thought to be evidence for the first step of the catalysed reaction being attack by a water molecule on C2 of PEP. None of the non-phosphorylated five-carbon sugars, or erythrose itself are substrates for *E. coli* DAH7P synthase.[15] Crystal structures have shown that the phosphate group has many binding interactions, so it is probably very important for positioning the substrate into the active site. The Iα DAH7P synthase from *N. gonnorrhoeae* has also been shown to take A5P as a substrate.[85]

Glyceraldehyde-3-phosphate **35**

Ribose-5-phosphate **33**   2-Deoxyribose-5-phosphate **34**   Arabinose-5-phosphate **8**

Glucose-6-phosphate **36**
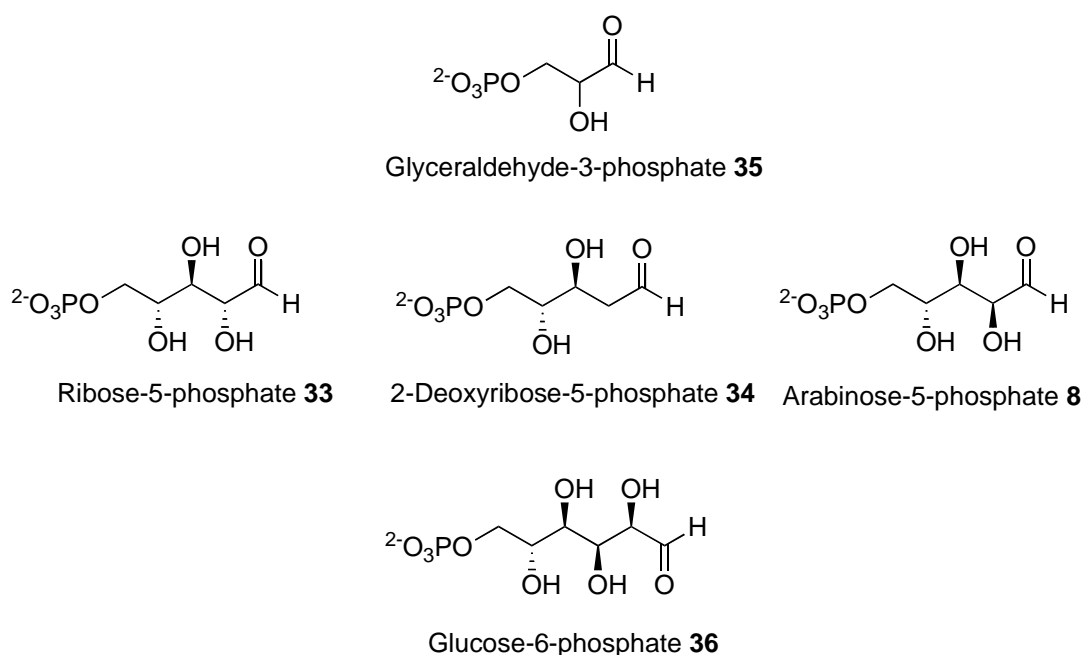
Figure 1.20: E4P analogues tested as substrates for *E. coli* DAH7P synthase (phe)

Substrate specificity studies of the type Iβ protein from *P. furiosus* have shown this enzyme to have a very broad substrate specificity. It is able to utilise the five-carbon sugars A5P **8**, R5P **33** and 2-deoxyR5P **34** with similar k_{cat} values as the natural substrate E4P **1**.[20] This is in contrast to the studies with the Iα protein, *E. coli*, which is only able to utilise five-carbon sugars with greatly decreased k_{cat} values. The other well characterised Iβ enzyme from *T. maritima* is reported to not be able to utilise either A5P **1** or R5P **33**, which means *P. furiosus* is unique in its ability to efficiently utilise a range of substrates. However, like *E. coli* DAH7P synthase, it cannot utilise the three-carbon sugar G3P **35** or the six-carbon sugar G6P **36**.

The substrate specificity of one type II DAH7P synthase has been determined.[86] *H. pylori* DAH7P synthase is able to utilise the five-carbon sugars A5P **8**, R5P **33** and 2-

deoxyR5P **34**. Similar to the observations with *P. furiosus* DAH7P synthase, *H. pylori* DAH7P synthase shows greatly elevated K_M values with these analogues, but the k_{cat} values, particularly those of R5P and 2-deoxyR5P, are comparable to those of E4P itself.

1.11.2 KDO8P synthase

PEP analogues that have been shown to be substrates for KDO8P synthase include the (*Z*) -and (*E*)-isomers of 3-deuteroPEP and 3-fluoroPEP (with a clear preference for the (*E*)-isomer, in contrast to DAH7P synthase, which takes both isomers equally). The phosphonate analogue **37**, where the carboxyl has been replaced by phosphonic acid is a weak substrate, while the phosphoamidate analogue **30** where the phosphate bridging oxygen is replaced with an NH group is not a substrate at all, suggesting that steric factors are important for recognition and catalysis by the enzyme.[87,88]
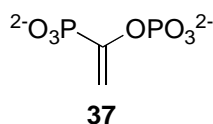
Figure 1.21: Phosphonate analogue of PEP

Howe *et al*[74] have investigated the substrate specificity of *E. coli* KDO8P synthase. They found that in the presence of E4P **1**, R5P **33** or 2-deoxyR5P **34**, KDO8P synthase catalyses the loss of PEP **2**. However, further investigation by ^{1}H NMR analysis showed that in the case of E4P and R5P, the PEP was not being converted to a KDO8P-like product, but was forming pyruvate (through water attack on C2 of PEP) and 2-phosphoglyceric acid (2-PGA), (through water attack on C3 of PEP). 2-PGA has since been shown to bind to the active site of *A. aeolicus* in a similar manner to PEP.[80] ^{1}H NMR analysis confirmed that a condensation reaction was occurring between PEP and 2-deoxyR5P to form the expected KDO8P-like product.

Other A5P analogue studies have found that 4-deoxyA5P is a good substrate for *E. coli* KDO8P synthase. Although the K_M is increased (probably due to the decrease in binding interactions), the k_{cat} is largely unchanged.[36] Despite initial claims by Subramaniam[9] that E4P was a substrate for *N. gonorrhoeae* KDO8P synthase, these claims have later been discounted.[62]

1.12 Outline of thesis

Although DAH7P and KDO8P synthase catalyse very similar reactions with similar mechanisms and have been shown to have very similar structures, the substrate specificities of these two evolutionary related enzymes are quite different. The natural substrate for DAH7P synthase is a four-carbon sugar, whereas the natural substrate for KDO8P synthase is a five-carbon sugar. The C2 configuration of the two substrates is opposite. DAH7P synthase is able to tolerate longer substrates, with the opposite C2 stereochemistry, whereas KDO8P synthase is specific to the correct C2 stereochemistry and is unable to accept longer (or shorter) substrates. Although it will not accept the opposite stereochemistry, KDO8P synthase will accept 2-deoxyR5P, where the C2-hydroxyl is missing altogether. The differences in substrate specificities of these two enzymes may indicate subtle differences in the mechanisms of these two otherwise similar enzymes, and may also help in deducing the evolutionary path that the two enzymes followed.

The objective of this project was to synthesise modified substrate analogues to probe the substrate specificities of these two related enzymes. In particular, we wished to investigate the importance and role of the C2- and C3-hydroxyl groups in E4P and A5P for binding and catalysis for both enzymes, as little is known about the important features of the phosphorylated monosaccharide. Specific goals of the project were to:

- Purify and characterise a type Iα DAH7P synthase from *N. meningitidis*.
- Chemically synthesise both the 2-deoxy and 3-deoxy E4P analogues.
- Chemically synthesise 3-deoxyA5P.
- Evaluate the activity of various deoxy substrate analogues, with a variety of DAH7P and KDO8P synthases from different classes in order to learn more about the comparative mechanisms of two similar enzymes.

CHAPTER TWO: PURIFICATION AND CHARACTERISATION OF A TYPE Iα DAH7P SYNTHASE FROM *NEISSERIA MENINGITIDIS*

2.1 Introduction

As part of these studies on the substrate specificity of DAH7P synthase and KDO8P synthase, enzymes from a variety of classes were required. In our laboratory, the type Iβ$_D$ enzyme from *P. furiosus*, the type Iβ$_K$ from *E. coli*, the type II enzyme from *M. tuberculosis* and the type Iα *E. coli* (phe) isozyme were available. Since *E. coli* DAH7P synthase (phe) is already widely characterised in the literature, it was decided to also purify and characterise another type Iα enzyme from *N. meningitidis*.

N. meningitidis is the causative agent of septicemia and meningitis. It is a major cause of disease worldwide, and can cause brain damage, hearing loss and is fatal in 4-10% of sufferers.[89-91] As aromatic amino acid synthesis is essential for the virulence of bacteria, hindering the shikimate pathway in this organism, and in particular DAH7P synthase, may result in an effective antibiotic against this disease.

There is one isozyme of *N. meningitidis* DAH7P synthase,[6] which belongs to the group of type Iα enzymes, along with the three isozymes of *E. coli* DAH7P synthase. *N. meningitidis* DAH7P synthase has 78% sequence similarity with *E. coli* (phe) DAH7P synthase, which is the most extensively characterised type Iα enzyme.[12,14,15,53,55,92] Some characterisation of *E. coli* (tyr),[11] *E. coli* (trp)[13,93] and the two isozymes of *S. cerevisiae* is also reported.[16-18] This chapter describes the purification and characterisation of *N. meningitidis* DAH7P synthase. This work was carried out in order to produce another enzyme to add to the range of enzymes already available in our laboratory to study the substrate specificity of DAH7P and KDO8P synthases with chemically synthesised substrate analogues. As well as this, it allowed for the determination of whether the features observed in the Iα DAH7P synthase enzymes can be generalised to all type Iα enzymes. This information is potentially useful for the design of narrow-spectrum antibiotics.

2.2   Cloning and expression

Prior to the beginning of this study, the cloning of *N. meningitidis* DAH7P synthase was carried out by Dr Fiona Cochrane. The gene was amplified from genomic DNA using standard PCR methodology. The PCR product was directly cloned onto the pT7-7 vector and the sequence verified after transformation of *E. coli* XL-1 competent cells. The pT7-7 *N. meningitidis* DAH7P synthase plasmid was then transformed into *E. coli* BL21(DE3) cells for expression, which were stored in glycerol at -80˚C.

At the beginning of the current study, the glycerol stock was used to inoculate 5mL culture tubes, which were allowed to grow overnight at 37˚C. These were then used to inoculate 250mL cultures in LB broth containing $100\mu gmL^{-1}$ ampicillin. Cells were grown at 37˚C for approximately three hours, until an OD_{600} of ~0.6 was reached, at which point the cells were induced with 1mM IPTG. The cells were harvested by centrifugation (5500*g* at 4˚C for 15 minutes) four hours after induction and lysed using a French Press, followed by sonication. Cell debris was then removed by centrifugation (27,000*g* at 4˚C for 20 minutes).

2.3   Purification

A two-step purification procedure based on the theoretical isoelectric point (pI) of *N. meningitidis* DAH7P synthase of 6.3, was developed using anion exchange chromatography followed by hydrophobic interaction chromatography. The results are summarised in table 2.1.

Step	Total protein (mg)	Total enzyme activity (Units)	Specific activity (Units mg^{-1})	Yield (%)	Relative purity
Crude Lysate	6.6	44	6.6	100	1.0
Source 15Q®	3.0	34	12	77	1.8
Source-Phe®	0.18	3.5	20	8	3.0

Table 2.1: Two step purification procedure of *N. meningitidis* DAH7P synthase

2.3.1 Purification by Ion Exchange Chromatography (IEC)

IEC separates proteins based on their different net charges at a given pH. The sidechains of surface amino acids can be either protonated or deprotonated depending on the pH of the environment, so that the overall charge on the protein can dictate its behaviour on an ion-exchange matrix. This type of chromatography allows purification of a given protein based on its isoelectric point (pI), the point at which the protein carries no net charge. Stationary phase matrices can carry groups that are either negatively charged (Cation Exchange Chromatography (CEC)) or positively charged (Anion Exchange Chromatography (AEC)). The charges on these matrices are balanced by counter-ions such as Cl^- in the case of anion exchange and Na^+ for cation exchange. The net charge of the protein of interest is the same as that of the counter-ions and therefore the protein competes with the counter-ions to bind to the charged matrix. If the protein carries no charge or the opposite charge of the counter-ions it will pass through the column in the mobile phase. In the case of *N. meningitidis* DAH7P synthase, the predicted pI is 6.3. At 1 pH unit above this (ie. pH 7.3) the overall charge on the protein is negative therefore AEC can be used as a purification step.

The crude lysate was diluted and applied to an anion exchange (Source 15Q®) column. Initial attempts showed that *N. meningitidis* DAH7P synthase did not bind to the column at either pH 7.3 or pH 8.0, despite being well above the pI of 6.3. Small scale adsorption tests using aliquots of the Source 15Q® resin found that the initial EDTA concentration of 10mM in the buffer was preventing binding and after reducing this to a concentration of 1mM, the protein bound to the Source 15Q® resin at pH 7.3. A fast, linear gradient of 0-1M NaCl was run and it was found that DAH7P synthase was eluted in approximately 175mM NaCl, so subsequent purifications ran a slow (70mL) gradient up to 0.4M NaCl, followed by a fast (20mL) gradient to 1M NaCl after all the DAH7P synthase had been eluted. Activity assays were carried out in order to determine which fractions contained DAH7P synthase activity.
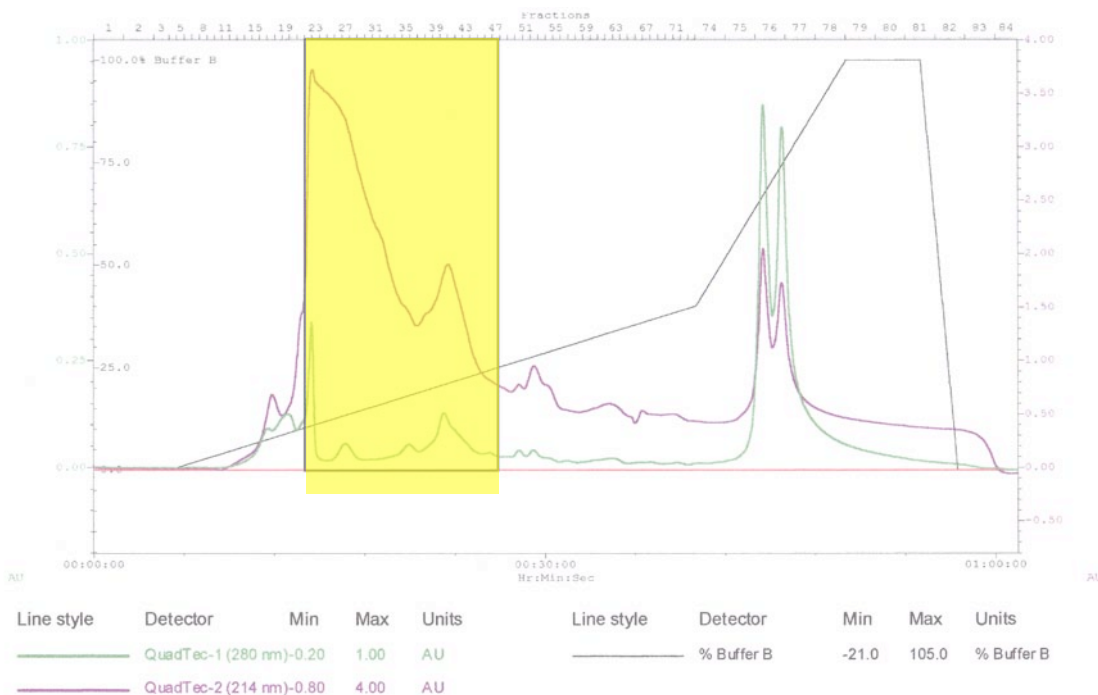
Figure 2.1 Chromatogram of AEC using Source 15Q® column. Fractions containing *N. meningitidis* DAH7P synthase activity are shaded yellow.

2.3.2 Purification by Hydrophobic Interaction Chromatography (HIC)

Following anion exchange chromatography, an SDS-PAGE gel showed a number of contaminants and hence, hydrophobic interaction chromatography was used to further purify the active fractions. Proteins differ from one another in their hydrophobic properties and this difference forms the basis of HIC separation. HIC separates proteins depending on the strength of their interaction with hydrophobic ligands attached to an uncharged base matrix. Samples bind at high ionic strength and are eluted as the ionic strength is lowered. Therefore, this separation technique was investigated to separate *N. meningitidis* DAH7P synthase from the contaminating proteins.

Fractions from the AEC containing active protein were pooled and ammonium sulfate added to a final concentration of 1M. The sample was then applied to a hydrophobic interaction (Source-Phe®) column at pH 7.3 and a linear gradient run from 1M-0M ammonium sulfate. *N. meningitidis* DAH7P synthase eluted at almost zero concentration ammonium sulfate, so subsequent runs involved a fast gradient (40mL) from 1M to 0.15M and a slower gradient (20mL) to 0M ammonium sulfate. This step of the purification procedure resulted in a large loss of protein (see table 2.1). This may be due to the protein binding very tightly to the column and hence not eluting efficiently, or losses may have occurred during subsequent concentration and desalting. Future HIC purification may require the use of a lower pH buffer in order to make the

protein bind less tightly to the resin. Fractions containing pure protein, as shown by SDS-PAGE, were pooled and desalted by repeated dilution and concentration using a 10kDa MWCO concentrator (Vivascience). The concentrated protein was then snap frozen in 100μL aliquots in liquid nitrogen and stored at -80°C. No appreciable loss of activity was observed after several months of storage at this temperature.
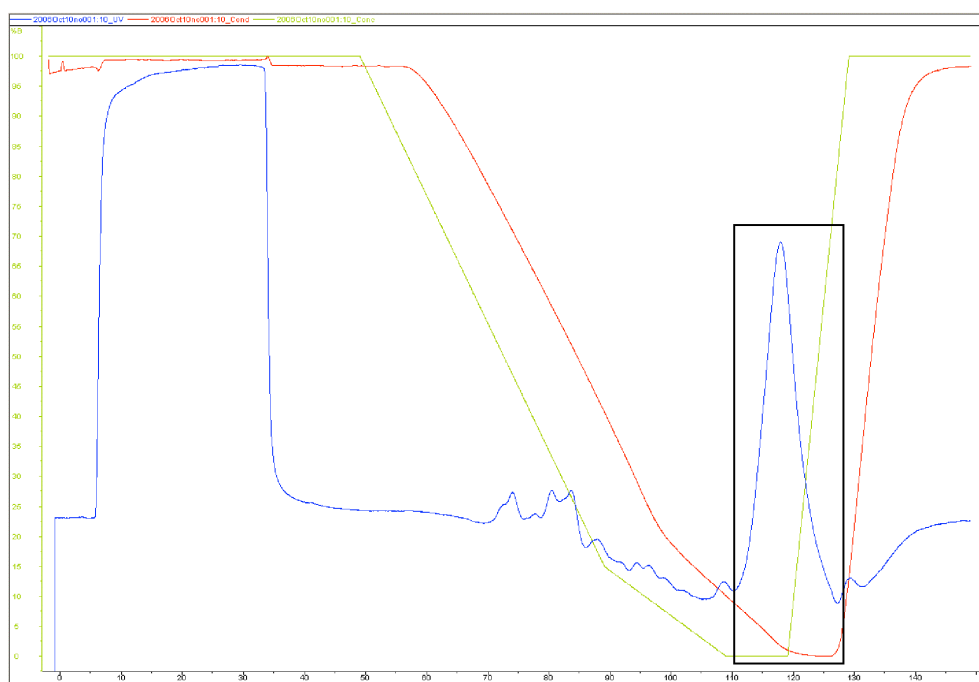
Figure 2.2: Chromatogram trace of HIC, using Source Phe® column. Fractions containing *N. meningitidis* DAH7P synthase activity are boxed.

The SDS-PAGE gel of the protein after these two steps showed relatively pure protein, but with two faint, higher molecular weight bands (Figure 2.3) at approximately 80kDa and 120kDa. It was originally thought that these may be due to the presence of a dimer and trimer of *N. meningitidis* DAH7P synthase, however longer boiling times of the sample before loading on the gel made no difference to the relative amounts of each band. If the minor bands were due to the presence of dimer or trimer, boiling of the sample in the presence of SDS would be expected to break these interactions.
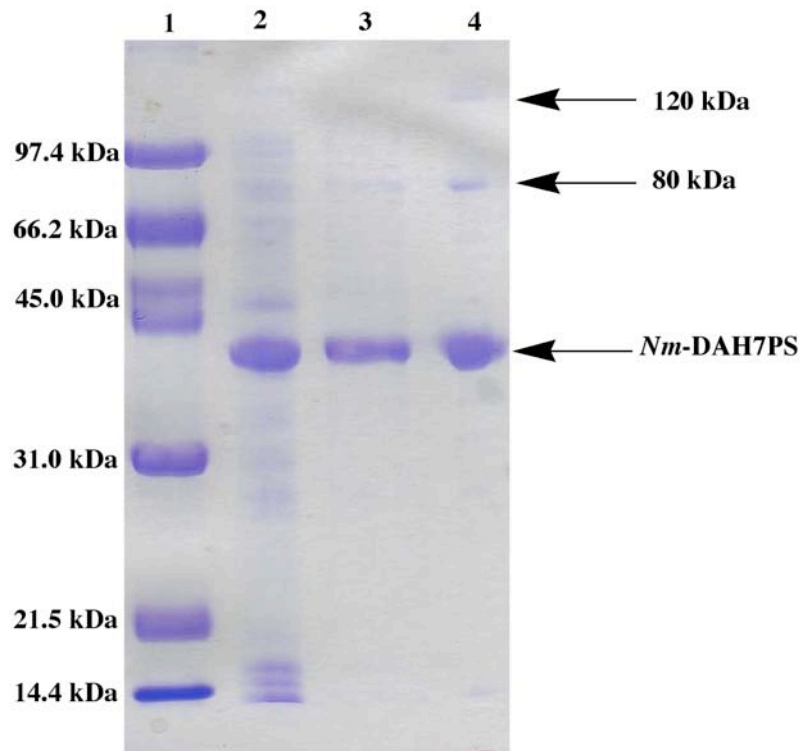
Figure 2.3: SDS-PAGE analysis of the stages of purification of *N. meningitidis* DAH7P synthase. SDS-PAGE analysis was performed on a 12% polyacrylamide gel and visualised with Coomassie Brilliant Blue R 250. Lane 1. MW markers; Lane 2. Crude lysate; Lane 3. After Source 15Q[®] column; Lane 4. After Source-Phe[®] column, desalting and concentration.

In order to attempt to separate *N. meningitidis* DAH7P synthase from these contaminating proteins, size-exclusion chromatography was performed using a Superdex S200 column. However, the SDS-PAGE gel (Figure 2.4) showed little difference in purity between the two samples, so this step was omitted in subsequent purifications.
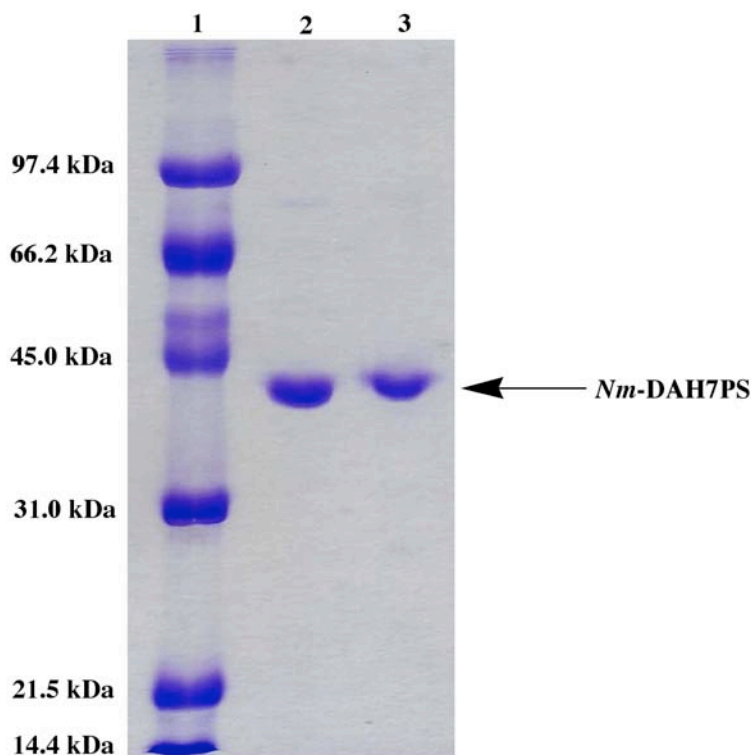
Figure 2.4: SDS-PAGE analysis of *N. meningitidis* DAH7P synthase, before and after size-exclusion chromatography. SDS-PAGE analysis was performed on a 12% polyacrylamide gel and visualised with Coomassie Brilliant Blue R 250. Lane 1. MW markers; Lane 2. Before Superdex S200 column; Lane 3. After Superdex S200 column.

2.3.3 Summary

The purification procedure described above resulted in a three-fold purification of *N. meningitidis* DAH7P synthase over two steps, although the hydrophobic interaction chromatography resulted in large losses as described above. Despite these losses, HIC chromatography was considered worthwhile for the increase in specific activity, which almost doubled after HIC. The reported purification of the phenylalanine-sensitive isozyme from *S. cerevisiae* by Paravicini *et al*[17] utilised HIC with only very small losses, suggesting that varying the HIC conditions in this purification may result in a better yield for this step. Purifications of other Iα DAH7P synthases have reported yields of 11-52%, with many of them requiring several more steps than utilised in the purification of *N. meningitidis* DAH7P synthase.[11-13,17,55,92] Several of these have also reported the presence of contaminating proteins which have been difficult to separate from DAH7P synthase, as found in this purification.[12,13,55]

2.4   Molecular mass determination

Although the Iα DAH7P synthases are very similar in size and sequence, variations in quaternary structure of the enzyme from different organisms and among different isozymes from the same organism have been reported. *E. coli* (phe) DAH7P synthase is a tetramer in solution,[12,55] whereas the tyrosine and tryptophan-sensitive isozymes are both dimers.[11,13] *S. cerevisiae* (tyr) has also been shown to be a dimer in solution, with some evidence of the presence of monomer and higher molecular weight aggregates,[18] while the phenylalanine inhibited isozyme has been shown to exist as a monomer in solution.[17]

Iβ DAH7P synthases have been reported to be tetrameric in the case of *T. maritima*[21] and *B. subtilis*,[52] while the *P. furiosus* enzyme is dimeric.[19]

 To determine the molecular mass of *N. meningitidis* DAH7P synthase in solution, protein standards of known molecular mass were also applied to the Superdex S200 column. A plot of the log of molecular mass against V_e/V_o (where V_e is elution volume and V_o is the void volume, determined using Blue Dextran with a molecular weight of 2000kDa) allows the molecular mass of *N. meningitidis* DAH7P synthase to be determined by interpolation. The molecular mass of *N. meningitidis* DAH7P synthase was determined to be 146kDa. As the theoretical molecular weight of *N. meningitidis* DAH7P synthase is 38.66kDa, this suggests that it exists as a tetramer in solution.

Protein	Molecular Mass (kDa)	V_e/V_o
Cytochrome C	12.4	2.17
Carbonic anhydrase	29	1.86
N. meningitidis DAH7P synthase	146 (by interpolation)	1.44
Alcohol dehydrogenase	150	1.44
β-Amylase	200	1.36
Blue dextran	2000	1.00

Table 2.2: Protein standard molecular masses and elution times from the Superdex S200 column
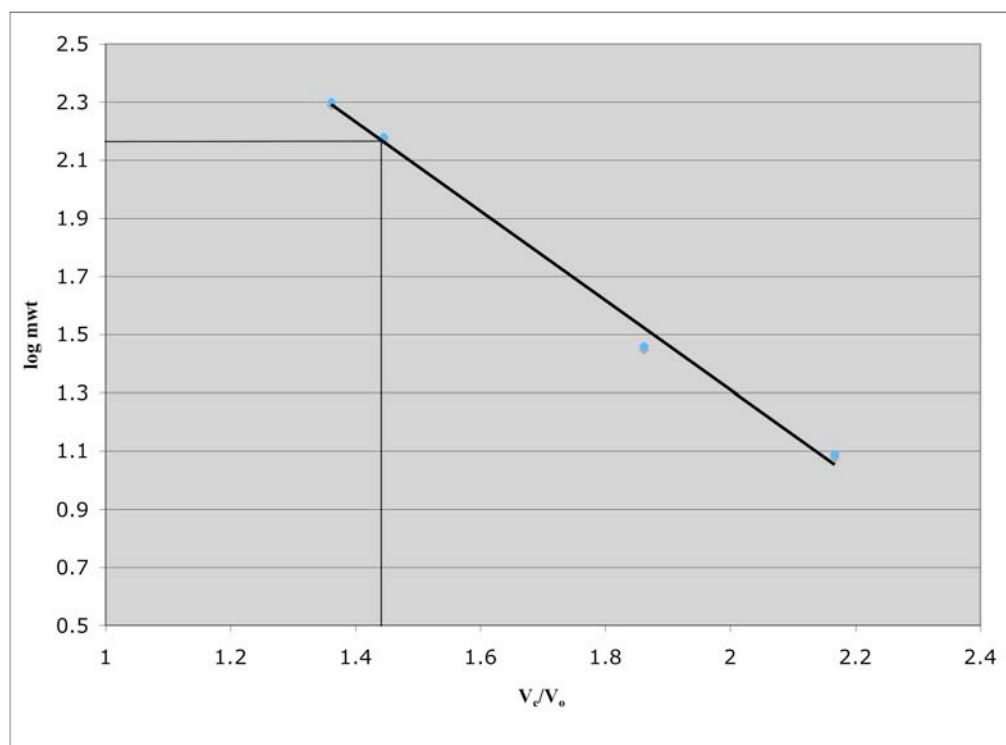
Figure 2.5: Standard curve of log molecular mass versus elution time for *N. meningitidis* DAH7P synthase. The molecular mass of *N. meningitidis* DAH7P synthase was determined by plotting the logarithm of the known mass of protein standards against V_e/V_o, where V_e is elution time and V_o is the void volume at which blue dextran is eluted.

Comparison of *N. meningitidis* DAH7P synthase with *E. coli* DAH7P synthase (phe) on a native gel (Figure 2.6) showed that they traveled a similar distance, also suggesting that they are both similar sized tetramers in solution.
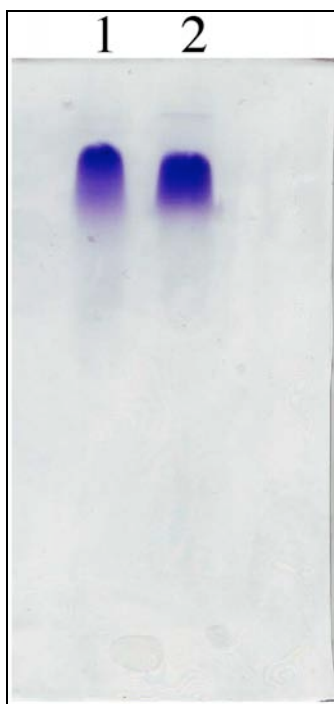
Figure 2.6: Native PAGE analysis of *N. meningitidis* DAH7P synthase (lane 1) and *E. coli* DAH7P synthase (lane 2). Gels were performed on a 12% polyacrylamide gel and protein bands visualised with Coomassie Brilliant Blue R 250.

2.5 Initial kinetic parameters

The steady-state kinetic constants for freshly purified *N. meningitidis* DAH7P synthase were determined by monitoring the loss of PEP as observed at 232nm. Initial velocity values were determined as a function of the concentration of one substrate at various fixed concentrations of the other substrate. The apparent K_M values for E4P and PEP respectively were 25±2μM and 17±1 μM, and the k_{cat} value was calculated as 9.4±0.1s^{-1}. These results are broadly in line with those reported for the other characterised type Iα enzymes from *E. coli* and *S. cerevisiae* (table 2.3). It has been suggested that the reasonably broad range of K_M values for E4P may be a consequence of the dimeric nature of E4P in solution, leading to the concentration of E4P available to the enzyme being overestimated.[17]

Organism	E4P K_M (µM)	PEP K_M (µM)	k_{cat} (s^{-1})	Reference
E. coli (phe)	39	2.0	26	[94,95]
E. coli (tyr)	96.5	5.8	121	[11]
S. cerevisiae (phe)	130	18	10	[17]
N. meningitidis	25	17	9.4	This study

Table 2.3: Kinetic parameters of characterised type Iα DAH7P synthases
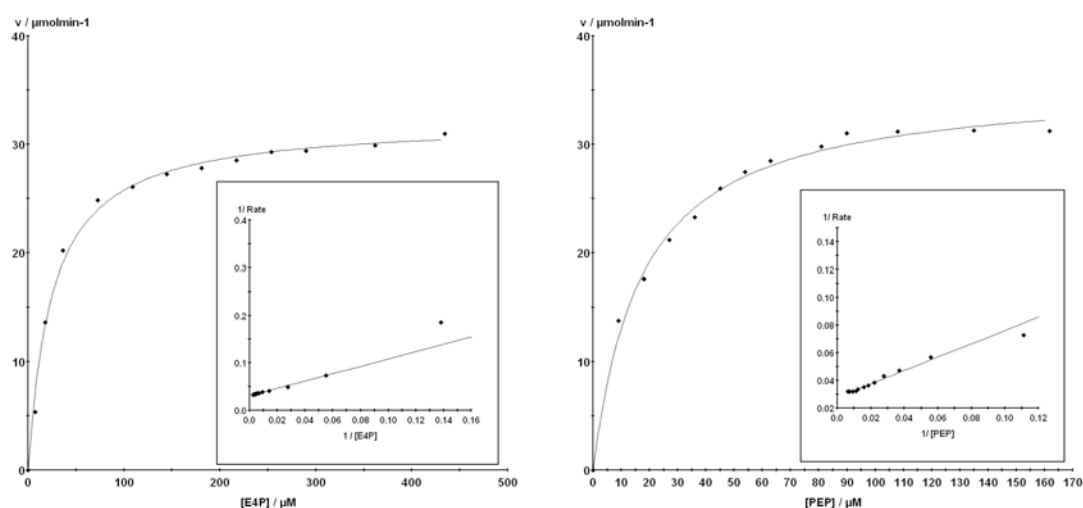
Figure 2.7: Michaelis-Menten and Lineweaver-Burk plots for determination of K_M values for E4P and PEP with *N. meningitidis* DAH7P synthase. The reaction mixtures for the determination of the K_M of E4P consisted of PEP (270µM), MnSO$_4$ (100µM) and E4P (7-430µM), in 50mM BTP pH 6.8 buffer. The reaction mixtures for the determination of PEP consisted of E4P (360µM), MnSO$_4$ (100µM) and PEP (9-180µM) in 50mM BTP pH 6.8 buffer. The reaction was initiated by the addition of *N. meningitidis* DAH7P synthase (2µL, 1mg/mL) and carried out at 25˚C. K_M and k_{cat} values were determined by fitting the data to the Michaelis-Menten equation using Enzfitter (Biosoft).

2.6 Metal dependency

As with all DAH7P synthases characterised to date, *N. meningitidis* DAH7P synthase activity is dependent on the presence of a divalent metal ion. To carry out these studies, all solutions except for the divalent metals were pre-treated with Chelex resin before

use. In addition, 10µM EDTA was added to all solutions in order to remove any residual metal ions from solution, and the enzyme preparation contained 10mM EDTA. Enzyme activity was not detectable in the absence of divalent metals but could be restored by the addition of various divalent metals. Assays were carried out by pre-incubating the enzyme with metal and PEP prior to initiation with E4P. The order of reactivation was $Mn^{2+} > Cd^{2+} > Co^{2+} > Zn^{2+} > Fe^{2+} > Cu^{2+} > Mg^{2+}$, (table 2.4) with Ni^{2+}, Ca^{2+}, Ba^{2+} and Sr^{2+} not activating the enzyme at all. These results are similar to those reported for other type Iα enzymes. The order of reactivation by divalent metals for *E. coli* DAH7P synthase (phe) is $Mn^{2+} > Cd^{2+} > Fe^{2+} > Co^{2+} > Ni^{2+}$, Cu^{2+}, $Zn^{2+} >> Ca^{2+}$, with the other two isozymes showing a very similar hierarchy of activity with the different metal ions.[14] The phenylalanine-sensitive isozyme from *S. cerevisiae* is also reported to have a similar reactivation order, with Mn^{2+} and Co^{2+} being the most activating and Fe^{2+} and Zn^{2+} being relatively poor.[17] The tyrosine-sensitive isozyme from *S. cerevisiae* in contrast, is reported to show the greatest activity with Cu^{2+} and Fe^{2+}, with Cd^{2+} and Ni^{2+} able to activate the enzyme to 70% of the activity of the untreated enzyme. Mn^{2+} and Mg^{2+} are both poor activators, with the activity only reaching approximately 20% of that of the untreated enzyme.

Divalent metal	% Activity
Mn	100
Cd	69
Co	34
Zn	24
Fe	15
Cu	8
Mg	1
Ni	0
Ca	0
Ba	0
Sr	0

Table 2.4: Activation of purified *N. meningitidis* DAHPS by various divalent metal ions. All solutions contained 10µM EDTA and (except the metal solutions) were chelexed before use. The assay mixture contained PEP (180µM), divalent metal salt (100µM) and *N. meningitidis* DAH7P synthase (5µL, 1.7mg/mL) in BTP buffer, pH 6.8. Assays were carried out at 25˚C. The reaction was initiated by the addition of E4P (150µM).

2.7 Temperature studies

To determine the optimum operating temperature for *N. meningitidis* DAH7P synthase, assays were carried out at a range of temperatures and the initial rates measured. Due to the reported instability of E4P at higher temperatures,[19] E4P was added to the assay after six minutes of pre-incubation at the required temperature. The reaction was initiated by the addition of enzyme one minute later. *N. meningitidis* DAH7P synthase is active over a range of temperatures up to 50˚C, with the greatest activity around 40˚C (Figure 2.8). However, in order to compare the activity of *N. meningitidis* DAH7P synthase with other characterised Iα DAH7P synthases, which used the assay conditions originally described by Schoner and Herrmann,[11] all assays with *N. meningitidis* DAH7P synthase were carried out at 25˚C.
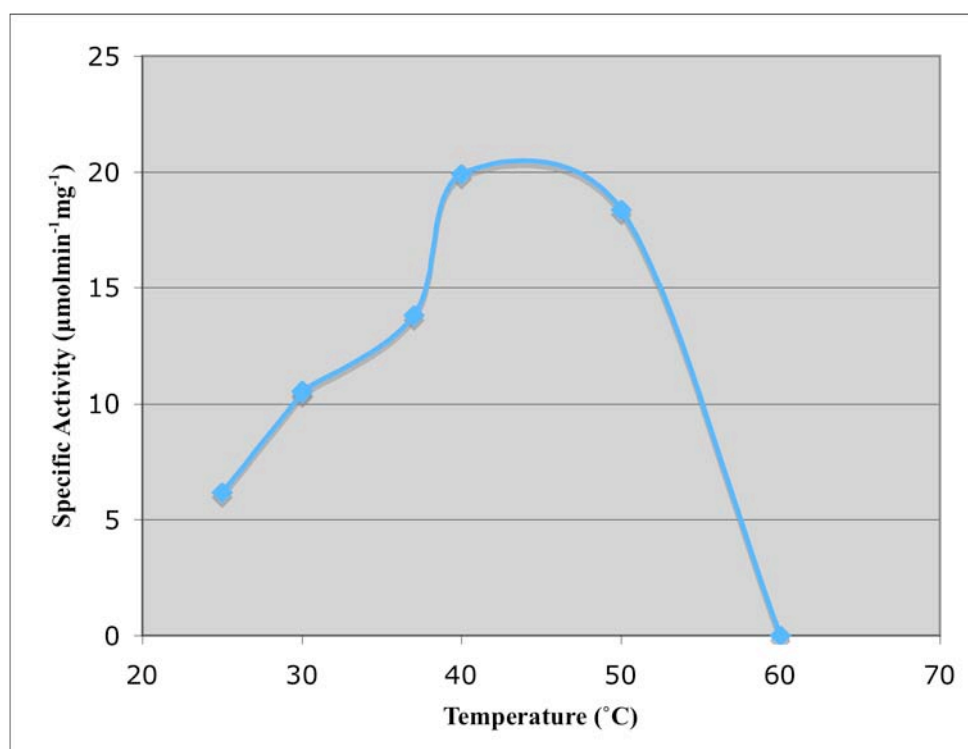
Figure 2.8: Effect of temperature on specific activity of purified *N. meningitidis* DAH7P synthase. Reaction mixtures contained PEP (200µM) and $MnSO_4$ (100µM) in 50mM BTP buffer at pH 6.8 at the required temperature. Assays were initiated by the addition of purified *N. meningitidis* DAH7P synthase (5µL, 1.7mg/mL) 1 minute after the addition of E4P (200µM).

2.8 Feedback inhibition studies

While DAH7P synthases from *S. cerevisiae* and *E. coli* have two and three isozymes respectively, each being regulated by a single amino acid, *N. meningitidis* DAH7P synthase has only a single isozyme. It has been proposed by Hartmann *et al*[16] that feedback sensitivity can be predicted by sequence. All tyrosine-regulated DAH7P synthases have a conserved Gly within the regulatory region, at the bottom of the inhibitor-binding cavity. This Gly is replaced by a conserved Ser in all phenylalanine-regulated DAH7P synthases. Hence, the feedback regulation of an enzyme may be predicted from the primary sequence.

```
Sce_Phe    GLSFPIGFKNGTDGGLQVAIDAMRAAAHEHYFLSVTKPGVTAIVGTEG
Sce_Tyr    GLSFPVGFKNGTDGTLNVAVDACQAAAHSHHFMGVTKHGVAAITTTKG
Eco_Tyr    GLSMPVGFKNGTDGSLATAINAMRAAAQPHRFVGINQAGQVALLQTQG
Eco_Phe    GLSCPVGFKNGTDGTIKVAIDAINAAGAPHCFLSVTKWGHSAIVNTSG
Nme        GLSCPVGFKNGTDGNLKIAIDAIGAASHSHHFLSVTKAGHSAIVHTGG
```

Figure 2.9: Partial sequence alignment of *S. cerevisiae* (phe), *S. cerevisiae* (tyr), *E. coli* (tyr), *E. coli* (phe) and *N. meningitidis* DAH7P synthases. The residue predicating feedback inhibition by phenylalanine or tyrosine is highlighted.

The sequence of *N. meningitidis* DAH7P synthase reveals a Ser in this position, indicating that its activity should be inhibited by phenylalanine. The feedback sensitivity of *N. meningitidis* DAH7P synthase was investigated using standard assay conditions (as described in chapter six). The three aromatic amino acids phenylalanine, tyrosine and tryptophan were added to the assay in order to determine whether there was any loss of activity. As predicted, the presence of tyrosine or tryptophan had no effect on the activity, whereas phenylalanine inhibited activity of *N. meningitidis* DAH7P synthase (table 2.5).

Inhibitor	% activity
None	100
Tryptophan	102
Tyrosine	103
Phenylalanine	44

Table 2.5: The effect of aromatic amino acids on the activity of *N. meningitidis* DAH7P synthase. Standard assays were performed which consisted of E4P (125μM), PEP (100μM), MnSO$_4$ (100μM) and the amino acid (200μM) in 50mM BTP buffer, pH 6.8. Assays were carried out at 25˚C. Reactions were initiated by the addition of *N. meningitidis* DAH7P synthase (2μL, 1.1mg/mL). Assays were performed in duplicate and averaged.

2.9   Substrate specificity

Substrate specificity studies with the Iα *E. coli* DAH7P synthase (phe) have reported little tolerance for changes to the phosphorylated monosaccharide substrate.[15] The five-carbon sugars arabinose 5-phosphate **8**, ribose 5-phosphate **33** (with the C2-hydroxyl in the opposite configuration to A5P) and 2-deoxy-D-ribose 5-phosphate **34** (with the C2-hydroxyl group removed) were all very poor substrates and the three-carbon sugar glyceraldehyde 3-phosphate (G3P) **35** and the six-carbon glucose-6-phosphate (G6P) **36** were not substrates.

Like *E. coli* DAH7P synthase (phe), *N. meningitidis* DAH7P synthase has very narrow substrate specificity. It is unable to utilise either G3P or G6P. There was some evidence that the five-carbon sugars A5P **8**, R5P **33** and 2-deoxyR5P **34** were substrates, albeit very poor ones. An enzyme-dependent loss of PEP was observed in the presence of all of these five-carbon sugars. However, the rates were extremely slow compared to those observed with E4P, making quantification difficult. Proof that the loss of PEP was due to a condensation reaction between the two substrates, resulting in a DAH7P-like product would require large amounts of the monosaccharide and enzyme, which were not available at the time. 3-DeoxyA5P, the synthesis of which is described in chapter four, was not a substrate.

In the case of the four-carbon sugars, both (*S*)-2-deoxyE4P **38** and (*R*)-3-deoxyE4P **39** were able to be utilised as substrates, as was also found for various other enzymes (details of the synthesis of these compounds and kinetic data is presented in chapters three and four).
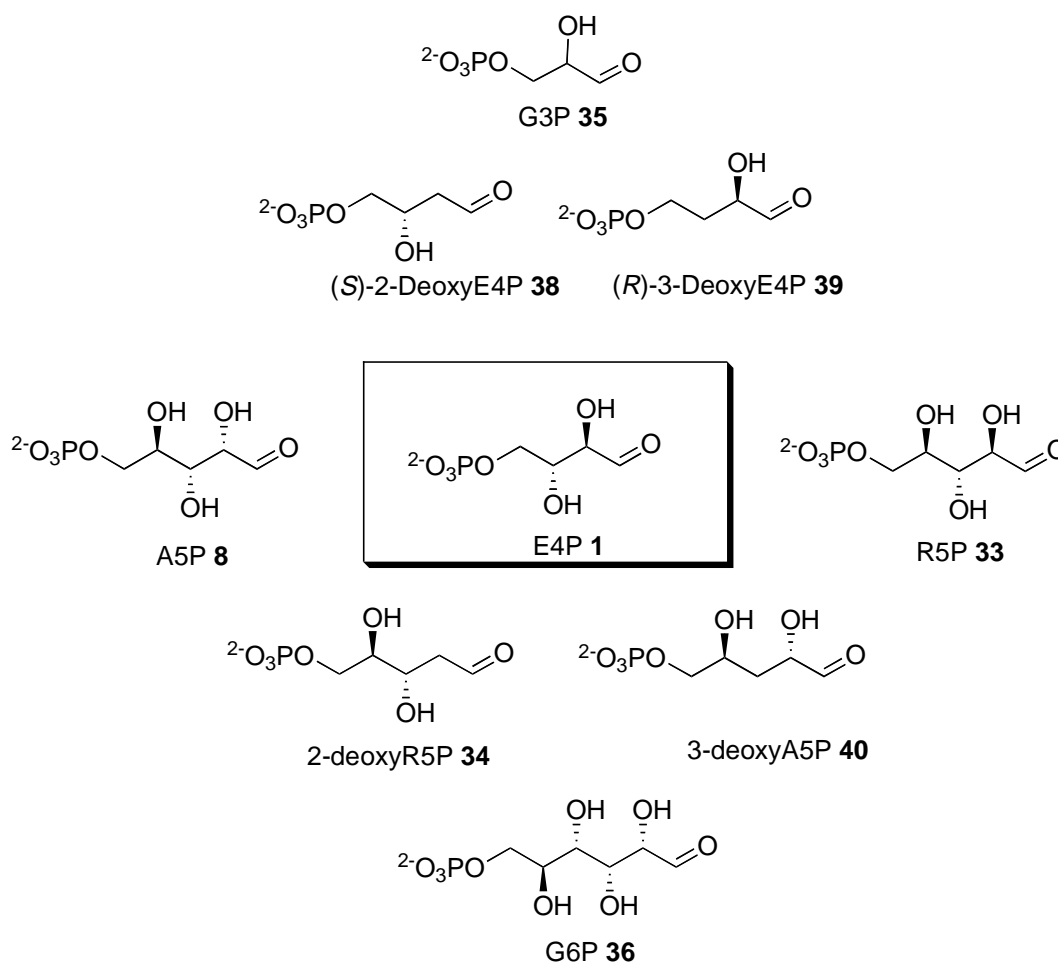
Figure 2.10: Phosphorylated monosaccharides tested as substrates for *N. meningitidis* DAH7P synthase.

2.10 Summary

N. meningitidis DAH7P synthase has been successfully purified and characterised. In the case of metal dependency, kinetic parameters for the substrates E4P and PEP, and the narrow substrate specificity, *N. meningitidis* DAH7P synthase is very similar to the already characterised Iα proteins from *E. coli* and *S. cerevisiae*. The enzyme has been confirmed to be feedback-inhibited by phenylalanine. Molecular weight studies and the native gel suggest that *N. meningitidis* DAH7P exists as a tetramer in solution, as does

the phenylalanine-sensitive *E. coli* isozyme. The substrate specificity of *N. meningitidis* DAH7P synthase with chemically synthesised analogues is described in chapters three and four.

CHAPTER THREE: EVALUATION OF 2-DEOXYE4P AND A5P ANALOGUES WITH DAH7P AND KDO8P SYNTHASES

3.1 Introduction

In our laboratory, we have chosen to target E4P analogues to investigate the importance of the hydroxyl groups on carbons two and three for binding and catalysis in the active site of DAH7P synthase. DideoxyE4P has been synthesised by Dr Rachel Williamson and was not a substrate for *E. coli* DAH7P synthase.[96] Other target analogues include D- and L-threose-4-phosphate (T4P) in which the stereochemistry is reversed at C2 and C3 respectively, which is the focus of Meekyung Ahn's PhD studies,[95] and 2-deoxy and 3-deoxyE4P. A synthesis of racemic 2-deoxyE4P, following a procedure similar to that outlined by André *et al*[97] and Guerard *et al*[98] detailed below in Figure 3.1, was carried out in our laboratory by Dr Rachel Williamson.[99]
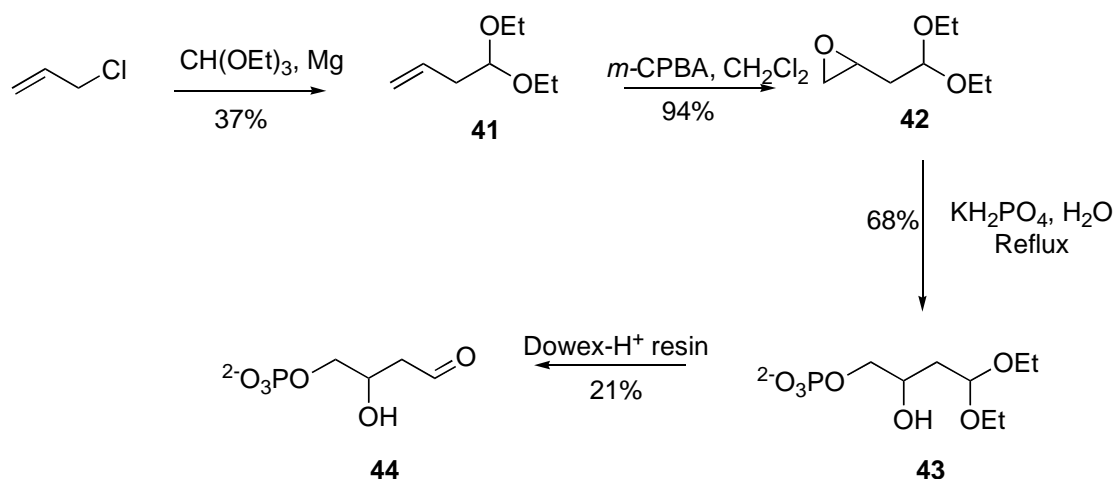
Figure 3.1: Synthesis of racemic 2-deoxyE4P

In this synthesis, allyl chloride was converted into 4,4-diethoxy-1-butene **41** by formation of the Grignard derivative and treatment with triethyl orthoformate.[100] Epoxidation to give **42** was then carried out using *meta*-chloroperbenzoic acid in dichloromethane. The phosphate was introduced by opening of the epoxide with inorganic phosphate under reflux conditions, giving **43**, and the aldehyde moiety was revealed using Dowex-H^{+} cation exchange resin. Treatment with Dowex-Na^{+} followed

by lyophilisation of the aqueous solution provided racemic 2-deoxyE4P **44** as its disodium salt.

3.2   Use of γ-butyrolactones to synthesise E4P analogues

Preliminary results from our laboratory indicated that racemic 2-deoxyE4P was a substrate for DAH7P synthase from *E. coli* and *P. furiosus*. However, enantiopure (*S*)-2-deoxyE4P would enable more detailed investigation of the role of the C2-hydroxyl group, and a route to 3-deoxyE4P was still required. It was proposed to use γ-butyrolactones to try to synthesise these two targets by analogous routes. These seemed suitable starting materials because they already have the correct number of carbon atoms and functionalities on the appropriate carbon atoms. Figure 3.2 shows the potential products from various γ-butyrolactones using our developed synthetic route in which the lactone carbon becomes the aldehyde in the final product.
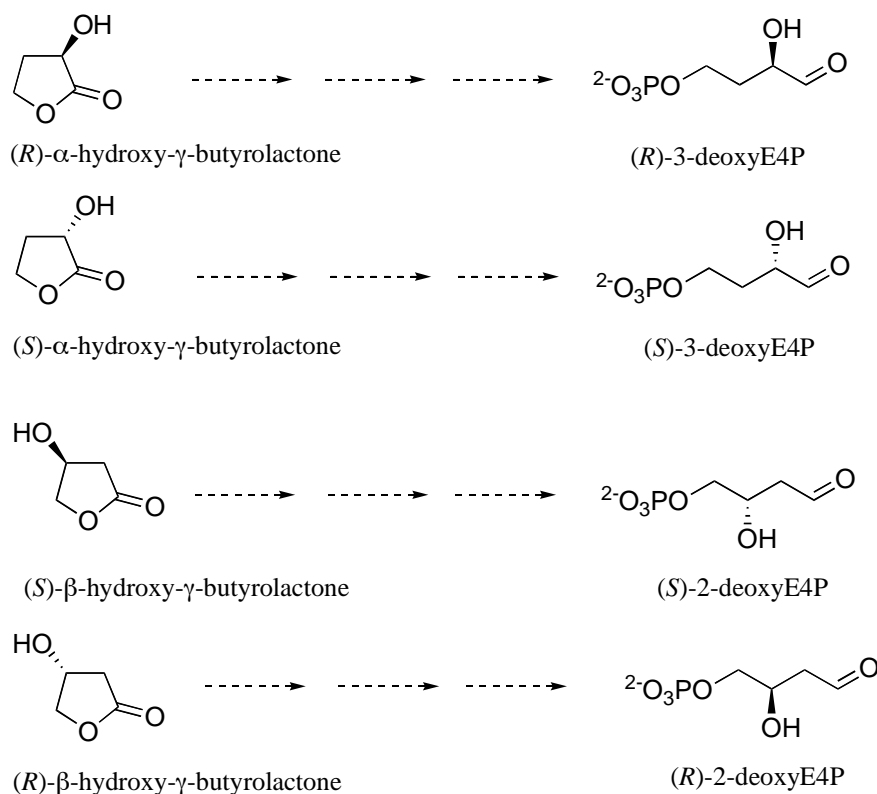
Figure 3.2: Potential E4P analogue products from γ-butyrolactones

Currently α-hydroxy-γ-butyrolactone is commercially available in both (*S*)- and (*R*)-forms, as well as the racemic form. β-Hydroxy-γ-butyrolactone is only available in the enantiomerically pure (*S*)-form, but fortunately this has the same C3 configuration as E4P itself. This thesis describes the development of a synthetic strategy that is generally applicable to any of these lactones to synthesise a variety of deoxy E4P analogues, although we have found that the position of the hydroxyl group has a significant influence on the reactivity of the lactone. This chapter outlines the synthesis of 2-deoxyE4P from β-hydroxy-γ-butyrolactone and its evaluation as a substrate for DAH7P synthases from various organisms. In addition, in order to compare the relative importance of the C2-hydroxyl group for substrate recognition and catalytic activity in DAH7P and KDO8P synthases, commercially available 2-deoxyR5P (which is equivalent to 2-deoxyA5P) was evaluated as a substrate for KDO8P synthase.

3.3 Synthesis of (*S*)-2-deoxyE4P from β-hydroxy-γ-butyrolactone

The successful synthesis of (*S*)-2-deoxyE4P from β-hydroxy-γ-butyrolactone is outlined below in Figure 3.3.
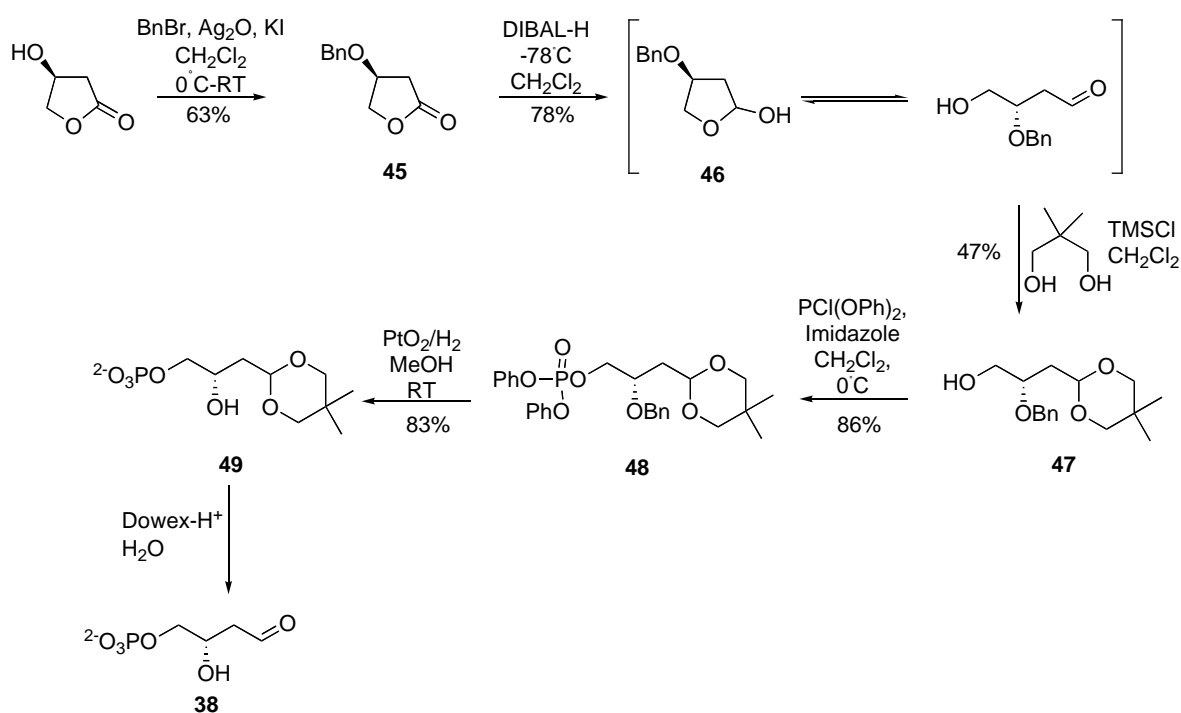
Figure 3.3: Synthesis of (*S*)-2-deoxyE4P

The synthesis starts with protection of the β-hydroxyl group as the benzyl ether to give **45**.[101-103] Reduction to aldehyde **46**, followed by protection with 2,2-dimethylpropane-1,3-diol then exposes the 1° alcohol for phosphorylation.[104] Deprotection of the benzyl and phenyl groups then gives the protected aldehyde **49**, which is treated with acid to give 2-deoxyE4P.[98]

Benzylation was carried out using silver oxide, benzyl bromide and a catalytic amount of potassium iodide in dichloromethane.[101] This step was difficult, and the yields achieved were often inconsistent. The highest yield achieved was 63%. The same reaction in DMF was less promising, with no product detected. The freshness of the Ag_2O appeared to be an important factor. Yields were significantly lower when using Ag_2O that had been prepared more then a fortnight before. The highest yield of 63% was achieved using silver oxide that had been prepared the day before the benzylation reaction and this yield was reproducible, providing the silver oxide was freshly prepared.

Benzylation with benzyltrichloroacetimidate (BTCA), as reported by Larsen *et al*,[105] was also attempted, but no product was detected using this method.

Other methods attempted for protection of the 2° alcohol included silylation with both TBDMSCl and TBDPSCl and imidazole in DMF. However, these reactions were lower yielding than the benzylation reaction already investigated and it was decided to persist with protection through the benzyl group. Although this reaction was relatively low yielding at 65%, it was convenient in that it provided a UV marker for TLC analysis, and was known to be stable throughout the rest of the synthesis, based on the work carried out by Dr Matthias Rost on the synthesis of 3-deoxyE4P (described in chapter four). In his work, Dr Rost also found that the TBDMS group was cleaved during the protection of the aldehyde, whereas the benzyl group was more stable.

The next step involved reduction of the lactone to the lactol **46**.[106] The lactol is in equilibrium with the open-chain form, allowing access to both the aldehyde functionality and the 1° alcohol. The reduction was carried out using diisobutylaluminium hydride in dichloromethane with the temperature reduced to –78°C to prevent over reduction to the alcohol. The DIBAL was added in small amounts until

no starting material was visible by TLC. Analysis by ^{1}H NMR spectroscopy established that reduction had occurred, producing a mixture of diastereomers of the lactol **46**, evidenced by the pair of acetal protons at 5.85 and 5.41 ppm. The two diastereomers were present in a 1:0.8 ratio. A small peak in the ^{13}C NMR spectrum at 207.6ppm, as well as a triplet peak in the ^{1}H NMR spectrum at 9.78ppm, suggested there was also a small amount of the open-chain aldehyde form present.

Investigations already carried out on the analogous synthesis of 3-deoxyE4P from α-hydroxy-γ-butyrolactone (described in chapter four) have shown that the most successful method of opening the lactol ring and protecting the aldehyde is to use 2,2-dimethylpropane-1,3-diol to form the six-membered dioxalane ring. This was carried out on the lactol product **46** using the method described by Chan *et al*[104] in which chlorotrimethylsilane is used both as an acid catalyst and a dehydrating reagent, eliminating the need for molecular sieves or other dehydrating agents in the reaction mixture. There are several potential products from this reaction. The desired product, in which the lactol ring has opened, releasing the primary alcohol is shown in Figure 3.4 below.

47
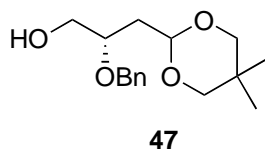
Figure 3.4: The six membered ring product **47** with the primary alcohol exposed

There are two conformations of this product, but one is much more favourable then the other because it allows the bulky side chain to be in an equatorial position rather than an axial position of the six-membered ring. Two diastereomers, shown in Figure 3.5 can also be formed in which the five-membered lactol ring is still intact.
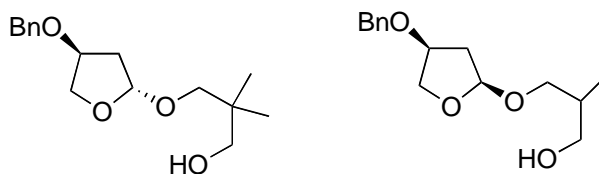
Figure 3.5: The two possible five-membered ring products **50** from the protection of the aldehyde of **46**

A mixture of the six-membered dioxalane ring **47** and the five-membered ring **50** was formed during this reaction, consistent with reports from Barton *et al.* TLC analysis of the reaction mixture showed two major products, which were able to be separated by flash column chromatography. It was difficult to distinguish the two compounds by ^{1}H NMR spectroscopic analysis, as the spectra of **47** and **50** were very similar. Hence, in order to determine that the lower R_F spot was the desired **47**, the product was phosphorylated, which allowed for identification of the product, through the coupling patterns in the ^{13}C NMR spectrum. For the six-membered ring **47**, ^{13}C-^{31}P coupling to two methylene carbons (carbons three and four) was expected, whereas for the five-membered ring **50**, ^{13}C-^{31}P coupling would be expected to be evident in a quaternary carbon as well as a methylene carbon. This analysis showed that the lower R_F spot was the desired six membered ring product **47**.

Unfortunately, **47** was the minor product (16%), with **50** being the major product (24%). Barton *et al*[107] reportedly converted the five-membered ring to the six-membered ring to give an overall yield of 80%. However, we found the reverse to be true. A mixed fraction of **47** and **50** was stirred in dichloromethane with a catalytic amount of *p*-toluenesulfonic acid at room temperature. After three hours, TLC analysis showed all of **47** ring had been converted to **50**.

Through varying the reaction time and temperature, it was found that the highest yields of the desired product **47** were achieved when the reaction was carried out at 0˚C with a shorter reaction time. If the reaction mixture was allowed to heat up, or was not worked up as soon as TLC analysis confirmed the consumption of all of the starting material, a higher yield of **50** was formed. Through careful monitoring of the reaction mixture, a yield of 47% of the desired product **47** was achieved.

With the aldehyde protected, the 1˚ alcohol was exposed for phosphorylation. This was carried out with diphenylchlorophosphate and imidazole in dichloromethane, which conveniently allowed the phosphate group to be added in an already protected form. A yield of 83% of the phosphate **48** was achieved after stirring overnight at room temperature.

The phenyl and benzyl protecting groups on the phosphate group and 2° alcohol of **48** were removed by hydrogenation at atmospheric pressure in the presence of a platinum catalyst. The reaction was followed by TLC and quenched once there were no UV-active baseline spots by TLC analysis representing aromatic groups still present on the polar product. ^{1}H NMR spectroscopic analysis of the product **49** confirmed the absence of all aromatic groups.

In order to deprotect the aldehyde, a solution of **49** was treated with Dowex-H^{+} cation exchange resin and heated to 40°C overnight.[98] The presence of (*S*)-2-DeoxyE4P **38** was confirmed using the DAH7P synthase reaction, with a modified form of the continuous assay of Schoner and Herrmann (see Section 3.4).[11] With PEP in excess, the yield of (*S*)-2-deoxyE4P was calculated to be 50% over the two deprotection steps. This yield is comparable to similar deprotections carried out within our laboratory.[95] A longer heating time made no difference to the yield. For use in enzyme assays, the pH of the solution was increased to 6.8 with NaOH, giving the sodium salt. All enzyme tests with this compound have been carried out using this solution directly, as lyophilisation was found to destroy this compound. When stored at -18°C, the solutions were found to be stable over a period of at least three months, with little loss in concentration over this time; however, wherever possible, for kinetic analyses the solutions were used within days of carrying out the deprotection and were stored at 4°C.

This synthetic route has been successful in producing (*S*)-2-deoxyE4P. Although the overall yield is not particularly high (<10%), it is a useful route to this compound, as only very small amounts of the compound are required for the subsequent enzyme assays. It also allowed for a comparison with the already available racemic 2-deoxyE4P. Analysis of the behaviour of both racemic and (*S*)-2-deoxyE4P with enzymes from various sources is described in the next section.

3.4 Enzymatic reaction of (*S*)-2-deoxyE4P with DAH7P synthase

In our laboratory we are interested in the comparison of different classes of DAH7P synthases. The use of DAH7P synthases from various sources allows us to compare

and contrast the interaction of our synthesised substrates with different classes of DAH7P synthases.

The DAH7P synthase used for most of our enzyme tests on 2-deoxyE4P is the phenylalanine-sensitive isozyme of *E. coli* DAH7P synthase. This is a type Iα enzyme and is the DAH7P synthase utilised in most of the DAH7P synthase studies reported in the literature, as described in chapter one. The type Iα DAH7P synthase from *N. meningitidis*, the purification of which is described in chapter two, was also used. The Iβ$_D$ DAH7P synthase from *P. furiosus* has also been used in our studies with 2-deoxyE4P. *P. furiosus* is a hyperthermophile found in deep sea hydrothermal vents and usually grows at 100˚C.[19] DAH7P synthase from *P. furiosus* is closely related to the KDO8P synthases, which belong to Iβ$_K$ subfamily, and this DAH7P synthase has a broad substrate specificity, as described in chapter one. It is particularly tolerant to changes at C2 of E4P, as will be described in this section. Due to the elevated temperatures that *P. furiosus* usually lives at, the assays carried out in our laboratory with this DAH7P synthase are performed at 60˚C, which still allows for reasonable stability of the substrates.[19] Finally, kinetic analysis has also been carried out with the type II DAH7P synthase from *M. tuberculosis*.

We have used a modified form of the continuous assay of Schoner and Herrmann[11] to determine the use of 2-deoxyE4P (and other substrates) by the enzymes described above. All assays were performed in 50mM BTP buffer at a pH and temperature detailed in chapter six. All buffers and solutions were Chelex-treated to remove any residual metal ions. The enzymatic reaction was initiated by the addition of purified enzyme, except in the case of *P. furiosus* DAH7P synthase, where it was initiated by the addition of 2-deoxyE4P. The progress of the reaction was monitored by the loss of PEP as observed at 232nm. During the reaction, PEP loses its double bond between C2 and C3, causing the disappearance of absorption at 232nm when the enzyme catalyses the formation of DAH7P from E4P, or in the case of 2-deoxyE4P being used as a substrate, 5-deoxyDAH7P. Therefore, with PEP in excess, the loss of absorbance will be proportional to the phosphorylated monosaccharide concentration.

When 2-deoxyE4P was incubated with any of the DAH7P synthase enzymes described above, a time-dependent loss of absorbance at 232nm was observed. The magnitude of

the absorbance decrease and the rate were proportional to the amount of 2-deoxyE4P added and to the enzyme concentration respectively. This was consistent with 2-deoxyE4P being a substrate for all the enzymes tested.

3.5 Analysis of the product formed by the reaction of 2-deoxyE4P and PEP

Initial enzyme assays showed that (*S*)-2-deoxyE4P was a substrate for all the DAH7P synthases described above. However, while this assay system is a convenient method for following the reaction between DAH7P synthase and 2-deoxyE4P, it does not provide proof that a DAH7P-like product is being formed. PEP loss could come about by other mechanisms, including the formation of pyruvate through the attack of water on the phosphorus or at C2 of PEP. In order to confirm that the PEP loss was due to the consumption of 2-deoxyE4P and to the generation of a DAH7P-like product, a large-scale reaction was followed and the product purified and analysed by ^{1}H NMR spectroscopy.

The reaction was carried out with racemic 2-deoxyE4P on a relatively large scale (4mg of 2-deoxyE4P) in water instead of buffer, with the pH adjusted to 6.8 using 1M NaOH. The reaction was then followed in the usual manner, but using a 0.1cm path length cuvette and observing the loss of PEP at 260nm instead of the usual 232nm, due to the relatively large concentrations of PEP causing the absorbance to be beyond the linear range at 232nm. The reaction progress was monitored overnight until the loss of PEP, which was present in excess, had stopped, indicating that all the 2-deoxyE4P had been consumed. After removal of the enzyme using an ultrafiltration device with a molecular weight cutoff of 10kDa, the mixture was purified by anion-exchange chromatography using Source-15Q® resin and a linear gradient of 0-1M NaHCO$_3$. Fractions containing product were pooled, lyophilised and re-dissolved in D$_2$O for ^{1}H NMR spectroscopic analysis, which confirmed the formation of 5-deoxyDAH7P **51**.
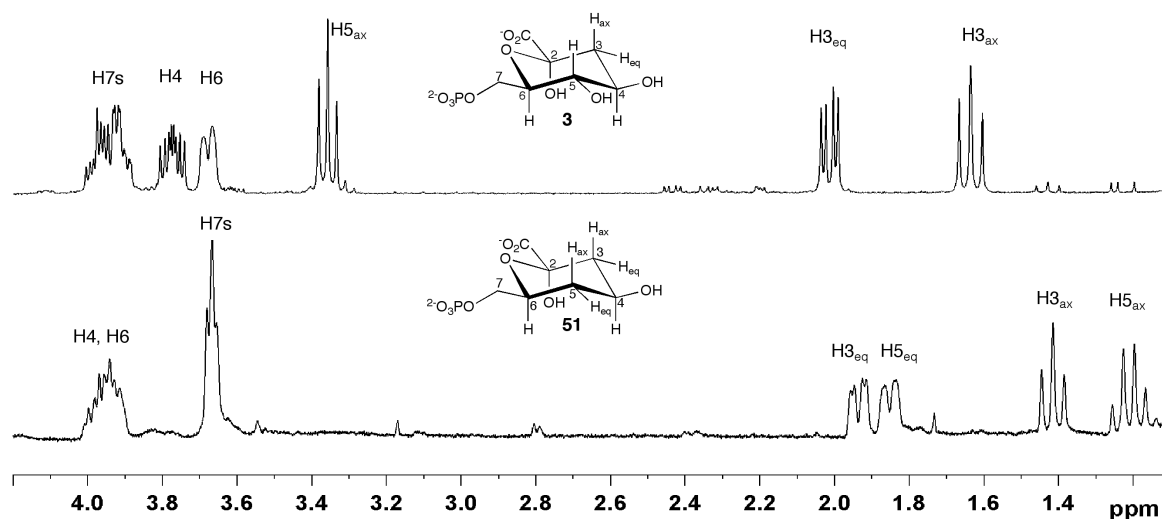
Figure 3.6: ^{1}H NMR spectra of DAH7P **3** (top) and 5-deoxyDAHP **51** (400MHz) formed from the reaction of 2-deoxyE4P with PEP and *E. coli* DAH7P synthase.

Figure 3.6 shows the ^{1}H specta of 5-deoxyDAH7P **51**, as well as DAH7P **3** prepared in the same manner using E4P for comparison. The spectra have been assigned with the aid of 2-dimensional NMR spectral analyses. In the DAH7P spectrum, the downfield H7, H4 and H6 peaks are all multiplets due to their extensive coupling. H5$_{ax}$ appears as a triplet, due to the two large axial-axial couplings with the protons on H4 and H6. H3$_{eq}$ is a doublet of doublets, with a large geminal coupling and smaller coupling to the axial H4. H3$_{ax}$ again appears as a triplet, due to the large geminal coupling and axial-axial coupling to H4.

The spectrum of 5-deoxyDAH7P is very similar, but with an additional proton on C5 in the equatorial position where the hydroxyl group resides in DAH7P. The C5 axial proton peak has shifted upfield due to the absence of a hydroxyl group on that carbon, and a new peak corresponding to the equatorial proton on this carbon is evident at 1.85ppm. The spectrum also confirmed that there was only one product formed in the reaction, with evidence of only one stereochemistry at C6 of the product, which corresponds to C2 in the racemic mixture of 2-deoxyE4P. This suggested that although both the enantiomers of 2-deoxyE4P were present in the reaction, only one was a substrate for DAH7P synthase.

There are two possible ways that the product with this stereochemistry can be formed during reaction with a racemic mixture of 2-deoxyE4P, shown in Figure 3.7. The first (and most likely scenario) is by PEP attacking the *re* face of (*S*)-2-deoxyE4P.

Alternatively the enantiomer of this compound **52** (but with the same ^{1}H NMR spectrum) of 5-deoxyDAHP **51** would be formed if the *si* face of (*R*)-2-deoxyE4P were attacked by PEP. Assuming that the facial selectivity in this reaction is the same as is seen in the reaction between E4P and PEP (*ie*. the *si* face of PEP attacks the *re* face of E4P), and knowing that the (*S*)-enantiomer of 2-deoxyE4P is a substrate for DAH7P synthase from *E. coli* (with better kinetic parameters than the racemic mixture), it seems reasonable to assume that the product is formed by attack on the *re* face of (*S*)-2-deoxyE4P, rather than the less likely scenario of PEP attacking the *si* face of the (*R*)-enantiomer. This could be confirmed by carrying out a large scale reaction with the enantiopure (*S*)-2-deoxyE4P; however, due to having only small amounts of the enantiopure compound, which is formed from a relatively expensive starting material, this has not been carried out. Investigation of the synthesis of 3-deoxyE4P has revealed an alternative synthesis of 2-deoxyE4P (described in the chapter four) that may be used to synthesise larger amounts of (*S*)-2-deoxyE4P for this work.
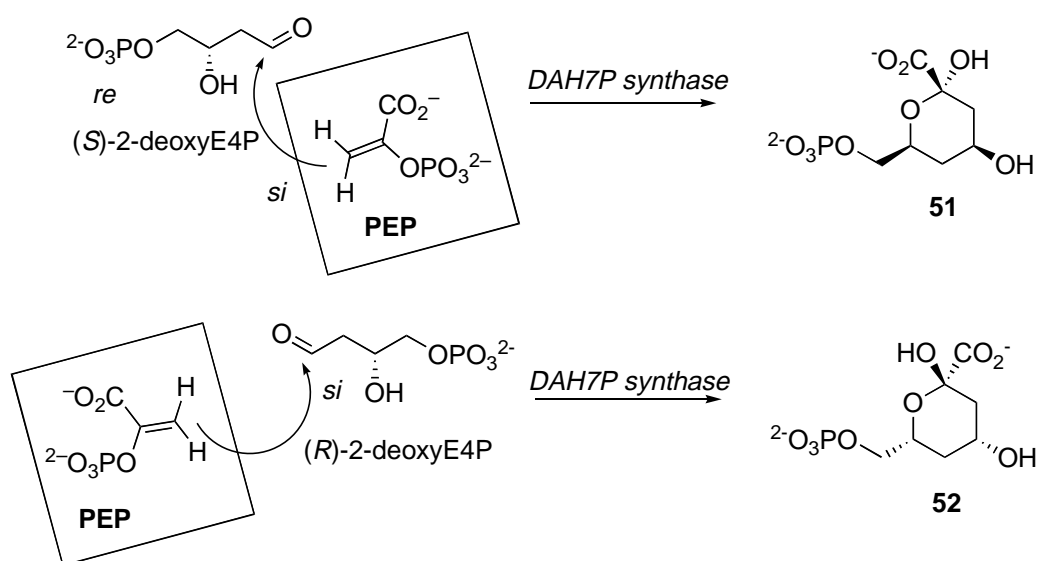
Figure 3.7: The two ways that 5-deoxyDAH7P could be formed by reaction of 2-deoxyE4P with PEP.

3.6 Determination of the utilisation of racemic 2-deoxyE4P by *E. coli* DAH7P synthase

The concentration of 2-deoxyE4P utilised during the enzyme-catalysed reaction can be easily determined by measuring the loss of absorbance due to PEP consumption at 232nm during the reaction. When PEP is present in excess, this loss of absorbance is proportional to the amount of phosphorylated monosaccharide consumed. However, as it appeared that only half of the 2-deoxyE4P in solution (ie. the (*S*)-enantiomer) was being utilised during the enzyme-catalysed reaction, it would be advantageous to determine the exact concentration of 2-deoxyE4P in the original solution in order to confirm that only half of the 2-deoxyE4P in solution is consumed. Weight per volume concentrations are not accurate enough for this work because such small masses are involved, i.e. 1-2mg of material is being weighed out. As well as this, we cannot be sure of the molecular weight as we do not know the ionisation state of the compound and therefore the number of counter-ions present.

In order to work out the proportion of racemic compound that is consumed during the catalysis reaction, ^{31}P NMR was used. Two solutions were made up containing ~4mg each of glucose-6-phosphate (G6P) and racemic 2-deoxyE4P. Equal volumes of each solution were then combined and a ^{31}P proton-decoupled NMR spectrum collected in order to determine the relative concentrations of the two solutions by integrating the peaks due to G6P and 2-deoxyE4P. Although ^{31}P NMR spectra are not routinely integrated, there are examples in the literature where this has been carried out successfully.[108-110]

To determine the exact concentration of the G6P solution, it was diluted to ~1mM and assayed at 340nm with G6P dehydrogenase to follow the oxidation of G6P *via* the increase of absorbance due to the formation of NADPH ($\varepsilon = 6.2 \times 10^3$ M^{-1} cm^{-1} at 25°C).[111]

The exact 2-deoxyE4P concentration could then be determined, as the relative concentrations of G6P and 2-deoxyE4P were known from the ^{31}P NMR spectrum.
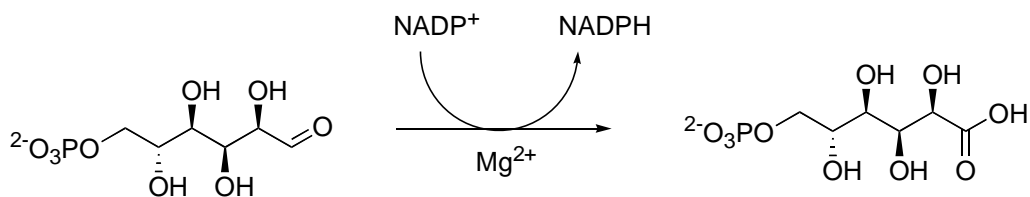
Figure 3.8: Glucose-6-phosphate dehydrogenase assay

The concentration of 2-deoxyE4P used by the enzyme was calculated using standard assay procedures. PEP was present in excess, so the loss of absorbance at 232nm is proportional to the 2-deoxyE4P concentration. A blank assay, which contains no E4P analogue, was used to determine how much absorbance increase was seen after the addition of enzyme. This was used to correct the assays as some loss of absorbance may have occurred after addition of the enzyme before the cuvette could be placed back into the holder.

The results from this experiment showed that 50% of the racemic 2-deoxyE4P was used by the enzyme. This result, along with the ^{1}H NMR data showing formation of only one product is consistent with only the (*S*)-enantiomer of 2-deoxyE4P being a substrate for *E. coli* DAH7P synthase (phe).

The results from this analysis allowed for comparison with other enzymes to determine whether one or both enantiomers were substrates. For *N. meningitidis* DAH7P synthase, assays were carried out with racemic 2-deoxyE4P in conjunction with assays with *E. coli* DAH7P synthase under identical conditions, with PEP present in excess. The assays showed the same consumption of PEP for both enzymes. As it had been determined that only the (*S*)-enantiomer of 2-deoxyE4P was a substrate for *E. coli* DAH7P synthase, the same case could be inferred for *N. meningitidis* DAH7P synthase. The same experiment also showed that only one enantiomer was a substrate for *M. tuberculosis* DAH7P synthase.

Interestingly, unlike what has been seen with the Iα and type II enzymes, when racemic 2-deoxyE4P was tested with the type Iβ *P. furiosus* DAH7P synthase by Dr Linley Schofield there was evidence that both the (*S*)- and (*R*)- enantiomers were substrates.[112] The assays with racemic 2-deoxyE4P (Figure 3.9) show a kink in the curve, presumably at the point where the second enantiomer starts to be utilised by the enzyme, and hence

we see a different rate in the reaction. The loss of absorbance in each phase of the curve is approximately equal. This change in rate is not observed with (*S*)-2-deoxyE4P. The slow upwards drift seen towards the end of the assays occurs in all assays with this enzyme, and is thought to be attributable to the high temperatures that the assays are carried out at (60°C).
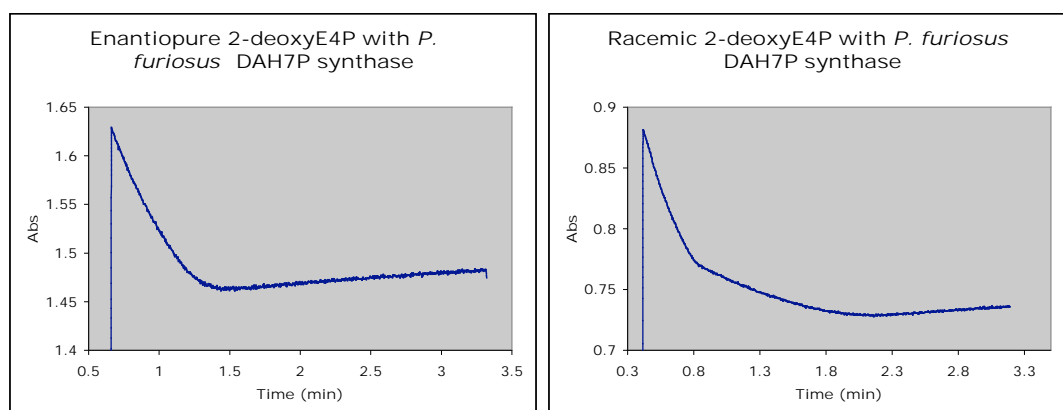
Figure 3.9: Assays of enantiopure and racemic 2-deoxyE4P with *P. furiosus* DAH7P synthase

Attempts to characterise the products from the enzyme-catalysed reaction in order to determine whether both enantiomers of 2-deoxyE4P are being converted to DAH7P-like products have proven difficult. In order to get large enough amounts of product to use for ^{1}H NMR analysis, the concentration of substrate analogue needs to be much higher than that used in normal assays. These large concentrations cause substrate inhibition of *P. furiosus* DAH7P synthase. As well as this, there are issues with substrate instability at high temperatures.

3.7 Initial kinetic parameters of 2-deoxyE4P with DAH7P synthase from various organisms

The apparent kinetic parameters for both the racemic and enantiopure 2-deoxyE4P with DAH7P synthase from a variety of organisms were determined by monitoring the loss of PEP as observed at 232nm. The steady state kinetic parameters were calculated by fitting data to the Michaelis-Menten equation using Enzfitter®. Tables 3.1 and 3.2 show the calculated kinetic parameters for 2-deoxyE4P with DAH7P synthase from a variety

of organisms. The kinetic parameters for these enzymes with E4P are presented in table 3.1 for comparison.

DAH7PS source	E4P K_M (μM)	PEP K_M (μM)	k_{cat} (s^{-1})	k_{cat}/K_M ^{E4P} (s^{-1}μM^{-1})	Reference
E. coli (phe)	39±4	2.0±0.2	26±2	0.67	[95]
N. meningitidis	25±2	17±1	9.4±0.1	0.38	Chapter two
P. furiosus	28±4	120±20	1.5±0.1	0.05	[19]
M. tuberculosis	25±3	37±3	3.1±0.1	0.12	[31]

Table 3.1: Kinetic parameters for E4P and PEP with enzymes from various organisms
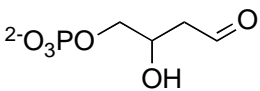
DAH7PS source	Racemic 2-deoxyE4P K_M (μM) $^{2-}O_3PO\!-\!\!\diagup\!\!\diagdown\!\!\diagup^{O}$ OH	PEP K_M (μM)	k_{cat} (s^{-1})	k_{cat}/K_M $^{2\text{-deoxyE4P}}$ (s^{-1}μM^{-1})
E. coli (phe)	650±30	9.1±2	14±0.1	0.02

Table 3.2: Kinetic parameters for racemic 2-deoxyE4P with *E. coli* DAH7P synthase (phe)
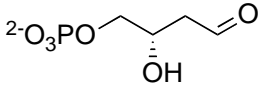
DAH7PS source	(*S*)-2-deoxyE4P K_M (μM) $^{2-}O_3PO\!-\!\!\diagup\!\!\diagdown\!\!\diagup^{O}$ OH	PEP K_M (μM)	k_{cat} (s^{-1})	k_{cat}/K_M $^{(S)\text{-2-deoxyE4P}}$ (s^{-1}μM^{-1})
E. coli (phe)	410±40	4.1±0.5	19±1	0.06
N. meningitidis	580±30	nd	12.3±0.2	0.02
P. furiosus[20]	6±1	33±4	3.0±0.1	0.5
M. tuberculosis	45±5	24±2	3.7±0.2	0.08

Table 3.3: Kinetic parameters for (*S*)-2-deoxyE4P with DAH7P synthase from various organisms.

3.7.1 *E. coli* DAH7P synthase

The apparent K_M of (*S*)-2-deoxyE4P with *E. coli* DAH7P synthase was found to be significantly lower than that for the racemic compound. As described above, only the (*S*)-enantiomer in the racemic mixture seemed to be utilised by the enzyme; hence, the difference in the K_M values suggests that the (*R*)-enantiomer is binding to the enzyme active site and inhibiting the reaction between the (*S*)-enantiomer and PEP. It was found when carrying out assays with racemic 2-deoxyE4P, that any concentration of more than ~1mM in the cuvette caused inhibition of the enzyme activity. As this only appears to be the case with the racemic compound, it again suggests that the (*R*)-enantiomer of 2-deoxyE4P is inhibiting the enzyme at these high concentrations.

The lower K_M of (*S*)-2-deoxyE4P compared to racemic 2-deoxyE4P is illustrated by the experiments shown in Figure 3.10. This Figure shows assays following the loss of absorbance due to PEP consumption at 232nm. Both assays have approximately the same concentration of 2-deoxyE4P (in the (*S*)-enantiomer). Although the two assays appear to have approximately the same initial rate, the assay with the racemic mixture shows greater curvature, indicating that as the relative concentration of the (*R*)-enantiomer to the (*S*)-enantiomer increases, there is more competition for the active site, and hence the K_M increases. Although the K_M of (*S*)-2-deoxyE4P with *E. coli* DAH7P synthase is lower than that for racemic 2-deoxyE4P, the K_M of both racemic and (*S*)-2-deoxyE4P is significantly higher than that for E4P.
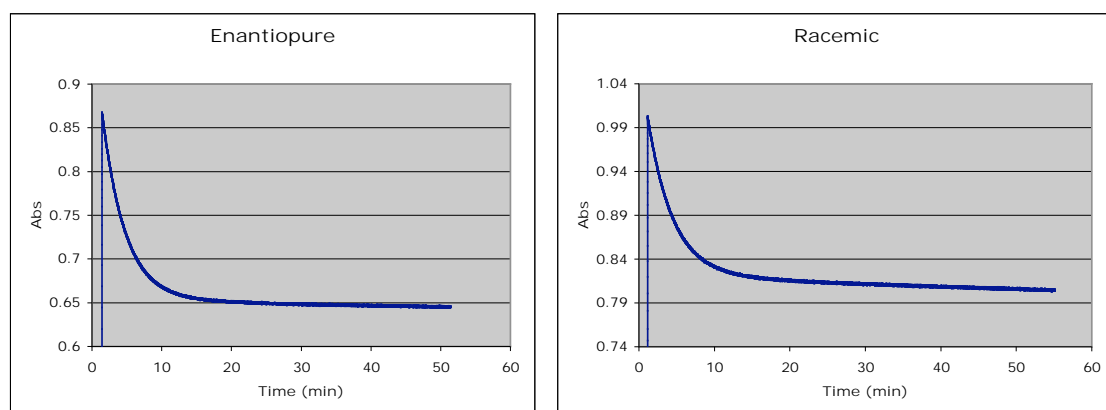
Figure 3.10: Assays following the loss of PEP at 232nm in the presence of enantiopure and racemic 2-deoxyE4P with *E. coli* DAH7PS (phe)

Assays with racemic 2-deoxyE4P and *E. coli* DAH7P synthase exhibit a continual downward drift even after all the (*S*)-2-deoxyE4P appears to have been consumed. However, this loss of absorbance is not proportional to the amount of enzyme present, (addition of further enzyme does not increase the rate of PEP loss), so this is probably due to non-enzyme-catalysed loss of PEP. There is no evidence in the ^{1}H NMR spectrum of the product for conversion of the remaining (*R*)-enantiomer to a DAH7P-like product.

The binding of PEP appears to be largely unaffected by the presence of either enantiomer of 2-deoxyE4P. The K_M for PEP in the presence of racemic and (*S*)-2-deoxyE4P is 9.1 and 4.1µM respectively, compared to 2.0 in the presence of E4P.[95]
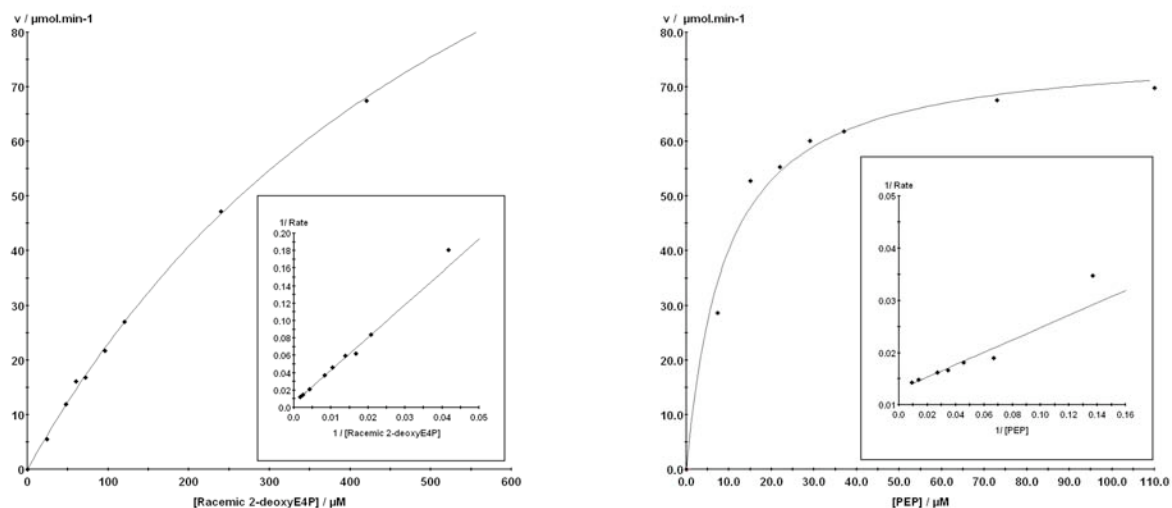
Figure 3.11: Michaelis–Menten and Lineweaver-Burk plots for determination of K_M values for racemic 2-deoxyE4P and PEP in the presence of racemic 2-deoxyE4P for *E. coli* DAH7P synthase (phe). The reaction mixtures for the determination of the K_M of 2-deoxyE4P consisted of PEP (150µM), MnSO$_4$ (100µM) and 2-deoxyE4P (24µM to 600µM), in 50mM BTP buffer, pH 6.8. The reaction mixtures for the determination of the K_M of PEP consisted of 2-deoxyE4P (1mM), MnSO$_4$ (100µM) and PEP (7-110µM) in 50mM BTP buffer, pH 6.8. The reaction was initiated by the addition of purified *E. coli* DAH7P synthase (5µL, 1.6mg/mL) and carried out at 25°C in a total volume of 1mL. K_M and k_{cat} values were determined by fitting the data to the Michaelis–Menten equation using Enzfitter (Biosoft).
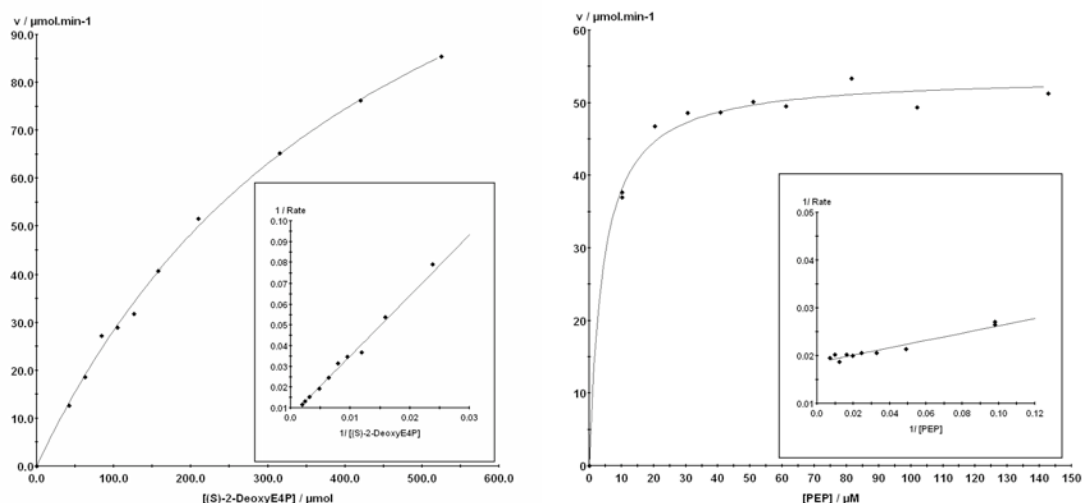
Figure 3.12: Michaelis–Menten and Lineweaver-Burk plots for determination of K_M values for (S)-2-deoxyE4P and PEP in the presence of (S)-2-deoxyE4P for *E. coli* DAH7P synthase (Phe). The reaction mixtures for the determination of the K_M of 2-deoxyE4P consisted of PEP (150μM), MnSO$_4$ (100μM) and 2-deoxyE4P (42-525μM), in 50mM BTP buffer, pH 6.8. The reaction mixtures for the determination of the K_M of PEP consisted of (S)-2-deoxyE4P (200μM), MnSO$_4$ (100μM) and PEP (10-200μM) in 50mM BTP buffer, pH 6.8. The reaction was initiated by the addition of purified *E. coli* DAH7P synthase (5μL, 1.6mg/mL) and carried out at 25°C in a total volume of 1mL. K_M and k_{cat} values were determined by fitting the data to the Michaelis–Menten equation using Enzfitter (Biosoft).

3.7.2 *N. meningitidis* DAH7P synthase

Similarly to the *E. coli* enzyme, *N. meningitidis* DAH7P synthase has a greatly increased apparent K_M with 2-deoxyE4P compared with E4P. The K_M of (S)-2-deoxyE4P with *N. meningitidis* was found to be 580μM, compared to 25μM for E4P. The k_{cat} however, is very similar, with a k_{cat} of 12.3s^{-1} with 2-deoxyE4P, compared with 9.4s^{-1} with E4P. The K_M of PEP with 2-deoxyE4P and *N. meningitidis* DAH7P synthase has not been determined due to limited amounts of 2-deoxyE4P being available.
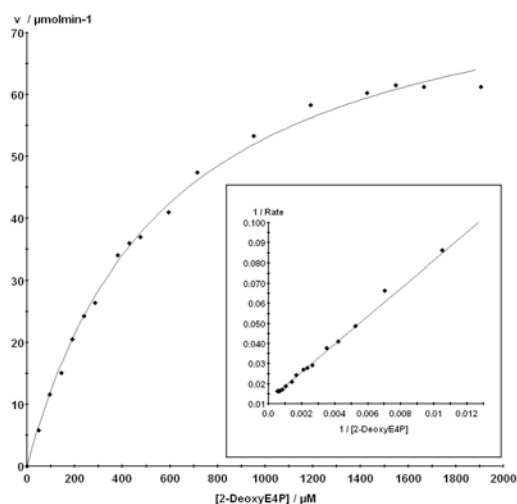
Figure 3.13: Michaelis–Menten and Lineweaver-Burk plots for determination of the K_M value for (*S*)-2-deoxyE4P with *N. meningitidis* DAH7P synthase. The reaction mixtures for the determination of the K_M of 2-deoxyE4P consisted of PEP (200µM), $MnSO_4$ (100µM) and 2-deoxyE4P (48-1900µM), in 50mM BTP buffer, pH 6.8. The reaction was initiated by the addition of purified *N. meningitidis* DAH7P synthase (4µL, 1.1mg/mL) and carried out at 25˚C in a total volume of 1mL. K_M and k_{cat} values were determined by fitting the data to the Michaelis–Menten equation using Enzfitter (Biosoft).

3.7.3 *P. furiosus* DAH7P synthase

The kinetic analysis of (*S*)-2-deoxyE4P was carried out by Dr Linley Schofield.[20] 2-DeoxyE4P is a considerably better substrate for DAH7P synthase from *P. furiosus* than it is for the Iα DAH7P synthases from *E. coli* and *N. meningitidis*. As discussed earlier, both enantiomers appear to be substrates, while in all the other enzymes tested, only one enantiomer is a substrate. Kinetic analysis carried out on (*S*)-2-deoxyE4P showed both a lower K_M and higher k_{cat} than for E4P itself, indicating that the 2-hydroxyl group has no significant role in the catalysis reaction for this enzyme. The structure of *P. furiosus* DAH7P synthase has been determined and E4P modeled into the active site.[20] It shows that the carbonyl group of Pro61 in one subunit faces inwards towards the E4P binding site, while in the other subunit it faces outwards, forming a hydrogen-bond with a tyrosine from a neighbouring subunit. This proline is conserved in all type I DAH7P synthases. In structures of other enzymes such as *E. coli*,[10] *S. cerevisiae*,[16] and *T. maritima*[22] with E4P modeled into the active site, the carbonyl of this residue is shown to be within hydrogen bond distance of the C2-hydroxyl. The flexibility of this group shown in the *P. furiosus* structure indicates that this interaction is not important for the binding or catalysis reaction for this enzyme. The difference in

the importance of the E4P C2-hydroxyl in binding and catalysis by different types of DAH7P synthases is discussed further in chapter five.

3.7.4 *M. tuberculosis* DAH7P synthase

2-DeoxyE4P is also a particularly efficient substrate for the type II enzyme from *M. tuberculosis*. The K_M and k_{cat} for (*S*)-2-deoxyE4P were 45µM and 3.7s^{-1} (table 3.3) which is in the same vicinity as E4P itself with a K_M of 25µM and k_{cat} of 3.1s^{-1}.[31]
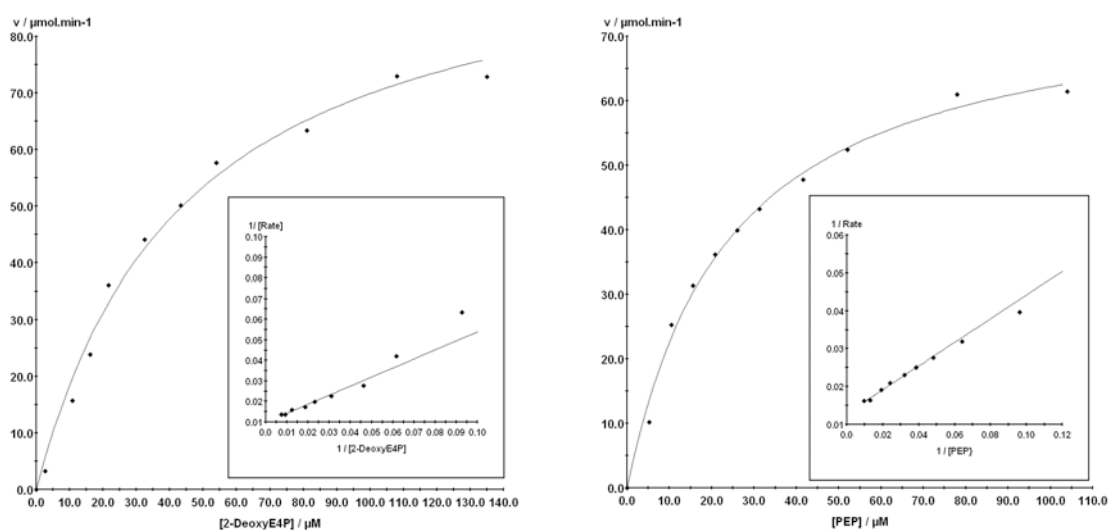
Figure 3.14: Michaelis–Menten and Lineweaver-Burk plots for determination of K_M values for (*S*)-2-deoxyE4P and PEP in the presence of (*S*)-2-deoxyE4P with *M. tuberculosis* DAH7P synthase. The reaction mixtures for the determination of the K_M of 2-deoxyE4P consisted of PEP (300µM), MnSO$_4$ (100µM) and 2-deoxyE4P (3 to 135µM), in 50mM BTP buffer, pH 7.5. The reaction mixtures for the determination of the K_M of PEP consisted of (*S*)-2-deoxyE4P (150µM), MnSO$_4$ (100µM) and PEP (5-100µM) in 50mM BTP buffer, pH 7.5. The reaction was initiated by the addition of purified *M. tuberculosis* DAH7P synthase (5µL, 4.6mg/mL) and carried out at 30˚C in a total volume of 1mL. K_M and k_{cat} values were determined by fitting the data to the Michaelis–Menten equation using Enzfitter (Biosoft).

3.8 Stereospecific deuteration by DAH7P synthase

When the enzyme-catalysed reaction between 2-deoxyE4P and PEP was followed by ^{1}H NMR in D_2O using *E. coli* DAH7P synthase, the product isolated contained only three, rather than the expected four, geminal protons. Comparison with the product from the reaction carried out in H_2O indicated that it was the equatorial proton on C5, where the hydroxyl group would be on DAH7P, which was missing. Mass spectrometry and 2D NMR spectra revealed the product to be (5S)-[5-^{2}H]-5-deoxyDAH7P **53**. Control experiments have shown that without DAH7P synthase present, no exchange of deuterium at C2 of 2-deoxyE4P occurs. No incorporation of deuterium into DAH7P is found when the enzymic reaction is carried out with the natural substrates, or when the non-deuterated 5-deoxyDAH7P is incubated with enzyme and phosphate in D_2O. As the reaction is carried out at neutral pH, and this proton would not be predicted to exchange for deuterium at an appreciable rate, as well as the fact that the exchange is stereospecific for one proton, it seems evident that this exchange must be enzyme-catalysed, and the proton must be abstracted from 2-deoxyE4P after it binds to the enzyme and prior to the reaction with PEP.
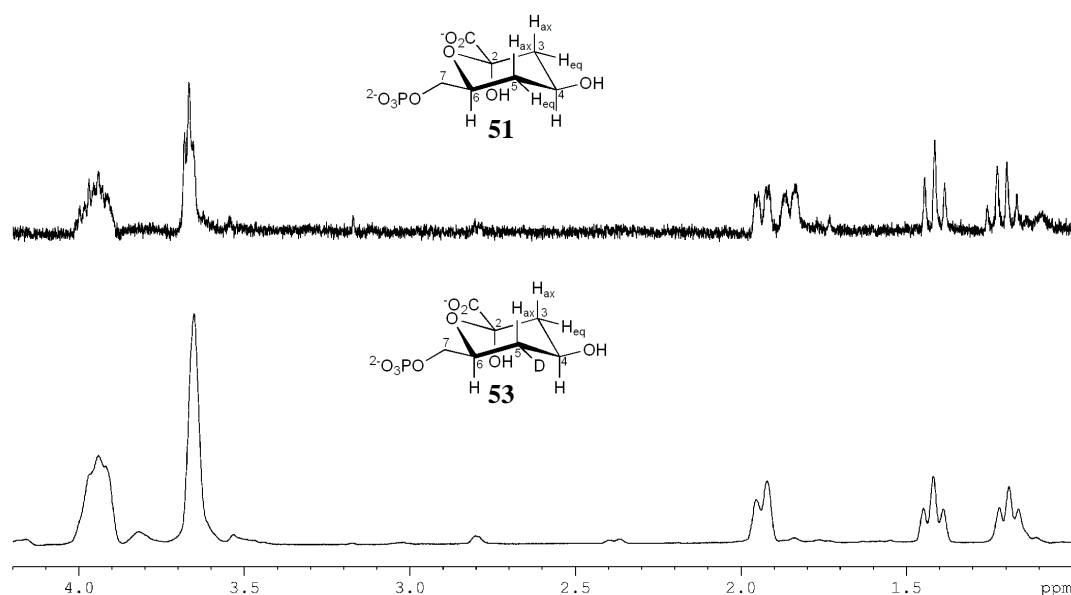
Figure 3.15: ^{1}H NMR spectra of 5-deoxyDAH7P **51** (top) and (5S)-[5-^{2}H]-5-deoxyDAH7P **53** (400MHz) showing the missing C5 equatorial proton.

Modeling studies of E4P in the active site of DAH7P synthase have suggested that the E4P C2-hydroxyl interacts with Arg165 and the main-chain carbonyl of Pro98.[16] Interaction of the proton now in this position in 2-deoxyE4P with these residues could be expected to increase its acidity, allowing for exchange with deuterium. Both of these active site residues are conserved in all DAH7P synthases, suggesting that the deuteration may be expected to occur in DAH7P synthase from any source.

Attempts were made to follow the reaction catalysed by *P. furiosus* DAH7P synthase by ^{1}H NMR spectroscopy in order to determine whether this stereospecific deuteration occurs with this enzyme. Racemic 2-deoxyE4P, PEP and $MnSO_4$ were dissolved in D_2O and the pH adjusted to 6.8 at 50˚C. After an initial spectrum was collected, *P. furiosus* DAH7P synthase was added and further spectra collected at intervals. After incubation at 50˚C overnight, some very small peaks indicative of 5-deoxyDAH7P were evident. However, the peaks were very small compared to the large peaks due to unreacted PEP and 2-deoxyE4P, and selective TOCSY experiments with an inverse probe were not consistent with the formation of 5-deoxyDAHP. This is thought to be due to substrate inhibition problems observed at high concentrations of racemic 2-deoxyE4P. The small peaks observed may also have been due to decomposition of the substrates at high temperatures.
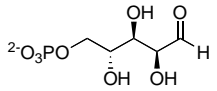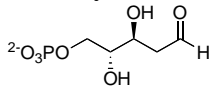
Since this work was carried out, DAH7P synthases from *N. meningitidis*, *M. tuberculosis*, and *H. pylori* have been purified in our laboratory. Future work could involve investigation of the deuteration reaction with any of these enzymes.

3.9 Initial kinetic parameters of 2-deoxyR5P with KDO8P synthase

In order to compare the importance of the hydroxyl groups in the substrates for the two enzymes DAH7P and KDO8P synthase, kinetic analysis of commercially available 2-deoxyR5P, the 2-deoxy analogue of A5P, was carried out with the non-metallo KDO8P synthase from *N. meningitidis*. The assay system used with KDO8P synthase is the same as the modified form of the Schoner and Herrman continuous assay used for

DAH7P synthase, where the reaction is followed by monitoring the loss of PEP as observed at 232nm.[11] Assays with *N. meningitidis* KDO8P synthase were carried out in 50mM BTP buffer at 30°C. As *N. meningitidis* KDO8P synthase is a non-metallo enzyme, the solutions used were not Chelex treated and do not contain EDTA. The enzymatic reaction was initiated by the addition of purified enzyme.

It was found that 2-deoxyR5P was a poor substrate for *N.meningitidis* KDO8P synthase. The natural substrate, A5P has a K_M and k_{cat} of $12\pm1\mu M$ and $2.7\pm0.6s^{-1}$ respectively,[95] whereas 2-deoxyR5P has a K_M and k_{cat} of $230\pm20\mu M$ and $0.13\pm0.01s^{-1}$ respectively. These results were consistent with results in the literature for *E. coli* KDO8P synthase, in which 2-deoxyR5P was reported to have an apparent K_M and k_{cat} of $50\pm8\mu M$ and $0.12\pm0.05s^{-1}$ respectively.

Monosaccharide	*N. meningitidis* KDO8P synthase			*E. coli* KDO8P synthase		
	K_M (μM)	k_{cat} (s^{-1})	k_{cat}/K_M ($\mu M^{-1}s^{-1}$)	K_M (μM)	k_{cat} (s^{-1})	k_{cat}/K_M ($\mu M^{-1}s^{-1}$)
A5P[a]	12 ± 1	2.7 ± 0.6	0.23	19 ± 4	6.8 ± 0.5	0.36
2-deoxyR5P[b]	230 ± 20	0.13 ± 0.01	0.0006	50 ± 8	0.12 ± 0.05	0.002

[a] Kinetic parameters of A5P with *N. meningitidis* KDO8P synthase were determined by M. Ahn[95] and with *E. coli* KDO8P synthase were reported by Howe *et al.*[74]
[b] Kinetic parameters of 2-deoxyR5P with *E. coli* KDO8P synthase were reported by Howe *et al*[74]

Table 3.4: Kinetic parameters of A5P and 2-deoxyR5P with KDO8P synthase from *E. coli* and *N. meningitidis*
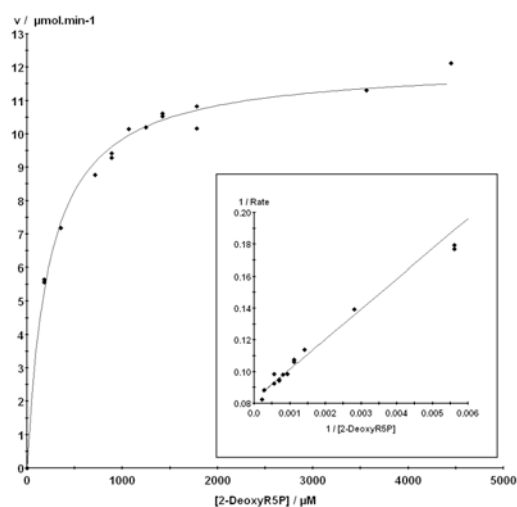
Figure 3.16: Michaelis–Menten and Lineweaver-Burk plots for determination of the K_M value for 2-deoxyR5P with *N. meningitidis* KDO8P synthase. The reaction mixture consisted of PEP (200μM) and 2-deoxyR5P (2-4450μM), in 50mM BTP buffer, pH 7.5. The reaction was initiated by the addition of purified. *N. meningitidis* KDO8P synthase (10μL, 4.8mg/mL) and carried out at 30°C in a total volume of 1mL. K_M and k_{cat} values were determined by fitting the data to the Michaelis–Menten equation using Enzfitter (Biosoft).

The poor ability of 2-deoxyR5P to act as an alternative substrate for KDO8P synthase indicates a significant role for the C2-hydroxyl of A5P in the KDO8P synthase catalysed reaction. This is in contrast to the results with 2-deoxyE4P and DAH7P synthase, which indicate a less crucial role for the C2-hydroxyl.

3.10 Summary

Characterisation of the behaviour of 2-deoxyE4P with two types of DAH7P synthase has been carried out. We have found that the (*S*)-enantiomer of 2-deoxyE4P is a substrate for the type Iα enzymes from *E. coli* and *N. meningitidis,* the type Iβ enzyme from *P. furiosus* and the type II enzyme from *M. tuberculosis.* To date, 2-deoxyE4P appears to be the best alternative substrate found for DAH7P synthase. In the case of *E. coli* DAH7P synthase, it has been shown that a DAH7P-like product has been formed. Although both (*S*)-and (*R*)-enantiomers appear to be substrates for the DAH7P synthase from *P. furiosus*, product characterisation has not been able to be carried out due to

-71-

issues with substrate inhibition. The elevated temperatures that are necessary in order to carry out assays with this enzyme make it difficult to probe some of the aspects of the catalysed reaction.

In comparison, the 2-deoxy analogue of A5P, 2-deoxyR5P was only a very poor substrate for KDO8P synthase from *N. meningitidis*. The results from 2-deoxyE4P and 2-deoxyR5P and implications for the reaction mechanisms of DAH7P synthase and KDO8P synthase are discussed in chapter five.

CHAPTER FOUR: SYNTHESIS AND EVALUATION OF 3-DEOXYE4P AND 3-DEOXYA5P WITH DAH7P AND KDO8P SYNTHASES

4.1   Introduction

As part of our laboratory's research into the role of the hydroxyl groups of E4P in the catalysis reaction of DAH7P synthase, we wished to synthesise 3-deoxyE4P, as well as 2-deoxyE4P, the synthesis of which is described in chapter three. The role of the hydroxyl group on C3 of E4P is of particular interest, due to its potential role in the enzyme-catalysed reaction. As discussed in chapter one, it was originally suggested that the reaction catalysed by KDO8P synthase went *via* a cyclic intermediate and required the C3-hydroxyl group to act as a nucleophile on the carbocation formed at C2 of PEP.[43] It has been reported that 3-deoxyA5P is not a substrate for *E. coli* KDO8P synthase.[44] However, there have been no reports on the analogous study of 3-deoxyE4P and DAH7P synthases. In order to compare the substrate specificity of these two enzymes, we wished to test 3-deoxyE4P as a substrate for DAH7P synthase from a variety of organisms, as well as testing 3-deoxyA5P as a substrate for KDO8P synthase. As these compounds were not commercially available, a method of synthesising them within our laboratory was investigated.

4.2   Synthesis of 3-deoxyE4P

The synthesis of 3-deoxyE4P has been carried out in our laboratory using both α-hydroxy-γ-butyrolactone and malic acid as starting materials. The following sections describe the development of these two synthetic routes.

4.2.1 Previous investigations into the synthesis of 3-deoxyE4P

The synthesis of 3-deoxyE4P was originally investigated in our laboratory by Dr Matthias Rost. The planned strategy was to use α-hydroxy-γ-butyrolactone in an analogous synthesis to that described for 2-deoxyE4P from β-hydroxy-γ-butyrolactone in chapter three. The proposed scheme, outlined in Figure 4.1 began by protecting the $2°$ hydroxyl group as the benzyl[101-103] or silyl ether and then reducing the lactone to the lactol with DIBAL at -78°C.[106] The crucial step then involved protecting the aldehyde, opening the lactol ring and exposing the $1°$ hydroxyl group.[104] It was found that the only ways to achieve this were by forming the dithiol acetal with 1,3-dithiane, or by forming the six membered dioxalane ring with dimethylpropanediol.[104] In both cases, the TBDMS group was not robust enough to handle the reaction conditions and was cleaved. Phosphorylation was still able to be carried out on the compounds with the $2°$ hydroxyl exposed, as it was found that the $1°$ phosphorylated compound was exclusively formed, whether the $2°$ hydroxyl group was protected or not. Hydrogenolysis of the benzyl, S,S-acetal protected compound was initially attempted using the method of Felix et al,[113] which utilised a palladium catalyst. However, this method was unsuccessful. As S,S-acetals are known to poison platinum catalysts,[114] methods to remove the S,S-acetal and replace it with an O,O-acetal were investigated. Removal of the S,S-acetal proved to be problematic. Methyliodide and calcium carbonate in aqueous acetonitrile[115,116] and cerium-IV-ammonium nitrate in aqueous acetone[117] were both found to be low yielding. A method outlined by Jones et al[118] where the S,S-acetal is replaced directly with a dimethyl acetal was also unsuccessful. Subsequently, the use of the S,S-acetal was discontinued and the 2,2-dimethylpropane-1,3-diol protecting group was used instead. Hydrogenolysis of this compound was straightforward, and heating in water removed the acetal protecting group to give 3-deoxyE4P. However, the final deprotection was very low yielding and further investigation was required to make this a useful synthetic route.
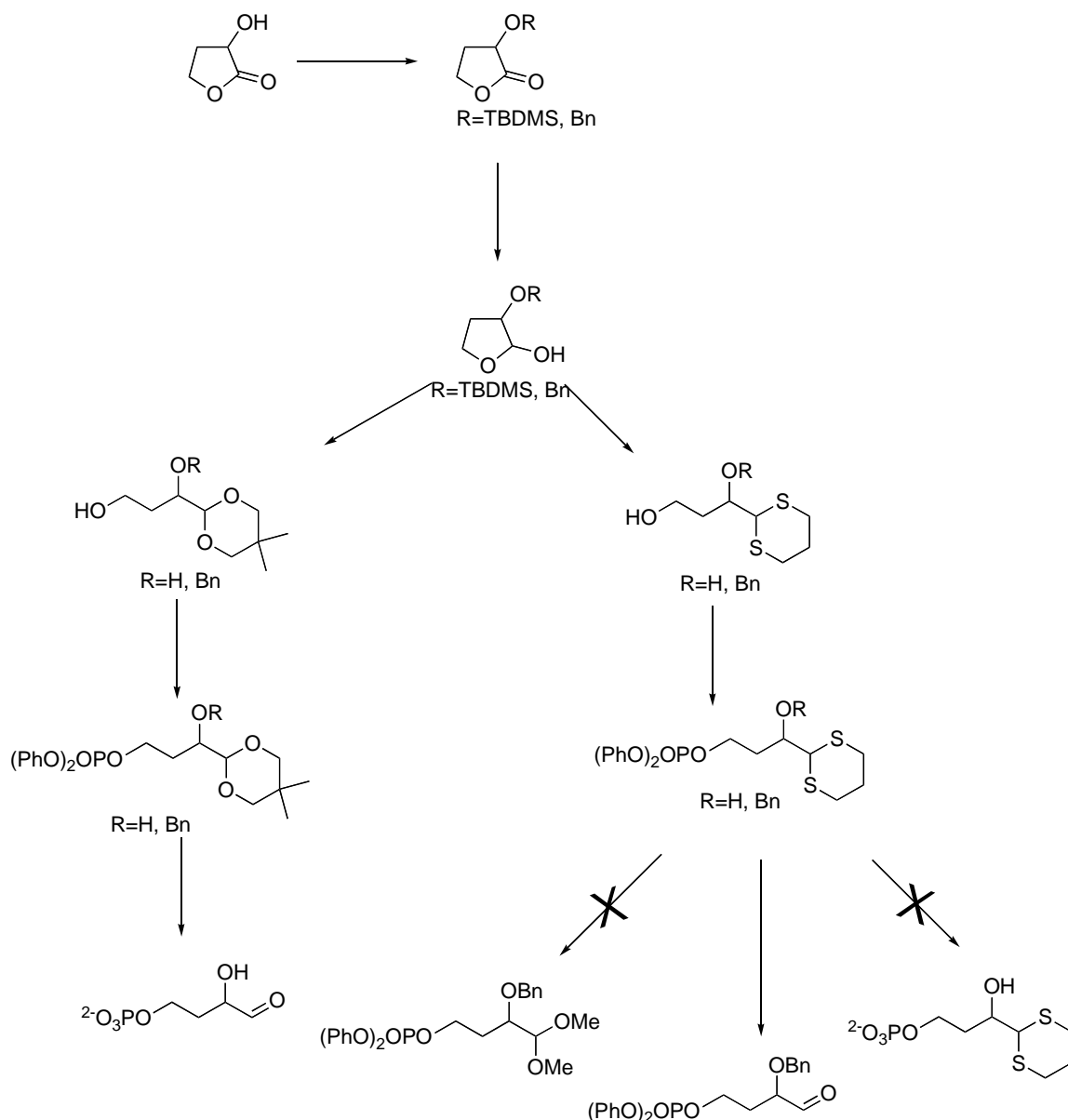
Figure 4.1: Outline of the strategy used by Dr Rost to synthesise 3-deoxyE4P

4.2.2 Synthesis of 3-deoxyE4P from α-hydroxy-γ-butyrolactone

The work carried out by Dr Rost described above suggested that the synthesis of 3-deoxyE4P from α-hydroxy-γ-butyrolactone was worthwhile pursuing. Although the yield for the final deprotection was very low, preliminary enzyme testing showed that some 3-deoxyE4P was being formed, and that it was a weak substrate for *E. coli* DAH7P synthase (phe). The convenience of being able to synthesise both deoxyE4P analogues *via* analogous routes suggested it was worthwhile carrying out further investigations into this route. As well as this, it was considered encouraging that the route to 2-deoxyE4P from β-hydroxy-γ-butyrolactone had previously been successful.

The synthesis described in this section (Figure 4.2) was carried out based on the earlier work by Dr Rost and the synthesis of 2-deoxyE4P, which is described in chapter three.
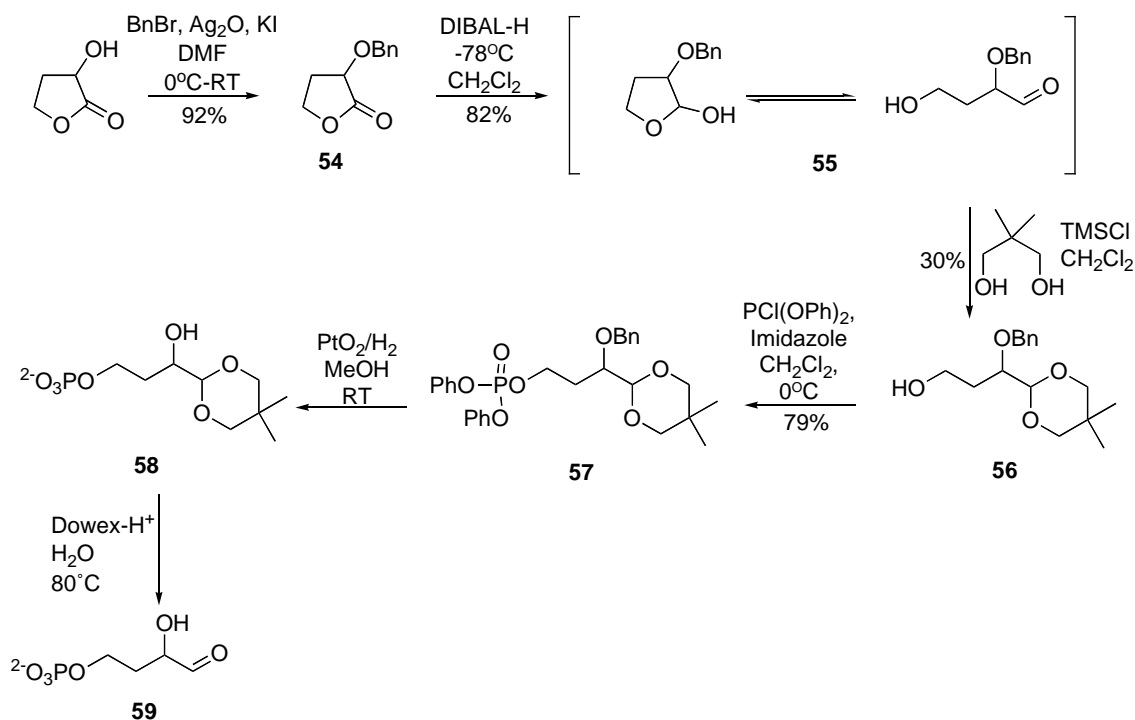
Figure 4.2: Synthesis of 3-deoxyE4P from α-Hydroxy-γ-butyrolactone

The synthesis was developed using racemic lactone, although both the (*R*)- and (*S*)-forms are both commercially available. α-Hydroxy-γ-butyrolactone was first protected with a benzyl group to give **54**.[101-103] In the synthesis of 2-deoxyE4P from β-hydroxy-γ-butyrolactone (described in chapter three) it was found that the benzylation reaction was more successful in CH_2Cl_2 than DMF. Conversely, the benzylation of α-hydroxy-γ-butyrolactone was much higher yielding in DMF (92%) than in CH_2Cl_2 (53%). The freshness of silver oxide also appeared to have less effect on the yield; the reaction was high yielding regardless of how recently the silver oxide was prepared. The DIBAL reduction to the lactol **55**, carried out in CH_2Cl_2 at -78°C was also found to be high yielding, at 82%, with no evidence of over-reduction occurring.[106]

The protection of the aldehyde with 2,2-dimethylpropane-1,3-diol was problematic, as was also found in the synthesis of 2-deoxyE4P.[104] After workup of the reaction mixture, only one spot was evident on the TLC plate. Identification of this compound as either the five-membered ring **60** or six-membered ring product **56** proved to be

difficult, as the ^{1}H and ^{13}C NMR spectra of the two products were expected to be very similar and the two products have the same molecular mass. Identification was easier once the phosphorylation step was carried out, as the [13]C-^{31}P coupling patterns in the ^{31}P NMR spectrum revealed whether the carbon with the phosphate group on it was adjacent to a methylene group (in the dioxalane product **57**), or a tertiary carbon (in the unwanted five-membered ring product **61**) (Figure 4.3). Analysis of the ^{31}P NMR spectrum confirmed that the desired dioxalane product **56** had been formed; however the yield was low (30%). It was anticipated that this reaction could be further investigated and the yield improved by varying the reaction conditions. However, due to problems with reagent availability encountered later, and promising results from an alternative route, it was not.
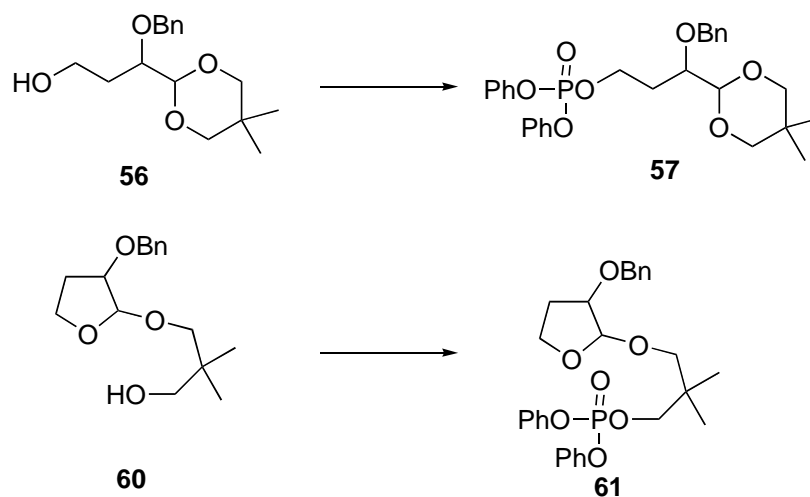
Figure 4.3: The possible products from the aldehyde protection reaction and their phosphorylated products

The phosphorylation with diphenylchlorophosphate and imidazole proceeded cleanly, with a yield of 79% of **57**, followed by hydrogenolysis at atmospheric pressure to give the protected aldehyde **58**.

As it was the final deprotection of the aldehyde functionality of the target compound that had proven to be the challenging step, it was attempted to follow this reaction by ^{1}H NMR spectroscopy, in conjunction with enzyme assays. The protected aldehyde **58** was dissolved in D_2O and an initial ^{1}H NMR spectrum was collected, which exhibited two methyl peaks at 0.63 and 1.03ppm, corresponding to the two methyl groups of the 2,2-dimethylpropane-1,3-diol protecting group. After heating overnight at 40°C and at a pH

of 1.5, these methyl groups were fully intact. A gradual increase in temperature eventually showed a proportional decrease of the integrals of these methyl groups (relative to the upfield methylene protons at 1.61 and 1.88ppm) and a new peak formed at 0.78ppm as the protecting group was cleaved. After heating overnight at 80°C, the peak integrals at 0.63 and 1.03ppm were reduced from an initial three protons to 0.4-0.5. Further heating at this temperature failed to reduce this integral any further, so the pH of the solution was increased and the solution tested by enzyme assay in order to determine whether 3-deoxyE4P had been formed. Unfortunately, although the ^{1}H NMR spectra showed that the aldehyde protecting group had been removed, when the product was tested by enzyme assay, it showed 3-deoxyE4P **59** to be present in only very small concentrations. The yield was less than 5% over the two deprotection steps. It is thought that the high temperatures necessary to remove the protecting group resulted in decomposition of the product, possibly by cleavage of the phosphate group. ^{31}P NMR spectra were collected during the experiment, but due to the low pH and ionic nature of the substrate, the peaks were very broad and unresolved and hence, difficult to interpret. There is some evidence of a new peak being formed at 0.78ppm after one hour of heating which gradually becomes bigger, but it remains much smaller than the original peak at 0.44ppm, so it seems unlikely that de-phosphorylation is the sole cause of the low yield. There are also some small additional peaks formed over time in the ^{1}H NMR spectrum, but again, they do not seem to be large enough to account for the very low yield determined.

As well as the problems producing 3-deoxyE4P from the protected analogue, the reduction step where the lactone is reduced to a lactol caused issues, as it became difficult to obtain DIBAL at this time. Due to these issues, a new strategy for producing this compound was sought. This is described in the next section.

4.2.3 Synthesis of 3-deoxyE4P from malic acid

Due to some of the problems encountered with the synthesis of 3-deoxyE4P from α-hydroxy-γ-butyrolactone, an alternative synthesis was sought. Malic acid seemed a suitable starting material for the synthesis of 3-deoxyE4P. It has a hydroxyl group already on C2 and carboxylic acid groups on both ends, one of which may be converted to an aldehyde and the other to a 1° alcohol to then be phosphorylated. Malic acid is

available in both (*S*)- and (*R*)- forms and is inexpensive compared to α-hydroxy-γ-butyrolactone, at approximately 25% of the cost for the appropriate stereoisomer. The straight chain structure was also thought to be easier to work with than the cyclic lactones previously found to be troublesome. Figure 4.4 outlines the strategy used.
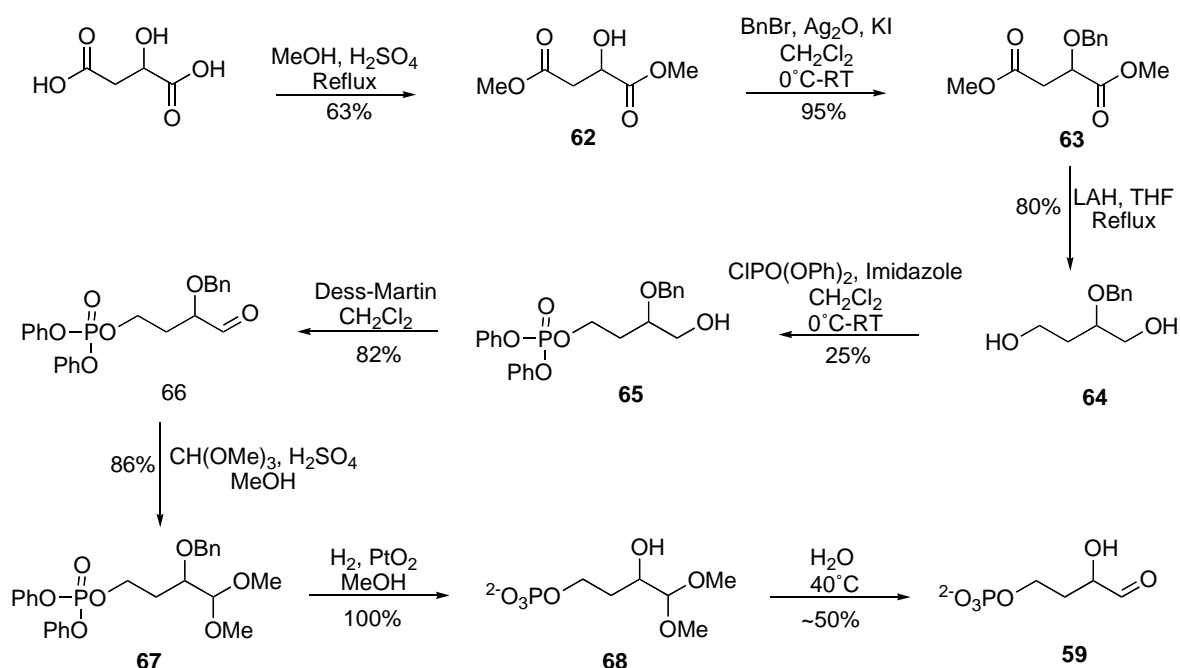
Figure 4.4: Synthesis of 3-deoxyE4P from malic acid

Malic acid was first esterified by treatment with methanol and concentrated sulfuric acid under reflux conditions to provide a 63% yield of dimethylmalate **62**.[105] The 2° alcohol was then protected as the benzyl ether using the same conditions as used previously to give **63**.[101-103] This reaction was much higher yielding than that found with the lactones and there was seemingly no need for the silver oxide to be freshly prepared. Reduction with lithium aluminium hydride provided a diol **64**, which needed to be phosphorylated at one end and oxidized at the other.[119,120] This same diol can also be formed by reduction of the benzyl lactone formed by the benzylation of the 2° hydroxyl of α-hydroxy-γ-butyrolactone, but malic acid is a much cheaper starting material. It was found that as expected, the benzyl group did provide some directing effects for the mono-phosphorylation. The yield of the desired compound **65** was 25%, compared to 11% for the other monophosphorylated product. Unfortunately, there was also a large amount of diphosphorylated compound (32%) formed in the reaction. A more dilute reaction solution or the use of less equivalents of phosphorylation reagent

did not improve the outcome of this reaction. Future work could investigate the use of a bulkier protecting group on the 2° alcohol, which could potentially increase the yield of the desired compound in this reaction and decrease the amount of side products, by adding to the steric hindrance for the phosphate group binding at the unwanted position. The other monophosphorylated compound formed in this reaction, is also potentially useful for the synthesis of 2-deoxyE4P (Figure 4.6). The two regioisomers were able to be separated by flash chromatography and the desired compound was oxidised to the aldehyde **66**,[121] using freshly prepared Dess-Martin periodinane. Aldehyde **66** was protected as the dimethylacetal, under standard conditions, affording the fully protected analogue **67**.[104]

The protected analogue **67** was treated to hydrogenolysis over PtO_2 in methanol and checked by ^{1}H NMR to ensure that cleavage to the protected aldehyde **68** was complete. The initial ^{1}H NMR spectrum subsequent to hydrogenolysis showed a singlet peak corresponding to the methyl acetal at 3.33ppm and another smaller peak, a third of the integral at 3.19ppm (Figure 4.5). An enzyme assay at this point revealed the concentration of 3-deoxyE4P in the solution to be 10% of the theoretical concentration. After heating to 40°C overnight, the ^{1}H peak due to the methyl glycoside protecting group at 3.33ppm had completely disappeared and the peak at 3.19ppm had proportionally increased in size. Enzyme assays at this point indicated a yield of 34% over the two deprotection steps had been achieved. This seemed reasonable as previous deprotections carried out in this manner within our laboratory in the synthesis of 2-deoxyE4P and of threose-4-phosphate (T4P), by Meekyung Ahn have had a maximum yield of 50%.[95] Additional investigation of this final deprotection step may allow for determination of the optimum time for the highest possible yield.
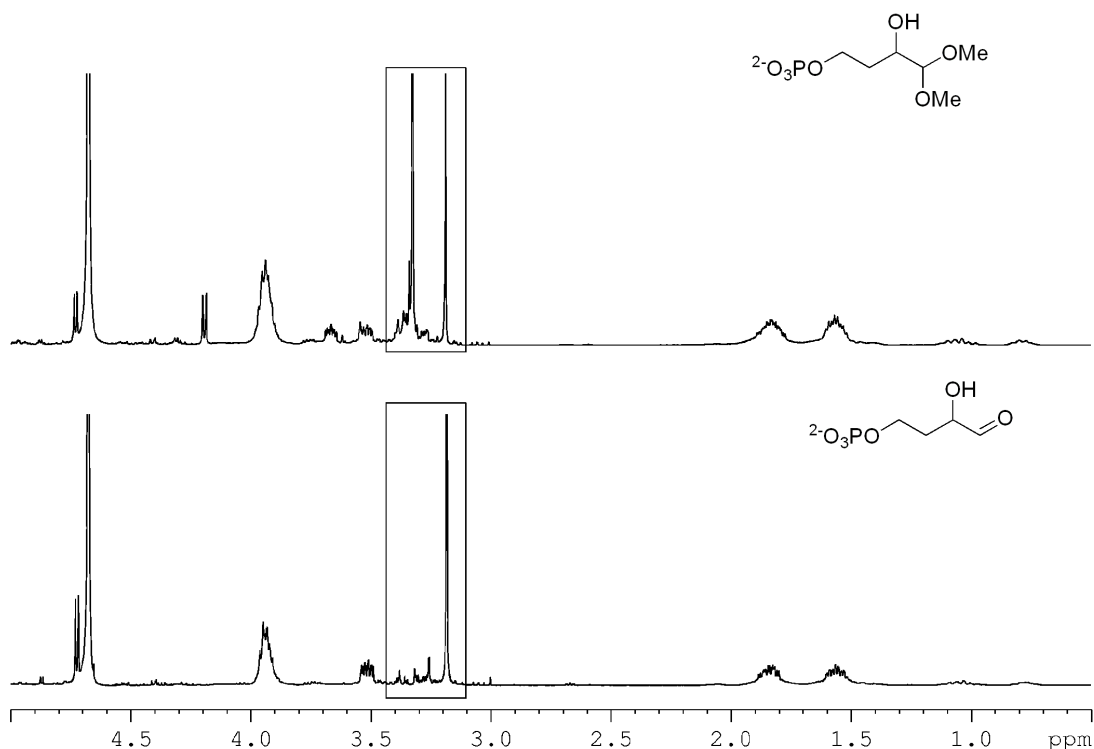
Figure 4.5: ^{1}H NMR (400MHz) spectra showing the deprotection of the dimethylacetal **68** (top) to 3-deoxyE4P **59**

Although this route to 3-deoxyE4P had one very low yielding step, the overall yield is better then that achieved from the lactone, due to the very low final deprotection step in that route. Other advantages to this route include the relative cost of malic acid being much lower than the lactone and the non-reliance on reagents for which supply can be difficult, such as DIBAL. After the route was established using racemic malic acid, it was repeated using (*R*)-malic acid to synthesise (*R*)-3-deoxyE4P **39**, with the same C2 stereochemistry as E4P itself. The opposite (*S*)-isomer of 3-deoxyE4P **76** could also be synthesised through the same route from (*S*)-malic acid, which may be useful for comparison with the (*R*)-isomer. There is also the potential to synthesise both the (*S*)- and (*R*)-enantiomers (**38** and **72** respectively) of 2-deoxyE4P by utilising the minor monophosphorylated products **71** and **75** formed in the phosphorylation reaction (Figure 4.6). The many different E4P analogues that can be formed using relatively inexpensive starting materials and reagents potentially make this a very useful synthetic route.
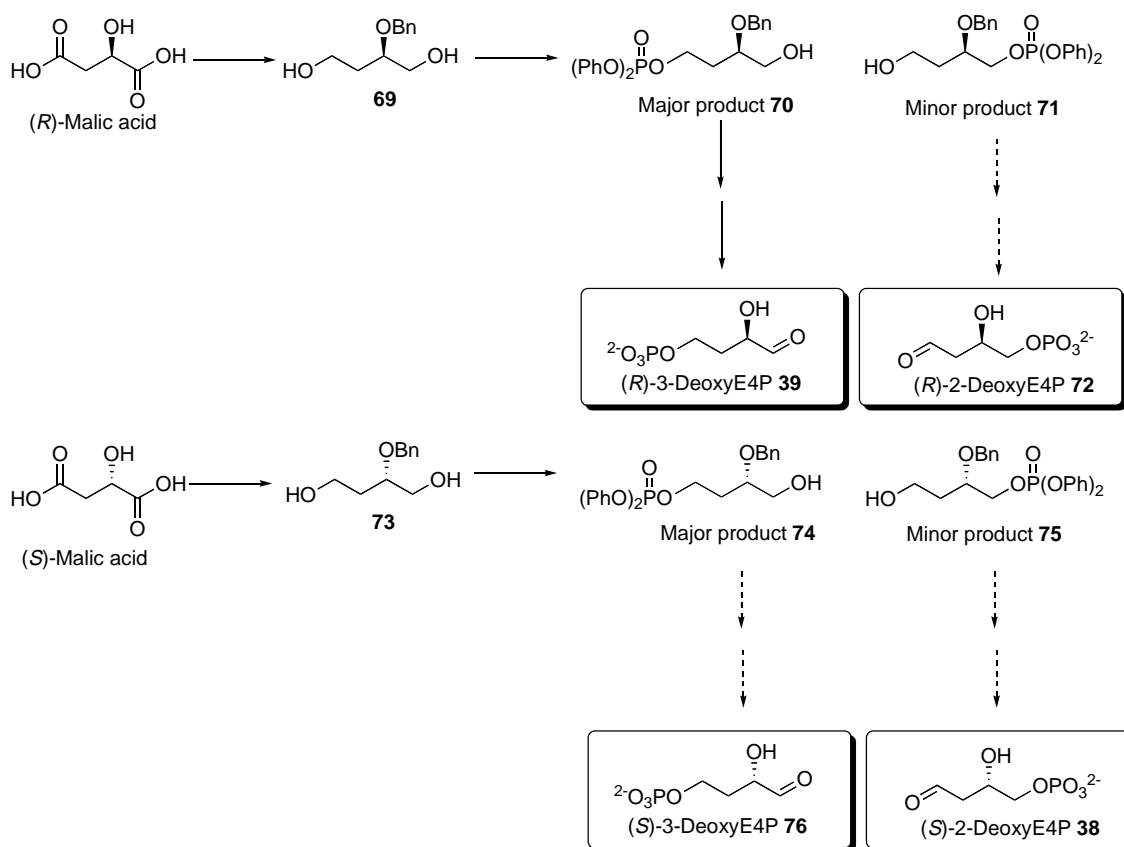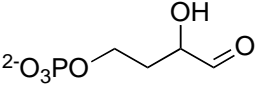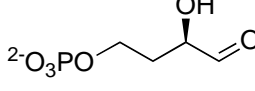
Figure 4.6: Potential products from the commercially available isomers of malic acid

Once synthesised, 3-deoxyE4P was tested as a substrate for DAH7P synthase from *E. coli*, *N. meningitidis*, *P. furiosus*, and *M. tuberculosis*. Interaction of both the racemic and enantiopure 3-deoxyE4P analogues with these enzymes is described in the next section.

4.3 Initial kinetic parameters of 3-deoxyE4P with DAH7P synthase from various organisms

The apparent initial kinetic parameters of 3-deoxyE4P with DAH7P synthase from a variety of organisms have been determined and are summarised in table 4.1

DAH7PS source	Racemic 3-deoxyE4P K_M (μM)	(R)-3-deoxyE4P K_M (μM)	PEP K_M (μM)	k_{cat} (s^{-1})	$k_{cat}/K_M^{\text{3-deoxyE4P}}$ (s^{-1}μM^{-1})
E. coli (phe)	2600±330	2700±140		4.5±0.1	0.002
N. meningitidis		2100±140		4.7±0.1	0.002
P. furiosus	Not a substrate	200±30	27±4.6	2.1±0.1	0.01
M. tuberculosis		280±30	24±1.6	2.4±0.1	0.01

pTable 4.1: Kinetic analysis of 3-deoxyE4P with DAH7P synthase from various organisms

4.3.1 *E. coli* DAH7P synthase (phe)

Initially, racemic 3-deoxyE4P was tested as a substrate for *E. coli* DAH7P synthase (phe). It was found to be a very poor substrate, with both a high K_M and low k_{cat} compared to E4P, which has a K_M of 39±4 and a k_{cat} of 26±3.[95]

However, it did appear that both (R)-and (S)-enantiomers were substrates, with no detectable change in the rate of reaction between the two. This was confirmed by concentration studies using G6P dehydrogenase and ^{31}P NMR spectroscopy, as described in the work with 2-deoxyE4P in chapter three. 100% utilisation of the racemic 3-deoxyE4P in solution was seen.
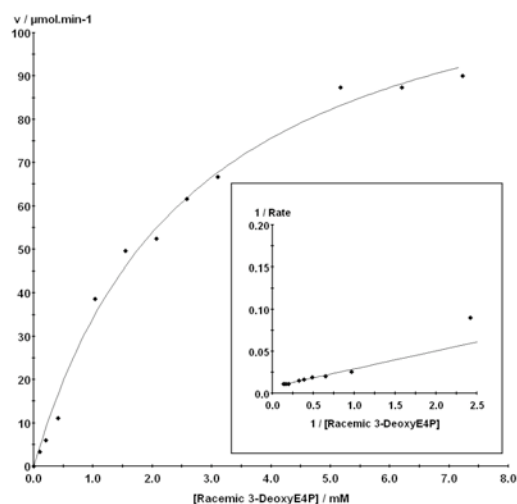
Figure 4.7: Michaelis–Menten and Lineweaver-Burk plots for determination of the K_M value for racemic 3-deoxyE4P with *E. coli* DAH7P synthase (phe). The reaction mixtures for the determination of the K_M of 3-deoxyE4P consisted of PEP (250µM), $MnSO_4$ (100µM) and 3-deoxyE4P (100µM to 7000µM), in 50mM BTP buffer, pH 6.8. The reaction was initiated by the addition of purified *E. coli* DAH7P synthase (2.5µL, 8.3mg/mL) and carried out at 25°C in a total volume of 1mL. K_M and k_{cat} values were determined by fitting the data to the Michaelis–Menten equation using Enzfitter (Biosoft).

Upon successful synthesis of the (*R*)-form of 3-deoxyE4P, the kinetic studies with *E. coli* DAH7P synthase (phe) were repeated and it was found that there was little change in the K_M or k_{cat}. 3-DeoxyE4P remained a very poor substrate, albeit seemingly with no preference for either stereochemistry at C2.
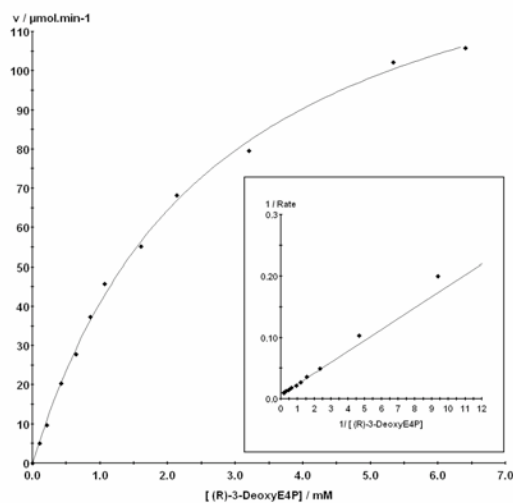
Figure 4.8: Michaelis–Menten and Lineweaver-Burk plots for determination of the K_M value for (*R*)-3-deoxyE4P with *E. coli* DAH7P synthase (phe). The reaction mixtures for the determination of the K_M of 3-deoxyE4P consisted of PEP (200µM), MnSO$_4$ (100µM) and (*R*)-3-deoxyE4P (100µM-9.6mM), in 50mM BTP buffer, pH 6.8. The reaction was initiated by the addition of purified *E. coli* DAH7P synthase (2.5µL, 8.3mg/mL) and carried out at 25°C in a total volume of 1mL. K_M and k_{cat} values were determined by fitting the data to the Michaelis–Menten equation using Enzfitter (Biosoft).

4.3.2 *N. meningitidis* DAH7P synthase

The behaviour of *N. meningitidis* DAH7P synthase with 3-deoxyE4P is different to that with *E. coli* DAH7P synthase (phe). In order to determine whether one or both enantiomers of 3-deoxyE4P was a substrate for *N. meningitidis* DAH7P synthase, two assays were carried out under identical conditions with racemic 3-deoxyE4P and PEP present in excess. The reaction was initiated by the addition of *E. coli* DAH7P synthase to one assay and *N. meningitidis* DAH7P synthase to the other. The loss of PEP in each assay was followed to completion. It was found that the *N. meningitidis* DAH7P synthase assay showed only half the amount of PEP lost, compared to the *E. coli* DAH7P synthase (phe) assay, indicating that only one enantiomer (presumably the (*R*)-enantiomer) had reacted with PEP.

The initial kinetic parameters, determined with the pure (*R*)-form of 3-deoxyE4P show it to be a poor substrate for *N. meningitidis* DAH7P synthase, as it was for *E. coli* DAH7P synthase (phe). The apparent K_M was 2100µM, compared to 25µM for E4P and k_{cat} 4.7s^{-1}, compared to 9.4s^{-1} for E4P (refer to chapter two).
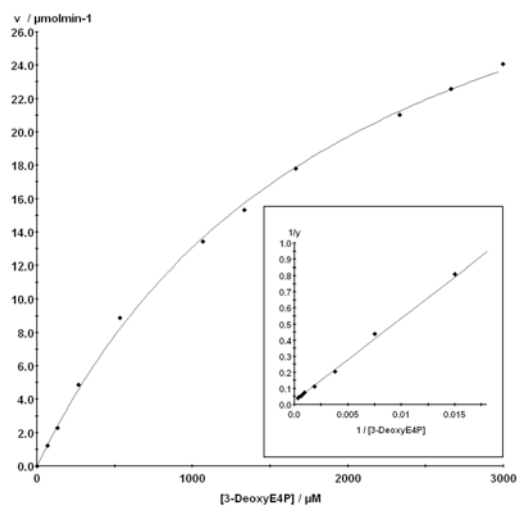
Figure 4.9: Michaelis–Menten and Lineweaver-Burk plots for determination of the K_M value for (R)-3-deoxyE4P with *N. meningitidis* DAH7P synthase. The reaction mixtures for the determination of the K_M of 3-deoxyE4P consisted of PEP (200μM), MnSO$_4$ (100μM) and (R)-3-deoxyE4P (67μM-3mM), in 50mM BTP buffer, pH 6.8. The reaction was initiated by the addition of purified *N. meningitidis* DAH7P synthase (5μL, 1.1mg/mL) and carried out at 25°C in a total volume of 1mL. K_M and k_{cat} values were determined by fitting the data to the Michaelis–Menten equation using Enzfitter (Biosoft).

Due to the very large 3-deoxyE4P K_M values for the type Iα enzymes and hence the large concentrations that would be needed to determine the K_M of PEP in the presence of 3-deoxyE4P, this has not been determined.

4.3.3 *P. furiosus* DAH7P synthase

When racemic 3-deoxyE4P was initially tested with the type $1\beta_D$ DAH7P synthase from *P. furiosus*, it did not appear to be a substrate. However, the pure (R)-form of 3-deoxyE4P was a substrate, with a K_M of 200± 30 and k_{cat} of 2.1±0.1, suggesting that the (S)-form of 3-deoxyE4P, the form with different stereochemistry to E4P itself is acting as an inhibitor of the enzyme. This could be tested by synthesising (S)-3-deoxyE4P from (S)-malic acid, using the synthetic scheme described in Section 4.2.3. The inability of *P. furiosus* DAH7P synthase to accept the opposite stereochemistry of 3-deoxyE4P is in contrast to the observed behaviour with 2-deoxyE4P, where both enantiomers are able to act as a substrate.

While the binding of 3-deoxyE4P to *P. furiosus* DAH7P synthase is significantly reduced compared to that of E4P (the E4P K_M with *P. furiosus* is 9±1[20]), the k_{cat} is very

similar (E4P k_{cat} is 1.4±0.1[20]). This pattern is seen in all the alternative substrates tested with *P. furiosus* DAH7P synthase to date, except for 2-deoxyE4P, which has both a lower K_M and higher k_{cat} than E4P itself. 3-DeoxyE4P has a lower K_M than that for the five-carbon analogues tested with *P. furiosus* DAH7P synthase, but is a significantly poorer substrate than 2-deoxyE4P or E4P itself. The PEP K_M in the presence of 3-deoxyE4P, is slightly decreased, with a K_M of 27µM, compared to 93µM in the presence of E4P.
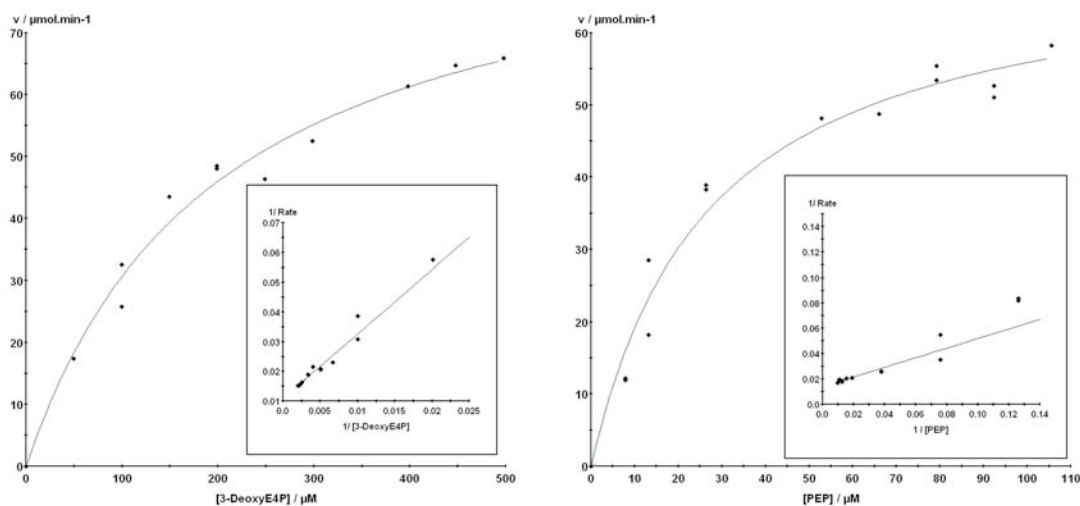
Figure 4.10: Michaelis–Menten and Lineweaver-Burk plots for determination of K_M values for (*R*)-3-deoxyE4P and PEP in the presence of (*R*)-3-deoxyE4P with *P. furiosus* DAH7P synthase. The reaction mixtures for the determination of the K_M of 3-deoxyE4P consisted of PEP (200µM), MnSO$_4$ (100µM), (*R*)-3-deoxyE4P (50-800µM) and purified *P. furiosus* DAH7P synthase (2.5µL, 9.0mg/mL) in 50mM BTP buffer, pH 6.8 at 60˚C. The reaction mixtures for the determination of the K_M of PEP consisted of (*R*)-3-deoxyE4P (500µM), MnSO$_4$ (100µM) PEP (13-160µM) and purified *P. furiosus* DAH7P synthase (2.5µL, 9.0mg/mL) in 50mM BTP buffer, pH 6.8 at 60˚C. The reaction was initiated by the addition of 3-deoxyE4P and carried out at 60˚C in a total volume of 1mL. K_M and k_{cat} values were determined by fitting the data to the Michaelis–Menten equation using Enzfitter (Biosoft).

4.3.4 *M. tuberculosis* DAH7P synthase

3-DeoxyE4P is also a poor substrate for *M. tuberculosis* DAH7P synthase, which has an apparent K_M value of 25±3µM for E4P, 37±3µM for PEP and a k_{cat} value of 3.1±0.1.[31] The apparent K_M value of 3-deoxyE4P is significantly larger than that for E4P, but as seen for *P. furiosus* DAH7P synthase, the k_{cat} is not as affected by the use of the alternative substrate. There is little difference in the apparent K_M of PEP in the presence of 3-deoxyE4P.
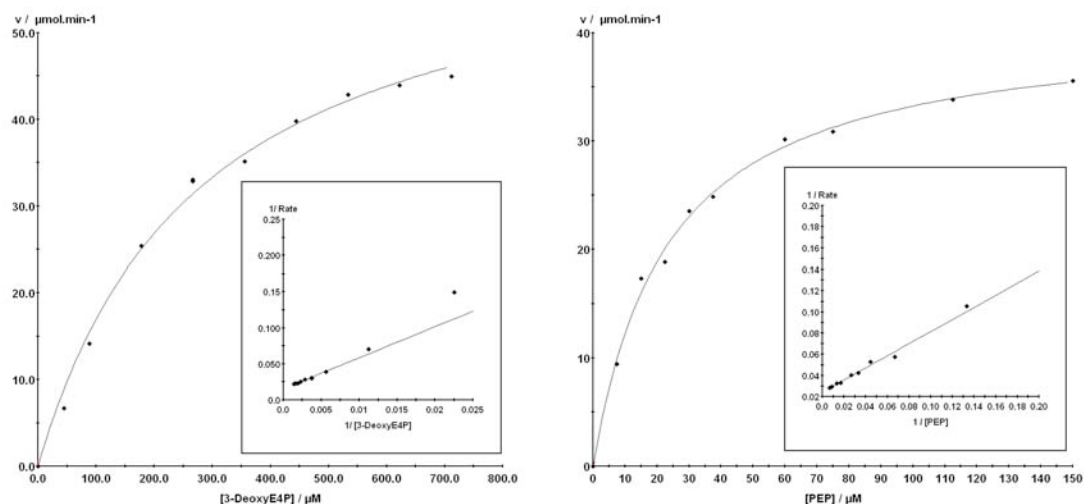
Figure 4.11: Michaelis–Menten and Lineweaver-Burk plots for determination of K_M values for (R)-3-deoxyE4P and PEP in the presence of (R)-3-deoxyE4P with *M. tuberculosis* DAH7P synthase. The reaction mixtures for the determination of the K_M of 3-deoxyE4P consisted of PEP (300µM), MnSO$_4$ (100µM) and 3-deoxyE4P (44µM-2.7mM), in 50mM BTP buffer, pH 6.8. The reaction mixtures for the determination of the K_M of PEP consisted of (R)-3-deoxyE4P (500µM), MnSO$_4$ (100µM) and PEP (8-150µM) in 50mM BTP buffer, pH 7.5. The reaction was initiated by the addition of purified *M. tuberculosis* DAH7P synthase (5µL, 4.6mg/mL) and carried out at 30°C in a total volume of 1mL. K_M and k_{cat} values were determined by fitting the data to the Michaelis–Menten equation using Enzfitter (Biosoft).

Overall, 3-deoxyE4P is a very poor substrate for DAH7P synthases from all the organisms tested, which represent type Iα, Iβ and type II enzymes. The K_M values tend to be significantly higher, and rates of reaction in most cases are slightly slower. The C3-hydroxyl group seems to be more important for binding to the enzyme than the C2-hydroxyl investigated in chapter three. The implications of these results for the reaction mechanism of DAH7P synthase is discussed further in chapter five.

4.4   Proof of product formation

The thiobarbituric acid test was used to determine whether the slow, enzyme-catalysed reaction observed between PEP and 3-deoxyE4P was producing the expected product 6-deoxyDAH7P **77**. The thiobarbituric acid assay is a colourimetric method for the detection of of 3-deoxyaldulosonic acids.[122] In this test, NaIO$_4$ is used to cleave any

1,2-diols in the molecule. This test is useful for detecting the presence of DAH7P or KDO8P in solution.[15] In DAH7P (or KDO8P), cleavage of the 1,2-diol gives β-formyl pyruvate **78**, which reacts with thiobarbituric acid to give a pink complex that can be spectrophotometrically detected at 549nm ($\varepsilon = 1.03 \times 10^5 \, M^{-1} cm^{-1}$). It could not be used for product characterisation in the reaction between 2-deoxyE4P and PEP, due to the product not having the necessary 1,2-diol for cleavage by $NaIO_4$ to give β-formyl pyruvate. However, it can be used to detect the presence of 6-deoxyDAH7P, formed through the reaction of PEP with 3-deoxyE4P.
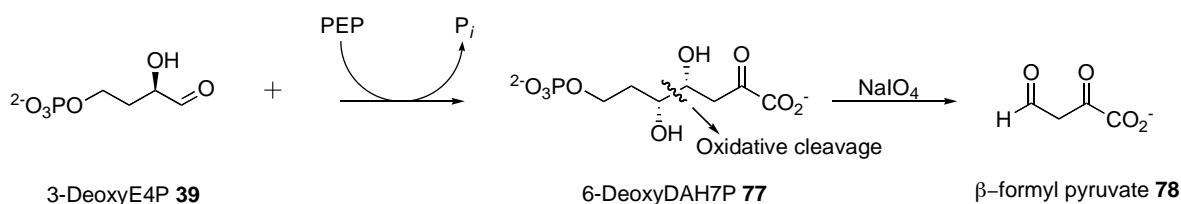
Figure 4.12: Thiobarbituric acid test

This test, carried out with DAH7P synthase from *E. coli* and the type II enzymes *M. tuberculosis* and *H. pylori*, with E4P used as a control, all produced a dark, pink-coloured compound and absorbed light at 549nm, which is consistent with the formation of a DAH7P-like product.

4.5   Use of erythronic lactone to synthesise fluorinated E4P analogues

As we had already developed synthetic schemes using γ-butyrolactones to synthesise 2- and 3-deoxyE4P, it was considered that some of this chemistry may be applied in the synthesis of other E4P analogues, in which the hydroxyl groups are replaced with something else. We were particularly interested in replacing the hydroxyl groups with fluorine as fluorine has a similar electronegativity as a hydroxyl group, without the ability to be a hydrogen-bond donor. Analogues of E4P where the hydroxyl group is replaced with a fluorine may help in determining the important interactions in the binding of E4P to the enzyme.

Figure 4.13 outlines the initial approach that was taken. It was proposed to protect one of the secondary hydroxyls of erythronic lactone, and then use diethylaminosulfur trifluoride (DAST) to fluorinate the remaining hydroxyl. DAST works by replacing a hydroxyl group with a fluorine in an S_N^2-type reaction, and hence the stereochemistry at the carbon involved is inverted. As we are interested in both 2- and 3-deoxy analogues, the expected lack of regiocontrol in the benzylation reaction was not considered to be a problem, as both potential products **79** and **80** could be carried through to synthesise the E4P analogues **84** and **85**. Even the dibenzylated product **81** which we would also expect to be formed is potentially useful in the synthesis of E4P **1** which although commercially available is relatively expensive.
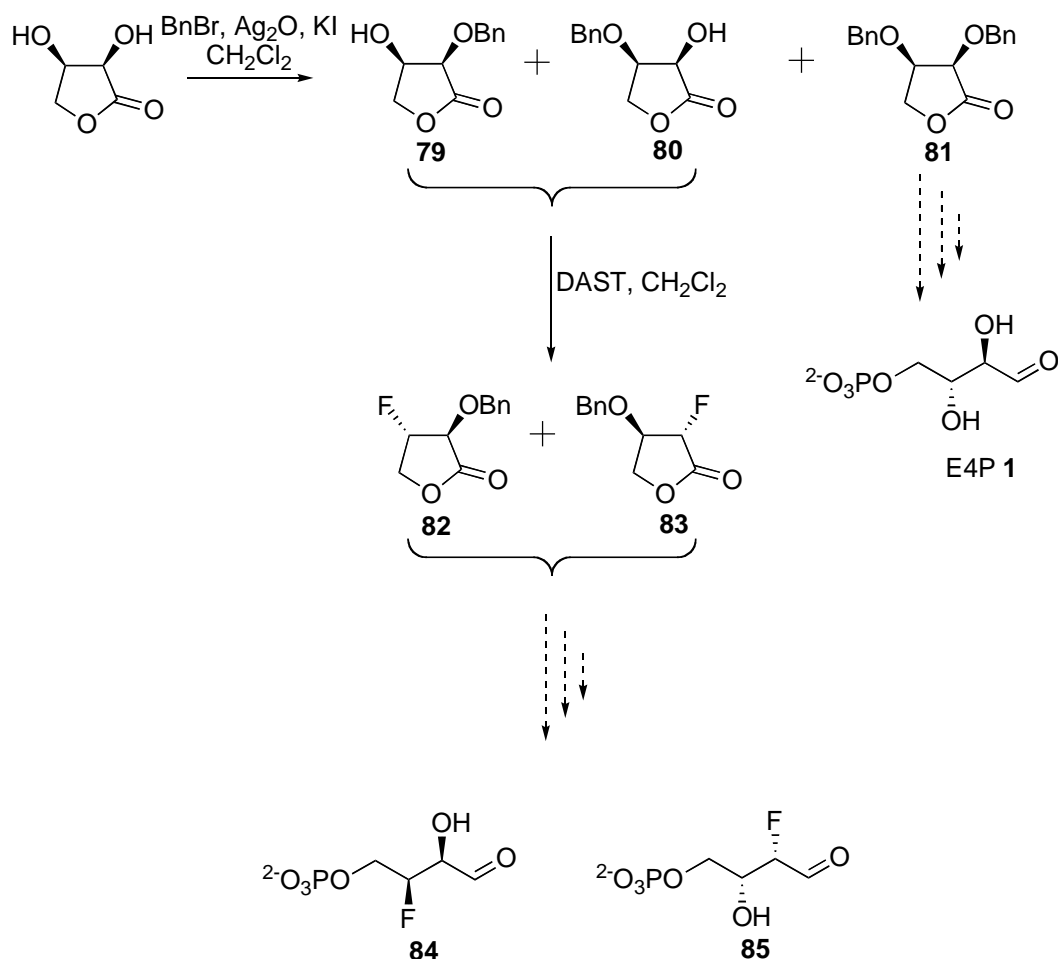
Figure 4.13: Potential route to fluorinated E4P analogues

There is little information in the literature to support such a strategy, although Dunigan and Weigel[123] have reported a regioselective tosylation at the C2-hydroxyl of erythronic lactone and Flasche and Scharf[124] have reported selective benzylation at the same

position. The fluorination of (S)-α-hydroxy-γ-butyrolactone with DAST has also been previously reported by Shiuey *et al.*[125]

Benzylation of erythronic lactone was attempted using the same reaction conditions previously found to be successful in the benzylation of lactones; benzyl bromide, silver oxide and potassium iodide, in two different solvents, CH_2Cl_2 and DMF.[101-103] The reaction in CH_2Cl_2 showed two major spots by TLC. The higher R_F spot was identified by NMR as the dibenzylated product **81**, with a yield of 21%, and the lower R_F spot identified as a mixture of both monobenzylated products **79** and **80**, evidenced by the two sets of benzyl protons in the ^1H NMR spectrum which were present in approximately a 1:1.7 ratio. The two monobenzylated products **79** and **80** combined had a yield of only 31% and were not able to be separated by flash chromatography. The addition of less benzyl bromide reduced the yield of **81**, but was unsuccessful in increasing the yield of **79** and **80**. As well as this, there were solubility issues with erythronic lactone in CH_2Cl_2, suggesting that the reaction was unlikely to be high yielding, hence an alternative solvent was used.

The same reaction in DMF had a different outcome. Again, two major spots were isolated, however, there was no evidence of any **80** being formed. The higher R_F spot with a yield of 35% was identified by ^1H NMR as the elimination product **86** resulting from loss of the acidic proton on C2 and the hydroxyl (or benzyl) group on C3 (Figure 4.14). The lower spot was identified as a single, monobenzylated compound, with 18% yield. This corresponded to the isomer that was present in larger amounts in the CH_2Cl_2 reaction. Distinguishing which of the two regioisomers (**79** or **80**) had been formed was difficult. It was assumed that assignment would become easier once the remaining hydroxyl was replaced by a fluorine, as ^{13}C-^{19}F coupling would enable assignment of the spectra, however, difficulties were encountered in the fluorination reactions. As it is reported in the literature that both tosylation and benzylation of erythronic lactone led to only the C2-protected compound, it was assumed at this point that the product formed was **79**.

86
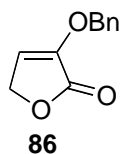
Figure 4.14: Elimination product **86** from the benzylation of erythronic lactone in DMF

In order to try to increase the yield of the desired compound **79** and reduce the amount of elimination product **86**, the reaction temperature was reduced to -26°C. Dunigan *et al*[123] in their tosylation reaction found that the lowered temperature resulted in a higher yield of the desired product, while reducing the likelihood of elimination. However, this was not successful in this case. Although a lower yield of **86** was detected, there was no increase in the amount of the desired product **79** formed. Reducing the reaction time also reduced the amount of **86** formed, but with no apparent corresponding increase in the amount of **79** formed.

With the small amount of monobenzylated product that had been formed, some fluorination reactions with DAST were investigated. Firstly, in order to confirm that the lactones could be fluorinated with DAST without opening up the lactone ring, the reaction was trialed on α-hydroxy-γ-butyrolactone (Figure 4.15). The fluorination conditions described by Mikhailopulo for carbohydrate fluorinations were used.[126] The substrate was first dissolved in CH_2Cl_2 at room temperature and an excess of DAST added. The reaction proceeded cleanly, with a 60% yield of **87** isolated. Previous reports have shown **87** to be volatile, which probably accounts for the other 40% as TLC analysis suggested the starting material was fully converted to a single product.[125] ^{1}H NMR analysis indicated that fluorination of the lactone had occurred, with a large [1]H-^{19}F coupling evident in the H2 signal. The ^{19}F NMR spectrum showed a peak appearing as a doublet of doublet of doublets, due to coupling interactions with H2 and both H3s.

87

Figure 4.15: Fluorination of α-hydroxy-γ-butyrolactone with DAST

-92-

The same reaction was carried out on the mixture of benzyl erythronic lactone regioisomers **79** and **80** formed in the CH$_2$Cl$_2$ reaction described above. After stirring for two hours, TLC analysis showed the formation of one new, less polar product and only a very small amount of starting material. ^{19}F NMR analysis of the crude product was consistent with the presence of both possible fluorinated products **82** and **83** (Figure 4.16). There was a signal appearing as a doublet of doublets, consistent with the formation of **83** and another peak appearing as a doublet of doublet of doublet of doublets, consistent with the formation of **82**.
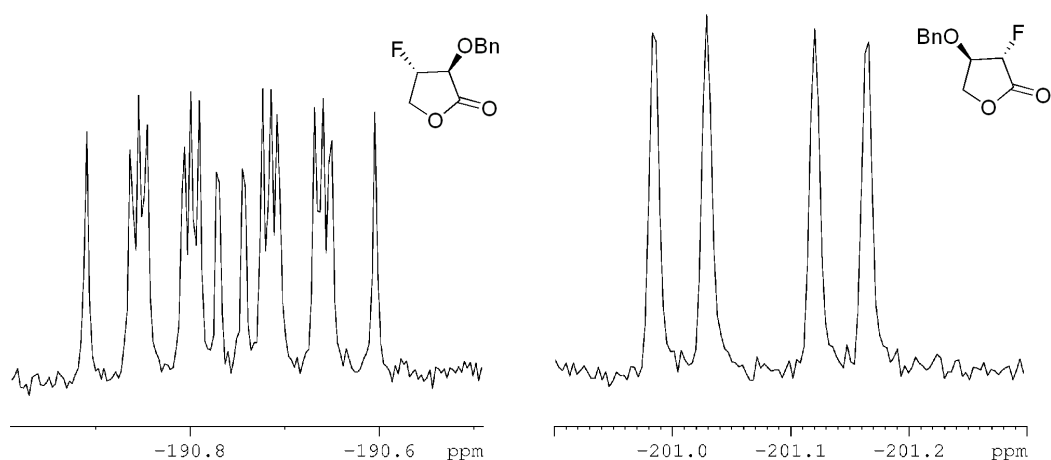
Figure 4.16: ^{19}F NMR spectra (376MHz) of **82** (left) and **83** (right)

However, purification of the crude product gave only 17% of the theoretical yield. Some elimination product **86** resulting from the loss of HF across the C2-C3 bond was also isolated. Further attempts to fluorinate both mixtures of **79** and **80** and the single monobenzylated compound formed in the DMF reaction have been unsuccessful. Although TLC analysis of the reaction mixtures show only the fluorinated product to be present, it is not able to be isolated with any reasonable yield and only **86** is detected after work-up. Clearly the product **82** is being formed, but is undergoing rapid base-catalysed elimination to form **86**.

Since the benzylated erythronic lactone has been found to be so unstable, the use of alternative protecting groups has been investigated. It was anticipated that the use of a bulkier protecting group would reduce the amount of diprotected product formed. The remaining hydroxyl group could then be protected with a benzyl group and the lactone reduced to the lactol to reduce the likelihood of elimination occurring as the C2 proton

would no longer be acidic. Some of the chemistry already developed on the α-and β-hydroxy-γ-butyrolactones (described in chapters three and four) may then be used, with the fluorination carried out later in the synthesis.

The use of silyl groups were investigated due to the possibility that these groups could be removed and fluorination carried out in one step, reducing the number of steps necessary.

Firstly it was attempted to protect with a *tert*-butyldimethylsilyl (TBDMS) group in CH_2Cl_2 with TBDMSCl and imidazole.[127] This resulted in a low yield (38%) of monosilylated compound **88**, as well as a reasonable amount of disilyated product **89** (20%). It was however, encouraging that by ^{1}H NMR spectroscopy, there appeared to be only one of the two possible regioisomers. The same reaction in DMF was more encouraging, with a yield of 67% of a single monosilylated product **88** and only a 5% yield of **89**. The monosilylated product formed in each case was the same isomer, as they were identical by both ^{1}H and ^{13}C NMR spectroscopy. Although it is difficult to determine by NMR analysis which isomer has been formed, prior experience reported in the literature has led us to assume that the C2-protected, rather than the C3-protected product has been formed.
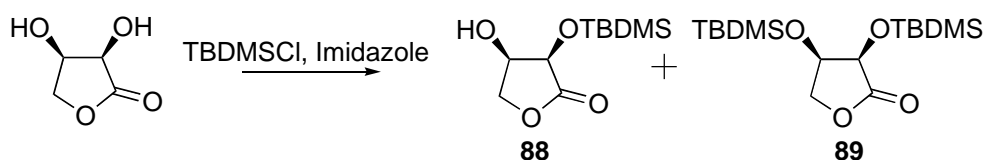
Figure 4.17: Protection of erythronic lactone with TBDMSCl

Benzylation of the remaining 2° alcohol of **88** was carried out under the same conditions as previously used. Unfortunately, this time it was not successful, with the yield only 30% in CH_2Cl_2 and no product at all was detected from the reaction in DMF.

 The next step planned in this synthesis was to reduce the lactone to a lactol using DIBAL at -78°C and then protect the aldehyde formed with 2,2-dimethylpropane-1,3-diol as originally carried out in the synthesis of 2-deoxyE4P from β-hydroxy-γ-butyrolactone. However, this has not been investigated due to the limited availability of DIBAL and the small amounts of diprotected lactone that were able to be formed. An

alternative route could involve reduction of the lactone to the diol with lithium aluminium hydride. The biggest disadvantage with this route is the resulting lack of control over the two 1° alcohols formed, one of which needs to be phosphorylated, while the other oxidised to the aldehyde. If starting materials were unlimited this would not be so much of an issue, as both possible combinations may be useful. Erythronic lactone is expensive, so at this point, it was decided not to continue with these investigations.

4.6   Synthesis of 3-deoxyA5P

In order to compare the reactivity of the two enzymes DAH7P and KDO8P synthase, 3-deoxyA5P was required. Unlike 2-deoxyR5P, This is not commercially available. However, it has been reported that this compound is not a substrate or an inhibitor for KDO8P synthase from *E. coli*.[44] The synthesis of 3-deoxy-3-aminoA5P from methyl 2,3-anhydro-D-*lyxo*-furanoside **94**[44] has also been reported. Methyl 2,3-anhydro-D-*lyxo*-furanosides are potentially useful intermediates for the synthesis of a variety of substituted A5P derivatives *via* epoxide openings with the required nucleophile. We used the method outlined by Thome *et al*[128] to produce the intermediate methyl 2,3-anhydro-D-lyxofuranoside **94** which was then used to synthesise 3-deoxyA5P, as well as investigating the formation of other A5P analogues.
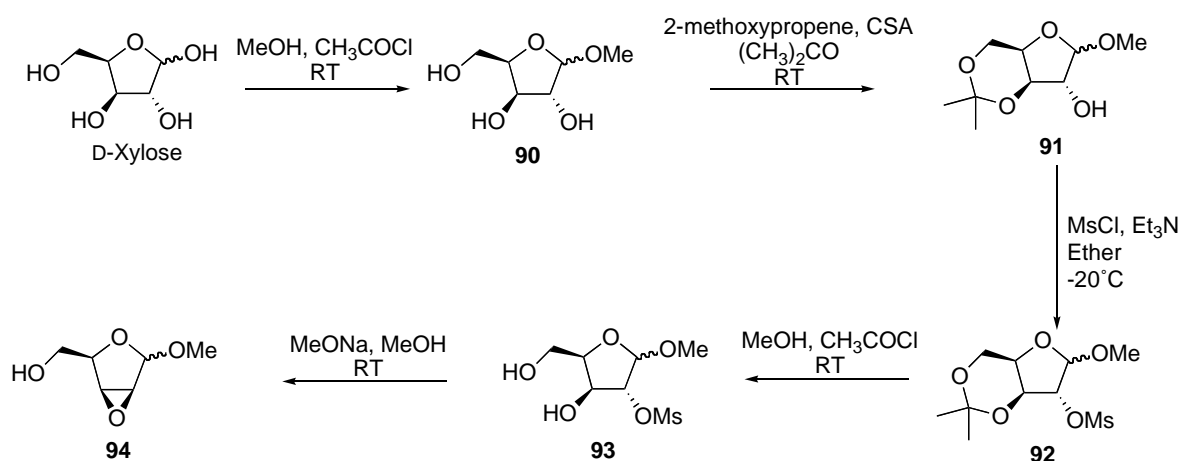
Figure 4.18: Synthesis of 2,3-anhydro-D-*lyxo*-furanoside from D-xylose

The synthesis of methyl 2,3-anhydro-D-*lyxo*-furanoside **94** from D-xylose is outlined in Figure 4.18. The methyl glycoside of D-xylose **90** was formed by stirring D-xylose overnight in MeOH and acetyl chloride. Treatment of glycoside **90** with 2-methoxypropene in acetone with a catalytic amount of camphor sulfonic acid at 0°C gave the acetal **91** after three hours of stirring. At this point, the two anomers were able to be separated by flash chromatography. However, as pure product was not necessary for the rest of the synthesis to work satisfactorily, the bulk of the crude product was carried through to the next step without purification or separation of the two anomers. An aliquot was purified for NMR analysis and characterisation of the two anomers. These were identified using ^{1}H NMR spectroscopy by the acetal proton at 4.83ppm or 5.18ppm for the two different anomers. The lack of coupling to H1 in one of the anomers suggests that it is the β-anomer, whereas an H1-H2 coupling is evident for the α-anomer.[129] The α-anomer was eluted first, as evidenced by the ^{1}H NMR spectrum, which showed a doublet acetal proton at 4.83ppm.

Mesylation at the 2-position of crude **91** was carried out at -20°C with mesyl chloride and triethylamine in ether to give a 78% yield of crude mesylate **92**. To deprotect the 3,5-acetal, **92** was stirred in MeOH and acetyl chloride at room temperature. After two hours, TLC analysis indicated the deprotection was complete and two equivalents of sodium methoxide in MeOH were added drop-wise to the solution. After stirring overnight the reaction was complete and the two anomers of **94** were separated easily by flash chromatography, with the α-anomer being eluted first, giving an overall yield of 33% with approximately a 1:1 ratio of the two anomers. The ^{1}H and ^{13}C NMR data was consistent with that published in the literature.[128]

There are two possible products from epoxide opening with a hydride ion, resulting in either *arabino* or *xylo* stereochemistry (Figure 4.19). Reports in the literature suggest that the epoxide opening reaction tends to be regioselective, giving predominantly the C3 substituted product with *arabino* stereochemistry, as opposed to the *xylo* stereochemistry resulting from attack at the C2 position.[130] The factors that govern this preference are not fully understood, as there should be minimal difference in steric hindrance to attack at C3 or C2. One proposed explanation is that the partial positive charge formed during the S_N2 reaction is more favorable at C3 than C2, due to C3 being further away from the electron withdrawing anomeric centre.[131] The regioselectivity is

observed for both the β-and α-anomers, and in some cases, slightly higher regioselectivity is seen for the α-anomer, presumably due to steric affects.[132] This regioselectivity has been exploited with varying success for the introduction of a variety of nucleophiles to the β-anomers, such as hydride,[131] amine and azide ions,[133,131] alkoxide[131] and fluoride ion.[130,132,134,135]

To open the epoxide with a hydride ion, the method described by Mastihubová and Biely was used.[136] Three equivalents of lithium aluminium hydride were suspended in THF and cooled to 0°C. α-Epoxide was added dropwise to the suspension and the mixture allowed to warm slowly to room temperature. After stirring overnight, the major product was isolated in 70% yield following purification.
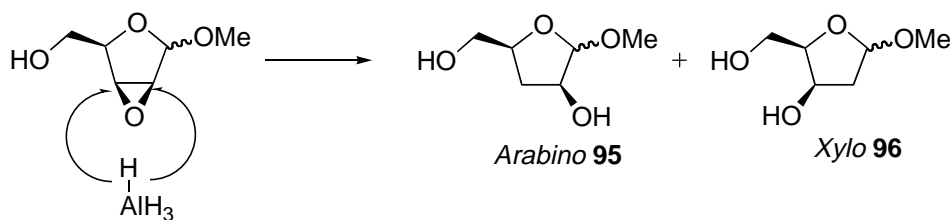
Figure 4.19: Potential products from the epoxide opening of **94** by the hydride ion

^{1}H and 2D NMR experiments were used to identify the major product as having the *arabino* stereochemistry **95**, formed by hydride attack on C3, rather than C2. The ^{1}H NMR spectrum is shown in Figure 4.20. H1 is a singlet with no apparent coupling. This supports the *arabino* stereochemistry, as the vicinal Karplus correlation predicts that the coupling constant for the *trans* protons will be zero.[129] If there were two protons on C2, then one would be *cis* to the C1 proton and the H1 peak would be expected to be a doublet. The C2 proton at 4.1ppm appears to have something else under it, presumably the C2-hydroxyl proton, as a weak coupling interaction is seen in the 2D spectrum, and the peak is very broad and integrates for two protons. 2D data confirms that this peak is H2, as it is coupled to one of the geminal upfield H3 protons. H3b at 2.5ppm, which is *cis* to H2 shows coupling to H2, the geminal H3b and H4, which it is also *cis* to, so displays as a doublet of doublet of doublets. H3a in contrast is a doublet of doublets, only showing coupling to the geminal H3b as well as a weak coupling to the *trans* H4. H4, as already mentioned, couples to both H3 protons, with a larger coupling constant to the *trans* H3a then the *cis* H3b.

A very faint second spot was observed on the TLC, with a smaller R_f, which may be attributed to the other product with the *xylo* stereochemistry, but the mass of this was only 3mg, giving a *arabino*:*xylo* ratio of at least 26:1.
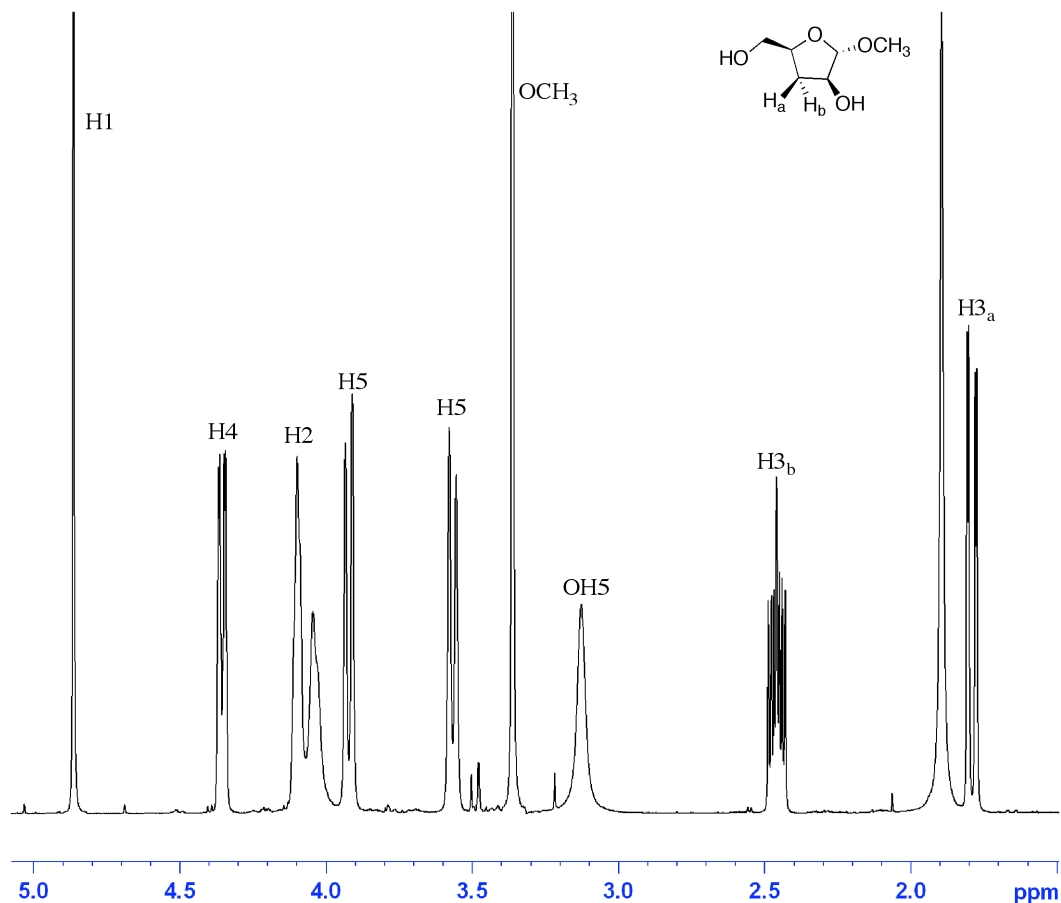
Figure 4.20: ^{1}H NMR spectrum (400MHz) of the α-anomer of **95**

Following opening of the epoxide, the 1° alcohol was phosphorylated using diphenylchlorophosphate and imidazole in dichloromethane to give a 37% yield of the 1° phosphorylated compound **97**, as well as an 18% yield of diphosphorylated compound **98**. It is anticipated that varying reaction conditions will enable this yield to be improved, although due to time constraints, this has not been trialled. Analysis of purified **97** gave further evidence that the starting material was the *arabino* stereochemistry as ^{13}C-^{31}P coupling was evident in the C4 and C5 peaks in the ^{13}C NMR spectrum. The 1° phosphorylated compound **97** was treated to hydrogenolysis with H_2 gas over PtO_2 overnight, the MeOH removed *in vacuo* and the remaining oil redissolved in D_2O to allow for NMR analysis of the removal of the methyl glycoside group.
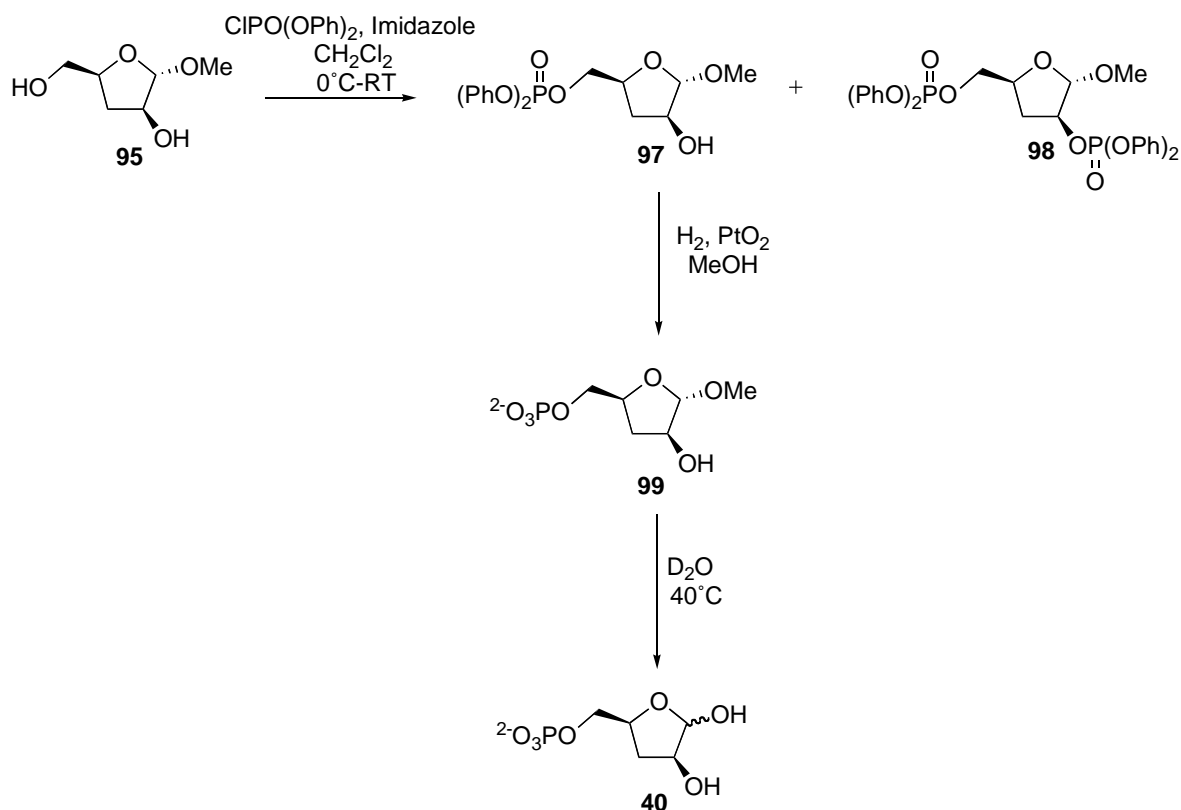
Figure 4.21: Synthesis of 3-deoxyA5P

The ^{1}H NMR spectrum of **99** in D$_2$O after hydrogenolysis and subsequent heating to 40°C overnight is shown in Figure 4.22. The ^{1}H NMR spectrum of **99** showed an absence of any peaks in the 7-8ppm region, confirming removal of the phenyl protecting groups from the phosphorus. The methyl glycoside peak at 3.24ppm remained, although there was a small peak beside it at 3.19ppm, indicating that a small amount of the methyl glycoside had been cleaved already. Heating the substrate to 40°C resulted in the methylglycoside peak becoming smaller as the methyl glycoside was removed and the methanol peak beside it became larger. The H1 peak at 4.81ppm also became smaller and another peak formed at 5.15ppm as the anomeric hydroxyl is released and both α- and β-anomers are formed. Eventually, after overnight heating, no further deprotection could be observed, even after heating to 60°C, so the solution was used in enzyme assays with some methylglycoside still remaining. The 3-deoxyA5P formed was then tested as a substrate for KDO8P synthase from *N. meningitidis*. As previously reported for the *E. coli* enzyme,[44] it was not a substrate. It was also found to not be a substrate for DAH7P synthase from *P. furiosus*. This is unsurprising given that

racemic 3-deoxyE4P had already been found to not be a substrate. The configuration at the 2-position of (*S*)-3-deoxyE4P (the opposite configuration to natural) is the same as the C2 configuration of 3-deoxyA5P.
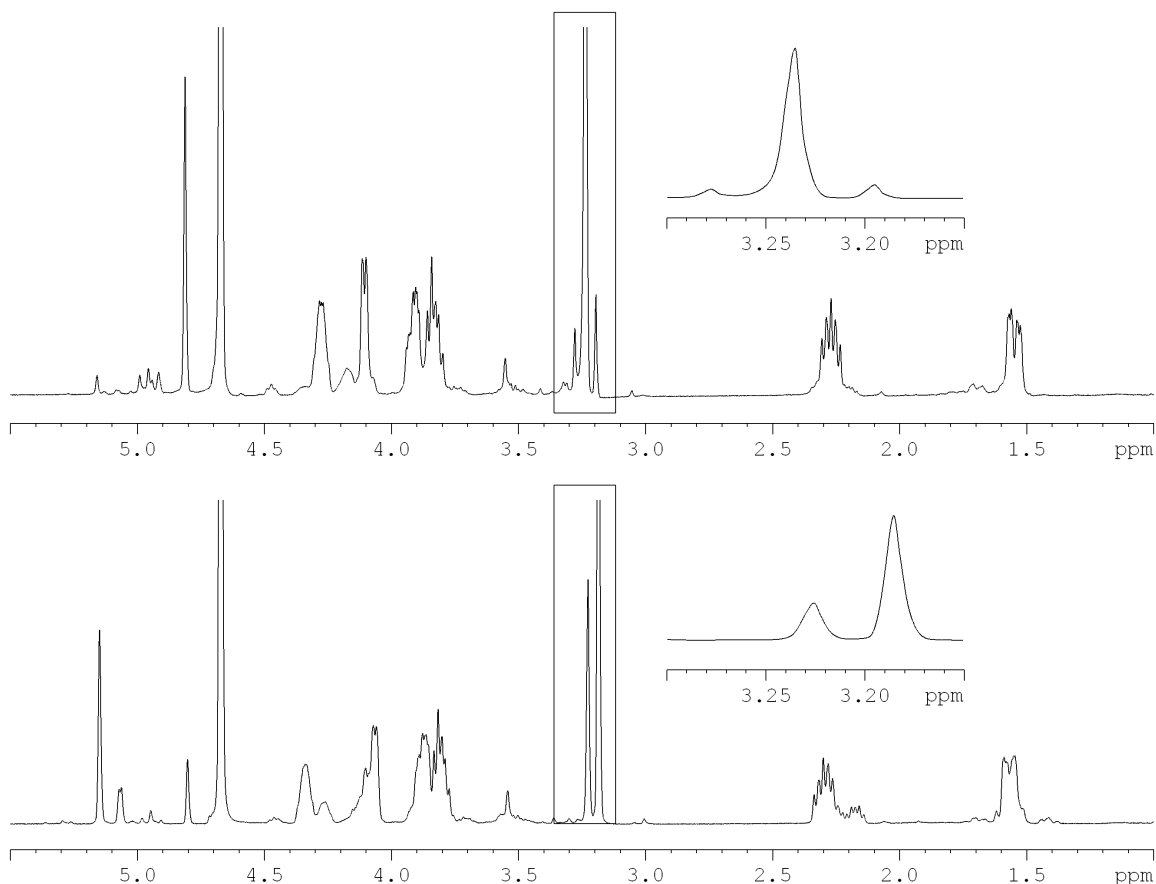
Figure 4.22: ^{1}H NMR spectra of **99** (top) and 3-deoxyA5P **40**

4.7 Investigation of methyl 2,3-anhydro-D-*lyxo*-furanoside as a precursor to C3-fluorinated A5P analogues

As part of our investigation of the role of the 3-hydroxyl group of A5P in the KDO8P synthase reaction, we also wished to open the epoxide moiety with other nucleophiles. Specifically fluorine, as it has a similar electronegativity to oxygen, whilst not having the ability to participate in hydrogen-bonding, which would allow us to further investigate the nature of the interaction of the 3-hydroxyl with the enzyme.

Wright and Taylor[135] reportedly opened the epoxide of α-methyl 2,3-anhydro-5-*O*-benzyl-D-*lyxo*-furanoside **100** with a fluoride ion. By treatment with sodium fluoride and potassium hydrogen fluoride at reflux in ethylene glycol they found that only the *arabino* stereochemistry was formed. A later publication[137] describing the same reaction on β-methyl 2,3-anhydro-5-*O*-benzyl-D-*lyxo*-furanoside **100** found that a mixture of *arabino* and *xylo* stereochemistry was formed with 31% and 23% yields respectively. Several studies since have used this same method, with differing results. Lim *et al*[132] used the same reaction conditions to fluorinate both α- and β-2,3-anhydro-D-*lyxo*-furanoside **94** and reported a 96% and 82% yield respectively, with only *arabino* stereochemistry formed, however, no experimental details were included in this report. Mikhailopulo[126] also cited Wright and Taylor's method for the fluorination of both α- and β-anomers of 2,3-anhydro-5-*O*-benzyl-D-*lyxo*-furanoside **100** and found that contrary to what had been previously reported, only the *arabino* stereochemistry was formed in both instances, with a 45% yield for the α-anomer and 31% for the β-anomer.
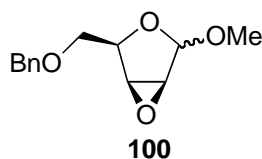
Figure 4.23: Methyl 2,3-anhydro-5-*O*-benzyl-D-*lyxo*-furanoside **100**

The fluorination of 2,3-anhydro-D-*lyxo*-furanoside **94** using the reaction conditions described by Wright and Taylor were investigated in this study (Figure 4.24).[135] It was initially attempted to fluorinate the α-epoxide on a small scale (~0.1mmol) with 2 equivalents of KHF_2 and 3.5 equivalents of NaH heated to reflux in ethylene glycol. After a reaction time of three hours, TLC analysis indicated that all the starting material had disappeared and two higher R_F products were evident. ^{19}F NMR analysis of the crude material showed a doublet of doublet of doublets due to coupling with H3, H4 and H2, and so was potentially the desired product **101** (Figure 4.25), but the yield was too low to allow for purification. A scale-up of this reaction to 0.5mmol gave the same result by ^{19}F NMR, but no more product was formed.
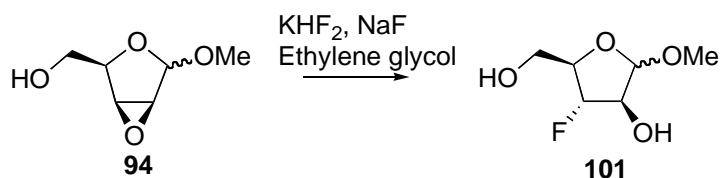
Figure 4.24: Fluorination of epoxide **94** to give **101**

Attempts to fluorinate the β-epoxide were no more promising. Before carrying out the reaction, the ethylene glycol was distilled and the KHF$_2$ and NaF dried under vacuum. TLC analysis after heating of the reaction mixture overnight revealed a lower R$_F$ spot as well as evidence of remaining starting material. ^{19}F NMR analysis of the crude material looked promising, with only one peak, a doublet of doublet of doublets, but after flash chromatography, the yield of purified product was only 13%, still much lower than the yield of 45% reported by Mikhailopulo *et al*. The scale-up of this reaction however was again unsuccessful, the percentage yield was lower in the larger scale reaction.
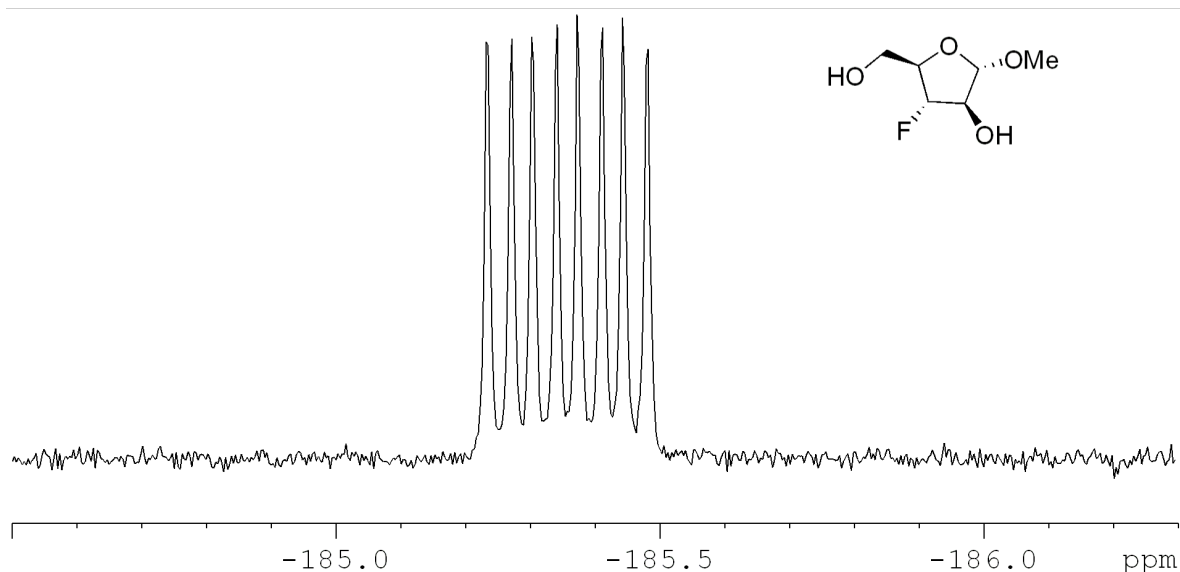
Figure 4.25: ^{19}F NMR (376MHz) of **101**

It was decided to attempt to protect the primary alcohol prior to the fluorination. The literature suggested that the fluorination could be carried out with a benzyl group on the 1° alcohol.[137] This would allow for easier TLC visualisation as the product would then be visible by UV light. Also, it was suspected that unreacted starting material was being lost during the aqueous work-up and a non-polar group on the primary alcohol may prevent this from occurring. The reaction conditions used previously for the benzylation of the lactones were used (Figure 4.26).[101-103] The β-epoxide was stirred

with benzyl bromide, silver oxide and potassium iodide in dichloromethane. Even after stirring for twenty-hours TLC indicated a large amount of starting material remained as well as a higher R_F spot which after purification was identified as the desired methyl 2,3-anhydro-5-*O*-benzyl-D-*lyxo*-furanoside **100**. However, the yield was very low and hence the same reaction was carried out using DMF as a solvent instead of dichloromethane. However, this proved no more successful, as again, a lot of starting material remained after stirring overnight. ^{1}H NMR analysis of the product formed in DMF suggested that the epoxide ring had been opened, and benzylation of the primary alcohol had occurred, as the aromatic protons integrated for two benzyl groups, rather than the expected one.
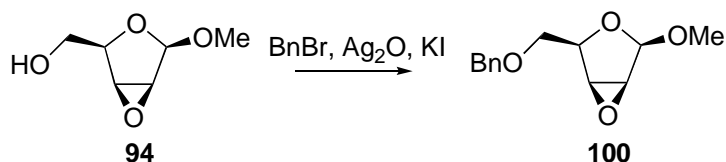
Figure 4.26: Benzylation of **94** to give **100**

It was also attempted to protect the primary alcohol with a phosphate group as that is what was ultimately required at the 5-position. The conditions used for the phosphorylation were the same as previously described; diphenylchlorophosphate and imidazole, in CH_2Cl_2. This reaction provided a 50% yield of the phosphorylated 1°alcohol, however, attempts to then open the epoxide with fluoride ions resulted in the phosphate group being cleaved.

Due to the lack of success in these investigations, this line of work has not been pursued. However, the evidence of some product detected, as well as success reported in the literature suggests that it may be worth revisiting at a later date.

4.8   Summary

The successful synthesis of 3-deoxyE4P has allowed for evaluation of its behaviour with DAH7P synthase from the type Iα (*E. coli* (phe) and *N. meningitidis*), Iβ (*P. furiosus*) and type II (*M. tuberculosis*) DAH7P synthases. It has been found that although 3-deoxyE4P is a substrate for DAH7P synthase from all of these organisms, it is a very poor substrate, with higher K_M and lower k_{cat} values than observed with 2-deoxyE4P, as described in the previous chapter.

Synthesis of 3-deoxyA5P has allowed for evaluation with the non-metallo KDO8P synthase from *N. meningitidis*. There is no evidence that 3-deoxyA5P is a substrate for *N. meningitidis* KDO8P synthase, in agreeance with previous reports from *E. coli* KDO8P synthase. The implication of these results for the kinetic mechanisms of DAH7P and KDO8P synthase is discussed in chapter five.

The synthesis of α-methyl 2,3-anhydro-5-*O*-benzyl-D-*lyxo*-furanoside also allowed for the potential synthesis of other A5P analogues.

CHAPTER FIVE: MECHANISTIC INSIGHT INTO DAH7P AND KDO8P SYNTHASES

5.1 Introduction

This study has explored the substrate specificity of the two enzymes DAH7P and KDO8P synthase. These two enzymes catalyse a similar aldol-like condensation reaction, where the *si* face of PEP attacks the *re* face of E4P or A5P (Figure 5.1).[39,138] Both reactions involve the cleavage of the C-O bond,[34,38] rather than the more usual cleavage of the O-P bond, and both catalyse the reaction by an ordered sequential mechanism in which PEP binds first and the sugar phosphate product is released last.[34,37] As well as the mechanistic similarities, structural studies have shown that the active sites of these two enzymes are very similar.[10,20,22,23,31,68,72] Hence, it has been assumed that the finer details of the mechanisms are also the same.
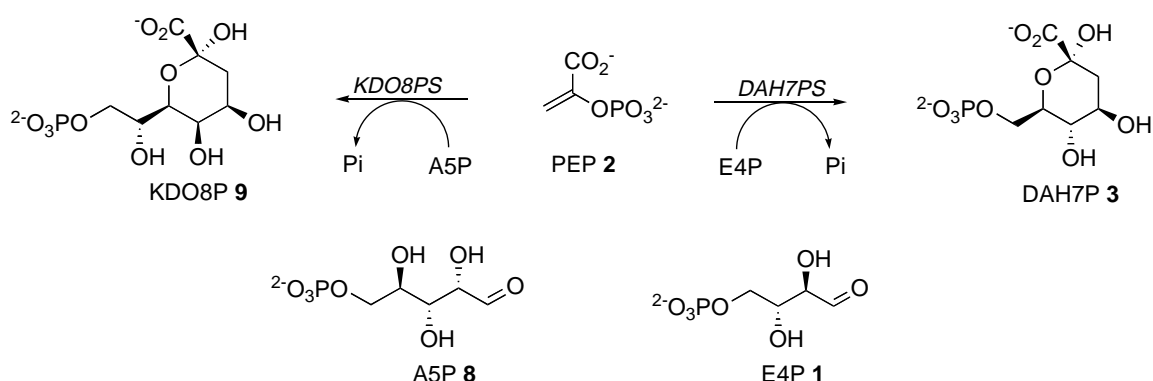
Figure 5.1: The reactions catalysed by DAH7P and KDO8P synthases

Differences between these two enzyme-catalysed reactions include the metal requirement and the phosphorylated monosaccharide substrate preference. All DAH7P synthases characterised to date require a divalent metal ion for activity, whereas both metallo and non-metallo KDO8P synthases have been characterised. The natural substrate for KDO8P synthase, A5P **8,** has different C2 configuration and is one carbon longer than the natural substrate for DAH7P synthase, E4P **1**. The aim of this study was to investigate the roles of the 2- and 3-hydroxyl groups on the substrates E4P and A5P

in the enzymic reactions, in order to gain some insight into the finer details of the mechanisms of these enzyme-catalysed reactions.

5.2 The role of the E4P hydroxyl groups in DAH7P synthase

As well as those outlined within this thesis, other substrate analogue studies carried out with D- and L-threose 4-phosphate (T4P) within our laboratory and other reports in the literature provide some insight into the role of the E4P hydroxyl groups in the DAH7P synthase catalysed reaction. A summary of available kinetic data for E4P substrate analogues with DAH7P synthase available is presented in tables 5.1 and 5.2.

5.2.1 Role of the C2-hydroxyl of E4P

The data presented in table 5.1 indicate that the C2-hydroxyl of E4P is not essential for binding or catalysis in DAH7P synthase. As well as 2-deoxyE4P **38** being shown to be a substrate for all of the DAH7P synthases tested, the analogue D-T4P **102**, with the stereochemistry inverted at C2 is also a substrate for *E. coli* DAH7P synthase (phe) and *P. furiosus* DAH7P synthase. Reports from the literature and studies carried out within our laboratory have also shown that the five-carbon sugars A5P **8** (with the opposite C2 stereochemistry as E4P), R5P **33** (with the same C2 stereochemistry as E4P) and 2-deoxyR5P **34** (with no C2-hydroxyl) (Figure 5.2) are all able to be utilised as substrates (table 5.2).[15,20] All of these alternate five-carbon substrate analogues have been shown to produce DAH7P-like products in the enzyme-catalysed reaction with *E. coli* DAH7P synthase (phe).[15,95]

D-Threose 4-phosphate **102**

Ribose 5-phosphate **33**   2-Deoxyribose 5-phosphate **34**   Arabinose 5-phosphate **8**
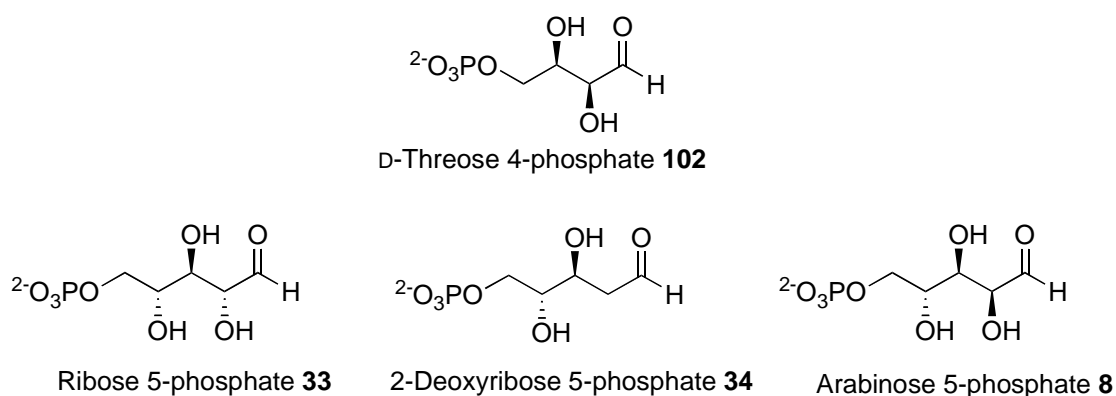
Figure 5.2: Phosphorylated monosaccharides shown to be substrates for DAH7P synthase

Although there have been no structures solved of DAH7P synthase with E4P bound in the active site in a catalytically competent manner, modeling studies with *S. cerevisiae*[68] and *T. maritima*[22] have identified the probable binding site of E4P. These studies have suggested that the carbonyl oxygen of E4P coordinates to the metal ion, activating it for attack. While the C2-hydroxyl of E4P is not essential for this interaction, which ultimately allows the condensation reaction to take place, the interactions it makes with the active site residues are likely to be important in positioning the molecule in the right orientation allowing for the carbonyl to coordinate the metal and in placing the C1 of E4P in an appropriate position to be attacked by C3 of PEP.

These modeling studies with DAH7P synthase have placed the E4P C2-hydroxyl group in a position allowing it to interact with the carbonyl group of the Pro residue of the absolutely conserved LysProArgThr motif in DAH7P synthases. In the Iα enzymes from *E. coli* and *N. meningitidis*, the loss of, or change in orientation of the C2-hydroxyl group has a significant effect on the catalysis reaction, with a 10-20-fold increase in the apparent K_M for both 2-deoxyE4P and D-T4P. This can be explained by the lack of interaction of the C2-hydroxyl with the Pro residue. In 2-deoxyE4P, this interaction would not be possible, and in D-T4P, the C2-hydroxyl is pointed in the wrong direction. The lowered k_{cat} seen for the Iα enzymes can also be explained in that without the C2-hydroxyl holding E4P in the correct orientation, the carbonyl would not always be in a position to coordinate the metal and hence the rate of turnover decreases. The k_{cat} of T4P with *E. coli* DAH7P synthase (phe) is significantly lower than that of 2-deoxyE4P. This may be explained by the C2-hydroxyl forming interactions within the active site and essentially trapping T4P in a less catalytically competent manner. Crystal structures of D-T4P within the active site may explain this further.

Conversely, kinetic analyses of the two substrates 2-deoxyE4P and D-T4P with the Iβ enzyme from *P. furiosus* have shown little effect in the binding and catalysis of these analogues. Intriguingly, 2-deoxyE4P appears to be a better substrate than E4P itself with both a lower apparent K_M and higher k_{cat}. D-T4P is utilised with a similar efficiency to E4P itself. As well as this, the five-carbon sugar analogues A5P, 2-deoxyR5P and R5P have been shown to be utilised by *P. furiosus* DAH7P synthase[20] with a greater efficiency than reported for *E. coli* DAH7P synthase.[15] The crystal

structure of *P. furiosus* DAH7P synthase provides clues about these observed differences in substrate specificities.[20] The Pro residue implicated in E4P binding (Pro61 in *P. furiosus* DAH7P synthase) is located on the β2-α2 loop. The conformation of this loop in the Iα enzymes is constrained by intersubunit interactions to form a dimer, close to the active site. However, in *P. furiosus* DAH7P synthase in solution, these interactions are thought to be absent, resulting in an active site with greater flexibility. In particular, this additional flexibility seems to have an effect on the conformation of Pro61. This conserved Pro is observed in two different conformations in the two subunits of the structure. In the first, it is in the same position as already observed in other structures,[10,16,22] whereas in the adjacent subunit, the carbonyl faces outward, forming a hydrogen bond with a tyrosine from a neighboring subunit in the crystallographic tetramer (Figure 5.3). This flexibility within the active site explains why 2-deoxyE4P and D-T4P are so efficiently used by *P. furiosus* DAH7P synthase.

2-DeoxyE4P is utilised by the type II DAH7P synthase from *M. tuberculosis* with a similar efficiency as seen in *P. furiosus* DAH7P synthase. The apparent K_M of 2-deoxyE4P is only twice that of E4P and the k_{cat} shows little difference between the two substrates. Structural studies on *M. tuberculosis* DAH7P synthase reveal a different intersubunit interface than that of the type I DAH7P synthases. The β2-α2 loop which contains residues that interact with E4P, including the Pro that interacts with the C2-hydroxyl, is involved in dimer formation in the type I DAH7P synthases, but is not in *M. tuberculosis* DAH7P synthase. This lack of involvement of the β2-α2 loop in interdimer interactions may indicate a higher level of flexibility in this region, which could explain the lack of reliance on an interaction with the C2-hydroxyl of E4P for binding and catalysis.
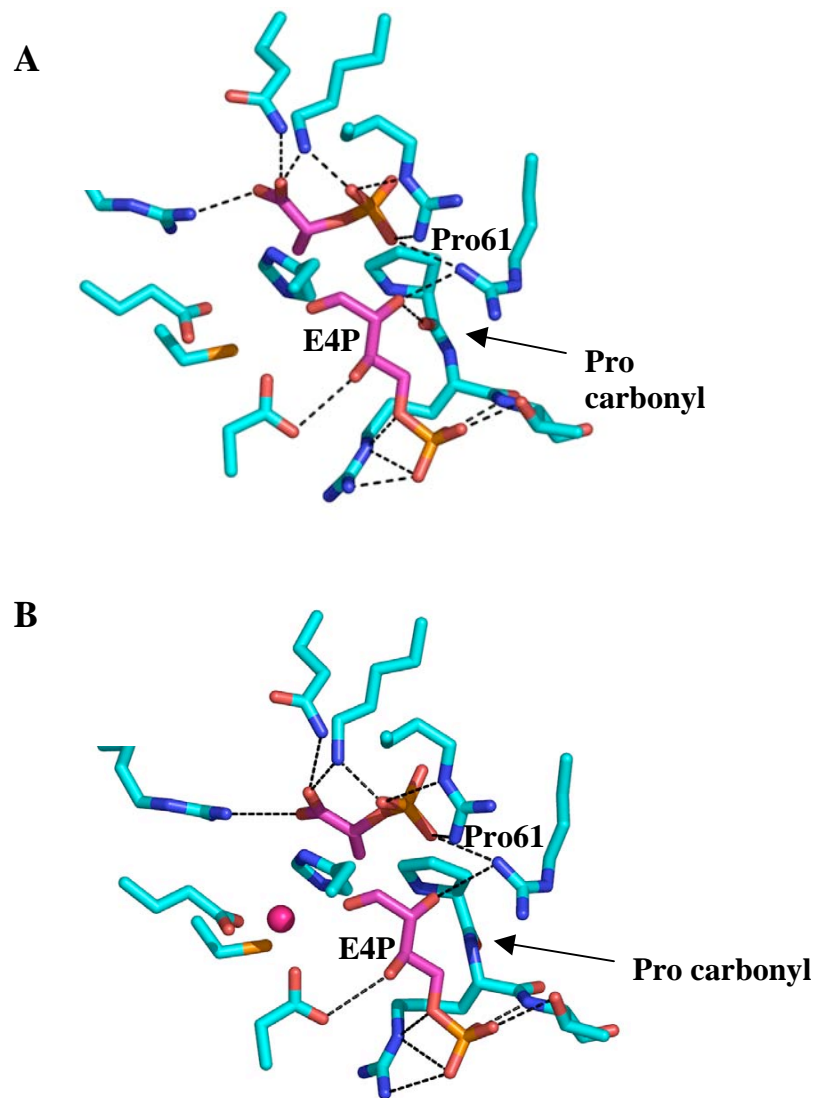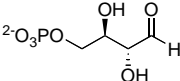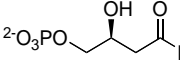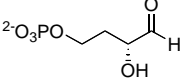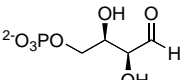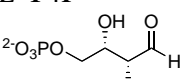
Figure 5.3: Active site of *P. furiosus* DAH7P synthase (PDB code 1ZCO) with E4P modeled in, showing the two different conformations of Pro61. In subunit A, the carbonyl interacts with the E4P C2-hydroxyl. In subunit B, the carbonyl is pointed away from the binding site of E4P.
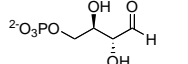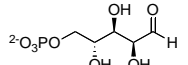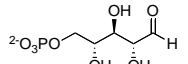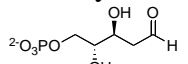
Monosaccharide	*E. coli* DAH7P synthase (phe)			*N. meningitidis* DAH7P synthase			*P. furiosus* DAH7P synthase			*M. tuberculosis* DAH7P synthase		
	K_M (µM)	k_{cat} (s⁻¹)	k_{cat}/K_M (µM⁻¹s⁻¹)	K_M (µM)	k_{cat} (s⁻¹)	k_{cat}/K_M (µM⁻¹s⁻¹)	K_M (µM)	k_{cat} (s⁻¹)	k_{cat}/K_M (µM⁻¹s⁻¹)	K_M (µM)	k_{cat} (s⁻¹)	k_{cat}/K_M (µM⁻¹s⁻¹)
E4P[a]	39±4	26±2	0.67	25±2	9.4±0.1	0.38	9±1	1.4±0.1	0.16	25±3	3.1±0.1	0.12
2-deoxyE4P[b]	410±40	19±1	0.06	580±30	12.3±0.2	0.02	6±1	3.0±0.1	0.49	45±5	3.7±0.2	0.08
3-deoxyE4P	2700±140	4.5±0.1	0.002	2100±140	4.7±0.1	0.002	200±30	2.1±0.1	0.01	280±30	2.4±0.1	0.009
D-T4P[c]	390±13	2.5±0.1	0.006				21±1	2.4±0.1	0.11			
L-T4P	750±10	1.5±0.1	0.002				47±3	4.0±0.1	0.09			

[a] Kinetic parameters for E4P with *E. coli* DAH7P synthase were determined by M. Ahn,[94] for *P. furiosus* DAH7P synthase by Dr L. Schofield[20] and for *M. tuberculosis* DAH7P synthase by Dr C. Webby.[31]

[b] Kinetic parameters for 2-deoxyE4P with *P. furiosus* DAH7P synthase were determined by Dr L. Schofield.

[c] Kinetic parameters for D- and L-T4P with *E. coli* DAH7P synthase (phe) and *P. furiosus* DAH7P synthase were determined by M. Ahn.

Table 5.1: Kinetic parameters of DAH7P synthase with four-carbon sugar analogues of E4P

Monosaccharide	*E. coli* DAH7P synthase (phe)			*P. furiosus* DAH7P synthase			*H. pylori* DAH7P synthase		
	K_M (μM)	k_{cat} (s^{-1})	k_{cat}/K_M (μM^{-1}s^{-1})	K_M (μM)	k_{cat} (s^{-1})	k_{cat}/K_M (μM^{-1}s^{-1})	K_M (μM)	k_{cat} (s^{-1})	k_{cat}/K_M (μM^{-1}s^{-1})
E4P[a]	39±4	26±2	0.67	9±1	1.4±0.1	0.16	6±1	3.0±0.3	0.5
A5P[b]	30	0.054	0.002	2700±200	1.1±0.1	0.0004	4800±360	0.3±0.01	0.00006
R5P[b]	6000	0.72	0.001	1580±110	2.5±0.1	0.002	1050±95	1.2±0.01	0.001
2-deoxyR5P[b]	6800	0.46	0.00007	2500±150	1.7±0.1	0.0007	3040±230	1.0±0.03	0.0003

[a] Kinetic parameters for E4P with *E. coli* DAH7P synthase were determined by M. Ahn,[94] for *P. furiosus* DAH7P synthase by Dr L. Schofield,[20] and for *H. pylori* DAH7P synthase by Dr C. Webby.[86]

[b] Kinetic parameters for the five carbon sugars with *E. coli* DAH7P synthase are calculated from the reported results of Sheflyan *et al,*[15] with *P. furiosus* DAH7P synthase determined by Dr L Schofield,[20] and with *H. pylori* DAH7P synthase determined by Dr C. Webby.[86]

Table 5.2: Kinetic parameters of DAH7P synthase with five-carbon sugar analogues of E4P

5.2.2 Role of the C3-hydroxyl of E4P

Kinetic data with 3-deoxyE4P **39** and L-T4P **103** indicate that the C3-hydroxyl of E4P is more important for binding and catalysis than the C2-hydroxyl. Removal of the C3-hydroxyl or a change in the stereochemistry at this position has a much larger impact on the reaction than any change to the C2-hydroxyl for all the DAH7P synthases tested. L-T4P, with the opposite C3 stereochemistry to E4P (Figure 5.4) is a very poor substrate, with a 20-fold increase of the apparent K_M compared with E4P for *E. coli* DAH7P synthase (phe). 3-DeoxyE4P, where the C3-hydroxyl is missing altogether is an even poorer substrate for this enzyme, with a K_M almost 100-fold larger than that for E4P. Both L-T4P and 3-deoxyE4P have significantly lower k_{cat} values. Kinetic data for 3-deoxyE4P with the Iα DAH7P synthase from *N. meningitidis*, and the Iβ *P. furiosus* enzyme and type II *M. tuberculosis* enzyme show a similar pattern. Although these enzymes appear to have more flexibility in their substrate specificity than found with *E. coli* DAH7P synthase (phe), the K_M of 3-deoxyE4P is still significantly higher than the K_M for 2-deoxyE4P.

103
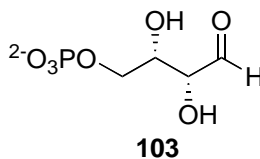
Figure 5.4: L-T4P

An early proposal for the mechanism of KDO8P and DAH7P synthases suggested that the C3 of E4P played a vital role in the reaction mechanism. In this proposed mechanism, PEP would act as a nucleophile on the aldehyde of E4P, resulting in the formation of an oxocarbenium ion intermediate **11**. The C3-hydroxyl of E4P would then act as a nucleophile on C2 of PEP, directly forming cyclic DAH7P **3** (Figure 5.5). Structural studies are not consistent with this mechanism as modeling of E4P into the active site of DAH7P synthase has shown that C3 of E4P is not close enough to form a bond with C2 of PEP. However, while this role for the C3-hydroxyl has been discounted, the results presented in this thesis suggest that the C3-hydroxyl of E4P does play an important role in the enzyme-catalysed reaction.
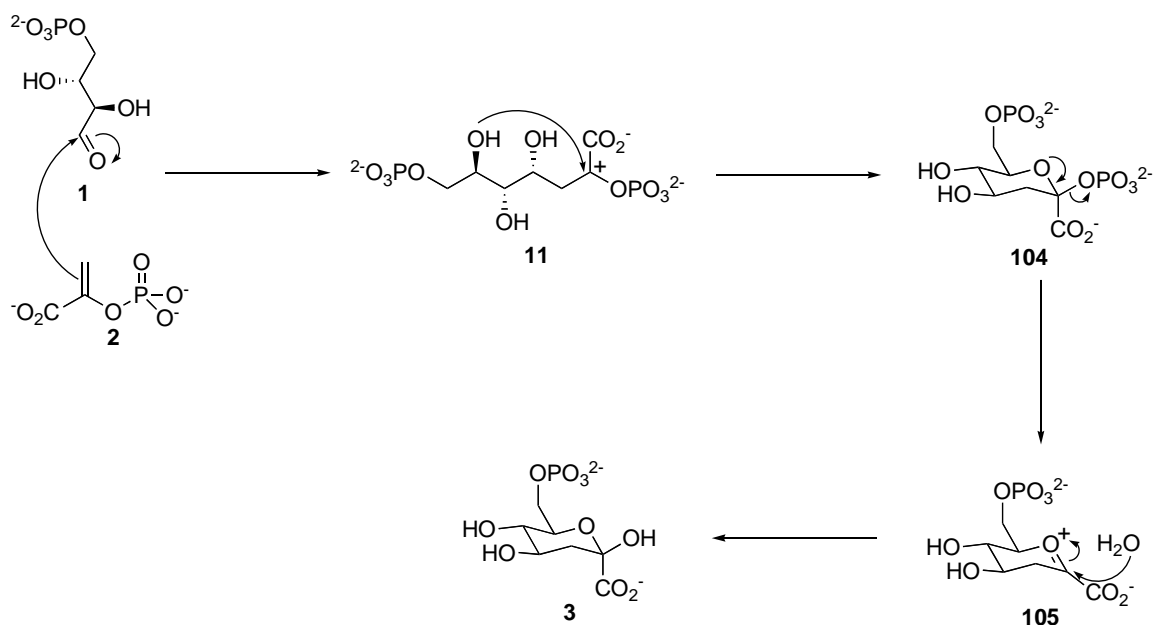
Figure 5.5: Proposed cyclic mechanism of DAH7P synthase

Modeling studies of E4P in the active site of *S. cerevisiae*[68] and *T. maritima*[22] DAH7P synthases have indicated that the C3-hydroxyl interacts with the conserved metal-binding Asp residue. As discussed earlier, the activation of the E4P carbonyl by the metal ion appears to be the key step for the condensation reaction. The hydrogen-bonding interaction of the C3-hydroxyl with the metal-binding Asp is likely to strengthen the metal-E4P aldehyde interaction by activating the metal and making it a stronger Lewis acid, further activating the C1 of E4P for attack by PEP. Therefore when the C3-hydroxyl is not present, the binding is reduced and the rate of reaction is slower.

These substrate specificity studies on DAH7P synthase have shown that the C2 and C3-hydroxyl groups on E4P are not absolutely vital for the enzyme-catalysed reaction. The reaction can proceed with them missing, or in the opposite configuration. The C3-hydroxyl appears to play a more important role, as both 3-deoxyE4P and L-T4P show considerably reduced k_{cat} values compared with 2-deoxyE4P. As it has been shown that the C3-hydroxyl normally coordinates to the metal-ion binding Asp, this suggests an important role for the metal in the reaction mechanism.
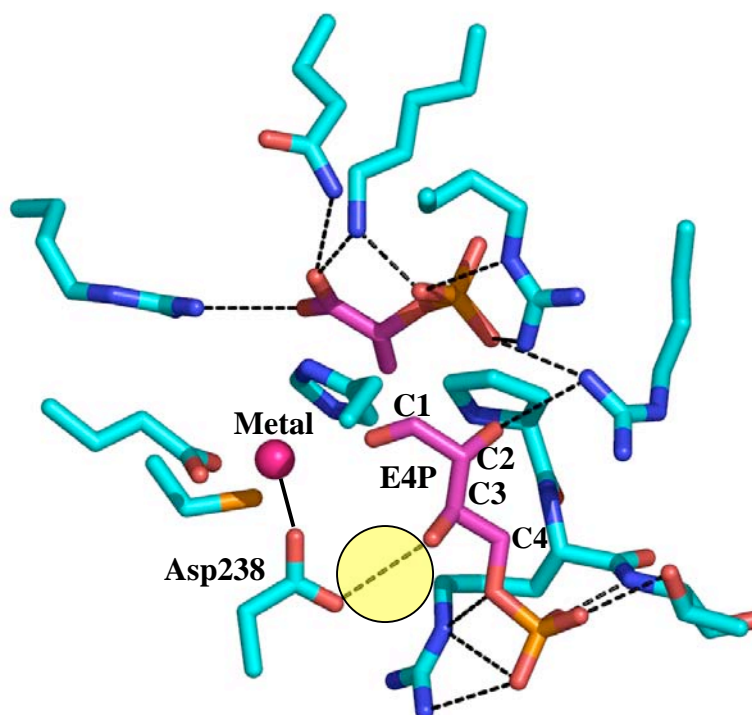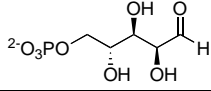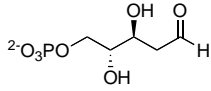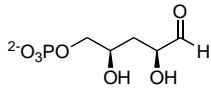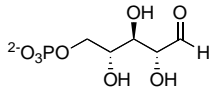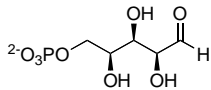
Figure 5.6: Active site of *P. furiosus* DAH7P synthase (PDB code 1ZCO) with E4P modeled in. The C3-hydroxyl of E4P interacts with Asp238 (shaded yellow), which interacts with the metal ion.

5.3 The role of the A5P hydroxyl groups in KDO8P synthase

Prior to this work, substrate specificity studies in the literature had demonstrated a narrow substrate specificity for *E. coli* KDO8P synthase. The A5P analogues 2-deoxyR5P and 4-deoxyA5P have been reported to be poor substrates for *E. coli* KDO8P synthase,[36,74] whereas R5P and 3-deoxyA5P are not able to be utilised at all.[44] These results, as well as the results presented in this thesis and other results from within our laboratory (presented in table 5.3) have allowed for a more detailed analysis of the substrate specificity of KDO8P synthase and comparison with the results discussed for DAH7P synthase.

Monosaccharide	N. meningitidis KDO8P synthase			E. coli KDO8P synthase		
	K_M (µM)	k_{cat} (s^{-1})	k_{cat}/K_M (µM^{-1}s^{-1})	K_M (µM)	k_{cat} (s^{-1})	k_{cat}/K_M (µM^{-1}s^{-1})
A5P[a]	12±1	2.7±0.6	0.23	19±4	6.8±0.5	0.36
2-deoxyR5P[b]	230 ± 20	0.13±0.01	0.0006	50±8	0.12±0.05	0.002
3-deoxyA5P[c]	Not a substrate			Not a substrate		
R5P[a]	Not a substrate			829±54[d]	0.02±0.004[d]	0.00002[d]
L5P[a]	Not a substrate					

[a] Kinetic parameters for A5P, R5P and L5P with N. meningitidis KDO8P synthase were determined by M. Ahn[95] and for A5P with E. coli KDO8P synthase are from the reported results of Howe et al.[74]

[b] Kinetic parameters for 2-deoxyR5P with E. coli KDO8P synthase are from the reported results of Howe et al.[74]

[c] Results for 3-deoxyA5P with E. coli KDO8P synthase are reported by Baasov et al[44]

[d] Although enzyme-dependent loss of PEP was observed in the presence of R5P, it was shown to not result in the formation of a KDO8P-like product.

Table 5.3: Kinetic parameters of KDO8P synthase with five-carbon sugar analogues of A5P

5.3.1 Role of the C2-hydroxyl of A5P

The removal of the A5P C2-hydroxyl has much more of a catastrophic effect on the reaction of the KDO8P synthases from N. meningitidis and E. coli than the loss of the E4P C2-hydroxyl in the DAH7P synthase catalysed reaction. 2-DeoxyR5P, with the C2-hydroxyl missing is an extremely poor substrate for N. meningitidis DAH7P synthase, with both high K_M and low k_{cat}, and similar results have been reported for this compound with E. coli KDO8P synthase. R5P, with the opposite stereochemistry at C2 to A5P is not a substrate for N. meningitidis KDO8P synthase. It has also been reported to not be a substrate for E. coli KDO8P synthase, although enzyme-dependent loss of PEP has been observed in the presence of R5P.[74]

The recent high resolution structure of *A. aeolicus* KDO8P synthase with A5P bound has allowed for analysis of the possible role of the C2-hydroxyl group.[42] As discussed previously, modeling of E4P in the active site of DAH7P shows the carbonyl coordinating to the metal. This is not the case for A5P in KDO8P synthase. In this structure the C2-hydroxyl of A5P coordinates either to the metal ion, or to a water molecule, which in turn coordinates the metal ion (Figure 5.7). In non-metallo enzymes, the conserved Asn residue is thought to replace this metal ion. Although the reaction can proceed without the C2-hydroxyl group present, it cannot when the stereochemistry is reversed. This suggests that the role of the C2-hydroxyl of A5P is in positioning the molecule into the correct conformation for attack by PEP.

5.3.2 Role of the C3-hydroxyl of A5P

Although KDO8P synthase has limited ability to accept modifications to C2 of A5P, the C3-hydroxyl group of A5P is vital for the enzyme-catalysed reaction. Whereas DAH7P synthase is able to utilise both the C3 epimer of E4P, L-T4P and 3-deoxyE4P, there is no evidence of any reaction with the C3 epimer of A5P, L5P, or with 3-deoxyA5P with *N. meningitidis* KDO8P synthase. The *A. aeolicus* KDO8P synthase structure shows that the C3 of A5P interacts with the Asn residue from the fully conserved LysAlaAsnArgSer motif of KDO8P synthases, which replaces the absolutely conserved LysProArgThr motif of DAH7P synthases. Clearly this interaction is vital for binding and catalysis. The significance of this conserved motif and a possible explanation for the narrower substrate specificity of KDO8P synthase compared to DAH7P synthase is discussed in the next section.
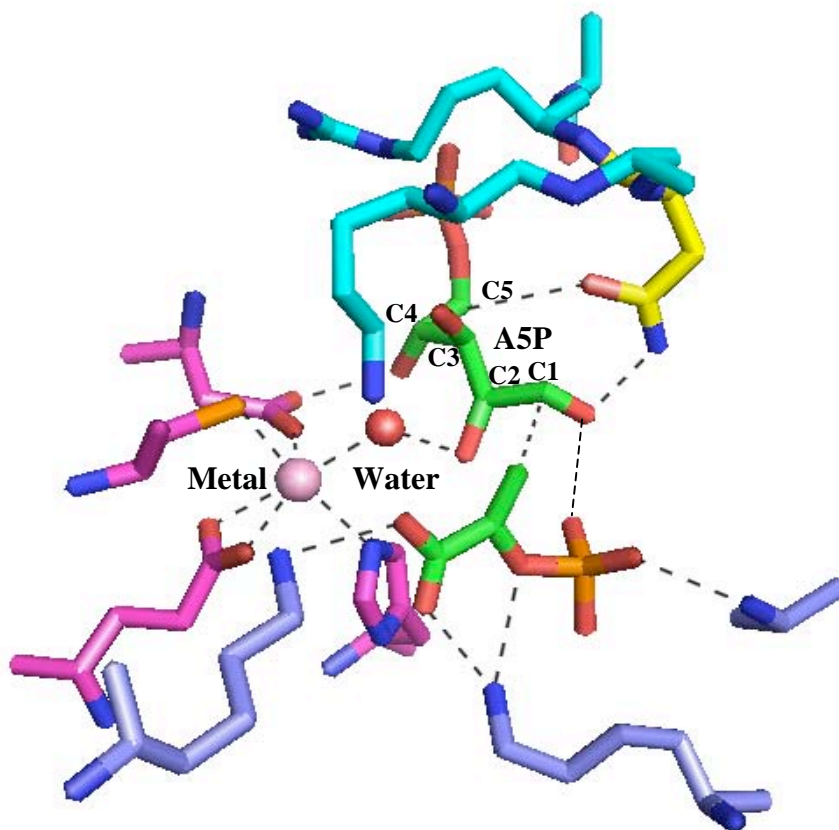
Figure 5.7: Active site of *A. aeolicus* KDO8P synthase (PDB code IFWW) showing the C2-hydroxyl of A5P interacting with the metal ion *via* a water molecule.

5.4   Mechanism of DAH7P and KDO8P synthases

While early studies on DAH7P and KDO8P synthase have shown many similarities in the mechanisms, the role of the metal is still under debate. Early studies on KDO8P synthase focused on *E. coli* KDO8P synthase, which did not require a metal ion for activity and it was assumed that the requirement for a divalent metal ion for activity was a key difference between DAH7P synthase and KDO8P synthase. However, a later study showed KDO8P synthase from *A. aeolicus* to require a divalent metal ion for activity and identified a new class of metallo KDO8P synthases.[24] Given the close evolutionary relationship between these two enzymes, the very similar active sites and the already demonstrated similarities in mechanisms, it would be reasonable to expect that the metallo KDO8P synthases may share a common mechanism with DAH7P synthases, and that a mechanistic difference exists between these two enzymes and the non-metallo KDO8P synthase. However, recent structural, functional and mutational studies in the literature suggest that all KDO8P synthases have the same mechanism

(and a different mechanism to DAH7P synthases) regardless of whether they are metallo or non-metalloenzymes.

The metal dependency of KDO8P synthase can be predicted by its primary sequence.[29] All metallo KDO8P synthases share with the DAH7P synthases a conserved Cys residue, which is replaced by an Asn residue in the non-metallo counterparts. Mutation studies have found that the metal-dependent KDO8P synthases from *A. pyrophilus* and *A. aeolicus* can be converted to metal-independent enzymes by the single mutation of the metal-binding Cys to Asn.[65,66] In contrast, the same mutation in *P. furiosus* DAH7P synthase produced an enzyme which no longer bound metal, but which showed no activity in the presence or absence of metal.[94] Hence, while the metal plays a dispensable role in the KDO8P synthase catalysed reaction, it is vital for the DAH7P synthase reaction.

Studies by Furdui *et al*[139] are also consistent with a different reaction mechanism for these two enzymes. These studies showed that both the metallo KDO8P synthase from *A. pyrophilus* and the non-metallo KDO8P synthase from *E. coli* showed a clear preference for (*Z*)-3-fluoroPEP over (*E*)-3-fluoroPEP. In contrast, *E. coli* DAH7P synthase showed no preference for either isomer, indicating a key difference in mechanism between the two enzymes, depending on the reaction they catalysed.

Structural studies of DAH7P synthase and the metallo KDO8P synthase from *A. aeolicus* have suggested a different role for the metal in these two enzymes. Modeling studies of DAH7P synthase have placed E4P in the active site in such a way that the E4P carbonyl is a metal ligand, allowing for Lewis acid catalysis.[22,68] In comparison, the carbonyl of A5P in *A. aeolicus* KDO8P synthase is too far away from the metal to be considered a ligand and so attack of PEP on A5P is likely to be initiated by protonation (Brønsted acid catalysis). The earlier proposed mechanism where the role of the metal is to deprotonate a water molecule which then attacks PEP[34] is considered unlikely due to the metal-binding ligand mutation studies highlighting the dispensable role of the metal in KDO8P synthases.[65,66]

The structure of *A. aeolicus* KDO8P synthase solved with R5P bound in the active site supports a mechanism for KDO8P synthase where the crucial step is to correctly

orientate the substrate A5P.[73] In this structure, R5P is reportedly found bound in the active site in the same place as A5P is found, but with the carbonyl bound in a different orientation to that observed for A5P. As R5P is not a substrate for *A. aeolicus* KDO8P synthase,[73] or for KDO8P synthase from *E. coli* or *N. meningitidis* (table 5.3), this is consistent with the R5P carbonyl not being in the correct orientation for reaction.

All of the above studies are consistent with a different mechanism for DAH7P and KDO8P synthase, regardless of requirement for metal. Hence, the substrate specificity results from the non-metallo KDO8P synthase from *N. meningitidis* presented in this study, as well as those in the literature from *E. coli* KDO8P synthase may be generalised to other KDO8P synthases, including the metallo enzymes.

The substrate specificity studies presented in this thesis, combined with others from our laboratory and in the literature have revealed some significant differences in the roles of the C2 and C3-hydroxyl groups of E4P and A5P. Whereas the hydroxyl groups of both substrates appear to have a role in positioning the substrate into the right conformation for reaction with PEP, this role seems much more vital in the case of KDO8P synthase. DAH7P synthase is able to utilise 2-deoxyE4P and D-T4P, 3-deoxyE4P and L-T4P with reasonable efficiency. In contrast, the removal of, or change in orientation of either the C2 or C3-hydroxyl of A5P is much more catastrophic for the KDO8P synthase reaction and results in an extremely slow reaction or no reaction at all. Along with the differences in metal requirement, these findings are consistent with a different mechanism for DAH7P and KDO8P synthase and suggest a mechanism for KDO8P synthase where the crucial step is correct positioning of A5P. In KDO8P synthase, activation and positioning of the aldehyde moiety is critical for the reaction to proceed. The C2 and C3-hydroxyl groups play an important role in positioning A5P in such a way that the dihedral angle about the C1–C2 bond of A5P is controlled. Consequently, altering the configuration or removing the C2-hydroxyl of A5P is catalytically catastrophic. This is in contrast to DAH7P synthase, where the crucial step appears to be coordination of the carbonyl to the metal. Although the C2-hydroxyl is likely to be important for the positioning of E4P within the active site to allow this interaction to take place, and the C3-hydroxyl of E4P appears to have a role in activating the metal to make it a stonger Lewis acid, the hydroxyl groups are less essential for catalysis.

The data presented in this thesis is consistent with the reaction mechanisms proposed by Ahn.[94,95] In this model, the differences in the reactivity of DAH7P synthase and KDO8P synthase is attributed to two conserved differences within the active site. Firstly, an Arg in the PEP phosphate binding site of DAH7P synthase is substituted with a Phe in KDO8P synthase. Secondly, the Pro residue in the conserved LysProArgThr motif of DAH7P synthases (which interacts with the E4P C2 hydroxyl) is replaced by Ala and Asn residues, giving the conserved LysAlaAsnArgSer motif in KDO8P synthases. The effect of the first substitution is elimination of a salt bridge to the PEP phosphate in the DAH7P synthase active site, increasing the hydrophobicity in the vicinity of the PEP phosphate in KDO8P synthase, and allowing PEP to be bound in its dianionic form, rather than the trianionic form found in DAH7P synthase. This also allows for the carbonyl of A5P to be positioned differently, forming hydrogen bonds with the phosphate of PEP.

The second substitution of an AlaAsn for a Pro gives an additional interaction between the A5P C3-hydroxyl and the Asn residue in order to position A5P for attack by PEP. In DAH7P synthase, the coordination of the carbonyl to the metal fulfils this role. The proposed differences in the binding and catalysis of E4P and A5P in the active sites of DAH7P and KDO8P synthases are shown in Figure 5.8.
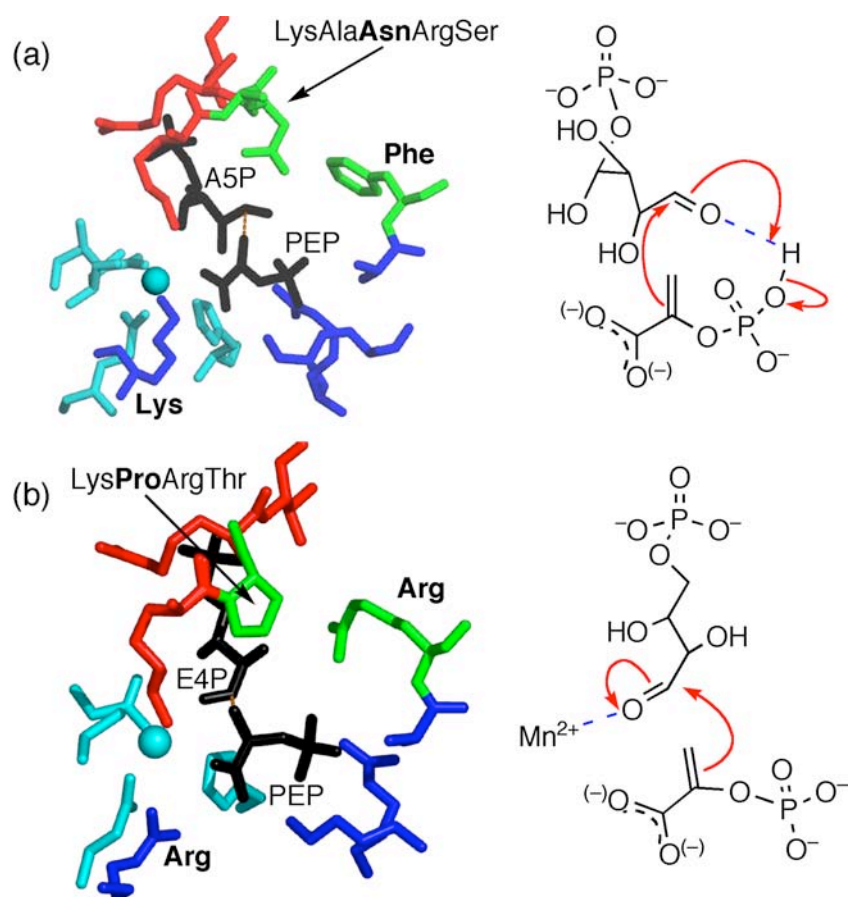
Figure 5.8: Comparison of active sites and proposed (partial) reaction mechanisms for (a) *A. aeolicus* KDO8P synthase (PDB code 1FWW) (b) *P. furiosus* DAH7P synthase (PDB code 1ZCO). E4P has been modeled into this structure based on the observed binding of glycerol 3-phosphate to *S. cerevisiae* DAH7PS[68] and the proposed binding of E4P to *T. maritima* DAH7PS.[22] The key changes discussed in the text are highlighted in green. Metal and metal ligands are in cyan and PEP ligands are shown in blue. Substrates, PEP and A5P (or E4P) are shown in black.

5.5   Summary and future directions

The substrate specificity studies presented in this thesis are consistent with the findings of Ahn and the mechanism proposed to explain these findings.[94,95]   The different substrate specificities of the two enzymes DAH7P and KDO8P synthase along with the different requirements for metal ions can be explained by the two enzymes having different mechanisms to catalyse what are two seemingly very similar reactions. Phylogenetic and structural analyses have shown that the two enzymes are related.[6,10,16,20,22,31,40,42,48,68,69,72,73]   However the evolutionary changes that have led to the difference in substrate specificity and metal requirement are not fully understood.

Site-directed mutagenesis studies on *P. furiosus* DAH7P synthase, which with its extended substrate specificity and lack of feedback regulation appears to be the contemporary protein closest to ancestral DAH7P synthase, would allow for testing of the proposed mechanism outlined in Section 5.4.[20] The residues to be mutated are the conserved Pro in DAH7P synthase to the AlaAsn in KDO8P synthase and the conserved Arg in the PEP binding phosphate site to the Phe in the same position in KDO8P synthase. This should theoretically turn a DAH7P synthase into a KDO8P synthase; however, it is likely that additional changes, not identified in these studies, have also facilitated the development of KDO8P synthase activity from DAH7P synthase. Structural analysis of wild-type protein and these mutants, particularly with substrate analogues, such as those detailed within this thesis may help to confirm the different mechanisms of these two related enzymes.

The substrate analogue studies on KDO8P synthase described in this study have all been carried out on the non-metallo KDO8P synthase from *N. meningitidis*. Future work could also involve the testing of 2-deoxyR5P and 3-deoxyA5P with a metallo KDO8P synthase. This would allow for confirmation that both metallo and non-metallo KDO8P synthases exhibit the narrow substrate specificity demonstrated in these studies and hence that they share a common mechanism.

CHAPTER SIX: EXPERIMENTAL PROCEDURES

6.1   General biochemical methods

Buffers

Chemicals used for buffer preparation were purchased from commercial sources.

BTP buffers were prepared by adjusting the pH with concentrated HCl. The following buffers were used in standard assays for the following enzymes:

E. coli DAH7P synthase (phe) – 50mM BTP, 10µM EDTA, pH 6.8 at 25˚C

N. meningitidis DAH7P synthase - 50mM BTP, 10µM EDTA, pH 6.8 at 25˚C

P. furiosus DAH7P synthase – 50mM BTP, 10µM EDTA, pH 6.8 at 60˚C

M. tuberculosis DAH7P synthase – 50mM BTP, 10µM EDTA, pH 7.5 at 30˚C

N. meningitidis KDO8P synthase – 50mM BTP, pH 7.5 at 30˚C

Enzymes

Glucose-6-phosphate dehydrogenase was purchased from Sigma Chemical Company.

Purified *E. coli* DAH7P synthase was kindly supplied by Dr Fiona Cochrane or Dr Linley Schofield. Purified *P. furiosus* DAH7P synthase was kindly supplied by Dr Linley Schofield. Purified *M. tuberculosis* DAH7P synthase was kindly supplied by Dr Celia Webby. Purified *N. meningitidis* KDO8P synthase was kindly supplied by Dr Fiona Cochrane.

Standard enzyme assay for DAH7P synthase and KDO8P synthase

The assay system for DAH7P synthase and KDO8P synthase was a modified form of the assay used by Schoner and Herrman.[11] The consumption of PEP was monitored at 232nm (ε = 2.8 x 10^3 M^{-1} cm^{-1} at 25˚C or 2.6 x 10^3 M^{-1} cm^{-1} at 60˚C) using a Varian Cary 1 UV Visible spectrophotometer. Measurements were made using 1cm path-length quartz cuvettes. Standard reaction mixtures contained PEP (~150µM) (Research Chemicals), E4P or A5P (~150µM) (Sigma) (or E4P or A5P analogue), and in the case

of DAH7P synthase, $MnSO_4$ (~100µM) (Sigma) in BTP buffer. All buffer solutions and reagents except metal solutions and those used with *N. meningitidis* KDO8P synthase were pre-treated with Chelex 100 resin (Bio-Rad) to remove metal ions. Metal solutions were made up using water that had been pretreated with Chelex resin. Solutions were filtered through a 0.45µm membrane to remove any particulate matter prior to use. Assay mixtures were incubated for two minutes at 25°C or 30°C or six minutes at 60°C before initiation. For *P. furiosus* DAH7P synthase, the reaction was initiated by the addition of E4P to give a final volume of 1mL. For all other enzymes, the reaction was initiated by the addition of enzyme to give a final volume of 1mL. Assays were carried out at 25°C for *E. coli* DAH7P synthase and *N. meningitidis* DAH7P synthase, 60°C for *P. furiosus* DAH7P synthase and 30°C for *N. meningitidis* KDO8P synthase and *M. tuberculosis* DAH7P synthase. One unit (1 U) of activity is defined as the loss of 1µmol of PEP per minute at the stated temperature. Specific activity (U/mg) is defined as the loss of 1µmol of PEP per minute at the stated temperature per mg of protein. K_M and k_{cat} values were determined by fitting the data to the Michaelis-Menten equation using Enzfitter (Biosoft, 1999).

Accurate concentrations of PEP and E4P or E4P analogue were determined by following the loss of PEP on complete conversion of one of the substrates (with the other in excess) using *E. coli* DAH7P synthase. Allowance was made for the change in absorbance due to initiation by addition of the enzyme. Concentrations were calculated using Beer's law where $\varepsilon = 2.8 \times 10^3 M^{-1}cm^{-1}$ at 25°C.

Determination of protein concentration

Protein concentrations were determined by Bradfords assay using BSA (bovine serum albumin) as a standard.[140] Assays were carried out by adding 1mL of the Bradford reagent to 100µL of standard solutions (0.05, 0.1, 0.2 and 0.4mg/mL) or diluted samples. A blank solution was made using 100µL of MilliQ water. The assays were allowed to stand for 10 minutes and the absorbance measured at 595nm. The protein concentrations of the unknown samples were determined from a standard plot.

Purified water

All water used was Milli-Q water. Milli-Q water was generated by passage through a Sybron/Barnstead NANOpure II filtration system (Maryland, USA), containing two ion-exchange and two organic filters.

Centrifugation

Centrifugation was performed in either a SORVALL Evolution RC centrifuge®, a SORVALL Heraeus multifuge® 1S/1SR or an Eppendorf Minispin® centrifuge.

Sonication

Sonication was performed using a VirTis Virsonic digital 475 ultrasonic cell disrupter using an 1/8 inch probe at ~60 Watts.

pH measurements

The pH of buffers used in this project was measured using a model 20 pH/Conductivity Meter (Denver Instrument Company) and a Sartorius Professional Meter. For small volumes, an ORION Model 410A pH meter was used. The pH of solutions was adjusted using 10M NaOH or ~12M HCl.

Fast Protein Liquid Chromatography (FPLC)

FPLC was carried out using either a Bio-Rad BioLogic Duo-Flow protein chromatography system at 4°C or an ÄKTAprime plus protein chromatography system at room temperature. All buffers and solvents for FPLC were filtered using a 0.2µm filter (Millipore).

UV-Visible spectrophotometry

UV-Visible spectrophotometry was performed on a Varian Cary® 1 UV-Vis spectrophotometer at 25°C, 30°C or 60°C as indicated, controlled by a Cary temperature controller using 1cm path length quartz cells.

6.2   General chemical methods

Solvents

All organic solvents were freshly distilled before use. Dichloromethane was distilled from calcium hydride. Diethyl ether was distilled from sodium hydroxide. THF was distilled from sodium wire. Analytical grade acetone, methanol and ethanol were used as supplied from commercial sources.

Reagents

All chemical reagents used for experiments were purchased from commercially available sources and used as supplied unless otherwise noted.

Silver oxide (Ag_2O) was freshly prepared using the published procedure[141].

Dess-Martin periodinane was prepared according to the modified procedure of Ireland and Liu.[142,143]

Chromatography

Analytical thin layer chromatography (tlc) was performed on Merck Silica Gel 60 F254 aluminium backed sheets. Spots on plates were visualised under UV (254nm) followed by staining with aqueous potassium permanganate or vanillin.

Flash column chromatography was carried out on Scharlau silica gel 60, 230-400 mesh. Chromatographic solvents, ethyl acetate and hexane, were distilled prior to use.

Reactions and work-up

All reactions were performed under an inert atmosphere of dry nitrogen (N_2), argon (Ar) or hydrogen (H_2) unless otherwise stated. Crude organic extracts were dried with anhydrous magnesium sulfate. Evaporations were carried out on a rotary evaporator.

pH measurements

pH measurements were made using Whatman's Full range pH Paper.

Spectroscopy

^{1}H NMR spectra were performed on a Bruker Avance® 400MHz or Bruker Avance® 500MHz instrument, utilizing a QNP or QXI probe respectively. All spectra were recorded in deuterated solvents as indicated. When samples were dissolved in D_2O, the spectra were referenced to HOD at 4.7ppm. When samples were dissolved in $CDCl_3$, the spectra were referenced to TMS at 0ppm.

^{13}C NMR spectra were performed on either a Bruker Avance® 400MHz instrument operating at 100.613 MHz or a Bruker Avance® 500MHz instrument operating at 125.758 MHz.

^{31}P spectra were recorded on a Bruker Avance® 400MHz instrument operating at 161.975 MHz.

^{19}F spectra were recorded on a Bruker Avance® 400MHz instrument operating at 376.46 MHz.

All signal assignments were consistent with the appropriate 2D NMR experiments (^{1}H/^{1}H COSY and ^{1}H/^{13}C HMQC).

Mass spectrometry

High-resolution mass spectrometry was carried out either by the Department of Chemistry at the University of Auckland on a VG-70SE High-resonance mass spectrophotometer or the Department of Chemistry at the University of Canterbury on a Micromass LCT.

Optical rotation

Optical rotations of compounds were performed in $CHCl_3$ unless otherwise noted, in a Perkin Elmer 341 polarimeter.

6.3 Experimental methods for chapter two: Purification and characterisation of a type Iα DAH7P synthase from *Neisseria meningitidis*

Media

Cultures were grown in Luria Broth (LB) base. LB broth (Invitrogen) was made up (25g/L) with Milli-Q water and sterilised by autoclaving at 121°C and 15psi for 20 minutes.

Antibiotic stocks

Stock solutions of ampicillin (100mg/mL) in Milli-Q water were filter sterilised (0.2μm) and stored at -20°C.

Growth of cells

250mL cultures were grown from an overnight 5mL culture of LB which had been inoculated with a scraping of glycerol stock of *E. coli* cells containing the *N. meningitidis* DAH7P synthase-plasmid construct. The cells were grown in LB containing ampicillin (100μg/mL) in baffled flasks (250mL per 1L flask) at 37°C with shaking (230rpm) for approximately three hours, until mid-logarithmic phase (OD$_{600}$~0.4-0.6).

Induction of protein expression

Expression of genes inserted into the cloning site of pT7-7 is under the control of the *lac* promoter and is therefore induced by the addition of lactose or isopropyl-β-D-thiogalactopyranoside (IPTG) (Applichem). IPTG is a non-physiological analogue of lactose, which activates gene expression but is not metabolised by the cell like lactose. IPTG was added to cultures to a final concentration of 1mM to induce protein expression at mid logarithmic phase.

Harvesting and lysis of cells

The cells were harvested approximately 4 hours after induction by centrifuging at 5500*g* for 15 minutes at 4°C. The cell pellet was stored at -80°C until lysis. The cell pellet

was resuspended in lysis buffer (10mM BTP pH 7.3, 1mM EDTA, 200mM KCl, 200µM PEP) and the cells lysed using a French press (8000psi). The DNA was broken up by sonication on ice and the cell debris removed by centrifugation (27,000g at 4˚C for 20 minutes).

Polyacrylamide gel electrophoresis

Sodium dodecyl sulfate-polyacrylamide gel electrophoresis was performed using the method of Laemmli[144] with a 4% (w/v) stacking gel and a 12% (w/v) separating gel, using a Mini Protean III cell (Bio-Rad). All samples were prepared in SDS loading buffer and were boiled for two minutes. Low range SDS-PAGE molecular weight standards (Bio-Rad) were used. Native PAGE was performed similarly, with a 4% (w/v) stacking gel and a 15% (w/v) running gel, and with the omission of SDS from all buffers. A constant voltage of 260V was applied across the electrodes until the dye front reached the bottom of the separating gel. After electrophoresis, gels were stained for protein using Coomassie Brilliant Blue R 250 (Park Scientific) in 50% (v/v) methanol, 10% acetic acid (v/v) in water for approximately 20 minutes. To remove excess dye, the gels were de-stained in an identical solution without the dye.

Storage of enzymes

All enzyme preparations were stored as aliquots of volumes no more than 200µL, snap-frozen in liquid nitrogen and stored at -80˚C.

Purification using AEC and HIC

The supernatant fraction collected after cell lysis and centrifugation was filtered using a 0.2µm filter (Millipore), diluted five-fold with buffer A (10mM BTP, 1mM EDTA, pH 7.3) and loaded onto a column (8mL) of Source 15Q® (10/10) (Amersham) equilibrated in buffer A at 4˚C. The unbound protein was removed with two column volumes (16mL) of buffer A and the bound protein was eluted with a 75mL linear gradient between buffer A and buffer A + 1M NaCl at a flow rate of 2mL/min. Active fractions were pooled, ammonium sulfate added to a final concentration of 1M and loaded onto a source Phe® (Amersham) column (8mL), equilibrated in buffer C (Buffer A + 1M ammonium sulfate) at room temperature. The unbound protein was removed with two column volumes of buffer C and the bound protein was eluted with a 40mL linear

gradient between buffer C and buffer A at a flow rate of 1mL/min. Active fractions were pooled, concentrated and washed with buffer A using a 20mL Vivaspin 10kDa MWCO concentrator.

Determination of molecular mass using SEC

Size exclusion chromatography (Superdex S200, Amersham Biosciences) was used to determine the molecular mass of *N. meningitidis* DAH7P synthase in solution by comparing elution volumes with those for molecular weight standards (MW-GF-200, Sigma). The molecular weight standards were cytochrome C (12.5kDa), carbonic anhydrase (29kDa), alcohol dehydrogenase (150kDa), and β-amylase (200kDa). Blue dextran, with a molecular weight of 2000kDa was used to determine the void volume. The gel filtration buffer contained 10mM BTP, pH 7.3, 10µM EDTA, 200µM PEP and 50mM KCl. The same buffer was used to elute both DAH7P synthase and the standards. All SEC was performed at a flow rate of 0.4mL/min at 4˚C.

For the determination of the molecular mass of *N. meningitidis* DAH7P synthase, ~0.2mg of blue dextran was dissolved in 400µL of gel filtration buffer, filtered through a 0.2µm filter (Millipore) and injected onto the column. The elution volume was designated the void volume. A second run contained ~0.2mg of β-amylase and ~0.4mg of cytochrome C in 400µL, and a third run, ~0.3mg carbonic anhydrase and ~0.5mg alcohol dehydrogenase in 400µL. The elution volumes for each standard were divided by the void volume and a standard curve was constructed. The elution volume for *N. meningitidis* DAH7P synthase allowed the molecular weight to be estimated by reading off the standard curve. Elution volumes for the standards and *N. meningitidis* DAH7P synthase are in chapter two.

Determination of kinetic parameters

Standard assay conditions were used for the determination of kinetic parameters of *N. meningitidis* DAH7P synthase. To determine kinetics for PEP, the reaction mixture contained PEP (9–180µM), $MnSO_4$ (100µM), and E4P (360µM) in 50 mM BTP buffer with 10µM EDTA at pH 6.8. To determine kinetics for E4P, the reaction mixture contained E4P (7-450µM), PEP (270µM), and $MnSO_4$ (100 µM) in 50mM BTP buffer with 10µM EDTA at pH 6.8. In each case, the reaction was initiated by the addition of

purified *N. meningitidis* DAH7P synthase (2μL, 1.1mg/mL). All assays were carried out at 25°C. K_M and k_{cat} values were determined by fitting the data to the Michaelis–Menten equation using Enzfitter (Biosoft).

Metal activation

Metal activation studies were carried out with *N. meningitidis* DAH7P synthase preparations containing 10mM EDTA. All solutions contained 10μM EDTA and (except the metal solutions) were treated with Chelex resin before use. The assay mixture contained PEP (180μM), divalent metal salt (100μM) and *N. meningitidis* DAH7P synthase (5μL, 1.7mg/mL). The reaction was initiated with the addition of E4P (150μM). The metal salts used were $MnSO_4$, $ZnSO_4$, $CdSO_4$ (BDH), $CoSO_4$ (May and Baker), $NiCl_2$ (May and Baker), $CaCl_2$ (Prolabo), $CuSO_4$ (May and Baker), $FeCl_2$ (Riedel-de Haën), $MgSO_4$ (May and Baker), $SrCl_2$ (Unilab), and $BaCl_2$ (BDH).

Feedback inhibition studies

Solutions of phenylalanine, tyrosine and tryptophan (10mM) (Sigma) in water were added to standard assay reaction mixtures (PEP (100μM), E4P (125μM) and $MnSO_4$ (100μM) in BTP buffer (50mM, pH 6.8) containing 10μM EDTA) to give a final concentration of 200μM. The reaction was initiated by the addition of *N. meningitidis* DAH7P synthase (2μL, 1.1mg/mL) to give a total reaction volume of 1mL. All assays were performed in duplicate.

Substrate specificity

Assays to determine activity with DL-glyceraldehyde 3-phosphate (G3P) and D-glucose 6-phosphate (G6P) contained 180μM PEP and 6mM G3P (Sigma) or 1mM G6P (Sigma).

Assays to determine activity with the five-carbon sugars contained 180μM PEP and 1.5-2.6M of the monosaccharide phosphate. The assays were initiated by the addition of enzyme (20μL, 1.8mg/mL).

To determine whether one or both enantiomers of the racemic mixtures of 2-deoxyE4P were substrates, two identical assays were set up with ~100μM of the racemic mixture (in the (*S*) enantiomer), 180μM PEP and 100μM $MnSO_4$. The first reaction was

initiated by the addition of *N. meningitidis* DAH7P synthase (10µL, 1.8mg/mL), and the second by the addition of *E. coli* DAH7P synthase (5µL, 8mg/mL). After being monitored overnight, the loss of PEP in each assay was compared and found to be approximately the same (110µM in the *N. meningitidis* DAH7P synthase assay, 114µM in the *E. coli* assay).

The same experiment was carried out for racemic 3-deoxyE4P, with 97µM 3-deoxyE4P in the cuvette. In this experiment, the PEP loss for the *N. meningitidis* DAH7P synthase assay was 49µM, whereas the PEP loss for the *E. coli* assay was 95µM.

Temperature studies

The assays for temperature studies contained 180µM PEP and 100µM $MnSO_4$ in 50mM BTP solution containing 10µM EDTA, which was pH 6.8 at the required temperature. After incubation at the required temperature for six minutes, E4P (150µM) was added, and then one minute later, the reaction was initiated by the addition of enzyme (5µL, 1.7mg/mL).

6.4 Experimental methods for chapter three: Evaluation of 2-deoxyE4P and A5P analogues with DAH7P and KDO8P synthases

Synthesis of 45

45
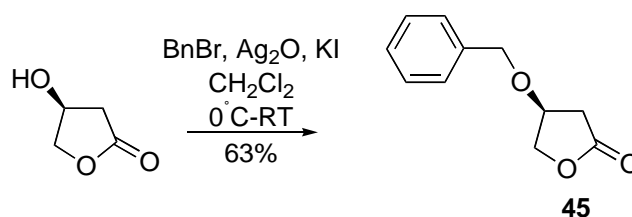
β-Hydroxy-γ-butyrolactone (0.3229g, 3.16mmol) was dissolved in 5mL of dry CH_2Cl_2 and cooled to 0°C. BnBr (564µL, 4.74mmol), Ag_2O (1.0985g, 4.74mmol), and KI (0.0670g, 0.40mmol) were added and the solution stirred and allowed to warm to room temperature. After 5.5 hours, the reaction mixture was filtered through Celite and washed with saturated aqueous $NaHCO_3$ solution (25mL), H_2O (25mL), and saturated aqueous NaCl solution (25mL). The combined aqueous washings were extracted with

CH_2Cl_2 (10mL x 3). The combined organic extracts were dried ($MgSO_4$) and the solvent removed *in vacuo*. The product **45** was then purified using flash chromatography, to provide 383mg (63%) of the title compound, a colourless oil.

R_F=0.53 (1:1 Hexane:EtOAc).

m/z (+ve FAB) cal 192.0786 found 192.0781

^{1}H NMR (CDCl$_3$, 400MHz) δ 7.40-7.27 (m, 5H, Ph-<u>H</u>), 4.54 (d. J=11.9Hz, 1H, Bn), 4.51 (d, J=11.9Hz, 1H, Bn), 4.42-4.37 (m, 3H, H3, H4), 2.74-2.62 (m. 2H, H2) ppm.

^{13}C NMR (CDCl$_3$, 100MHz) δ 175.8 (C1), 137.3 (C6), 129.0 (Ph), 128.6 (Ph), 128.1 (Ph), 74.2 (C4), 73.5 (C3), 71.6 (Ph-<u>C</u>H$_2$), 35.3 (C2) ppm.

Synthesis of 46
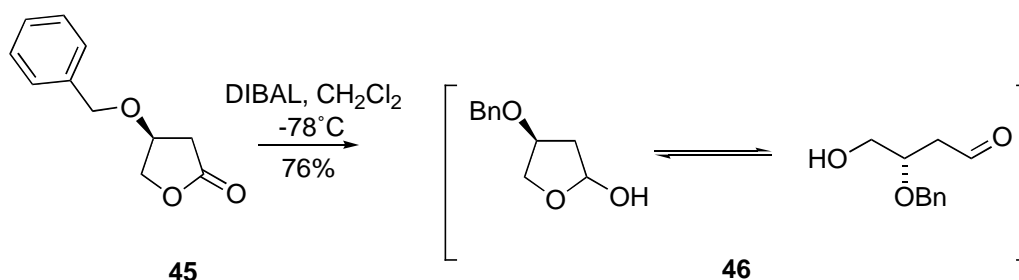
45 (300mg, 1.56mmol) was dissolved in dry CH_2Cl_2 (25mL) and cooled to –78˚C. DIBAL in CH_2Cl_2 (2.18mL of 1M solution) was added drop-wise, and the solution stirred at -78˚C. Once the starting material had been consumed, the reaction was quenched by the addition of 3mL of 10% HCl and allowed to warm to room temperature. The reaction mixture was partitioned between H_2O (20mL) and CH_2Cl_2 (40mL). The organic layer was removed and washed with Rochelle's salt (50mL), H_2O (50mL), and saturated aqueous NaCl solution (20mL). The combined aqueous extracts were washed with CH_2Cl_2 (20mL). The combined organic extracts were dried ($MgSO_4$) and the solvent removed *in vacuo*. The product was purified by flash chromatography to give 230mg (76%) of **46**, as a colourless oil.

R_F=0.47 (1:1 Hexane:EtOAc).

m/z (+ve FAB) cal 193.0865 found 193.0865

^{1}H NMR (CDCl$_3$, 400MHz) δ 9.78 (t, J=1.8Hz, 0.05H), 7.32 (m, 10H), 5.85 (m, 1H), 5.41 (m, 1H), 4.24 (m, 4H), 4.10 (m, 3H), 4.08 (m, 3H), 4.05 (m, 1H), 4.03 (m, 2H), 2.01 (m, 2H), 1.99 (m, 3H), 1.98 (m, 4H), 0.84 (m, 2H) ppm.

^{13}C NMR (CDCl$_3$, 100MHz) δ 207.6, 141.4, 138.3, 137.7, 129.0, 128.9, 128.8, 128.6, 128.4, 128.3, 128.1, 128.0, 127.3, 99.3, 99.0, 78.8, 78.4, 73.5, 72.8, 71.8, 71.6, 71.5, 67.6, 65.6, 40.8, 40.0, 38.7, 31.3 ppm.

Synthesis of 47
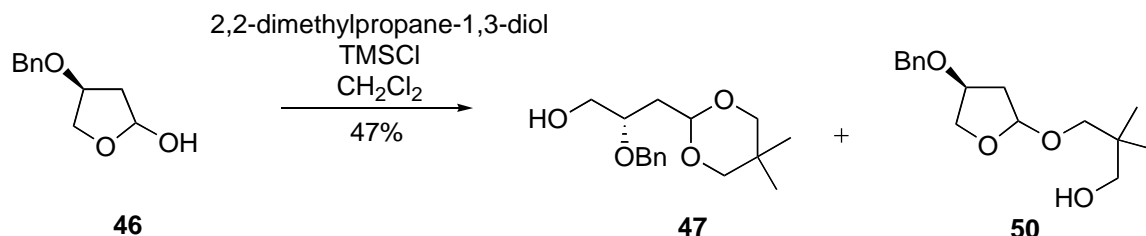
2,2-Dimethylpropane-1,3-diol (0.1007g, 0.97mmol) and TMSCl (245µL, 1.94mmol) were dissolved in CH$_2$Cl$_2$ (10mL) and cooled to 0˚C for 15 minutes. **46** (120mg, 0.64mmol) in CH$_2$Cl$_2$ (5mL) was added to the reaction mixture and stirred for four hours. The mixture was washed with saturated aqueous NaHCO$_3$ solution (20mL x 3) and the combined aqueous extracts washed with CH$_2$Cl$_2$ (20mL x 3). The organic extracts were dried (MgSO$_4$) and the solvent removed *in vacuo*. The product was then purified by flash chromatography to yield 85mg of the desired product **47** (47%), as well as 8mg (4%) of the five-membered ring **50**.

R$_F$=0.52 (1:1 Hexane:EtOAc)

m/z (+ve FAB) cal 280.1675 found 280.1676

^{1}H NMR (CDCl$_3$,, 400MHz) δ 7.33-7.23 (m, 5H), 4.59-4.51 (m, 3H, H1, Bn), 3.73-3.69 (m, 2H, H3, H4), 3.57-3.53 (m, 3H, H4, H5, -O-C$\underline{H}_2$), 3.40-3.34 (m, 2H, -O-C$\underline{H}_2$), 2.01-1.97 (m, 2H, H2, OH), 1.86-1.81(m, 1H, H2), 1.14 (s, 3H, CH$_3$), 0.68 (s, 3H, CH$_3$) ppm.

^{13}C NMR (CDCl$_3$, 100MHz) δ 128.9 (CH, Ph), 128.3 (CH, Ph), 128.2, (CH, Ph), 100.1 (CH, C1), 77.7 (CH$_2$, C5 and C7), 77.6 (CH$_2$, Bn), 76.2 (CH, C3), 72.0 (CH$_2$, Bn), 64.8 (CH$_2$, C4), 36.9 (CH$_2$, C2), 23.5 (CH$_3$), 22.2 (CH$_3$) ppm.

Synthesis of 48
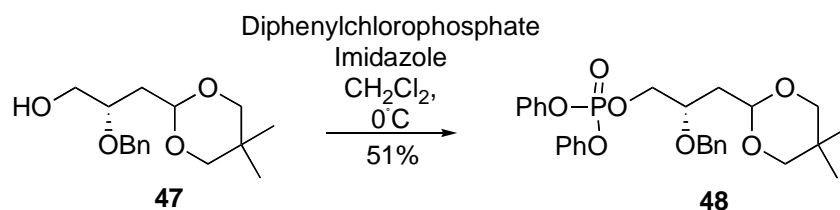
47 (97mg, 0.34mmol) was dissolved in CH_2Cl_2 (4mL) and cooled to 0°C. Imidazole (88mg, 0.42mmol) and diphenylchlorophosphate (32µL, 1.4mmol) were added, and the reaction mixture stirred for five hours while being allowed to warm to room temperature. H_2O (5mL) and CH_2Cl_2 (10mL) were then added to the reaction mixture, and it was transferred to a separating funnel. 10% HCl (3mL) was added and the aqueous layer extracted with CH_2Cl_2 (10mL x 3). The combined organic layers were then washed with saturated aqueous $NaHCO_3$ solution (10mL), H_2O (10mL), and saturated aqueous NaCl solution (10mL). The combined organic extracts were then dried ($MgSO_4$) and the solvent removed *in vacuo* to give 87mg (51%) of the title compound.

R_F=0.48 (2:1 Hex:EtOAc)

^{1}H NMR (CDCl$_3$, 400MHz) δ 7.29-7.13 (m, 15H, Ph), 4.57 (d, J=11.5Hz 1H, Bn), 4.52-4.50 (m, 1H, H1), 4.45 (d, J=11.5Hz, 1H, Bn), 4.39-4.30 (m, 1H, H4), 3.90-3.86 (m, 1H, H4), 3.54-3.50 (m, 2H, H3), 3.34 (d, J=11.3Hz, 2H, -O-C$\underline{H}_2$), 3.28 (d, J=11.3Hz, 2H, -O-C$\underline{H}_2$), 1.92-1.89 (m, 1H, H2), 1.84-1.64 (m, 1H, H2), 1.12 (s, 3H, C$\underline{H}_3$), 0.67 (s, 3H, C$\underline{H}_3$) ppm.

^{13}C NMR (CDCl$_3$, 100MHz) δ 130.2, 128.7, 128.3, 128.1, 125.7, 120.6, 120.5, 99.6 (CH, C1), 77.8 (CH$_2$), 77.6 (CH$_2$), 74.2 (d, $^3J_{POCC}$=7.6Hz, CH, C3), 72.6 (CH$_2$, Bn), 71.0 (d, $^2J_{POC}$=6.9Hz, CH$_2$, C4), 37.0 (CH$_2$, C2), 30.5 (CH, C1), 23.4 (CH$_3$), 22.2 (CH$_3$) ppm.

Synthesis of 49
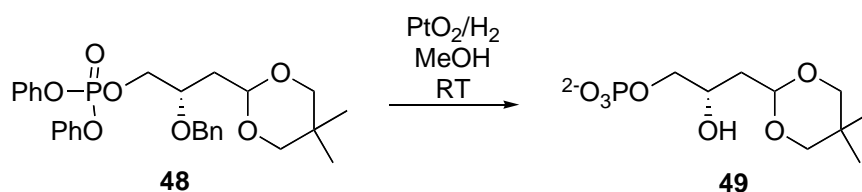
48 (33mg, 0.06mmol) was dissolved in MeOH (1mL) and PtO$_2$ added (15mg, 0.06mmol). The flask was evacuated and filled with H$_2$ gas three times and the mixture allowed to stir overnight until TLC analysis showed no UV active spot on the baseline. The solution was filtered and the pH adjusted to 9.5 using Et$_3$N. The product was then freeze-dried, giving 18.1mg (83%) of the triethylamine salt.

^{1}H NMR (D$_2$O, 400MHz) δ 4.67-4.63 (m, 1H, H1), 3.84-3.79 (m, 1H, H3), 3.68-3.65 (m, 1H), 3.61-3.57 (m, 1H), 3.52-3.44 (m, 5H), 1.69-1.66 (dd, J=6Hz, 6Hz, 2H, H2), 0.98 (s, 3H, CH$_3$), 0.69 (s, 3H, CH$_3$) ppm.

^{13}C NMR (D$_2$O, 100MHz) δ 100.0(C1), 77.2, 68.8, 67.1, 37.6 (C2), 29.9, 22.3 (CH$_3$), 20.9 (CH$_3$) ppm.

Synthesis of (*S*)-2-deoxyE4P 38
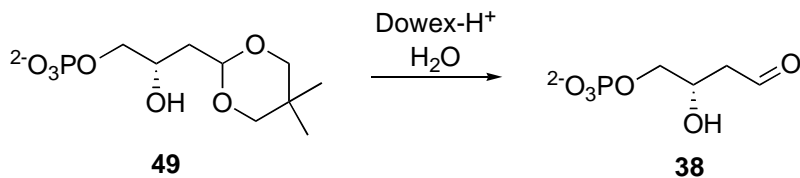
The dioxalane **49** (24mg, 0.05mmol) was dissolved in H$_2$O (1.5mL) and freshly activated Dowex$^®$ 50W-H$^+$ form cation exchange resin was added to give a pH of 2. The solution was then heated to 40˚C and stirred overnight. The Dowex$^®$ 50W resin was removed by filtration and the pH of the filtrate adjusted to 6.8 using 10M NaOH. Charcoal was used to decolourise the solution, which was then filtered and used directly in the enzyme assays.

Large scale synthesis of 5-deoxyDAH7P 51

Large scale enzymatic synthesis of 5-deoxyDAH7P was carried out using *E. coli* DAH7P synthase (phe). 4.5mg each of PEP and racemic 2-deoxyE4P were dissolved in water and MnSO$_4$ added to a final concentration of 500μM. The pH was adjusted to 6.8 using 1M NaOH. The reaction was initiated by the addition of enzyme (10μL, 1.8mg/mL) and the loss of PEP was monitored for 48 hours at 270nm. Once the loss of PEP had ceased, the enzyme was removed by ultrafiltration using a Vivaspin 10kDa MWCO concentrator and the products purified by anion-exchange chromatography (SourceQ$^®$ resin, Amersham) using a linear gradient of ammonium bicarbonate from 0-1M. The fractions containing 5-deoxyDAHP were pooled, lyophilised and stored in the freezer at -20˚C.

Determination of the utilisation of racemic 2-deoxyE4P by *E. coli* DAH7P synthase

A solution containing 4.2mg of racemic 2-deoxyE4P in 600μL D$_2$O was prepared. Another solution containing ~4.0mg of G6P in D$_2$O 600μL was also prepared. These two concentrated solutions were diluted 5-fold for use in the enzyme assays described below.

For the ^{31}P NMR analysis, 300µL of each undiluted solution were mixed together. A ^{31}P NMR spectrum was collected and the peaks due to 2-deoxyE4P and G6P were integrated to give a relative concentration of 1:0.37 G6P:2-deoxyE4P.

Assays with DAH7P synthase contained an unknown concentration of racemic 2-deoxyE4P (200µL of dilute solution), PEP (~500µM) and $MnSO_4$ (100µM) in 50mM BTP buffer containing µM EDTA, pH 6.8. Reactions were initiated by the addition of *E. coli* DAH7P synthase (10µL, 1.0mg/mL) to give a final volume of 1mL. Assays were carried out at 25°C. The control assays used to determine the absorbance increase due to the addition of enzyme contained no E4P analogue but were otherwise identical to the experimental assays. The decrease in absorbance due to the loss of PEP was monitored at 232nm ($\varepsilon = 2.8 \times 10^3 \ M^{-1} \ cm^{-1}$ at 25°C) to completion and the concentration of 2-deoxyE4P consumed by the enzyme calculated from the change in absorbance observed after correction for the blank assay containing no 2-deoxyE4P. Assays were carried out in duplicate.

Assays with G6P dehydrogenase contained an unknown concentration of G6P (50µL of the dilute solution), $MgCl_2$ (100µM), and $NADP^+$ (150µM) in 0.1M BTP buffer, pH 8. Reactions were initiated by the addition of G6P dehydrogenase (5µL, 1mg/mL) to give a final volume of 1mL. Assays were carried out at 25°C. The increase in absorbance due to the formation of NADPH was monitored at 340nm ($\varepsilon = 6.2 \times 10^3 \ M^{-1} \ cm^{-1}$ at 25°C) to completion and the concentration of G6P consumed by the enzyme calculated from the change in absorbance at 340nm. The assays were carried out in duplicate.

The results and calculations are given below.

[2-deoxyE4P] determined from assay 1 (after correction for blank)	3.53mM
[2-deoxyE4P] determined from assay 2 (after correction for blank)	3.58mM
[G6P] determined from assay 1	20mM
[G6P] determined from assay 2	19mM

The amount of 2-deoxyE4P in solution can be calculated using the average concentration of 2-deoxyE4P to G6P; 19.5 x 0.37 = 7.22mM. This is the concentration of both isomers of 2-deoxyE4P. The average concentration of 2-deoxyE4P determined by enzyme assay was 3.56mM, which is 49% of the average concentration determined by comparison to G6P by ^{31}P NMR.

This entire experiment was repeated under the same conditions with (*S*)-2-deoxyE4P and 100% utilisation was observed.

Determination of initial kinetic parameters of 2-deoxyE4P with DAH7P synthase

The determination of the initial kinetic parameters of 2-deoxyE4P with *E. coli* DAH7P synthase (phe), *N. meningitidis* DAH7P synthase and *M. tuberculosis* DAH7P synthase were carried out using standard assay conditions.

The determination of the initial kinetic parameters of 2-deoxyE4P with *P. furiosus* were carried out by Dr Linley Schofield as described in the literature.[20]

Deuteration studies

Large scale enzymatic synthesis of 5-deoxyDAH7P in D_2O was carried out using *E. coli* DAH7P synthase (phe). 4mg each of PEP and racemic 2-deoxyE4P were dissolved in D_2O and $MnSO_4$ added to a final concentration of 500µM. The pH was adjusted to 6.8 using 1M NaOH. The reaction was initiated by the addition of enzyme (10µL, 1.8mg/mL) and the reaction allowed to proceed at room temperature. ^{1}H NMR analysis was carried out directly on this solution.

Determination of initial kinetic parameters of 2-deoxyR5P with *N. meningitidis* KDO8P synthase

The determination of the initial kinetic parameters of 2-deoxyR5P with *N. meningitidis* KDO8P synthase were carried out using standard assay conditions.

6.5 Experimental methods for chapter four: Synthesis and evaluation of 3-deoxyE4P and 3-deoxyA5P with DAH7P and KDO8P synthases

Synthesis of 54
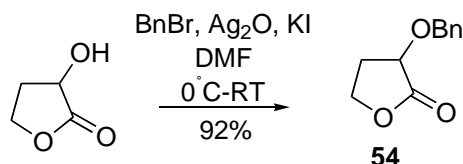
α-Hydroxy-γ-butyrolactone (0.2018g, 1.98mmol) was dissolved in DMF (5mL) and cooled to 0˚C. BnBr (352μL, 2.96mmol), Ag$_2$O (0.6896g, 2.96mmol) and KI (0.0329g, 0.20mmol) were added and the mixture allowed to warm slowly to room temperature. After four hours, the mixture was filtered through Celite and the filtrate washed with saturated aqueous NaHCO$_3$ solution, H$_2$O, and saturated aqueous NaCl solution (20mL each). The organic extract was dried (MgSO$_4$) and the solvent removed *in vacuo*. Purification by flash column chromatography provided 0.3507g (92%) of **54**, a colourless oil.

R$_F$=0.67 (1:1 Hex:EtOAc)

m/z (+ve FAB) cal 192.0786 found 192.0785

^{1}H NMR (CDCl$_3$, 400MHz) δ 7.36-7.24 (m, 5H), 4.92 (d, J=11.5Hz, 1H, Bn), 4.72 (d, J=11.5Hz, 1H, Bn), 4.41-4.40 (m, 1H, H4), 4.21-4.14 (m, 2H, H2, H4), 2.49-2.39 (m, 1H, H3), 2.30-2.29 (m, 1H, H3) ppm.

^{13}C NMR (CDCl$_3$, 100MHz) δ 175.5 (Q, C1), 137.3 (Q, Ph), 129.0, 128.6, 128.6 (CH, Ph) 72.8 (CH, C2), 75.5 (CH$_2$, Bn), 65.9 (CH$_2$, C4), 30.3 (CH$_2$, C3) ppm.

Synthesis of 55
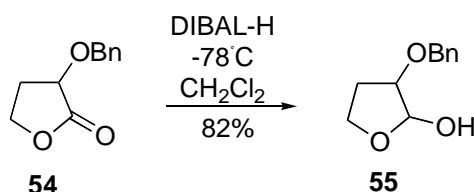
54 (0.206g, 1.07mmol) was dissolved in CH$_2$Cl$_2$ (15mL) and cooled to -78˚C. DIBAL (1.6mL, 1.61mmol) was added and the mixture kept at -78˚C. A further 0.4mL (0.4mmol) of DIBAL was added after one hour of stirring After another hour, the

reaction was quenched by drop-wise addition of 10% HCl (5mL) and allowed to warm to room temperature. The reaction mixture was then washed with saturated aqueous Rochelles salt and saturated aqueous NaCl solution (20mL each), dried (MgSO$_4$) and the solvent removed *in vacuo*. Flash chromatography provided 0.169g (82%) of **55**.

R$_F$=0.61 (1:2 Hex:EtOAc)

^{1}H NMR (CDCl$_3$, 400MHz) δ 7.36-7.24 (m, 7H), 5.42 (d, J=2.6Hz, 1H), 5.30 (dd, J=8.0Hz, 4.2Hz, 0.3H), 4.59 (d, J=6.3Hz, 0.4H), 4.54 (s, 2H), 4.07 (dd, J=8.2Hz, 6.1Hz, 2H), 3.99 (dd, J=5.7Hz, 1.9Hz, 1H), 3.83-3.77 (m, 0.5H), 2.74 (d, J=2.7Hz, 1H), 2.25-2.16 (m, 1H), 2.11-2.94 (m, 1.6H) ppm.

^{13}C NMR (CDCl$_3$, 100MHz) δ 128.6, 128.5, 128.2, 127.9, 127.8, 127.7, 100.7, 96.3, 83.3, 78.1, 72.4, 71.4, 67.1, 64.8, 29.9, 29.8 ppm.

Synthesis of 56
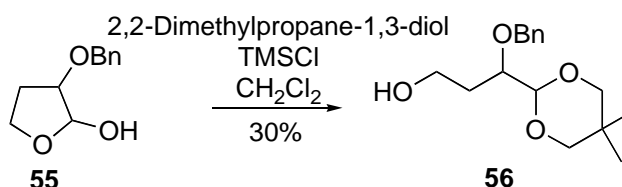
2,2-Dimethylpropane-1,3-diol (0.1087g, 1.04mmol) was dissolved in CH$_2$Cl$_2$ (5mL), TMSCl (264μL, 2.09mmol) added, and the mixture stirred at 0°C for 15 minutes. **55** (0.148g, 0.76mmol) was added and the mixture stirred overnight while being allowed to warm slowly to room temperature. The mixture was diluted with CH$_2$Cl$_2$ and washed with saturated aqueous NaHCO$_3$ solution (10mL). The aqueous phase was extracted with CH$_2$Cl$_2$ (15mL x 2). The combined organic extracts were dried (MgSO$_4$) and the solvent removed *in vacuo*. Flash chromatography provided 0.0658g (30%) of **56**, a colourless oil.

R$_F$=0.65 (1:2 Hex:EtOAc)

^{1}H NMR (CDCl$_3$, 400MHz) δ 7.35-7.23 (m, 5H, Ph), 4.78 (d, J=11.5Hz, 1H, Bn), 4.58 (d, J=11.5Hz, 1H, Bn), 4.51 (d, J=3.6Hz, 1H, H1), 3.73-3.60 (m, 5H, H2, H4s, -O-C$\underline{H}_2$), 3.43-3.38 (m, 2H, -O-C$\underline{H}_2$), 1.80 (br s, 1H, OH), 1.90-1.79 (m, 2H, H3s), 1.17 (s, 3H, CH$_3$), 0.70 (s, 3H, CH$_3$) ppm.

^{13}C NMR (CDCl$_3$, 100MHz) δ 138.2 (Q, Ph), 128.4, 128.1, 127.8 (CHs, Phs), 102.0 (CH, C1), 78.2 (CH, C2), 77.2 (CH$_2$, C5 and C7), 73.0 (CH$_2$, Bn), 60.1 (CH$_2$, C4), 32.2 (CH$_2$, C3), 30.4 (Q, C6), 23.0 (CH$_3$), 21.8 (CH$_3$) ppm.

Synthesis of 57
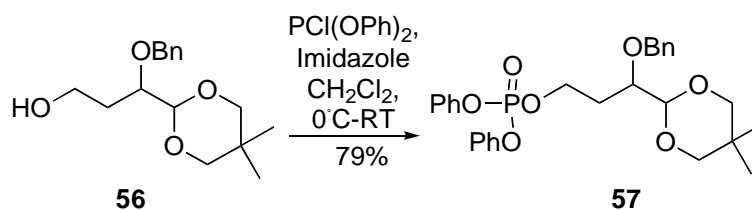
56 (0.0658g, 0.24mmol) was dissolved in CH$_2$Cl$_2$ (4mL) and cooled to 0˚C. Imidazole (0.0640g, 0.94mmol) and diphenylchlorophosphate (73µL, 0.35mmol) were added and the solution allowed to warm slowly to room temperature. After stirring overnight, the solution was diluted with CH$_2$Cl$_2$ (10mL) and washed with saturated aqueous NaHCO$_3$ solution and saturated aqueous NaCl solution three times (10mL each). The combined aqueous washings were extracted with CH$_2$Cl$_2$ (3 x 10mL) and the combined organic extracts dried (MgSO$_4$) and the solvent removed *in vacuo*. Flash chromatography provided 0.094g (79%) of the phosphorylated compound **57**.

R$_F$=0.81 (1:1 Hex:EtOAc)

m/z (+ve FAB) cal 513.2042 found 513.2069

^{1}H NMR (CDCl$_3$, 400MHz) δ 7.33-7.12 (m, 15H, Ph), 4.71 (d, J=11.6Hz, 1H, Bn), 4.49-4.46 (m, 2H, Bn, H1), 4.42-4.35 (m, 2H, H4s), 3.64-3.57 (m, 3H, H2, -O-C$\underline{H}_2$), 3.41-3.35 (m, 2H, -O-C$\underline{H}_2$), 2.17-2.08 (m, 1H, H3), 1.99-1.90 (m, 1H, H3), 1.16 (s, 3H, CH$_3$), 0.69 (s, 3H, CH$_3$) ppm.

^{13}C NMR (CDCl$_3$, 100MHz) δ 150.6 (d, ^{2}J$_{COP}$=7Hz, Q, P-O-$\underline{Ph}$), 138.3 (Q, CH$_2$-$\underline{Ph}$), 129.8, 128.3, 128.0, 127.7, 125.3, 120.1 (CHs, Phs), 101.8 (CH, C1), 77.1 (CH$_2$, C5, C7), 75.9 (CH, C2), 73.3 (CH$_2$, Bn), 66.2 (d, ^{2}J$_{COP}$=6.6Hz, CH$_2$, C4), 30.5 (d, ^{3}J$_{CCOP}$=7.5Hz, CH$_2$, C3), 30.4 (Q, C6), 23.0 (CH$_3$), 21.8 (CH$_3$) ppm.

^{31}P NMR (CDCl$_3$, 160 MHz) δ -11.85 (t, ^{3}J$_{POCH}$=7.8Hz).

Synthesis of 58
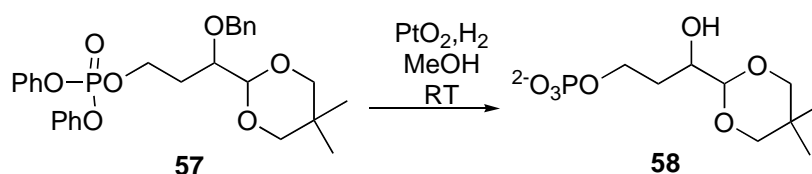
The protected analogue **57** (0.0944g, 0.18mmol) was dissolved in MeOH (5mL) and PtO$_2$ (0.0418g, 0.18mmol) added. The flask was evacuated and filled with H$_2$ gas and left to stir vigorously overnight. The PtO$_2$ was then filtered off and the filtrate lyophilised and the product was used without purification in the next step.

^{1}H NMR (D₂O, 400MHz) δ 4.59 (d, J=4.0Hz, 1H), 4.16-4.08 (m, 2H), 3.87-3.83 (m, 1H), 3.73 (d, J=11.3Hz, 2H), 3.63 (dd, J=11.3Hz, 3.0Hz, 2H), 2.07-1.99 (m, 1H), 1.86-1.77 (m, 1H), 1.19 (s, 3H), 0.80 (s, 3H) ppm.

Synthesis of racemic 3-deoxyE4P 59 from 58

58   **59**
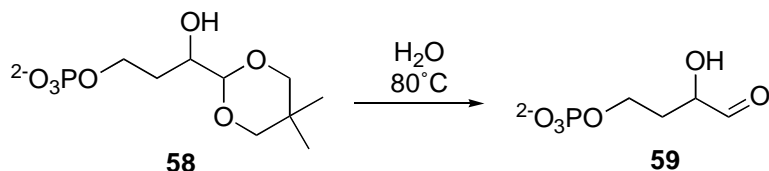
The lyophilised product **58** from the hydrogenolysis (5mg) was dissolved in D₂O (500µL) and heated gradually while being monitored by ^{1}H NMR spectroscopy. Once 80˚C was reached, the integral of the methyl groups from the protecting group began to decrease. The sample was maintained at 80˚C for 8 hours until less than 20% of the original integral remained. Enzyme assays showed the yield of 3-deoxyE4P to be <5%.

Synthesis of 62

62
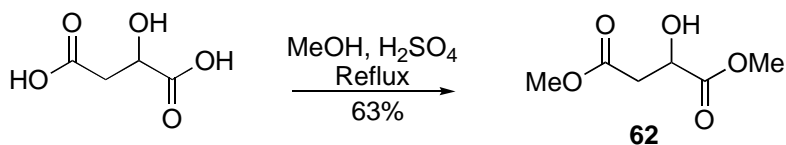
Malic acid (2.0g, 14.9mmol) was dissolved in MeOH (6mL), conc. H₂SO₄ added, and the solution was heated to reflux for 50 hours. After being allowed to cool, the mixture was poured into a separating funnel containing saturated aqueous NaCl solution (40mL) and EtOAc (10mL). The organic phase was removed and the aqueous phase extracted with EtOAc (10mL x 3). The combined organic extracts were dried (MgSO₄) and the solvent removed *in vacuo* to give 1.5295g (63%) of **62**, which was used without purification in the next step.

R_F=0.42 (1:1 Hex:EtOAc)

m/z (+ve FAB) cal 163.0601 found 163.0609

^{1}H NMR (CDCl₃, 400MHz) δ 4.46 (d, J=6.2Hz, 4.4Hz, 1H, H2), 3.74 (s, 3H, CH₃), 3.65 (s, 3H, CH₃), 3.46 (br s, 1H, OH), 2.82 (dd, J=16.5Hz, 4.4Hz, 1H, H3), 2.78 (dd, J=16.5Hz, 6.2Hz, 1H, H3) ppm.

Synthesis of 63
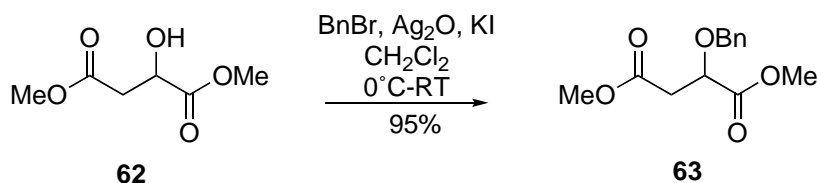
62 (1.0028g, 6.2mmol) was dissolved in CH_2Cl_2 (10mL) and cooled to 0°C. BnBr (1.1mL, 9.25mmol), Ag_2O (2.1476g, 9.27mmol) and KI (0.1055g, 0.64mmol) were added and the solution allowed to warm slowly to room temperature. After six hours, the mixture was filtered through celite and the filtrate washed with saturated aqueous $NaHCO_3$ solution, H_2O, and saturated aqueous NaCl solution (40mL each). The combined aqueous washings were extracted with CH_2Cl_2 (3 x 25mL), the combined organic extracts dried ($MgSO_4$) and the solvent removed *in vacuo.* Flash chromatography provided 0.1488g (95%) of **63**, a colourless oil.

R_F=0.82 (1:1 Hex:EtOAc)

m/z (+ve FAB) cal 253.1076 found 253.1081

$[\alpha]^{20}_D$ +70.9 (*c* 1.00, $CHCl_3$)

^{1}H NMR ($CDCl_3$, 400MHz) δ 7.31-7.23 (m, 5H, Ph), 4.74 (d, J=11.6Hz, 1H, Bn), 4.51 (d, J=11.6Hz, 1H, Bn), 4.37 (dd, J=7.6Hz, 5.3Hz, 1H, H2), 3.74 (s, 3H, CH_3), 3.65 (s, 3H, CH_3), 2.79-2.76 (m, 2H, H3s) ppm.

^{13}C NMR ($CDCl_3$, 100MHz) δ 171.8 (Q, C=O), 170.5 (Q, C=O), 137.2 (Q, Ph), 128.4, 128.1, 128.0 (CHs, Ph), 74.5 (CH, C2), 73.1 (CH_2, Bn), 37.8 (CH_2, C3) ppm.

Synthesis of 2-(benzyloxy)butane-1,4-diol
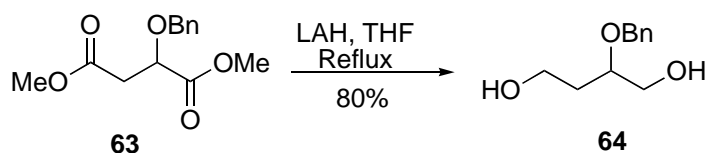
LAH (0.3403g, 8.97mmol) was suspended in THF (10mL) and cooled to 0°C. **63** in THF (10mL) was added dropwise to the LAH suspension over 30min. The reaction was then heated to reflux for 3 hours. After allowing to cool, H_2O and 1M NaOH solution were added sequentially until bubbling had ceased and the LAH was white in colour. The mixture was filtered through celite, the filtrate dried ($MgSO_4$) and the solvent removed *in vacuo.* Flash chromatography provided 0.7063g (80%) of **64** a colourless oil.

R_F=0.30 (1:3 Hex:EtOAc)

m/z (+ve FAB) cal 197.1178 found 197.1178

$[\alpha]^{20}_D$ +15.1 (*c* 1.00, CHCl$_3$)

^{1}H NMR (CDCl$_3$, 400MHz) δ 7.34-7.24 (m, 5H, Ph), 4.58 (d, J=11.8Hz, 1H, Bn), 4.54 (d, J=11.8Hz, 1H, Bn), 3.74-3.54 (m, 5H, H1s, H2, H4s), 2.80 (br s, 2H, O<u>H</u>), 1.88-1.73 (m, 2H, H3) ppm.

^{13}C NMR (CDCl$_3$, 100MHz) δ 138.1 (Q, Ph), 128.6, 127.9, 127.9 (CH, Phs), 77.8 (CH, C2), 71.6 (CH$_2$, Bn), 63.9 (CH$_2$, C1/C4), 59.4 (CH$_2$, C1/C4), 33.9 (CH$_2$, C3) ppm.

Synthesis of 65
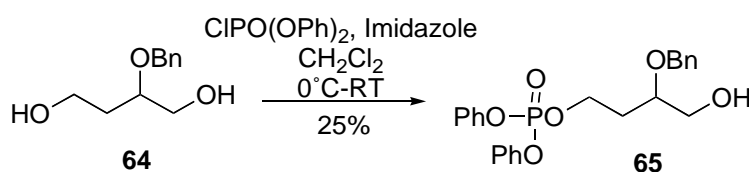
To a solution of **64** (0.1698g, 0.87mmol) in CH$_2$Cl$_2$ (5mL) was added diphenylchlorophosphate (162μL, 0.78mmol) and imidazole (0.2356g, 3.46mmol) at 0˚C. The solution was allowed to warm slowly to room temperature. After stirring overnight, further diphenylchlorophosphate (18μL, 0.09mmol) was added. After a further two hours stirring, the mixture was diluted with CH$_2$Cl$_2$ and washed with saturated aqueous NaHCO$_3$ solution and saturated aqueous NaCl solution. The combined aqueous extracts were extracted with CH$_2$Cl$_2$ (10mL x 2). The combined organic extracts were dried (MgSO$_4$) and the solvent removed *in vacuo*. Flash chromatography provided 0.0936g (25%) of the desired compound, as well as 0.0420g (11%) of the other monophosphorylated compound and 0.1823g (32%) of the diphosphorylated compound.

R_F=0.67 (1:3 Hex:EtOAc)

m/z (+ve FAB) cal 429.1467 found 429.1483

$[\alpha]^{20}_D$ +17.8 (*c* 1.00, CHCl$_3$)

^{1}H NMR (CDCl$_3$, 400MHz) δ 7.24-7.07 (m, 15H, Ph), 4.42 (d, J=11.5Hz, 1H, Bn), 4.40 (d, J=11.5Hz, 1H, Bn), 4.41-4.34 (m, 2H, H4), 3.69 (dd, J=11.6Hz, 3.7Hz, 1H, H1), 3.60 (dt, J=11.6Hz, 3.8Hz, 1H, H2), 3.46 (dd, J=11.6Hz, 3.7Hz, 1H, H1), 2.01-1.86 (m, 2H, H3) ppm.

^{13}**C NMR (CDCl$_3$, 100MHz)** δ 150.5 (d, $^2J_{COP}$=7Hz, Q, P-O-<u>Ph</u>), 138.1 (Q, CH$_2$-<u>Ph</u>), 129.9, 128.5, 127.9, 127.8, 125.4, 120.1 (CHs, Ph), 75.8 (CH, C2), 72.0 (CH$_2$, Bn), 66.1 (d, $^2J_{COP}$=6.4Hz, CH$_2$, C4), 63.6 (CH$_2$, C1), 32.1 (d, $^3J_{CCOP}$=6.8Hz, CH$_2$, C3) ppm.

^{31}**P NMR (CDCl$_3$, 160 MHz)** δ -11.93 (t, $^3J_{POCH}$= 6.9Hz) ppm.

Synthesis of 66
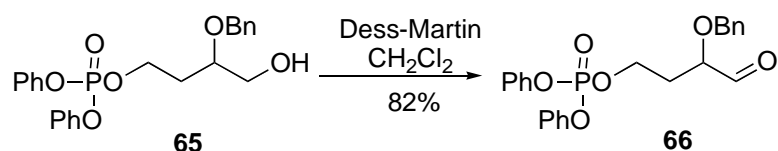
65 (0.0936g, 0.22mmol) was dissolved in CH$_2$Cl$_2$ (5mL) and freshly prepared Dess Martin periodinane (0.1854g, 0.44mmol) added. The mixture was stirred for three hours, after which Et$_2$O, saturated aqueous NaHCO$_3$ solution, and saturated aqueous Na$_2$S$_2$O$_3$ solution were added (3 mL each) and the mixture stirred until it was clear. The mixture was transferred to a separating funnel and the aqueous layer extracted with Et$_2$O (10mL x 3). The combined organic extracts were washed with saturated aqueous NaHCO$_3$ solution, H$_2$O and saturated aqueous NaCl solution (10mL each), dried (MgSO$_4$) and the solvent removed *in vacuo.* Flash chromatography provided 0.0768g (82%) of aldehyde **66**.

R$_F$=0.62 (1:3 Hex:EtOAc)

m/z (+ve FAB) cal 426.1232 found 426.1221

$[\alpha]^{20}_D$ +41.8 (*c* 1.00, CHCl$_3$)

^{1}**H NMR (CDCl$_3$, 400MHz)** δ 9.58 (d, J=1.6Hz, 1H, H1), 7.34-7.15 (m, 15H, Ph), 4.61 (d, J=11.5Hz, 1H, Bn), 4.48 (d, J=11.5Hz, 1H, Bn), 4.42-4.37 (m, 2H, H4), 3.89 (ddd, J=8.6Hz, 4.3Hz, 1.6Hz, 1H, H2), 2.15-2.06 (m, 1H, H3), 1.99-1.89 (m, 1H, H3) ppm.

^{13}**C NMR (CDCl$_3$, 100MHz)** δ 202.6 (CH, C1), 150.4 (d, $^2J_{COP}$=7.5Hz, Q P-O-<u>Ph</u>), 137.0, 129.9, 128.6, 128.5, 128.3, 128.1, 127.7, 125.5, 120.1, 120.0 (CHs Ph), 79.6 (CH, C2), 73.1 (CH$_2$, Bn), 64.6 (d, $^2J_{COP}$=5.9Hz, CH$_2$, C4), 31.0 (d, $^3J_{CCOP}$=7.5Hz, CH$_2$, C3) ppm.

^{31}**P NMR (CDCl$_3$, 160 MHz)** δ -12.02 (t, $^3J_{POCH}$=7.8Hz) ppm.

Synthesis of 67
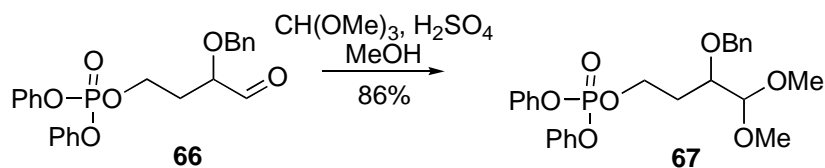
To **66** (0.213g, 0.5mmol) in MeOH (8mL) was added trimethylorthoformate (547µL, 5.0mmol) and conc. H_2SO_4 (4.3µL, 0.08mmol). After stirring overnight, the mixture was transferred to a separating funnel containing saturated aqueous $NaHCO_3$ solution (20mL) and Et_2O (10mL). The aqueous layer was extracted with Et_2O (10mL x 3). The combined organic extracts were washed with saturated aqueous NaCl solution (20mL), dried ($MgSO_4$) and the solvent removed *in vacuo*. Flash chromatography provided 0.202g (86%) of **67**.

R_F=0.78 (1:3 Hex:EtOAc)

m/z (+ve FAB) cal 473.1729 found 473.1743

$[\alpha]^{20}_D$ +28.5 (*c* 1.00, $CHCl_3$)

^{1}H NMR (CDCl$_3$, 400MHz) δ 7.35-7.12 (m, 15H, Ph), 4.69 (d, J=11.5Hz, 1H, Bn), 4.46 (d, J=11.5Hz, 1H, Bn), 4.41-4.36 (m, 2H, H4), 4.22 (d, J=5.2Hz, 1H, H1), 3.60-3.56 (m, 1H, H2), 3.40 (s, 3H, CH$_3$), 3.36 (s, 3H, CH$_3$), 2.10-2.02 (m, 1H, H3), 1.88-1.84 (m, 1H, H3) ppm.

^{13}C NMR (CDCl$_3$, 100MHz) δ 150.6 (d, $^2J_{COP}$=6.9Hz, Q, P-O-$\underline{Ph}$), 138.3 (Q, CH$_2$-$\underline{Ph}$), 129.8, 128.4, 128.0, 125.3 (CH, Phs), 120.1 (d, $^3J_{CCOP}$=4.4Hz, CH, Ph), 106.7 (CH, C1), 75.6 (CH, C2), 73.4 (CH$_2$, Bn), 66.0 (CH$_3$), 66.1 (d, $^2J_{COP}$=6.1Hz, CH$_2$, C4), 55.8 (CH$_3$), 31.0 (d, $^3J_{CCOP}$=7.4Hz, CH$_2$, C3) ppm.

^{31}P NMR (CDCl$_3$, 160 MHz) δ -11.96 (t, $^3J_{POCH}$=7.7Hz) ppm.

Synthesis of 3-deoxyE4P from 67
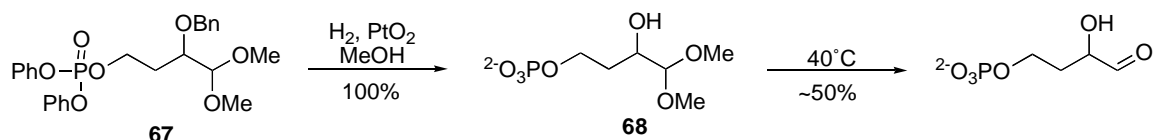
The protected analogue **67** (0.108g, 0.23mmol) was dissolved in MeOH (8mL) and PtO$_2$ (0.0519g, 0.23mmol) added. The flask was evacuated and filled with H$_2$ gas and left to stir for 50 hours. The PtO$_2$ was then removed by filtration and the filtrate evaporated *in vacuo,* giving 0.0528g (100%) of a colourless oil. The oil was dissolved

in H_2O and heated overnight at 40°C. Standard enzyme assay conditions were used to confirm the presence of 3-deoxyE4P with 50% yield.

Determination of initial kinetic parameters of 3-deoxyE4P with DAH7P synthase

The determination of the initial kinetic parameters of 3-deoxyE4P with *E. coli* DAH7P synthase (phe), *N. meningitidis* DAH7P synthase, *P. furiosus* DAH7P synthase and *M. tuberculosis* DAH7P synthase were carried out using standard assay conditions as described in Section 6.1.

Determination of the utilisation of racemic 3-deoxyE4P by *E. coli* DAH7P synthase

A ~10mM solution of racemic 3-deoxyE4P in D_2O and a ~3mM solution of G6P in D_2O were prepared. These solutions were used for the enzyme assays and ^{31}P NMR spectroscopy described below.

For the ^{31}P NMR analysis, 300µL of each solution were mixed together. A ^{31}P NMR was collected and the peaks due to 3-deoxyE4P and G6P were integrated to give a relative concentration of 1:4.2 G6P:3-deoxyE4P.

Assays with DAH7P synthase contained an unknown concentration of racemic 3-deoxyE4P (10µL of the solution described above), PEP (~300µM) and $MnSO_4$ (100µM) in 50mM BTP buffer, pH 6.8. Reactions were initiated by the addition of *E. coli* DAH7P synthase (5µL, 8.4mg/mL) to give a final volume of 1mL. Assays were carried out at 25°C. The decrease in absorbance due to the loss of PEP was monitored at 232nm ($\varepsilon = 2.8 \times 10^3$ M^{-1} cm^{-1} at 25°C) to completion and the concentration of 3-deoxyE4P consumed by the enzyme calculated from the change in absorbance observed at 232nm.

Assays with G6P dehydrogenase contained an unknown concentration of G6P (20µL of the solution described above), $MgCl_2$ (100µM), and $NADP^+$ (120µM) in 0.1M BTP buffer, pH 8. Reactions were initiated by the addition of G6P dehydrogenase (2.5µL, 1mg/mL) to give a final volume of 1mL. Assays were carried out at 25°C. The

increase in absorbance due to the formation of NADPH was monitored at 340nm (ε = 6.2 x 10^3 M^{-1} cm^{-1} at 25˚C) to completion and the concentration of G6P consumed by the enzyme calculated from the change in absorbance at 340nm. The assays were carried out in duplicate.

The results and calculations are given below.

[3-deoxyE4P] determined from assay 1 (after correction for blank)	13.04mM
[3-deoxyE4P] determined from assay 2 (after correction for blank)	12.65mM
[G6P] determined from assay 1	2.85mM
[G6P] determined from assay 2	3.17mM

The amount of 3-deoxyE4P can be calculated using the average concentration of G6P and the relative concentration of 3-deoxyE4P to G6P; 3.01 x 4.2 = 12.64mM. This is the concentration of both isomers of 3-deoxyE4P in solution. The average concentration of 3-deoxyE4P by enzyme assay was 12.85mM which is 98% of the concentration determination by comparison to G6P by NMR. This is also the concentration of both isomers.

Thiobarbituric acid assay[15,122]

The thiobarbituric acid test was carried out on the product of the enzyme-catalysed reaction with 3-deoxyE4P with DAH7P synthase from *E. coli*, *M. tuberculosis* and *H. pylori*.

Thiobarbituric acid assay reagents used were:
25mM sodium periodate ($NaIO_4$) in 0.125N H_2SO_4
Sodium metaarsenite ($NaAsO_2$) 2% w/v in 0.5M HCl
Thiobarbituric acid solution (0.36% w/v, pH 9 adjusted with NaOH)

A standard enzyme assay was carried out with 3-deoxyE4P (~140µM), PEP (200µM) and $MnSO_4$ (100µM). Once the reaction had gone to completion, the assay mixture

(100µL) was mixed with H_2O (50µL) and $NaIO_4$ (100µL in 0.125N H_2SO_4) and the mixture was heated at 60°C for one hour. The excess oxidising agent was reduced by the addition of 200µL of $NaAsO_2$. Following the disappearance of the yellow colour, 1mL of thiobarbituric periodate solution was added and the reaction mixture was heated at 100°C for ten minutes. Once the sample was cool, the absorbance at 549nm was measured ($\varepsilon = 1.03 \times 10^5 M^{-1}cm^{-1}$).

Benzylation of erythronic lactone in CH_2Cl_2
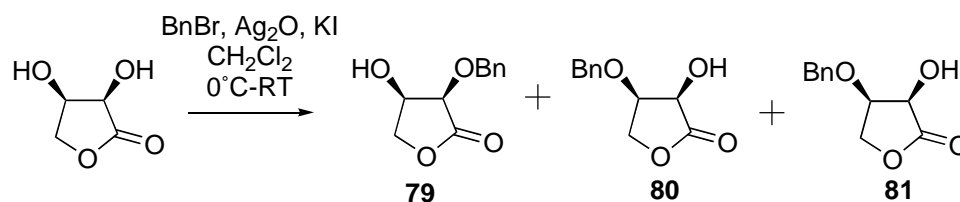
To a solution of erythronic lactone (0.1000g, 0.85mmol) in CH_2Cl_2 (5mL) at 0°C was added BnBr (101µL, 0.85mmol), Ag_2O (0.2965g, 1.28mmol) and KI (0.0142g, 0.085mmol). The mixture was allowed to warm slowly to room temperature. After six hours the reaction mixture was filtered through celite and the filtrate washed with saturated aqueous $NaHCO_3$ solution, H_2O and saturated aqueous NaCl solution (20mL each). The aqueous phase was extracted with CH_2Cl_2 (3 x 10mL), the combined organic extracts dried ($MgSO_4$) and the solvent removed *in vacuo*. Flash chromatography provided 0.0542g (31%) of a mixture of the two monobenzylated products products **79** and **80** as well as 0.0339g (21%) of the dibenzylated product **81**.

R_F (**79** and **80**)=0.50 (1:2 Hex:EtOAc)

R_F (**81** dibenzylated)=0.79 (1:2 Hex:EtOAc)

m/z (+ve FAB) cal 192.0786 found 192.0785

^{1}H NMR (79 **and** 80) **(CDCl$_3$, 400MHz)** δ 7.42-7.25 (m, 5H, Ph), 5.03 (d, J=12.0Hz, 1H, Bn), 4.82 (d, J=12.0Hz, 1H, Bn), 4.70 (d, J=12.0Hz, 0.3H, Bn), 4.66 (d, J=12.0Hz, 0.3H, Bn), 4.40-4.19 (m, 4H) ppm.

^{13}C NMR (CDCl$_3$, 100MHz) δ 173.3 (Q), 136.1 (Q), 128.8, 128.8, 128.7, 128.4, 127.9 (CH, Ph), 74.7 (CH), 74.0 (CH), 73.0 (CH$_2$) 71.2 (CH$_2$), 69.5 (CH), 69.9 (CH$_2$), 67.7 (CH$_2$) ppm.

Benzylation of erythronic lactone in DMF
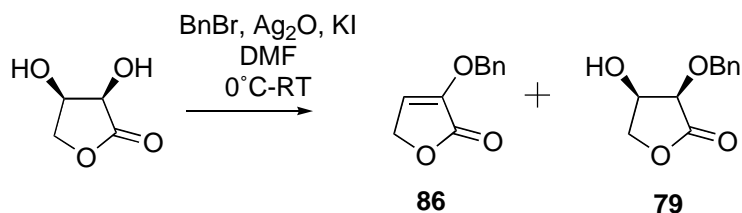
To a solution of erythronic lactone (0.1000g, 0.85mmol) in DMF (5mL) at 0°C was added BnBr (111μL, 0.93mmol), Ag_2O (0.2946g, 1.27mmol) and KI (0.0141g, 0.085mmol). The mixture was allowed to warm slowly to room temperature. After stirring overnight the reaction mixture was filtered through celite, and washed with saturated aqueous $NaHCO_3$ solution, H_2O and saturated aqueous NaCl solution (20mL each). The combined aqueous fractions were extracted with CH_2Cl_2 (3 x 10mL), filtered and the solvent evaporated *in vacuo*. Flash chromatography provided 0.0226g (13%) of **79** and 0.0569g (35%) of **86**.

R_F(**79**)=0.50 (1:2 Hex:EtOAc)

R_F(**86**)=0.70 (1:2 Hex:EtOAc)

^{1}H NMR (79) **($CDCl_3$, 400MHz)** δ 7.39-7.29 (m, 5H, Ph), 5.03 (d, J=11.7Hz, Bn), 4.82 (d, J=11.7Hz, Bn), 4.35-4.27 (m, 2H, H4), 4.21 (ddd, J=10.6Hz, 4.0Hz, 1.7Hz, 1H, H3), 4.14 (d, J=4.0Hz, 1H, H2) ppm.

^{13}C NMR ($CDCl_3$, 100MHz) δ 173.3 (Q, C1), 136.2 (Q, Ph), 128.8, 128.7, 128.4 (CH, Ph), 74.0 (CH, C2), 73.0 (CH_2, Bn), 71.2 (CH_2, C4), 67.7 (CH, C3) ppm.

Synthesis of 87
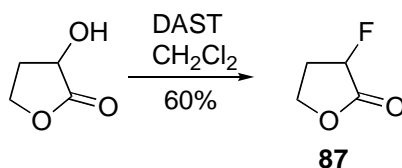
To α-hydroxy-γ-butyrolactone (0.2000g, 1.96mmol) in CH_2Cl_2 (10mL) at room temperature was added DAST (1.4mL, 11.7mmol). The mixture was allowed to stir at room temperature for four hours, at which point all the starting material had been consumed. The reaction mixture was cooled to 0°C and added to ice-cold saturated aqueous $NaHCO_3$ solution (50mL). The organic layer was removed and the aqueous layer extracted with CH_2Cl_2 (3 x 20mL). The combined organic extracts were dried ($MgSO_4$) and the solvent removed *in vacuo*. Flash chromatography provided 0.1234g (60%) of the product, a colourless oil.

R$_F$= 0.57 (1:1 Hex:EtOAc)

^{1}H NMR (CDCl$_3$, 400MHz) δ 5.14 (dt, J=51.3Hz, 7.9Hz, 1H, H2), 4.44-4.39 (m, 1H, H4), 4.27-4.21 (m, 1H, H4), 2.69-2.57 (m, 1H, H3), 2.50-2.35 (m, 1H, H3) ppm.

^{13}C NMR (CDCl$_3$, 100MHz) δ 171.9 (d, ^{2}J$_{CCF}$=21.3Hz, C1), 85.3 (d, J=189.6Hz, CH, C2), 64.9 (d, ^{3}J$_{CCCF}$=6.3Hz, CH$_2$, C4), 29.3 (d, ^{2}J$_{CCF}$=19.5Hz, CH$_2$, C3) ppm.

^{19}F NMR (CDCl$_3$, 376MHz) δ -195.84 (ddd, J=13.2Hz, 23.4Hz, 51.3Hz) ppm.

Fluorination of a mixture of 79 and 80

79 + **80** → **82** + **83** + **86**
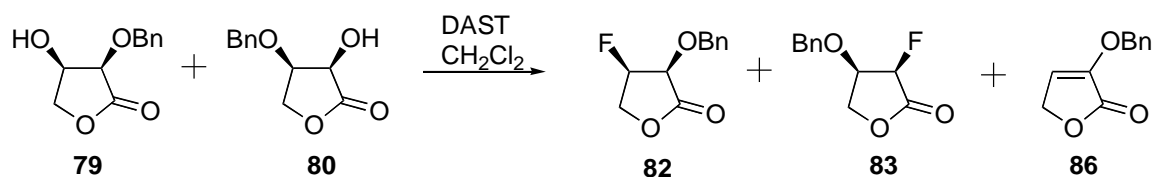
To a mixture of **79** and **80** (0.0423g, 0.20mmol) in CH$_2$Cl$_2$ (3mL) at room temperature was added DAST (150μL, 1.2mmol). The mixture was allowed to stir at room temperature for two hours. The reaction mixture was then poured into ice-cold saturated aqueous NaHCO$_3$ solution (25mL). The organic phase was removed and the aqueous phase extracted with CH$_2$Cl$_2$ (3 x 10mL). The combined organic extracts were dried (MgSO$_4$) and the solvent removed *in vacuo* to give 0.63g of crude product.

R$_F$ (**82** and **83**) = 0.69 (1:1 Hex:EtOAc)

R$_F$ (**86**) = 0.56 (1:1 Hex:EtOAc)

m/z (+ve FAB) (**86**) cal 190.06299 found 190.06340

m/z (+ve FAB) (**82** and **83**) cal 210.06922 found 210.06958

^{19}F NMR (82 and 83) (CDCl$_3$, 376MHz) δ $^-$190.8ppm (dddd, J=52.7Hz, 24;.3Hz, 10.3Hz, 3.0Hz), $^-$201.1ppm (dd, J=51.4Hz, 17.3Hz) ppm.

^{1}H NMR (86) (CDCl$_3$, 400MHz) δ 7.38-7.29 (m, 5H, Ph), 6.10 (t, J=2.2Hz, 1H, H3), 5.01 (s, 2H, Bn), 4.72 (d, J=2.2Hz, 2H, H4s) ppm.

^{13}C NMR (CDCl$_3$, 100MHz) δ 168.1 (Q, C1), 145.6 (Q. C2), 134.8 (Q, Ph), 128.7, 128.6, 127.6 (CH, Ph), 114.2 (CH, C3), 72.9 (CH$_2$, Bn), 67.5 (CH$_2$, C4) ppm.

Protection of erythronic lactone with TBDMSCl group

88 + **89**
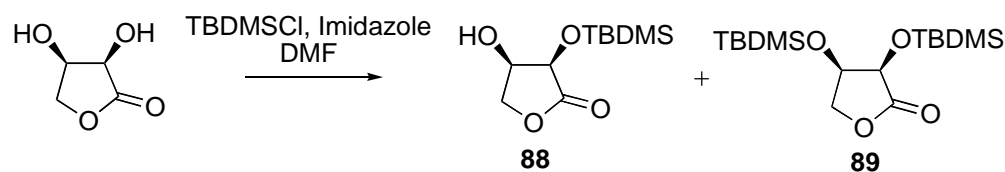
To a solution of erythronic lactone (0.132g, 1.1mmol) in DMF (5mL) at room temperature was added TBDMSCl (0.1853g, 1.23mmol). After five hours the reaction mixture was diluted with H_2O and EtOH. The aqueous phase was washed with EtOH (10mL x 2) and the organic phase washed with saturated aqueous NaCl solution (10mL), dried ($MgSO_4$) and the solvent removed *in vacuo*. Flash chromatography provided the monosilylated product **88** (0.1731g, 67%) as well as the disilylated product **89** (0.0213g, 5%).

R_F (**88**) = 0.81 (1:2 Hex:EtOAc)

R_F (**89**) = 0.95 (1:2 Hex:EtOAc)

^{1}H NMR (88) (CDCl$_3$, 400MHz) δ 4.50 (d, J=4.4Hz, H2), 4.40-4.37 (m, 2H, H3, H4), 4.30 (dd, J=10.7Hz, 3.0Hz, 1H, H4), 2.85 (br s, 1H, -OH), 0.98 (s, 9H, C(C$\underline{H}_3$)$_3$), 0.29 (s, 3H, Si-CH$_3$), 0.23 (s, 3H, Si-CH$_3$) ppm.

^{13}C NMR (CDCl$_3$, 100MHz) δ 173.8 (Q, C1), 70.9 (CH$_2$, C4), 70.3, 68.6 (CH, C2, C3), 25.7 (CH$_3$, C($\underline{C}$H$_3$)$_3$), 18.4 (Q, -$\underline{C}$(CH$_3$)$_3$), -4.5, -5.4 ((CH$_3$, Si-CH$_3$) ppm.

Benzylation of 88
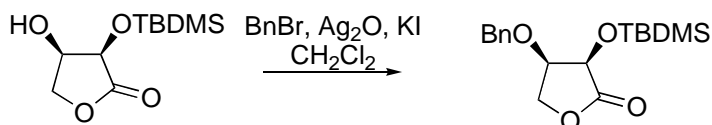
To a stirred solution of **88** (0.177g, 0.762mmol) in CH_2Cl_2 (5mL) at 0°C was added BnBr (136µL, 1.14mmol), Ag$_2$O (0.2641g, 1.14mmol), and KI (0.0126g, 0.076mmol). The mixture was allowed to warm slowly to room temperature. After stirring overnight, the reaction mixture was filtered through celite and washed with saturated aqueous NaHCO$_3$ solution, H_2O and NaCl (10mL each). The combined organic extracts were dried ($MgSO_4$) and the solvent removed *in vacuo*. Flash chromatography provided 0.074g of product (30%).

R_F=0.51 (1:3 Hex:EtOAc).

Synthesis of 90

90
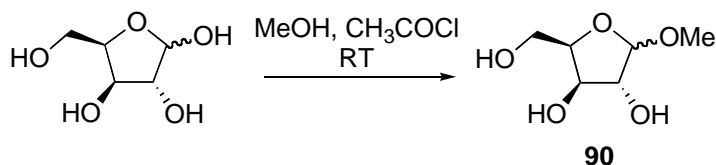
To a suspension of D-xylose (13.5g, 6.73mmol) in MeOH (270mL) was added acetyl chloride (2.7mL) drop-wise. The reaction mixture was allowed to stir at room temperature for a 24 hours, after which Ag_2CO_3 (8.1g) was added. The reaction was worked up according to Thome *et al* to give 16.3g of crude product **90**, which was used without purification in the next step.

Synthesis of 91
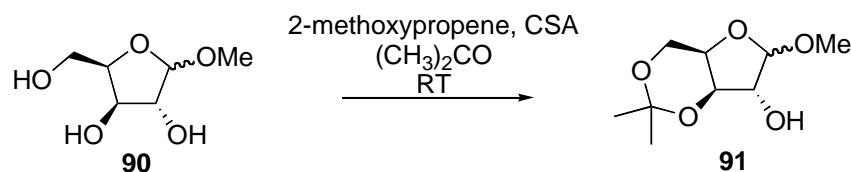
To the methyl glycoside **90** (16.36g, 0.1mol) and CSA (0.4060g, 1.6mmol) in acetone (130mL) at 0°C was added 2-methoxypropene (9.3mL, 0.1mol). The mixture was kept at 0°C and allowed to stir for 3 hours. K_2CO_3 (0.45g) was added and the mixture stirred for a further hour. The solvent was removed *in vacuo*, Et_2O added, the mixture dried ($MgSO_4$) and the solvent removed *in vacuo* to give 12.29g of the crude product. Although at this stage the two anomers could be separated by flash chromatography, the crude product was carried through to the next reaction.

R_F=0.47, 0.31 (1:1 Hex:EtOAc).

Synthesis of 92
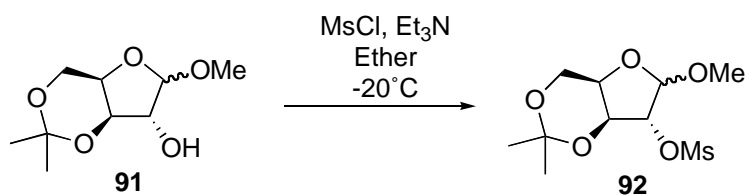
To a solution of crude **91** (11.83g, 57.9mmol) in Et_2O (150mL) at -20°C was added Et_3N (12mL, 86.9mmol). Mesyl chloride (5mL, 64mmol) was added drop-wise over 10 minutes. The reaction mixture was left to stir at -20°C for 4 hours, after which it was filtered and the solvent removed *in vacuo* to give 12.8g of the crude product, a yellow oil, which was used directly in the next reaction.

R_F=0.54 (1:1 Hex:EtOAc).

Synthesis of 2,3-anhydro-D-*lyxo*-furanoside 94
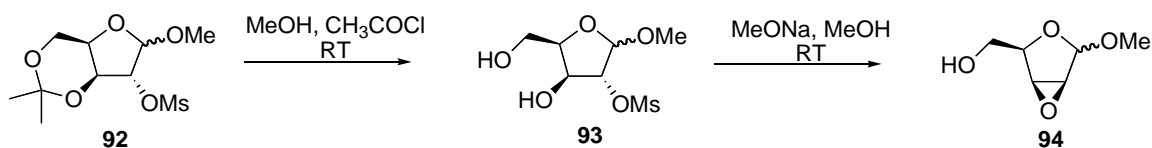
To a solution of the crude mesylate **92** (12.5g, 44mmol) in MeOH (150mL) was added acetyl chloride (632μL, 8.9mmol). The reaction mixture was allowed to stir at room temperature for 2.5 hours. Sodium metal (2g, 89mmol) was added to MeOH (20mL) and left at room temperature until all the sodium metal had dissolved. The MeONa was then added to the mesylate solution and the reaction mixture allowed to stir at room temperature overnight. Acetic acid was added to neutralize the reaction mixture and the solvent was removed *in vacuo*. The remaining liquid mixture was filtered through celite, washed with Et$_2$O and co-evaporated with toluene *in vacuo* to remove excess acetic acid. The remaining solid material was suspended in Et$_2$O and filtered. The Et$_2$O was removed *in vacuo* to give the crude product (4.396g). The α- and β-anomers were separated by flash chromatography.

R$_F$ (α-anomer)=0.40 (1:2 Hex:EtOAc)

R$_F$ (β-anomer)=0.16 (1:2 Hex:EtOAc)

m/z (+ve FAB) (β anomer) cal 164.09228 found 164.09158 for M+NH$_4^+$

m/z (+ve FAB) (β anomer) cal 147.06573 found 147.06566

^{1}H NMR (α-anomer) (CDCl$_3$, 400MHz) δ 4.94 (s, 1H, H1), 4.10 (t, J=5.1Hz, 1H, H4), 3.86 (d, J=5.1Hz, 2H, H5s), 3.72 (d, J=2.9Hz, 1H, H2), 3.63 (d, J=2.6Hz, 1H, H3), 3.40 (s, 3H, O-CH$_3$), 1.91 (br s, 1H, -OH) ppm.

^{13}C NMR (CDCl$_3$, 100MHz) δ 102.2 (CH, C1), 76.2 (CH, C4), 62.0 (CH$_2$, C5), 55.8 (CH, C3), 55.6 (CH$_3$, -OCH$_3$), 54.1 (CH, C2) ppm.

^{1}H NMR (β-anomer) (CDCl$_3$, 400MHz) δ 5.00 (s, 1H, H1), 4.00 (t, J=5.4Hz, 1H, H4), 3.86 (d, J=5.4Hz, 2H, H5s), 3.68 (br s, 2H, H2, H3), 3.50 (s, 3H, -OCH$_3$) ppm.

^{13}C NMR (CDCl$_3$, 100MHz) δ 102.4 (CH, C1), 77.2 (CH, C4), 62.1 (CH$_2$, C5), 60.0 (CH$_3$, -OCH$_3$), 55.4 (CH, C2), 54.9 (CH, C3) ppm.

Synthesis of 3-deoxyarabinose 95
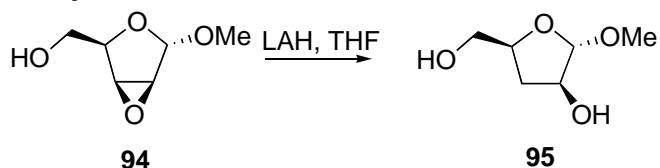
To a suspension of LAH (0.0903g, 2.38mmol) in THF (3mL) at 0°C was added a solution of **94** (0.1158g, 0.79mmol) in THF (2mL) dropwise. The reaction mixture was allowed to warm slowly to room temperature and stirred overnight. The mixture was then cooled to 0°C and H_2O (~1.5mL) added dropwise until the bubbling had ceased. The reaction mixture was filtered through celite, rinsing with EtOAc, the filtrate dried ($MgSO_4$) and the solvent removed *in vacuo*. The product was purified using flash chromatography to give **95** (0.0825g, 75%).

R_F=0.27 (1:3 Hex:EtOAc).

[1H] NMR (CDCl$_3$, 500MHz) δ 4.87 (s, 1H, H1), 4.34 (dd, J=9.5Hz, 2.6Hz, 1H, H4), 4.07 (br s, 1H, H2), 3.92 (d, J=11.7Hz, 1H, H5), 3.57 (d, J=11.7Hz, 1H, H5), 3.36 (s, 3H, OCH$_3$), 2.46 (ddd, J=13.8Hz, 9.5Hz, 5.3Hz, 1H, H3), 1.79 (dd, J=13.8Hz, 2.6Hz, 1H, H3) ppm.

[13C] NMR (CDCl$_3$, 125MHz) δ 109.7 (CH, C1), 78.1 (CH, C4), 74.1 (CH, C2), 63.5 (CH$_2$, C5), 54.4 (O-CH$_3$), 33.6 (CH, C3) ppm.

Synthesis of 97
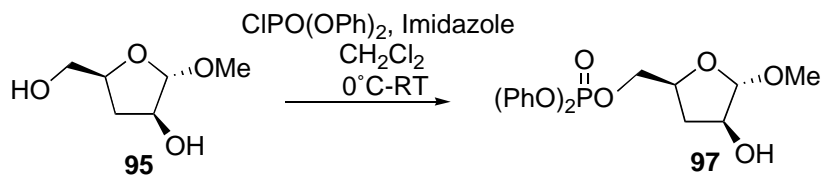
To a solution of **95** (0.0758g, 0.51mmol) in CH_2Cl_2 (5mL) at 0°C was added imidazole (0.1394g, 2.1mmol) and diphenylchlorophosphate (117µL, 0.56mmol). The reaction was allowed to warm slowly to room temperature and stirred overnight. The organic phase was then extracted with saturated aqueous NaHCO$_3$ solution and saturated aqueous NaCl solution (15mL each) and the combined aqueous extracts washed with CH_2Cl_2 (3 x 10mL). The combined organic extracts were dried ($MgSO_4$) and the solvent removed *in vacuo* to give the crude product. Flash chromatography provided 0.0723g (37%) of **97**.

R_F=0.23 (1:1 Hex:EtOAc).

[1H] NMR (CDCl$_3$, 400MHz) δ 7.32-7.13 (m, 10H, Ph), 4.79 (s, 1H, H1), 4,38-4.24 (m, 3H, H4, H5s), 4.09 (d, J=5.0Hz, 1H, H2), 3.26 (s, 3H, OCH$_3$), 2.30 (ddd, J=13.7Hz, 8.2Hz, 5.0Hz, 1H, H3), 1.64 (dd, J=13.7Hz, 2.8Hz, 1H, H3) ppm.

^{13}**C NMR (CDCl$_3$, 125MHz)** δ 150.4 (Q, d, ^{2}J$_{COP}$=7.3Hz, Ph), 129.8, 125.5 (CH, Ph), 120.1 (d, J=9.6Hz, ^{3}J$_{CCOP}$=9.6Hz), 109.7 (CH, C1), 76.1 (d, ^{3}J$_{CCOP}$=6.9Hz, C5), 74.8 (CH, C2), 70.6 (d, ^{4}J$_{CCCOP}$=6.4Hz, C4), 54.6 (CH$_3$, O-CH$_3$), 34.1 (CH$_2$, C3).

^{31}**P NMR (CDCl$_3$, 160 MHz)** δ -11.86 (t, ^{3}J$_{POCH}$=7.9Hz).

Synthesis of 3-deoxyA5P 40

97 → H$_2$, PtO$_2$ / MeOH → **99** → **40**
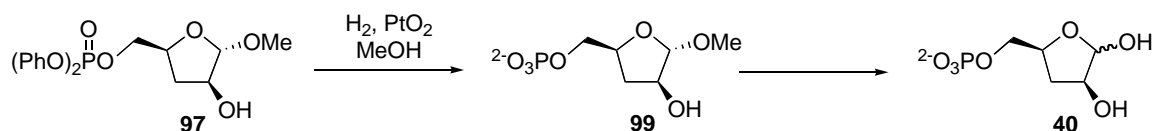
The protected analogue **97** (0.0774g, 0.20mmol) was dissolved in MeOH (6mL) and PtO$_2$ (0.0462g, 0.20mmol) added. The flask was evacuated and filled with H$_2$ gas and left to stir for 40 hours. The PtO$_2$ was filtered off and the filtrate evaporated *in vacuo,* giving 0.0468g (100%) of a colourless oil. The oil was dissolved in D$_2$O (1.5mL) and heated for 6-7 hours at 40˚C. The pH of the solution was then adjusted to 7.0 with 10M NaOH, filtered and diluted to 5mL with 50mmol BTP buffer, pH 7.5 for use in enzyme assays.

Synthesis of 101

94 → KHF$_2$, NaF / Ethylene glycol → **101**
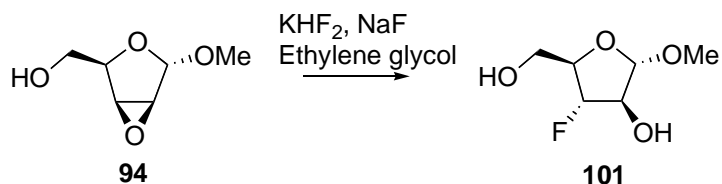
α-Epoxide **94** (0.11g, 0.75mmol) was dissolved in ethylene glycol and heated to reflux. NaF (0.1109g, 2.64mmol) and KHF$_2$ (0.1179g, 1.51mmol) were added and the mixture refluxed for three hours. After allowing to cool, saturated aqueous NaHCO$_3$ solution was added (10mL) and the mixture extracted with CHCl$_3$ (10mL x 3). The combined organic extracts were dried (MgSO$_4$) and the solvent removed *in vacuo* to give 0.0568g of crude product.

^{19}**F NMR (CDCl$_3$, 376MHz)** δ -184.4 (ddd, J=51.8Hz, 26.5Hz, 14.4Hz)

REFERENCES

1.	Bentley, R., The shikimate pathway - a metabolic tree with many branches. *Critical Reviews in Biochemistry and Molecular Biology* **1990,** 25, (5), 307-84.

2.	Steinrucken, H. C.; Amrhein, N., The herbicide glyphosate is a potent inhibitor of 5-enolpyruvyl-shikimic acid-3-phosphate synthase. *Biochemical and biophysical research communications* **1980,** 94, (4), 1207-12.

3.	Osborn, M. J.; Gander, J. E.; Parisi, E.; Carson, J., Mechanism of assembly of the outer membrane of *Salmonella typhimurium*. Isolation and characterization of cytoplasmic and outer membrane. *Journal of Biological Chemistry* **1972,** 247, (12), 3962-72.

4.	Rick, P. D.; Osborn, M. J., Lipid A mutants of *Salmonella typhimurium*. Characterization of a conditional lethal mutant in 3-deoxy-D-*manno*-octulosonate-8-phosphate synthetase. *Journal of Biological Chemistry* **1977,** 252, (14), 4895-903.

5.	Raetz, C. R. H., Biochemistry of endotoxins. *Annual Review of Biochemistry* **1990,** 59, 129-70.

6.	Jensen, R. A.; Xie, G.; Calhoun, D. H.; Bonner, C. A., The correct phylogenetic relationship of KdsA (3-deoxy-D-*manno*-octulosonate 8-phosphate synthase) with one of two independently evolved classes of AroA (3-deoxy-D-*arabino*-heptulosonate 7-phosphate synthase). *Journal of Molecular Evolution* **2002,** 54, (3), 416-423.

7.	Walker, G. E.; Dunbar, B.; Hunter, I. S.; Nimmo, H. G.; Coggins, J. R., Evidence for a novel class of microbial 3-deoxy-D-*arabino*-heptulosonate-7-phosphate synthase in *Streptomyces coelicolor* A3(2), *Streptomyces rimosus* and *Neurospora crassa*. *Microbiology (Reading, England)* **1996,** 142 (Pt 8), 1973-82.

8.	Gosset, G.; Bonner, C. A.; Jensen, R. A., Microbial origin of plant-type 2-keto-3-deoxy-D-*arabino*-heptulosonate 7-phosphate synthases, exemplified by the chorismate- and tryptophan-regulated enzyme from *Xanthomonas campestris*. *Journal of Bacteriology* **2001,** 183, (13), 4061-4070.

9.	Subramaniam, P. S.; Xie, G.; Xia, T.; Jensen, R. A., Substrate ambiguity of 3-deoxy-D-*manno*-octulosonate 8-phosphate synthase from *Neisseria gonorrhoeae* in the context of its membership in a protein family containing a subset of 3-deoxy-D-*arabino*-heptulosonate 7-phosphate synthases. *Journal of Bacteriology* **1998,** 180, (1), 119-127.

10.   Shumilin, I. A.; Kretsinger, R. H.; Bauerle, R. H., Crystal structure of phenylalanine-regulated 3-deoxy-D-*arabino*-heptulosonate-7-phosphate synthase from *Escherichia coli*. *Structure (London)* **1999,** 7, (7), 865-875.

11.   Schoner, R.; Herrmann, K. M., 3-Deoxy-D-*arabino*-heptulosonate 7-phosphate synthase. Purification, properties, and kinetics of the tyrosine-sensitive isoenzyme from *Escherichia coli*. *Journal of Biological Chemistry* **1976,** 251, (18), 5440-7.

12.   McCandliss, R. J.; Poling, M. D.; Herrmann, K. M., 3-Deoxy-D-*arabino*-heptulosonate 7-phosphate synthase. Purification and molecular characterization of the phenylalanine-sensitive isoenzyme from *Escherichia coli*. *Journal of Biological Chemistry* **1978,** 253, (12), 4259-65.

13.   Ray, J. M.; Bauerle, R., Purification and properties of tryptophan-sensitive 3-deoxy-D-*arabino*-heptulosonate-7-phosphate synthase from *Escherichia coli*. *Journal of Bacteriology* **1991,** 173, (6), 1894-901.

14.   Stephens, C. M.; Bauerle, R., Analysis of the metal requirement of 3-deoxy-D-*arabino*-heptulosonate-7-phosphate synthase from *Escherichia coli*. *Journal of Biological Chemistry* **1991,** 266, (31), 20810-17.

15.   Sheflyan, G. Y.; Howe, D. L.; Wilson, T. L.; Woodard, R. W., Enzymic Synthesis of 3-deoxy-D-*manno*-octulosonate 8-phosphate, 3-deoxy-D-*altro*-octulosonate 8-Phosphate, 3,5-dideoxy-D-*gluco*(*manno*)-octulosonate 8-phosphate by 3-deoxy-D-*arabino*-heptulosonate 7-Phosphate Synthase. *Journal of the American Chemical Society* **1998,** 120, (43), 11027-11032.

16.   Hartmann, M.; Schneider, T. R.; Pfeil, A.; Heinrich, G.; Lipscomb, W. N.; Braus, G. H., Evolution of feedback-inhibited β/α barrel isoenzymes by gene duplication and a single mutation. *Proceedings of the National Academy of Sciences of the United States of America* **2003,** 100, (3), 862-867.

17.   Paravicini, G.; Schmidheini, T.; Braus, G., Purification and properties of the 3-deoxy-D-*arabino*-heptulosonate-7-phosphate synthase (phenylalanine-inhibitable) of *Saccharomyces cerevisiae*. *European Journal of Biochemistry* **1989,** 186, (1-2), 361-6.

18.   Schnappauf, G.; Hartmann, M.; Kunzler, M.; Braus, G. H., The two 3-deoxy-D-*arabino*-heptulosonate-7-phosphate synthase isoenzymes from *Saccharomyces cerevisiae* show different kinetic modes of inhibition. *Archives of Microbiology* **1998,** 169, (6), 517-524.

19.   Schofield, L. R.; Patchett, M. L.; Parker, E. J., Expression, purification, and characterization of 3-deoxy-D-*arabino*-heptulosonate 7-phosphate synthase from *Pyrococcus furiosus. Protein Expression and Purification* **2004,** 34, (1), 17-27.

20.   Schofield, L. R.; Anderson, B. F.; Patchett, M. L.; Norris, G. E.; Jameson, G. B.; Parker, E. J., Substrate ambiguity and crystal structure of *Pyrococcus furiosus* 3-deoxy-D-*arabino*-heptulosonate-7-phosphate Synthase: an ancestral 3-deoxyald-2-ulosonate-phosphate synthase? *Biochemistry* **2005,** 44, (36), 11950-11962.

21.   Wu, J.; Howe, D. L.; Woodard, R. W., *Thermotoga maritima* 3-Deoxy-D-*arabino*-heptulosonate 7-Phosphate (DAHP) Synthase: The ancestral eubacterial DAHP synthase? *Journal of Biological Chemistry* **2003,** 278, (30), 27525-27531.

22.   Shumilin, I. A.; Bauerle, R.; Wu, J.; Woodard, R. W.; Kretsinger, R. H., Crystal Structure of the Reaction Complex of 3-Deoxy-D-*arabino*-heptulosonate-7-phosphate Synthase from *Thermotoga maritima* Refines the Catalytic Mechanism and Indicates a New Mechanism of Allosteric Regulation. *Journal of Molecular Biology* **2004,** 341, (2), 455-466.

23.   Duewel, H. S.; Sheflyan, G. Y.; Woodard, R. W., Functional and biochemical characterization of a recombinant 3-Deoxy-D-*manno*-octulosonic acid 8-phosphate synthase from the hyperthermophilic bacterium *Aquifex aeolicus. Biochemical and biophysical research communications* **1999,** 263, (2), 346-51.

24.   Duewel, H. S.; Woodard, R. W., A metal bridge between two enzyme families. 3-Deoxy-D-*manno*-octulosonate-8-phosphate synthase from *Aquifex aeolicus* requires a divalent metal for activity. *Journal of Biological Chemistry* **2000,** 275, (30), 22824-22831.

25.   Krosky, D. J.; Alm, R.; Berg, M.; Carmel, G.; Tummino, P. J.; Xu, B.; Yang, W., *Helicobacter pylori* 3-deoxy-D-*manno*-octulosonate-8-phosphate (KDO-8-P) synthase is a zinc-metalloenzyme. *Biochimica et Biophysica Acta, Protein Structure and Molecular Enzymology* **2002,** 1594, (2), 297-306.

26.   Ray, P. H., Purification and characterization of 3-deoxy-D-*manno*-octulosonate 8-phosphate synthetase from *Escherichia coli. Journal of bacteriology* **1980,** 141, (2), 635-44.

27.   Silakowski, B.; Kunze, B.; Muller, R., *Stigmatella aurantiaca* Sg a15 carries genes encoding type I and type II 3-deoxy-D-*arabino*-heptulosonate-7-phosphate synthases: involvement of a type II synthase in aurachin biosynthesis. *Archives of Microbiology* **2000,** 173, (5-6), 403-411.

28.	Fowden, L., The chemical approach to plants. *Sci. Progr. (London)* **1965,** 53, (212), 583-99.

29.	Birck, M. R.; Woodard, R. W., *Aquifex aeolicus* 3-deoxy-D-*manno*-2-octulosonic acid 8-phosphate synthase: a new class of KDO 8-P synthase? *Journal of Molecular Evolution* **2001,** 52, (2), 205-214.

30.	Jensen, R. A., Enzyme recruitment in evolution of new function. *Annual review of Microbiology* **1976,** 30, 409-25.

31.	Webby, C. J.; Baker, H. M.; Lott, J. S.; Baker, E. N.; Parker, E. J., The structure of 3-deoxy-D-*arabino*-heptulosonate 7-phosphate synthase from *Mycobacterium tuberculosis* reveals a common catalytic scaffold and ancestry for type I and Type II enzymes. *Journal of Molecular Biology* **2005,** 354, (4), 927-939.

32.	Floss, H. G.; Onderka, D. K.; Carroll, M., Stereochemistry of the 3-deoxy-D-*arabino*-heptulosonate 7-phosphate synthetase reaction and the chorismate synthetase reaction. *Journal of biological chemistry* **1972,** 247, (3), 736-44.

33.	Staub, M.; Denes, G., A kinetic study of the mechanism of action of 3-deoxy-D-*arabino* heptulosonate-7-phosphate synthase in *Escherichia coli* K 12. *Biochimica et Biophysica Acta* **1967,** 132, (2), 528-30.

34.	DeLeo, A. B.; Dayan, J.; Sprinson, D. B., Purification and kinetics of tyrosine-sensitive 3-deoxy-D-*arabino*-heptulosonic acid 7-phosphate synthetase from *Salmonella*. *Journal of Biological Chemistry* **1973,** 248, (7), 2344-53.

35.	Wanke, C.; Amrhein, N., Evidence that the reaction of the UDP-N-acetylglucosamine 1-carboxyvinyltransferase proceeds through the *O*-phosphothioketal of pyruvic acid bound to Cys115 of the enzyme. *European Journal of Biochemistry* **1993,** 218, (3), 861-70.

36.	Kohen, A.; Jakob, A.; Baasov, T., Mechanistic studies of 3-deoxy-D-*manno*-2-octulosonate-8-phosphate synthase from *Escherichia coli*. *European Journal of Biochemistry* **1992,** 208, (2), 443-9.

37.	Baasov, T.; Sheffer-Dee-Noor, S.; Kohen, A.; Jakob, A.; Belakhov, V., Catalytic mechanism of 3-deoxy-D-*manno*-2-octulosonate-8-phosphate synthase. The use of synthetic analogs to probe the structure of the putative reaction intermediate. *European Journal of Biochemistry* **1993,** 217, (3), 991-9.

38.	Hedstrom, L.; Abeles, R., 3-Deoxy-D-*manno*-octulosonate-8-phosphate synthase catalyzes the carbon-oxygen bond cleavage of phosphoenolpyruvate. *Biochemical and Biophysical Research Communications* **1988,** 157, (2), 816-20.

39.   Kohen, A.; Berkovich, R.; Belakhov, V.; Baasov, T., Stereochemistry of the KDO8P synthase. An efficient synthesis of the 3-fluoro analogs of KDO8P. *Bioorganic & Medicinal Chemistry Letters* **1993,** 3, (8), 1577-82.

40.   Asojo, O.; Friedman, J.; Adir, N.; Belakhov, V.; Shoham, Y.; Baasov, T., Crystal structures of KDOP synthase in its binary complexes with the substrate phosphoenolpyruvate and with a mechanism-based inhibitor. *Biochemistry* **2001,** 40, (21), 6326-6334.

41.   Lambert, J. M.; Boocock, M. R.; Coggins, J. R., The 3-dehydroquinate synthase activity of the pentafunctional arom enzyme complex of *Neurospora crassa* is zinc-dependent. *Biochemical Journal* **1985,** 226, (3), 817-29.

42.   Duewel, H. S.; Radaev, S.; Wang, J.; Woodard, R. W.; Gatti, D. L., Substrate and metal complexes of 3-deoxy-D-*manno*-octulosonate-8-phosphate synthase from *Aquifex aeolicus* at 1.9-.ANG. resolution. Implications for the condensation mechanism. *Journal of Biological Chemistry* **2001,** 276, (11), 8393-8402.

43.   Sheffer-Dee-Noor, S.; Belakhov, V.; Baasov, T., Insight into the catalytic mechanism of KDO8P synthase. Synthesis and evaluation of the isosteric phosphonate mimic of the putative cyclic intermediate. *Bioorganic & Medicinal Chemistry Letters* **1993,** 3, (8), 1583-8.

44.   Baasov, T.; Tkacz, R.; Sheffer-Dee-Noor, S.; Belakhov, V., Catalytic mechanism of 3-deoxy-D-*manno*-2-octulosonate-8-phosphate synthase. *Current Organic Chemistry* **2001,** 5, (2), 127-138.

45.   Liang, P.-H.; Lewis, J.; Anderson, K. S.; Kohen, A.; D'Souza, F. W.; Benenson, Y.; Baasov, T., Catalytic mechanism of Kdo8P synthase: Transient kinetic studies and evaluation of a putative reaction intermediate. *Biochemistry* **1998,** 37, (46), 16390-16399.

46.   D'Souza, F. W.; Benenson, Y.; Baasov, T., Catalytic mechanism of Kdo8P synthase: synthesis and evaluation of a putative reaction intermediate. *Bioorganic & Medicinal Chemistry Letters* **1997,** 7, (19), 2457-2462.

47.   Liang, P.-H.; Kohen, A.; Baasov, T.; Anderson, K. S., Catalytic mechanism of Kdo8P synthase. Pre-steady-state kinetic analysis using rapid chemical quench flow methods. *Bioorganic & Medicinal Chemistry Letters* **1997,** 7, (19), 2463-2468.

48.   Shumilin, I. A.; Bauerle, R.; Kretsinger, R. H., The high-resolution structure of 3-deoxy-D-*arabino*-heptulosonate-7-phosphate synthase reveals a twist in the plane of bound phosphoenolpyruvate. *Biochemistry* **2003,** 42, (13), 3766-3776.

49.	Staub, M.; Denes, G., Purification and properties of the 3-deoxy-D-*arabino*-heptulosonate-7-phosphate synthase (phenylalanine sensitive) of *Escherichia coli* K-12. II. Inhibition of activity of the enzyme with phenylalanine and functional group-specific reagents. *Biochimica et Biophysica Acta, Enzymology* **1969,** 178, (3), 599-608.

50.	Simpson, R. J.; Davidson, B. E., Studies on 3-deoxy-D-*arabino*-heptulosonate-7-phosphate synthetase(phe) from *Escherichia coli* K12. 2. Kinetic properties. *European Journal of Biochemistry* **1976,** 70, (2), 501-7.

51.	Jensen, R. A.; Nester, E. W., Regulatory enzymes of aromatic amino acid biosynthesis in *Bacillus subtilis*. I. Purification and properties of 3-deoxy-D-*arabino*-heptulosonate 7-phosphate synthetase. *Journal of Biological Chemistry* **1966,** 241, (14), 3365-72.

52.	Wu, J.; Sheflyan, G. Y.; Woodard, R. W., *Bacillus subtilis* 3-deoxy-D-*arabino*-heptulosonate 7-phosphate synthase revisited: resolution of two long-standing enigmas. *Biochemical Journal* **2005,** 390, (2), 583-590.

53.	Stephens, C. M.; Bauerle, R., Essential cysteines in 3-deoxy-D-*arabino*-heptulosonate-7-phosphate synthase from *Escherichia coli*. Analysis by chemical modification and site-directed mutagenesis of the phenylalanine-sensitive isozyme. *Journal of Biological Chemistry* **1992,** 267, (9), 5762-7.

54.	Baasov, T.; Knowles, J. R., Is the first enzyme of the shikimate pathway, 3-deoxy-D-*arabino*-heptulosonate-7-phosphate synthase (tyrosine sensitive), a copper metalloenzyme? *Journal of Bacteriology* **1989,** 171, (11), 6155-60.

55.	Simpson, R. J.; Davidson, B. E., Studies on 3-deoxy-D-*arabino*-heptulosonate-7-phosphate synthetase(phe) from *Escherichia coli* K12. 1. Purification and subunit structure. *European Journal of Biochemistry* **1976,** 70, (2), 493-500.

56.	McCandliss, R. J.; Herrmann, K. M., Iron, an essential element for biosynthesis of aromatic compounds. *Proceedings of the National Academy of Sciences of the United States of America* **1978,** 75, (10), 4810-13.

57.	Park, O. K.; Bauerle, R., Metal-catalyzed oxidation of phenylalanine-sensitive 3-deoxy-D-*arabino*-heptulosonate-7-phosphate synthase from *Escherichia coli*: inactivation and destabilization by oxidation of active-site cysteines. *Journal of Bacteriology* **1999,** 181, (5), 1636-1642.

58.	Webby, C. J. Structural & functional characterization of 3-deoxy-D-*arabino*-heptulosonate 7 phosphate synthase from *Helicobacter pylori* & *Mycobacterium tuberculosis*. Massey University, 2006.

59.   Nagano, H.; Zalkin, H., Tyrosine-inhibited 3-deoxy-D-*arabino*-heptulosonate 7-phosphate synthetase. Properties of the partially purified enzyme from *Salmonella typhimurium*. *Archives of biochemistry and biophysics* **1970,** 138, (1), 58-65.

60.   Parker, E. J.; Bulloch, E. M. M.; Jameson, G. B.; Abell, C., Substrate deactivation of phenylalanine-sensitive 3-deoxy-D-*arabino*-heptulosonate 7-Phosphate synthase by erythrose 4-phosphate. *Biochemistry* **2001,** 40, (49), 14821-14828.

61.   Taylor, W. P.; Sheflyan, G. Y.; Woodard, R. W., A single point mutation in 3-deoxy-D-*manno*-octulosonate-8-phosphate synthase is responsible for temperature sensitivity in a mutant strain of *Salmonella typhimurium*. *The Journal of biological chemistry* **2000,** 275, (41), 32141-6.

62.   Sheflyan, G. Y.; Sundaram, A. K.; Taylor, W. P.; Woodard, R. W., Substrate ambiguity of 3-deoxy-D-*manno*-octulosonate 8-phosphate synthase from *Neisseria gonorrhoeae* revisited. *Journal of Bacteriology* **2000,** 182, (17), 5005-5008.

63.   Cochrane, F., Personal communication

64.   Shulami, S.; Yaniv, O.; Rabkin, E.; Shoham, Y.; Baasov, T., Cloning, expression, and biochemical characterization of 3-deoxy-D-*manno*-2-octulosonate-8-phosphate (KDO8P) synthase from the hyperthermophilic bacterium *Aquifex pyrophilus*. *Extremophiles : life under extreme conditions* **2003,** 7, (6), 471-81.

65.   Li, J.; Wu, J.; Fleischhacker, A. S.; Woodard, R. W., Conversion of *Aquifex aeolicus* 3-Deoxy-D-*manno*-octulosonate 8-phosphate synthase, a metalloenzyme, into a nonmetalloenzyme. *Journal of the American Chemical Society* **2004,** 126, (24), 7448-7449.

66.   Shulami, S.; Furdui, C.; Adir, N.; Shoham, Y.; Anderson, K. S.; Baasov, T., A reciprocal single mutation affects the metal requirement of 3-deoxy-D-*manno*-2-octulosonate-8-phosphate (KDO8P) synthases from *Aquifex pyrophilus* and *Escherichia coli*. *Journal of Biological Chemistry* **2004,** 279, (43), 45110-45120.

67.   Oliynyk, Z.; Briseno-Roa, L.; Janowitz, T.; Sondergeld, P.; Fersht, A. R., Designing a metal-binding site in the scaffold of *Escherichia coli* KDO8PS. *Protein Engineering, Design & Selection* **2004,** 17, (4), 383-390.

68.   Konig, V.; Pfeil, A.; Braus, G. H.; Schneider, T. R., Substrate and Metal Complexes of 3-Deoxy-D-*arabino*-heptulosonate-7-phosphate Synthase from *Saccharomyces cerevisiae* Provide New Insights into the Catalytic Mechanism. *Journal of Molecular Biology* **2004,** 337, (3), 675-690.

69.   Wagner, T.; Shumilin, I. A.; Bauerle, R.; Kretsinger, R. H., Structure of 3-Deoxy-D-*arabino*-heptulosonate-7-phosphate Synthase from *Escherichia coli*: Comparison of the Mn^{2+}*2-Phosphoglycolate and the Pb^{2+}*2-Phosphoenolpyruvate Complexes and Implications for Catalysis. *Journal of Molecular Biology* **2000,** 301, (2), 389-399.

70.   Shumilin, I. A.; Zhao, C.; Bauerle, R.; Kretsinger, R. H., Allosteric inhibition of 3-deoxy-D-*arabino*-heptulosonate-7-phosphate synthase alters the coordination of both substrates. *Journal of Molecular Biology* **2002,** 320, (5), 1147-1156.

71.   Wagner, T.; Kretsinger, R. H.; Bauerle, R.; Tolbert, W. D., 3-Deoxy-D-*manno*-octulosonate-8-phosphate Synthase from *Escherichia coli*. Model of Binding of Phosphoenolpyruvate and D-arabinose-5-phosphate. *Journal of Molecular Biology* **2000,** 301, (2), 233-238.

72.   Radaev, S.; Dastidar, P.; Patel, M.; Woodard, R. W.; Gatti, D. L., Structure and mechanism of 3-deoxy-D-*manno*-octulosonate 8-phosphate synthase. *Journal of Biological Chemistry* **2000,** 275, (13), 9476-9484.

73.   Wang, J.; Duewel, H. S.; Woodard, R. W.; Gatti, D. L., Structures of *Aquifex aeolicus* KDO8P synthase in complex with R5P and PEP, and with a bisubstrate inhibitor: role of active site water in catalysis. *Biochemistry* **2001,** 40, (51), 15676-15683.

74.   Howe, D. L.; Sundaram, A. K.; Wu, J.; Gatti, D. L.; Woodard, R. W., Mechanistic Insight into 3-deoxy-D-*manno*-octulosonate-8-phosphate Synthase and 3-deoxy-D-*arabino*-heptulosonate-7-phosphate Synthase Utilizing Phosphorylated Monosaccharide Analogues. *Biochemistry* **2003,** 42, (17), 4843-4854.

75.   Ogino, T.; Garner, C.; Markley, J. L.; Herrmann, K. M., Biosynthesis of aromatic compounds: 13C NMR spectroscopy of whole *Escherichia coli* cells. *Proceedings of the National Academy of Sciences of the United States of America* **1982,** 79, (19), 5828-32.

76.   Tribe, D. E.; Camakaris, H.; Pittard, J., Constitutive and repressible enzymes of the common pathway of aromatic biosynthesis in *Escherichia coli* K-12: regulation of enzyme synthesis at different growth rates. *Journal of Bacteriology* **1976,** 127, (3), 1085-97.

77.   Liu, H.; Li, W.; Kim, C. U., Synthesis and evaluation of 3-deoxy-D-*manno*-2-octulosonate-8-phosphate (KDO8P) synthase inhibitors. *Bioorganic & Medicinal Chemistry Letters* **1997,** 7, (11), 1419-1420.

78.   Du, S.; Faiger, H.; Belakhov, V.; Baasov, T., Towards the development of novel antibiotics: synthesis and evaluation of a mechanism-based inhibitor of Kdo8P synthase. *Bioorganic & Medicinal Chemistry* **1999,** 7, (12), 2671-2682.

79.   Du, S.; Tsipori, H.; Baasov, T., Synthesis and evaluation of putative oxocarbenium intermediate mimic in the Kdo8P synthase-catalyzed reaction as a tool for the design of potent inhibitors for lipopolysaccharide biosynthesis. *Bioorganic & Medicinal Chemistry Letters* **1997,** 7, (19), 2469-2472.

80.   Xu, X.; Wang, J.; Grison, C.; Petek, S.; Coutrot, P.; Birck, M. R.; Woodard, R. W.; Gatti, D. L., Structure-based design of novel inhibitors of 3-deoxy-D-*manno*-octulosonate 8-phosphate synthase. *Drug Design and Discovery* **2003,** 18, (2-3), 91-99.

81.   Belakhov, V.; Dovgolevsky, E.; Rabkin, E.; Shulami, S.; Shoham, Y.; Baasov, T., Synthesis and evaluation of a mechanism-based inhibitor of KDO8P synthase. *Carbohydrate Research* **2004,** 339, (2), 385-392.

82.   Walker, S. R.; Parker, E. J., Synthesis and evaluation of a mechanism-based inhibitor of a 3-deoxy-D-arabino heptulosonate 7-phosphate synthase. *Bioorganic & Medicinal Chemistry Letters* **2006,** 16, (11), 2951-2954.

83.   Parker, E. J. Mechanistic studies on shikimate pathway enzymes. PhD, University Of Cambridge, 1996.

84.   Le Marechal, P.; Froussios, C.; Level, M.; Azerad, R., The interaction of phosphonate and homophosphonate analogs of 3-deoxy-D-*arabino*-heptulosonate 7-phosphate with 3-dehydroquinate synthetase from *Escherichia coli. Biochemical and Biophysical Research Communications* **1980,** 92, (4), 1104-9.

85.   Sundaram, A. K.; Woodard, R. W., *Neisseria gonorrhoeae* 3-deoxy-D-*arabino*-heptulosonate 7-phosphate synthase does not catalyze the formation of the *ribo* analogue. *Organic letters* **2001,** 3, (1), 21-4.

86.   Webby, C. J.; Patchett, M. L.; Parker, E. J., Characterization of a recombinant type II 3-deoxy-D-*arabino*-heptulosonate-7-phosphate synthase from *Helicobacter pylori. Biochemical Journal* **2005,** 390, (1), 223-230.

87.   Sheffer-Dee-Noor, S.; Baasov, T., A combined chemical-enzymic synthesis of a new phosphoramidate analog of phosphoenolpyruvate. *Bioorganic & Medicinal Chemistry Letters* **1993,** 3, (8), 1615-18.

88.   Benenson, Y.; Belakhov, V.; Baasov, T., 1-(Dihydroxyphosphynyl)vinyl phosphate: the phosphonate analog of phosphoenolpyruvate is a pH-dependent substrate

of Kdo8P synthase. *Bioorganic & Medicinal Chemistry Letters* **1996,** 6, (23), 2901-2906.

89.   Rosenstein, N. E.; Perkins, B. A.; Stephens, D. S.; Popovic, T.; Hughes, J. M., Meningococcal disease. *The New England journal of medicine* **2001,** 344, (18), 1378-88.

90.   Nokleby, H.; Aavitsland, P.; O'Hallahan, J.; Feiring, B.; Tilman, S.; Oster, P., Safety review: Two outer membrane vesicle (OMV) vaccines against systemic *Neisseria meningitidis* serogroup B disease. *Vaccine* **2007,** 25, (16), 3080-3084.

91.   Nikulin, J.; Panzner, U.; Frosch, M.; Schubert-Unkmeir, A., Intracellular survival and replication of *Neisseria meningitidis* in human brain microvascular endothelial cells. *International Journal of Medical Microbiology* **2006,** 296, (8), 553-558.

92.   Staub, M.; Denes, G., Purification and properties of the 3-deoxy-D-*arabino*-heptulosonate-7-phosphate synthase (phenylalanine sensitive) of *Escherichia coli* K-12. I. Purification of enzyme and some of its catalytic properties. *Biochimica et Biophysica Acta, Enzymology* **1969,** 178, (3), 588-98.

93.   Pittard, J.; Camakaris, J.; Wallace, B. J., Inhibition of 3-deoxy-D-*arabino*-heptulosonic acid 7-phosphate synthetase (trp) in *Escherichia coli*. *Journal of Bacteriology* **1969,** 97, (3), 1242-7.

94.   Ahn, M.; Pietersma, A. L.; Schofield, L. R.; Parker, E. J., Mechanistic divergence of two closely related aldol-like enzyme-catalysed reactions. *Organic & Biomolecular Chemistry* **2005,** 3, (22), 4046-4049.

95.   Ahn, M. Substrate analogues as mechanistic probes for 3-deoxy-D-*arabino*-heptulosonate 7-phosphate synthase and 3-deoxy-D-*manno*-octulosonate 8-phosphate synthase. PhD, Massey University, 2007.

96.   Williamson, R., Unpublished result.

97.   Andre, C.; Demuynck, C.; Gefflaut, T.; Guerard, C.; Hecquet, L.; Lemaire, M.; Bolte, J., Fructose-1,6-bisphosphate aldolase and transketolase: complementary tools for the de novo syntheses of monosaccharides and analogs. *Journal of Molecular Catalysis B: Enzymatic* **1998,** 5, (1-4), 113-118.

98.   Guerard, C.; Alphand, V.; Archelas, A.; Demuynck, C.; Hecquet, L.; Furstoss, R.; Bolte, J., Transketolase-mediated synthesis of 4-deoxy-D-fructose 6-phosphate by epoxide-hydrolase-catalysed resolution of 1,1-diethoxy-3,4-epoxybutane. *European Journal of Organic Chemistry* **1999**, (12), 3399-3402.

99.   Williamson, R. M.; Pietersma, A. L.; Jameson, G. B.; Parker, E. J., Stereospecific deuteration of 2-deoxyerythrose 4-phosphate using 3-deoxy-D-*arabino*-heptulosonate 7-phosphate synthase. *Bioorganic & Medicinal Chemistry Letters* **2005,** 15, (9), 2339-2342.

100.   Cloux, R.; Schlosser, M., Selective syntheses with organometallics. Part XI. An efficient synthesis of α,β-unsaturated aldehydes by a four-carbon unit extension of Grignard reagents. *Helvetica Chimica Acta* **1984,** 67, (6), 1470-4.

101.   Bouzide, A.; Sauve, G., Highly selective silver(I) oxide mediated monoprotection of symmetrical diols. *Tetrahedron Letters* **1997,** 38, (34), 5945-5948.

102.   Bouzide, A.; LeBerre, N.; Sauve, G., Silver(I) oxide-mediated facile and practical sulfonylation of alcohols. *Tetrahedron Letters* **2001,** 42, (50), 8781-8783.

103.   Bouzide, A.; Sauve, G., Silver(I) Oxide Mediated Highly Selective Monotosylation of Symmetrical Diols. Application to the Synthesis of Polysubstituted Cyclic Ethers. *Organic Letters* **2002,** 4, (14), 2329-2332.

104.   Chan, T. H.; Brook, M. A.; Chaly, T., A simple procedure for the acetalization of carbonyl compounds. *Synthesis* **1983**, (3), 203-5.

105.   Larsen, C. H.; Ridgway, B. H.; Shaw, J. T.; Woerpel, K. A., A Stereoelectronic model to explain the highly stereoselective reactions of nucleophiles with five-membered-ring oxocarbenium ions. *Journal of the American Chemical Society* **1999,** 121, (51), 12208-12209.

106.   Van Hijfte, L.; Little, R. D.; Petersen, J. L.; Moeller, K. D., Intramolecular 1,3-diyl trapping reactions. Total synthesis of (+-)-hypnophilin and (+-)-coriolin. Formation of the trans-fused bicyclo[3.3.0]octane ring system. *Journal of Organic Chemistry* **1987,** 52, (21), 4647-61.

107.   Barton, D. H. R.; Benechie, M.; Khuong-Huu, F.; Potier, P.; Reyna-Pinedo, V., Studies related to the synthesis of maytansinoids. *Tetrahedron Lett.* **1982,** 23, (6), 651-4.

108.   Aussenac, F.; Lavigne, B.; Dufourc, E. J., Toward bicelle stability with ether-linked phospholipids: temperature, composition, and hydration diagrams by 2H and 31P solid-state NMR. *Langmuir* **2005,** 21, (16), 7129-7135.

109.   Bravo, J.; Cativiela, C.; Chaves, J. E.; Navarro, R.; Urriolabeitia, E. P., 31P NMR spectroscopy as a powerful tool for the determination of enantiomeric excess and absolute configurations of α-amino acids. *Inorganic Chemistry* **2003,** 42, (4), 1006-1013.

110.   Gorenstein, D. G.; Rowell, R., Isotopic oxygen-18 shifts in phosphorus-31 NMR as a probe of stereochemistry of hydrolysis in phosphate triesters. *Journal of the American Chemical Society* **1980,** 102, (19), 6165-6.

111.   Loehr, G. W.; Waller, H. D., Glucose-6-phosphate dehydrogenase. *Methoden Enzym. Anal., 3. Neubearbeitete Erweiterte Aufl.* **1974,** 1, 673-81.

112.   Schofield, L. R., Personal communication.

113.   Felix, A. M.; Heimer, E. P.; Lambros, T. J.; Tzougraki, C.; Meienhofer, J., Rapid removal of protecting groups from peptides by catalytic transfer hydrogenation with 1,4-cyclohexadiene. *Journal of Organic Chemistry* **1978,** 43, (21), 4194-6.

114.   Kocienski, P. J., *Protecting groups.* Thieme: 1994.

115.   Kolb, H. C.; Ley, S. V.; Slawin, A. M. Z.; Williams, D. J., Chemistry of insect antifeedants from Azadirachta indica. Part 12. Use of silicon as a control element in the synthesis of a highly functionalized decalin fragment of azadirachtin. *Journal of the Chemical Society, Perkin Transactions 1: Organic and Bio-Organic Chemistry (1972-1999)* **1992**, (21), 2735-62.

116.   Ley, S. V.; Maw, G. N.; Trudell, M. L., Enantioselective synthesis of the C3-C11 hydrocarbon fragment of the ionophore antibiotic tetronasin (ICI 139603). *Tetrahedron Letters* **1990,** 31, (38), 5521-4.

117.   Okada, Y.; Minami, T.; Umezu, Y.; Nishikawa, S.; Mori, R.; Nakayama, Y., Synthesis of a novel type of chiral phosphinocarboxylic acids. Phosphine-palladium complex catalyzed asymmetric allylic alkylation. *Tetrahedron: Asymmetry* **1991,** 2, (7), 667-82.

118.   Jones, T. K.; Reamer, R. A.; Desmond, R.; Mills, S. G., Chemistry of tricarbonyl hemiketals and application of Evans technology to the total synthesis of the immunosuppressant (-)-FK-506. *Journal of the American Chemical Society* **1990,** 112, (8), 2998-3017.

119.   Cunningham, A. F., Jr.; Kuendig, E. P., An efficient synthesis of both enantiomers of trans-1,2-cyclopentanediol and their conversion to two novel bidentate phosphite and fluorophosphinite ligands. *Journal of Organic Chemistry* **1988,** 53, (8), 1823-5.

120.   Nemoto, H.; Takamatsu, S.; Yamamoto, Y., An improved and practical method for the synthesis of optically active diethyl tartrate dibenzyl ether. *Journal of Organic Chemistry* **1991,** 56, (3), 1321-2.

121.   Araki, K.; Suenaga, K.; Sengoku, T.; Uemura, D., Total synthesis of attenols A and B. *Tetrahedron* **2002,** 58, (10), 1983-1995.

122.   Aminoff, D., Methods for the quantitative estimation of N-acetyl-neuraminic acid and their application to hydrolyzates of sialomucoids. *Biochemical Journal* **1961,** 81, 384-92.

123.   Dunigan, J.; Weigel, L. O., Synthesis of alkyl (2*S*,3*R*)-4-hydroxy-2,3-epoxybutyrates from sodium erythorbate. *Journal of Organic Chemistry* **1991,** 56, (21), 6225-7.

124.   Flasche, M.; Scharf, H.-D., A straightforward preparation of both enantiomerically pure 2-*O*-benzyl-erythro-butanetetrols. *Tetrahedron: Asymmetry* **1995,** 6, (7), 1543-6.

125.   Shiuey, S. J.; Partridge, J. J.; Uskokovic, M. R., Triply convergent synthesis of 1a,25-dihydroxy-24(*R*)-fluorocholecalciferol. *Journal of Organic Chemistry* **1988,** 53, (5), 1040-6.

126.   Mikhailopulo, I. A.; Sivets, G. G., A novel route for the synthesis of deoxy fluoro sugars and nucleosides. *Helvetica Chimica Acta* **1999,** 82, (11), 2052-2065.

127.   Garcia, C.; Soler, M. A.; Martin, V. S., Enantiocontrolled synthesis of C-19 tetrahydrofurans isolated from the marine alga Notheia anomala. *Tetrahedron Letters* **2000,** 41, (21), 4127-4130.

128.   Thome, M. A.; Giudicelli, M. B.; Picq, D.; Anker, D., An improved synthesis of methyl 2,3-anhydro-α- and -β-D-*lyxo*furanosides. *Journal of Carbohydrate Chemistry* **1991,** 10, (5), 923-6.

129.   Silverstein, R.; Bassler, G. C.; Morril, T. C., *Spectrometric identification of organic compounds*. 5th ed.; John Wiley & Sons Inc: 1991.

130.   Mikhailopulo, I. A.; Poopeiko, N. E.; Prikota, T. I.; Sivets, G. G.; Kvasyuk, E. I.; Balzarini, J.; De Clercq, E., Synthesis and antiviral and cytostatic properties of 3'-deoxy-3'-fluoro- and 2'-azido-3'-fluoro-2',3'-dideoxy-D-*ribo*furanosides of natural heterocyclic bases. *Journal of Medicinal Chemistry* **1991,** 34, (7), 2195-202.

131.   Gadikota, R. R.; Callam, C. S.; Wagner, T.; Del Fraino, B.; Lowary, T. L., 2,3-Anhydro Sugars in Glycoside Bond Synthesis. Highly Stereoselective Syntheses of Oligosaccharides Containing α- and β-*arabino*furanosyl Linkages. *Journal of the American Chemical Society* **2003,** 125, (14), 4155-4165.

132.   Lim, M. H.; Kim, H. O.; Moon, H. R.; Lee, S. J.; Chun, M. W.; Gao, Z.-G.; Melman, N.; Jacobson, K. A.; Kim, J. H.; Jeong, L. S., Design, Synthesis and Binding

Affinity of 3'-Fluoro Analogues of C1-IB-MECA as Adenosine A3 Receptor Ligands *Bioorganic & Medicinal Chemistry Letters* **2003,** 13, (12), 2087.

133.   Schulze, O.; Voss, J.; Adiwidjaja, G., Convenient preparation of 3,5-anhydro- and 2,5-anhydropentofuranosides, and 5,6-anhydro-D-glucofuranose by use of the Mitsunobu reaction. *Carbohydrate Research* **2005,** 340, (4), 587-595.

134.   Kim Hea, O.; Lim Moo, H.; Park Jae, G.; Moon Hyung, R.; Jacobson Kenneth, A.; Kim, H.-D.; Chun Moon, W.; Jeong Lak, S., Design and synthesis of A3 adenosine receptor ligands, 3'-fluoro analogues of Cl-IB-MECA. *Nucleosides, nucleotides & nucleic acids* **2003,** 22, (5-8), 923-5.

135.   Wright, J. A.; Taylor, N. F., Fluorocarbohydrates. XVI. The synthesis of 3-deoxy-3-fluoro-D-xylose and 3-deoxy-3-fluoro-β-D-arabinose. *Carbohydrate Research* **1967,** 3, (3), 333-9.

136.   Mastihubova, M.; Biely, P., Deoxy and deoxyfluoro analogs of acetylated methyl β-D-xylopyranoside--substrates for acetylxylan esterases. *Carbohydrate Research* **2004,** 339, (12), 2101-2110.

137.   Wright, J. A.; Fox, J. J., Synthesis of 2-deoxy-2-fluoro-D-xylose. *Carbohydrate Research* **1970,** 13, (2), 297-300.

138.   Onderka, D. K.; Floss, H. G., Steric course of the chorismate synthetase reaction and the 3-deoxy-D-*arabino*-heptulosonate 7-phosphate (DAHP) synthetase reaction. *Journal of the American Chemical Society* **1969,** 91, (21), 5894-6.

139.   Furdui, C. M.; Sau, A. K.; Yaniv, O.; Belakhov, V.; Woodard, R. W.; Baasov, T.; Anderson, K. S., The Use of (*E*)- and (*Z*)-phosphoenol-3-fluoropyruvate as mechanistic probes reveals significant differences between the active sites of KDO8P and DAHP synthases. *Biochemistry* **2005,** 44, (19), 7326-7335.

140.   Bradford, M. M., A rapid and sensitive method for the quantitation of microgram quantities of protein utilizing the principle of protein-dye binding. *Analytical Biochemistry* **1976,** 72, (1-2), 248-54.

141.   Tanabe, M.; Peters, R. H., (*R*,*S*)-mevalonolactone-2-13C. *Organic Syntheses* **1981,** 60, 92-101.

142.   Dess, D. B.; Martin, J. C., A useful 12-I-5 triacetoxyperiodinane (the Dess-Martin periodinane) for the selective oxidation of primary or secondary alcohols and a variety of related 12-I-5 species. *Journal of the American Chemical Society* **1991,** 113, (19), 7277-87.

143.   Ireland, R. E.; Liu, L., An improved procedure for the preparation of the Dess-Martin periodinane. *Journal of Organic Chemistry* **1993,** 58, (10), 2899.

144.   Laemmli, U. K., Cleavage of structural proteins during the assembly of the head of bacteriophage T4. *Nature* **1970,** 227, (5259), 680-5.